Development of optical fibre distributed sensing for the structural health monitoring of bridges and large scale structures

António Barrias

doctoral thesis by

September, 2018

Development of optical fibre distributed sensing for the structural health monitoring of bridges and large scale structures.

Thesis by publications

Doctoral Thesis by:
António Barrias

Directed by:
Prof. Dr. Joan Ramon Casas
Dr. Sergi Villalba

Barcelona, September 2018

Universitat Politècnica de Catalunya - BarcelonaTech
Department of Civil and Environmental Engineering

DOCTORAL THESIS

UNIVERSITAT POLITÈCNICA DE CATALUNYA BARCELONATECH

DEPARTAMENT D'ENGINYERIA CIVIL I AMBIENTAL

PROGRAMA DE DOCTORAT D'ENGINYERIA DE LA CONSTRUCCIÓ

DOCTORAL THESIS

DEVELOPMENT OF OPTICAL FIBRE DISTRIBUTED SENSING FOR SHM OF BRIDGES AND LARGE SCALE STRUCTURES

Thesis by publications

PhD Candidate:

António José de Sousa Barrias

MSc, Civil Engineer

Thesis Supervisors:

Joan Ramon Casas Rius

Prof., PhD, Civil Engineer

Sergi Villalba Herrero

Asoc. Prof., PhD, Industrial Engineer

Barcelona, September 2018

GENERAL INFORMATION

Title of the thesis

"Development of optical fibre distributed sensing for SHM of bridges and large scale structures"

PhD student

Name	António José de Sousa Barrias
Academic Record	Civil Engineer (MSc in Structural Engineering)
Institution	Universitat Politècnica de Catalunya (UPC)
Email	antonio.jose.de.sousa@upc.edu

Thesis supervisors

Name	Joan Ramon Casas Rius
Academic Record	Catedrático Dr. Ingeniero de Caminos, C y P
Institution	Universitat Politècnica de Catalunya (UPC)
Email	joan.ramon.casas@upc.edu

Name	Sergi Villalba Herrero
Academic Record	Prof. Asoc. Doctor Ingeniero Industrial
Institution	Universitat Politècnica de Catalunya (UPC)
Email	sergio.villalba@upc.edu

To my parents, sister and godmother:

António, Persília, Ana Maria and Maria da Conceição, for the continuous, selfless and invaluable support.

"All truths are easy to understand once they are discovered; the point is to discover them"

Galileo Galileo

Acknowledgments

I would like to take this opportunity to thank everyone, which in some way have contributed for the success of my personal academic career, more precisely, during the conduction of my doctorate studies, and therefore making the accomplishment of this great challenge possible. Notwithstanding, and due to their specific roles during this period, special acknowledgements have to be directed to:

- My supervisor, Prof. Joan Ramon Casas Rius, for the opportunity and confidence entrusted in me and for the unmeasurable support, knowledge and guidance provided during the conduction of this work. Furthermore, I would like to thank him for the magnificent treatment and kindness directed to me and all others, which constituted as an exemplary role model throughout these years;
- My co-supervisor, Dr. Sergi Villalba, for the continuous availability and technical aid on the use of the OBR system in this research project. Furthermore, to the opportunity of obtaining real world application data, which enabled important results and conclusions presented in this thesis;
- To Gerardo Rodriguez for his friendship and the invaluable help provided when introducing me to the topic of distributed optical fiber sensors, its capabilities and limitations and moreover to his great quality work in his doctoral thesis which greatly helped the conduction of this research;
- To all the personnel of the Structures Technology Laboratory of the Technical University of Catalunya – BarcelonaTech, and to Ulric Celada and Noemi Duarte for all the help and assistance provided during the laboratorial experimental campaigns conducted during this research.
- To my colleagues Giorgio Anitori, John James Moughty and Mattia Bado for all the camaraderie and friendship which eased the conduction of this research with plenty of moments of leisure and amiability.
- To all my personal friends, from the ones I have always known to the ones I've met along the way, which fortunately are too many to name separately, for the absolute and boundless companionship and affection which always supported me and provided me with endless fond and cheerful experiences and memories;
- To all the members of the TRUSS ITN project, from all the professors and supervisors to the other early stage researchers who provided critical feedback to this work in our semi-annual meetings and whose friendship and shared experience will be forever remembered;
- To the vital financial support provided by the European Union's Horizon 2020 research and innovation programme under the Marie Sklodowska-Curie grant agreement funding No. 642453.
- To my parents, António and Persília, whose unconditional love and support have always provided me, to the maximum extent of their capabilities, with the tools for the pursue of my goals and dreams;
- To my sister, Ana Maria, for always believing in me and whose kindness, love and limitless assistance allowed me to successfully conduct this research away from home;

- Finally, to my godmother, Maria da Conceição, whose always present guidance and ever-growing affection, love and dedication, have always encouraged me to improve and allowed for the fruition of all my aspirations and objectives.

Abstract

In this doctoral thesis it is proposed to research and assess the performance of the use of distributed optical fiber sensors (DOFS), more specifically the case of the optical backscattered reflectometry (OBR) based system, to the structural health monitoring (SHM) of bridges and large scale structures. This is a relatively recent technology that has demonstrated great promise for monitoring applications in a wide range of fields but due to its novelty, still presents several uncertainties which prevent its use in a more systematic and efficient way in civil engineering infrastructures. This is even more evident and relevant in the case of the application of this sensing technique to concrete structures. In this way, this thesis pretends to continue and further analyse this topic following the initial applications using the OBR system as a possible alternative/complementary monitoring tool in concrete structures.

Therefore, in the present thesis, after an initial and thorough literature review on the use of DOFS in civil engineering applications, a set of experiments and analysis is planned and carried out. Firstly, different laboratory experimental campaigns are devised where multiple aspects of the instrumentation of DOFS technology in civil engineering applications are assessed and scrutinized. Consequently, the study of new implementation methods, comparison and performance analysis of different bonding adhesives and spatial resolution is performed through the conduction of load tests in reinforced concrete beam elements instrumented with OBR DOFS technology. Moreover, the long-term reliability of this sensing typology is also assessed through the conduction of a fatigue load test on two additional reinforced concrete beams.

Afterwards, the use of the OBR system technology is assessed for the application in two real world structures in Barcelona, Spain. The first application corresponds to a previous monitoring work conducted in a historical masonry building and UNESCO World Heritage Site, which was subjected to rehabilitation works and where the collected data was analysed and interpreted in this thesis. The second real world structure application is an urban prestressed concrete viaduct that was exposed to major renovation actions, which included the widening of its deck and the introduction of new steel elements on the improved pedestrian sidewalks. This second application was conducted through a relatively extended period of time, which spanned from early summer to deep winter and therefore causing subsequent important thermal variations effects implications on the performance of the instrumented OBR system leading to the necessity of its compensation.

Finally, taking into account the previous points, several conclusions are obtained related with the proficiency and limitations on the use of this particular type of optical sensing system in concrete structures. The advantages and disadvantages on the use of different types of bonding adhesives, implementation methodologies and spatial resolutions are described. Additionally, the performance of this technology in real world conditions is studied and characterized.

Resum

En aquesta tesi doctoral es proposa investigar i avaluar la possibilitat d´aplicació de sensors de fibra òptica distribuïda (DOFS), més concretament un sistema del tipus OBR (Optical Backscattered Reflectometry), a la monitorització de la salut estructural (SHM) de ponts i estructures de grans dimensions. Es tracta d'una tecnologia relativament recent que ha demostrat una gran versatilitat i validesa en diferents aplicacions en un ampli ventall de camps, però que, a causa de la seva novetat, encara presenta diverses incerteses que impedeixen el seu ús d'una manera més sistemàtica i eficient en el cas de les infraestructures d'enginyeria civil. Sent això especialment cert i rellevant en el cas de l'aplicació d'aquesta tipologia de detecció en estructures de formigó. D'aquesta manera, aquesta tesi pretén continuar i analitzar aquest tema seguint les aplicacions inicials utilitzant el sistema OBR com una possible eina i de control alternatiu o complementari en estructures de formigó.

Per tant, en aquesta tesi, després d'una revisió inicial i exhaustiva de la literatura sobre l'ús de DOFS en aplicacions d'enginyeria civil, es planifiquen i executen un conjunt d'assaigs experimentals i el seu posterior anàlisi. En primer lloc, es desenvolupen diferents campanyes experimentals de laboratori on s'avaluen i examinen múltiples aspectes de la tecnologia DOFS en aplicacions d'enginyeria civil. Com a conseqüència, s´estudien nous mètodes d'implementació, de comparació i anàlisi de rendiment de diferents adhesius de connexió i de resolució espaial mitjançant la realització de proves experimentals en elements a flexió a de formigó armat equipats amb tecnologia OBR DOFS. A més, la fiabilitat a llarg termini d'aquesta tipologia de sensors també s'avalua mitjançant la realització d'un assaig de fatiga en dos bigues de formigó armat addicionals.

Posteriorment, l'ús de la tecnologia del sistema OBR s'avalua de cara a la seva aplicació en dues estructures reals a Barcelona, Espanya. La primera aplicació correspon a un treball de seguiment previ dut a terme en un edifici històric de maçoneria i que és Patrimoni de la Humanitat de la UNESCO (l´hospital de Sant Pau), que es va sotmetre a obres de rehabilitació i on es van analitzar i interpretar les dades recollides durant l´execució de les obres. La segona aplicació és un pont de formigó pretensat urbà que va estar exposat a una important intervenció de renovació, que va incloure l'ampliació de la coberta i la introducció de nous elements d'acer a les voreres de vianants. Aquesta segona aplicació es va dur a terme a través d'un període de temps relativament estès, que va des del començament de l'estiu fins a ben entrat l'hivern i, per tant, va provocar variacions tèrmiques importants tant als materials com als propis sensors, que van tenir conseqüències sobre el rendiment del sistema OBR instrumentat i que va comportar la necessitat de la seva compensació.

Finalment, tenint en compte els punts anteriors, s'obtenen diverses conclusions relacionades amb la competència i les limitacions sobre l'ús d'aquest tipus particular de sistema de detecció òptica en estructures de formigó. Es descriuen els avantatges i desavantatges sobre l'ús de diferents tipus

d'adhesius de connexió, metodologies d'implementació i resolucions espaials. Addicionalment, s'estudia i caracteritza l'acompliment d'aquesta tecnologia en condicions reals i no de laboratori.

Acronyms

SHM – Structural Health Monitoring

OFS – Optical Fiber Sensors

DOFS – Distributed Optical Fiber Sensors

OFDR – Optical Frequency Domain Reflectometry

OBR – Optical Backscatter Reflectometry

SWI – Swept Wavelength Interferometry

OTDR – Optical Time Domain Reflectometry

BOTDR – Brillouin Optical Time Domain Reflectometry

BOTDA – Brillouin Optical Time Domain Analysis

BOCDA – Brillouin Optical Correlation Domain Analysis

GDP – Gross Domestic Product

IWI – Inclusive Wealth Index

GNSS – Global Navigation Satellite System

GPR – Ground Penetration Radar

UAV – Unmanned Aerial Vehicles

NDE – Non Destructive Evaluation

FBG – Fiber Bragg Grating

FRP – Fiber Reinforced Polymer

RC – Reinforced Concrete

SSQ – Spectral Shift Quality

RIAS – Refractive Index Apparent Strain

TEAS – Thermal Expansion Apparent Strain

Table of contents

List of Figures

List of Tables

Chapter 1 - General introduction

This chapter introduces the topic of this thesis related with the use of distributed optical fibre sensing on the structural health monitoring of bridges and large-scale structures for the attainment of the title of Doctor by the Universitat Politècnica de Catalunya – BarcelonaTech.

In this section, the overall motivation behind the conducted research is presented while outlining its main goals and objectives and the structure of this document.

1.1. Motivation for research

Civil engineering infrastructures such as highways and railway transportation systems are of extreme importance in the functioning and economic competitiveness of any society. These elements are invaluable assets that during their lifetime should meet a specific requirement for safety and sustainability. Notwithstanding, all infrastructures are subjected to adverse effects and degradation due to different conditions such as environmental agents, overloading, unexpected events such as earthquakes and the inevitable deterioration associated with the normal use of the structure and the passage of time.

Moreover, current research showcases that the world population (currently around 7.2 billion) will continue to rise throughout this century having a 80 % probability of reaching between 9.6 and 12.3 billion by 2100 [1]. Additionally, to the increase in need of new housing and infrastructure, this will create an added necessity of sustainably increase the lifetime of the current available infrastructure.

This is not an easy assignment as most of the present infrastructure in areas such as Europe and North America is relatively old and becoming gradually inadequate. As of 2016, in the United States alone, 39% of the bridges in the National Bridge Inventory were more than 50 years old and 9.1 % of the total number of bridges were considered structurally deficient. As a consequence, an average of 188 million trips were performed daily across these structurally deficient bridges. Furthermore, the most recent estimate projects the backlog of rehabilitation projects for these infrastructures at $123 billion [2].

Despite the considerable amount of investment required to improve the condition of these structures, there is only a limited amount of funds available. In this way, assessment and maintenance strategies that are able to target and identify those structures in most need of attention are highly in demand.

Civil engineering infrastructures, which are well maintained, can substantially increase a country's competitiveness in a global economy and enhance resilience to adverse circumstances. They are part of the social common capital as included and proposed by the GDP alternative and more sustainable looking indicator of Inclusive Wealth Index (IWI) [3]. Moreover, all infrastructure is exposed to a wide variety of possible natural hazards, which inevitably lead to immense economic and social losses. In 2017 alone, 318 natural disasters occurred which affected a total of 122 countries and resulting in 9503 deaths, 96 million people affected and US$ 314 billion in economic damages [4].

Therefore, a structure, especially in the present days, must be able to reliably produce information regarding the alterations in its structural health condition and communicate it to the responsible operators and decision makers both in time and either automatically or on-demand in order to decrease the maintenance costs. To achieve such goals, a modern structure needs to be prepared with a system

that includes a “nervous subsystem”, a “brain”, and “voice lines”, which is continuously in operation and able to sense structural condition [5].

In the same way, that we as humans perform check-ups regarding our body, infrastructures must be monitored and diagnosed. As doctors assess the health condition of their patients, also civil engineers must be able to evaluate the integrity and safety of infrastructures. While a doctor uses specialized equipment to verify the blood pressure for example, and in this way verify the patient health, engineers deploy particular sensors to infrastructures in order to evaluate its condition. If the patient presents a high blood pressure, the doctor prescribes a suitable treatment. Similarly, engineers must be able to provide appropriate measures in the case of structural faults detections.

This process is known as Structural Health Monitoring (SHM) and has been studied and practiced with great interest within the engineering and academic communities over the last two decades.

The fundamental goals of SHM are to monitor loading conditions of a structure, to access its performance under various service loads, to detect damage and deterioration and to provide important information to better and more effectively conduct inspection and maintenance [6].

Furthermore, this necessity is not restricted to already existing and built structures. When dealing with important new structures, sensors can be deployed during the construction phase so small issues can be identified at an early stage avoiding costly renovations or reconstructions later in the future [7]. Additionally, when deployed correctly, a SHM simultaneously provides valuable qualitative information on the state of the monitored structure for its owner and management agency while also gathering important qualitative real world structural behaviour data for design engineers.

The topic of SHM applied to civil engineering infrastructures has been greatly studied in the recent decades using different approaches and techniques and relying heavily on the use of a wide variety of sensors. These have started to help providing important information on the condition of structures in real time and efficaciously investigate both local and global damage.

With the application of SHM systems, unexpected structural behaviour can be detected at a very early and preventing stage, diminishing the danger of an abrupt collapse, protecting, in this way, human lives, the environment and goods. The early detection of structural malfunctions allows the increase of the service life-time of the structure at the same time that decreases the maintenance costs associated with every infrastructure and the economic losses related with repair/reconstruction in the case of structural failure, being critical for the emergence of sustainable civil and environmental engineering.

Bridge monitoring particularly, can be dated back to the construction of the Golden Gate and Bay bridges in San Francisco in the 1930s in the USA as reported by [8] where an intricate program of measuring periods of the different components during their construction was performed in an attempt to obtain more knowledge on the dynamic behaviour of these structures and its possible implications in

case of an earthquake. More recently, noticeable since the 1990s permanent long-term monitoring systems have been deployed in major bridges in Europe, Japan, China and the USA [6].

Depending on the complexity level of the SHM system, besides the possibility of performing the diagnosis, it is also possible to provide prognosis steps, delivering essential data to carry out the most adequate action. In this way, according to their sophistication, SHM systems could even be considered as a full smart structure, equipped with a detection system (sensing), post-processing analysis (algorithms, programs, etc.) and actuation measures subsystems [5]

The act of damage identification has been around probably, in a qualitative manner, since modern man has used tools [9]. The innovation in the SHM technologies as well as the development of the large-scale SHM systems has been a great subject of interest within the engineering and academic communities over the last two decades [10]–[17]. However, despite its great potential, SHM has not been applied in large scale and in a systematic manner to civil infrastructures. One significant reason for this is the deficit of reliable and affordable generic monitoring solutions [18].

Furthermore, several limitations are present on the conventionally used sensors such as accuracy, electromagnetic interference, transmission cabling length for large-scale structures, accessibility, and practicality of employment within others. Consequently, the trend in the past years has been to develop and study sensing systems, which are able to overcome these limitations and provide important information on the infrastructures condition. The sensors development field has strived for achieving better accuracy, resolution, precision, achieve wider coverage, be more dynamic by enabling faster data acquisition and be more robust.

Different recent technologies have been researched and developed in this way in the past years in structural integrity assessment field. New developments such as smart and wireless sensors [13], the use of global navigation satellite system (GNSS) based sensors [19], ground penetration radar (GPR), acoustic emission [20], vision based sensors [21] and the use of unmanned aerial vehicles (UAVs) [22] among others. Some of these research trends are depicted in Figure 1.1, Figure 1.2 and Figure 1.3.

Figure 1.1. GNSS antenna and station used for the monitoring of motion of Wilford pedestrian bridge in the UK [23]

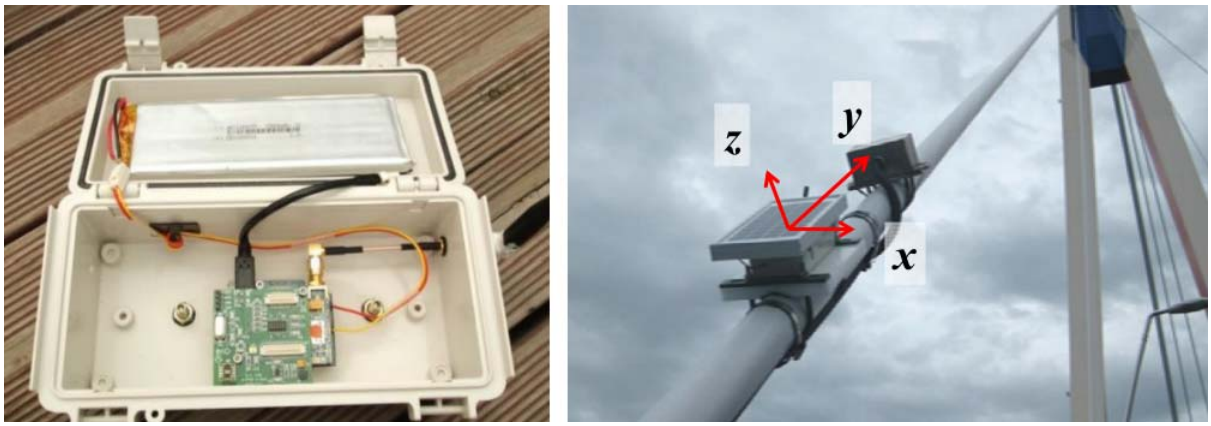

Figure 1.2. Wireless sensor node (left: inside, right: installed) as deployed in Jindo Bridges in South Korea [24]

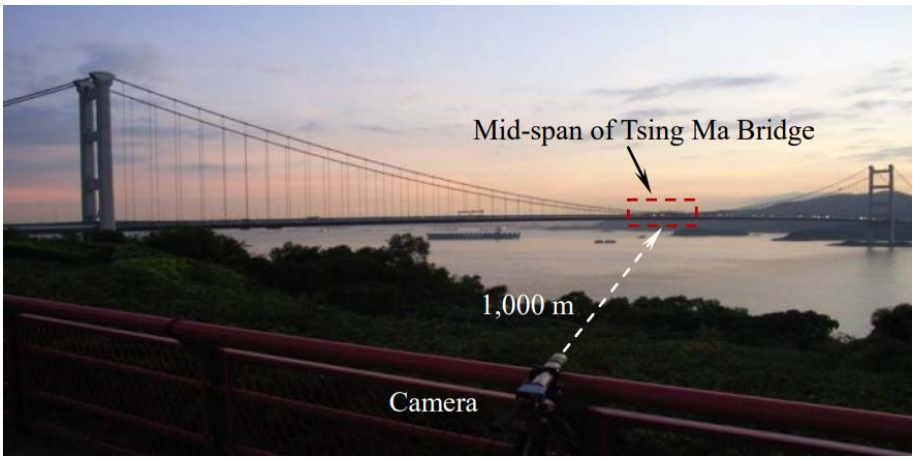

Figure 1.3. Vision-based displacement measurement of Tsing Ma Bridge in Hong Kong [25]

It is within these new sensor development trends that the use of optical fiber sensors (OFS) and more specifically distributed optical fiber sensors (DOFS), have been researched and practiced recently. It is based on this that in this research work it is proposed to further analyse and develop monitoring techniques using the Optical Backscatter Reflectometry (OBR) system which is a DOFS that has been a promising measurement technology in SHM applications in recent years, and depicted in Figure 1.4. In this image, it is possible to see the interrogation system on the left, an optical fiber cable which constitutes the sensor and the laptop computer used to operate the software interface of the system.

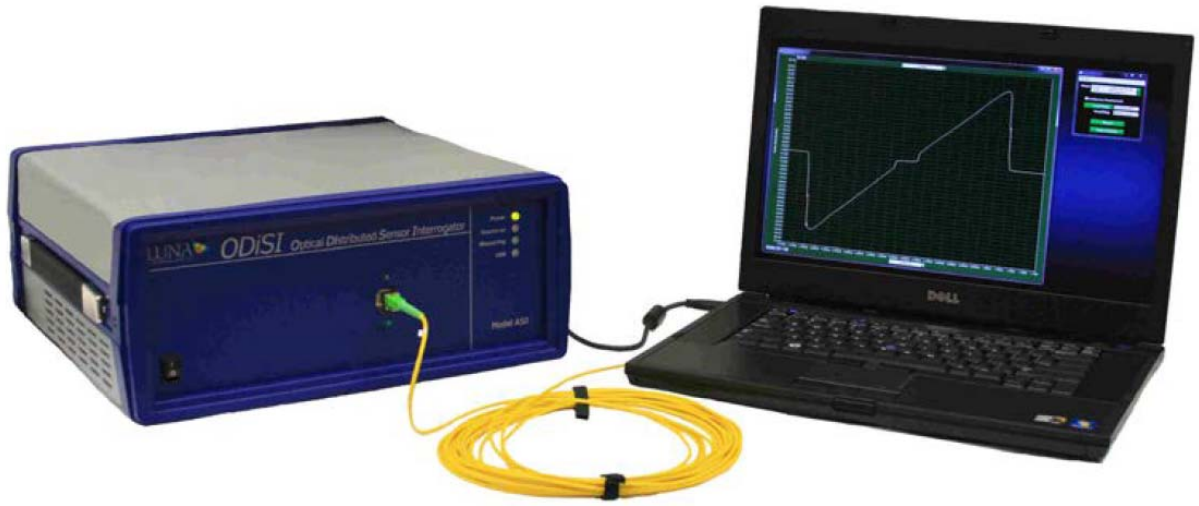

Figure 1.4. OBR system used in this investigation (ODiSI-A by LUNA Technologies) [26]

This is a system that is able to obtain distributed and continuous strain and temperature measurements using an optical fiber as the sensor providing numerous specific points of interest over an extended area of the monitored structure allowing for user-configurable sensing locations and gauge lengths.

The OBR system technique diverges from other frequency-domain optical fiber scattering techniques by the fact that is sensitive enough to measure levels of Rayleigh backscatter in standard single-mode fiber, allowing for an enhanced and unprecedented spatial resolution.

This technology has been effectively deployed in several applications in aeronautical construction, but the materials used here such as composites, steel and aluminium present a smooth and homogeneous surface permitting an easy bond between the sensor and the structure. Moreover, they also have a continuous strain field when subjected to external loading. Therefore, the study of the feasibility of using OBR in SHM of civil engineering constructions made of concrete assumes an even greater interest.

1.2. Problem Identification

Concrete (reinforced and prestressed) and steel are the most broadly used materials in civil engineering infrastructures and its inevitable decay and deterioration in the form corrosion and cracking is one of the main problems faced by infrastructure management agencies today. In these type of structures, the early detection of cracking is an important initial evidence of damage formation. Cracks can be categorized as unintentional discontinuities in the structural material that are usually consequence of local material failure and generated by different factors such as external loads, fatigue, chemical processes, corrosion and buckling. Small cracks may lead to not acceptable serviceability levels and large cracks can even result in structural failures. As a result, the early and effective detection

of all type of cracks before reaching critical levels, causing the failure of structural components or the entire structure, is of paramount importance.

Currently, most practiced methods for crack detection and characterization in civil engineering structures are based on periodical visual inspections and non-destructive evaluation (NDE) based on traditional instrumentation and techniques [27]. However, these methods can be expensive, time consuming and frequently inaccurate. Due to the different personal experience of each inspector and to the difficulty to detect inconspicuous cracks, visual inspections often become unreliable. Moreover, damage can occur and propagate until critical levels between two programed inspections. As a consequence, there is a real need for more accurate and reliable methods for quasi-real-time crack detection and characterization [28].

It is in this way that OFS is one of the fastest growing and most promising researched topic, due to their features of durability, stability, small size and insensitivity to external electromagnetic perturbations, which makes them ideal for the long-term health assessment of civil structures [29].

Furthermore, the most regularly practiced SHM approaches are based on electric strain sensors, accelerometers, inclinometers, GNSS-based sensors, acoustic emission, wave propagation, etc. Nevertheless, all of them present genuine challenges when deployed in real world applications. These challenges are mostly related with the difficulty on successfully capturing the system response associated with the lack damage sensitivity, the necessity of an adaptation learning period of these systems since data from damaged systems are not available, and finally the requirement of previously correctly defining the system properties before deployment in order to assure that the monitoring system itself will not be damaged when applied to an infrastructure [9]. Different kinds of sensors, embedded or attached to the structure, can be used in SHM systems but only those based on fiber technology provide the ability to accomplish integrated, quasi-distributed, and truly distributed measurements on or even inside the structure, along extensive lengths [5].

Furthermore, standard monitoring practice is normally based on the choice of a limited and relatively small number of points that are supposed to be illustrative of the structural behaviour [30]. However, for a large-scale structure, the number of point sensors needed to generate complete strain information can grow rapidly. Discrete short-gauge sensors provide useful and interesting data of the structure related with local behaviour but might omit important information in locations where degradation occurs but that it is not instrumented. There are ways of covering larger extensions of structures with the application of long-gauge sensors allowing the detection and characterization of phenomenon that have a global impact on the structure. Notwithstanding, the reliable detection and characterization that occurs far from instrumented areas continues to be challenging since it depends on high-level algorithms whose performance may decrease due to external interferences that can mask the

real damage, such as temperature variations, load changes, outliers and missing data in monitoring results [31], as seen in Figure 1.5.

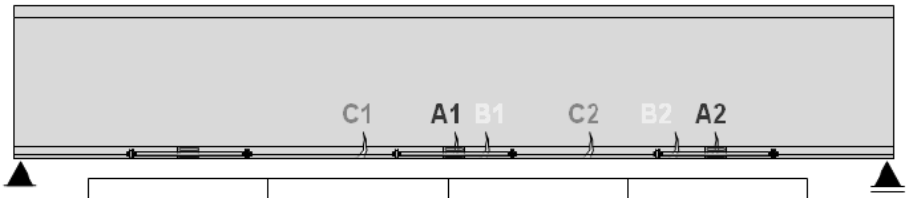

	Damages "A"	Damages "B"	Damages "C"
Short-gage	Direct detection	Indirect or impossible	Indirect or impossible
Long-gage	Direct detection	Direct detection	Indirect or impossible
Distributed	Direct detection	Direct detection	Direct detection

Figure 1.5. Schematic comparison between damage detection capabilities of short-gauge, long-gauge and distributed sensors [30]

Distributed optical fiber sensors (DOFS) offer an advantage over point sensors for global strain measurements. The thousands of sensing points that the DOFS provides enables mapping of strain distributions in two or even three dimensions. Thus, real measurements can be used to reveal the global behaviour of a structure rather than extrapolation from a few point measurements.

A truly distributed optical sensor is expected to measure temperature, strain and vibration data at any point along an entire fiber trough light scattering. The great challenge has been to develop these sensors in a way that they can achieve appropriate sensitivity and spatial resolution [29]. Fortunately, great advances have been made in the last decades in order to improve this area.

It is in this context that the capabilities and potential of the OBR system can be presented as a promising alternative for crack detection and general monitoring in concrete structures on civil engineering infrastructures. Therefore, due to the novelty and still relative uncertainty on the standard use of this type of sensor technology, in this doctoral thesis, the use and assessment of OBR based DOFS is performed specially aiming their application in concrete structures in order to establish more robust and confident guidelines for future and wider application.

1.3. Objectives

According to the problem statement presented, with the production of this doctoral thesis the following goals and objectives were stipulated at the beginning of the project timeline:

- Study and analysis of the spatial resolution and strain accuracy that are possible to be obtained through the use of Optical Backscattered Reflectometry (OBR) based DOFS;
- Verification of the potential and effectiveness of detecting and localizing crack or unusual deflections without failure or debonding of the optical fiber sensor;

- Optimization of the bond strain-transfer between the monitored structural specimen and the deployed DOFS.
- Demonstration of the feasibility of application of these type of sensors to reinforced concrete structures for long-term monitoring periods.

In this way, in order to achieve and fulfil the mentioned objectives, a set of particular goals were established and are presented as follows:

- Get acquainted with the background theoretical functioning of optical fiber sensors and their different categories including in more detail distributed optical fiber sensors (DOFS);
- Perform a detailed literature review of DOFS in civil engineering applications and withdraw their main challenges and points of research going into the future;
- Establish a set of laboratory experiments where novel implementation techniques, different bonding adhesives performance, and long-term reliability of OBR based DOFS to reinforced concrete structures, was to be explored and analysed.
- Perform and assess the behaviour of these sensors in real world monitoring scenarios and their capacity of being able to follow the structures' behaviour changes within safety limits during the monitoring period.
- With the experience obtained through the conduction of this project, provide future research lines to be pursued with the intent of improving OBR based DOFS as robust and effective sensor to be applied in civil engineering SHM applications.

1.4. Thesis Structure

This thesis is divided in five chapters and an annex where the actions conducted in order to fulfil the previous mentioned objectives and goals are described and discussed.

In the first chapter, where this thesis structure is outlined, it is initially presented the importance and relevance of structural health monitoring (SHM) systems to civil engineering infrastructures. This is followed by the identification of the problem intended to be researched in this thesis while introducing the topic of distributed optical fiber sensing (DOFS) and its role in SHM. Finally, the research objectives are outlined and presented.

In the second chapter, a brief historical revision of the origin of optical fiber technology is presented followed by its evolution until its sensing use. Then, a brief and general outline of the fundamentals of the theory that enables optical fiber sensing is presented as well as a comparison between the main used typology of sensors and practiced techniques. A general summary of previous conducted applications of DOFS in the civil engineering field is then presented both for laboratory experimental campaigns as in real world case scenarios. This is followed by the presentation of the most important takeaways from this literature review exercise and its implications for the schedule planning of the following actions in this thesis.

The third chapter constitutes the central core of this document as it presents the laboratory experimental campaigns and real world applications analysis conducted as a result of the objectives outlined in the first chapter. The summary of the conducted experiments and the discussion of the obtained results is showcased here while presenting the main encountered challenges and produced contributions to the state of the art of this researched topic.

As a thesis produced by the compendium of published journal articles, in the fourth chapter the articles used in this compendium are presented. These articles present in a vast greater detail part of the actions and results discussed in the third chapter. The content presented here follows its own numbering of figures, tables and sections as well as used references.

The fifth and final chapter describes the most important conclusions obtained through the conduction of the research performed in this thesis. Moreover, based on the obtained experience in this work, further developments and research topics are proposed and outlined which can continue to improve the work developed in this thesis.

Lastly, the annex of this document presents two articles, which were already submitted to international peer-reviewed journals and are currently under revision at the time of writing this thesis. The actions presented in these articles are summarized in the discussion of results presented in the third chapter while being described in this annex with greater detail. As in the fourth chapter, the contents presented in the annex follow its own numbering of figures, tables, sections and references.

Chapter 2 - State of the art

This chapter reviews the history behind optical fiber technology and its evolution towards sensing tools. A brief and general outline of the fundamentals of the theory that enables optical fiber sensing is presented as well as a comparison between the main used typology of sensors and practiced techniques. Finally, a global review of the application of this technology in the civil engineering field is presented followed by the most important takeaways that shaped the subsequent actions conducted in the materialization of this thesis.

2.1. Introduction

In this chapter, it is presented a brief and general state of the art on the use of OFS and more specifically distributed optical fiber sensors (DOFS) in civil engineering applications. The story and basic principles behind this technology are presented followed by the characterization of DOFS. Finally, a global review of applications of this technology in different fields of civil engineering is showcased.

Most of the information presented in this chapter is referred in the first published journal article produced within this thesis and which is presented later in Chapter 4. Therefore, in order to avoid repetitions in the text, the overall information described in the aforementioned journal article is briefly summarized here and referenced when appropriate while additional new references relevant for the subject of this thesis are added.

2.2. Fiber Optics Sensors

Despite the general idea of optical fiber sensing technology being a relatively recent breakthrough, its origin can be traced back until the 19th century where the principal of enclosing emitted light within a determined path through internal total reflection was first experimented. Daniel Colladon, a professor at the University of Geneva, firstly explored the properties of guiding light and reflecting it through a medium in his experiments using flowing water, Figure 2.1, which was later used to produce magnificent light stream illuminated fountains displayed mostly at great exhibitions of the time [32].

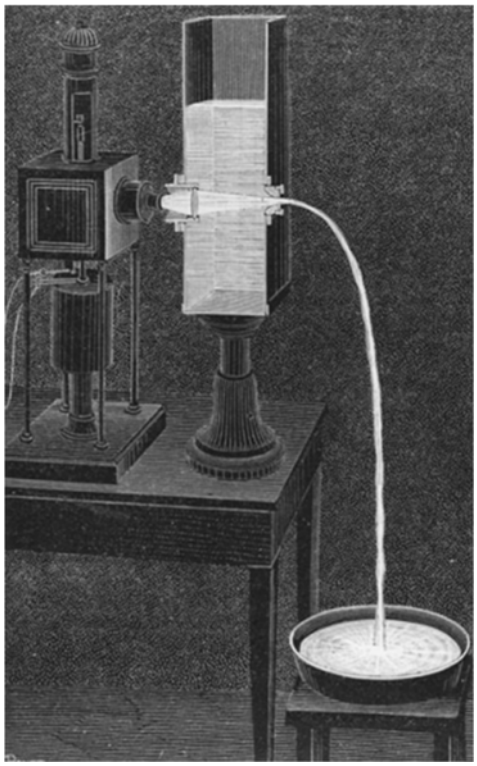

Figure 2.1. Colladon's fountain experiment [32]

This idea continued to be developed broadening its application to several fields, attempting to guide the light in short distances using glass. One of the most notable advances in this time is associated with the development of flexible endoscopes developed in the first half of the twentieth century, which propelled a revolution in the medicine field that continues to the present day [33]. In the 1930s a German medicine student, Heinrich Lamm, tried to find a better alternative for the rigid endoscope which was being used since the 19th century. In this way, Lamm observed that a bundle of glass fiber would be a much more flexible and pleasing for both the physicians and patients [32].

Nevertheless, light was still leaking when bare glass fibers touched each other or other surfaces. It was only in 1956, that a physics student from the University of Michigan, Lawrence E. Curtiss, produced glass-clad fiber which was the last piece needed to build the first functioning flexible endoscope by having a tube with an inferior refractive index around a rod of higher-index glass, Figure 2.2, trapping the light allowing for the total reflection of the light within the fiber [32].

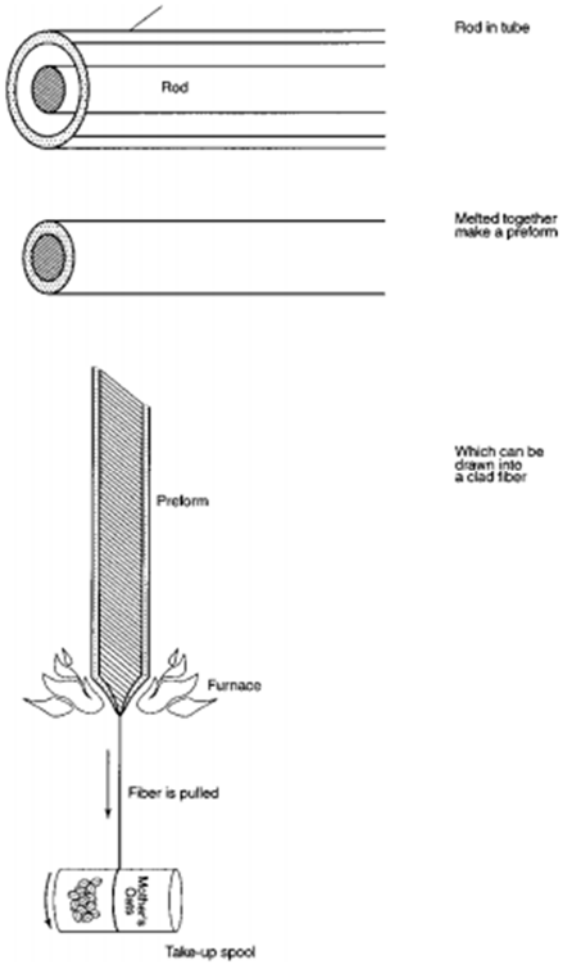

Figure 2.2. Production of glass-clad fiber by melting a glass of tube onto rod, heating the tip and stretching a fiber from it [32]

Nevertheless, the development of modern age of optical fiber sensors started in 1977 at the earliest for long distance telecommunications and it has experienced an exponential growth during the last four decades. In opposition to the use of this principle for producing endoscopes which only require relative short lengths, the communication field which required fibers able to transmit information over larger distances really catapulted the field of optical fiber technology.

Due to the wide dispersion of the light propagation, as the lengths necessary to cover by this technology increased, it was easily perceived that light suffered of attenuation and loss of power. In this way, communication through optical fiber systems was defective for distances even below 1 km [34]. Later with the development of the laser, it was possible to considerably decrease the light dispersion inside the optical fiber cables.

It was observed that impurities in the production of the fibers were the main cause behind the attenuation of the light. In order to make optical fibers competitive in the communication field it was necessary to reduce the loss due to attenuation to levels below 20 dB/km, which was achieved between 1970 and 1972 with the development of low-loss optical fibers [32].

Sensing applications are a small spin-off from this technology, taking profit of developments done for optoelectronic components and concepts. Initial exploration of optical fiber cables capabilities to measure deformation in structural mechanics were conducted by Butter and Hocker in 1978 [35]. By the year of 1982, magnetic, acoustic, pressure, temperature, acceleration, gyro, displacement, fluid level, torque, photo acoustic, current, and strain sensors were among the optical fiber sensors already developed and being researched [36] This modern age of optical fiber sensors was possible due to the aforementioned development of extremely low-loss optical fibers in the 1970s [33].

The fiber optic communications industry has literally revolutionized the telecommunications industry by providing higher-performance, more reliable telecommunication links with ever-decreasing bandwidth cost. As component prices have fallen and quality improvements have been made, the capability of fiber optic sensors to replace the more traditional electric sensors has been improved [37].

The initial introduction of optical fiber sensors into the markets was relatively slow, when competing with the conventional sensor technology in the last two decades of the 20th century. This was a result of the higher cost of the components needed for production of OFS. Nevertheless, this situation has since reverted.

2.3. Fundamentals of Optical Fiber Sensors

As explained in section 2.2 of the first published article available in Chapter 4 of this document, an optical fiber is essentially a cylindrical symmetric structure composed of a central “core” with a uniform refractive index which is then enclosed by a “cladding” with a lower refractive index which allows for the total reflection of the light waves being transported within the core. This cable is usually

produced of silica, allowing for the carrying of large amounts of information through great lengths with low–loss of power. Most of the time, in order to grant environmental and mechanical protection to the fiber, this cladding can be covered with an external plastic coating. The common dimensions of an optical fiber cable are depicted in Figure 2.3.

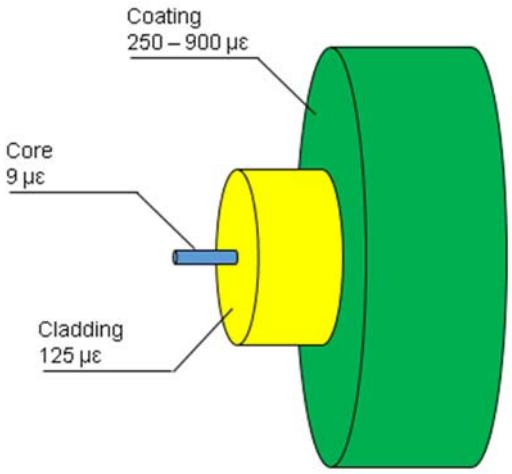

Figure 2.3. Typical dimensions of an optical fiber cable

External perturbations produce geometrical and optical changes in the optical fiber cable. These perturbations are avoided and minimized in the communication applications as they affect the transmission and reception of a reliable signal. On the other hand however, in optical fiber sensing technology the opposite happens as these external induced effects are intentionally enhanced [38].

When compared with the more traditional commonly used type of electric sensors, OFS provide several inherent advantages such as their immunity to electromagnetic interference and radio frequency, their small size, lightweight and flexibility, high sensitivity, good performance under a wide range of temperature, chemically inert (therefore free from corrosion) and large bandwidth.

In terms of typologies of optical fiber sensors there are several different ways of classifying them depending on the inherent property that is being considered. Nevertheless, regarding the topic in research in this thesis, it is best to assume the classification which divides the typologies of OFS in three different classes: interferometric sensors, grating-based sensors and distributed sensors [39]. This is depicted in Figure 3 of published journal article I. As mentioned in that document, the first two classes have been widely investigated and practiced in civil engineering monitoring applications [40]–[45].

Distributed sensors on the other hand only relatively recently have been starting to be researched and applied in a wide range of fields.

2.4. Distributed Optical Fiber Sensors (DOFS)

In the same way as the other categories of OFS, distributed optical fiber sensors (DOFS) also present the same inherent advantages mentioned in the previous section. Notwithstanding, they provide the unique capability of monitoring variations effects on the fiber cable along its entire length in a truly distributed way.

As it was already mentioned in Chapter 1, the use of point/discrete sensors might result in the omission of important data on the global structure's performance. This is even more significant in the case of large-scale structures such as bridges, dams, tunnels, high-rise buildings and power plants. Furthermore, when monitoring structures composed of heterogeneous materials such as the case of reinforced concrete members, it is practically impossible to accurately predict the exact location of possible damage formation (usually associated with cracking and corrosion). In this way, DOFS sensors provide a unique advantage of monitoring virtually every cross-section of the structure to which they are instrumented into, detecting damage that would be otherwise missed as depicted in Figure 2.4.

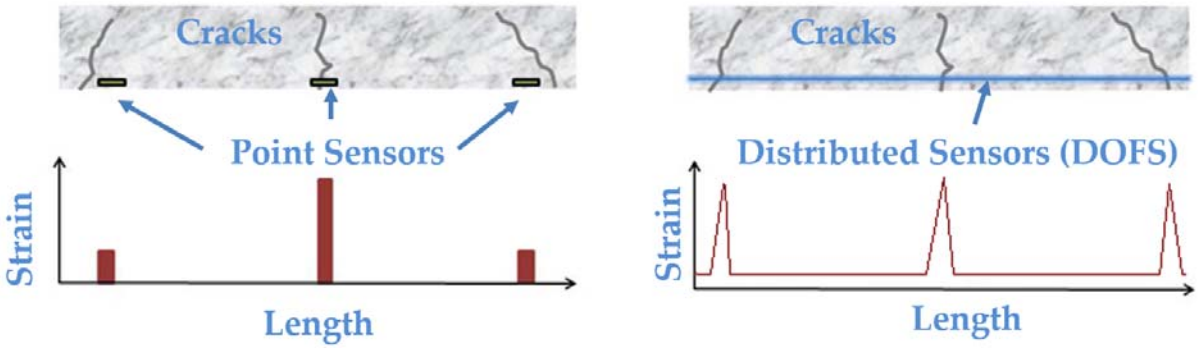

Figure 2.4. Spatial distribution detection using point sensors as OFS (left) and distributed sensors as DOFS (right)

Moreover, especially in large-scale structures, the necessary number of point sensors (and its corresponding connecting cables) to perform a suitable global monitoring can increase very rapidly or be most of the times practically unattainable, Figure 2.5. In this way, soaring the associated costs and technical challenges for effective deployment of a global monitoring sensing system.

Distributed sensing has also been achieved in a way through the use of quasi-distributed FBG sensors. In fact, this has been the most popular type of distributed optical fiber sensing technique as it represents 2/3 of the total number of SHM applications where any type of OFS was deployed for spatial continuous measurements [47].

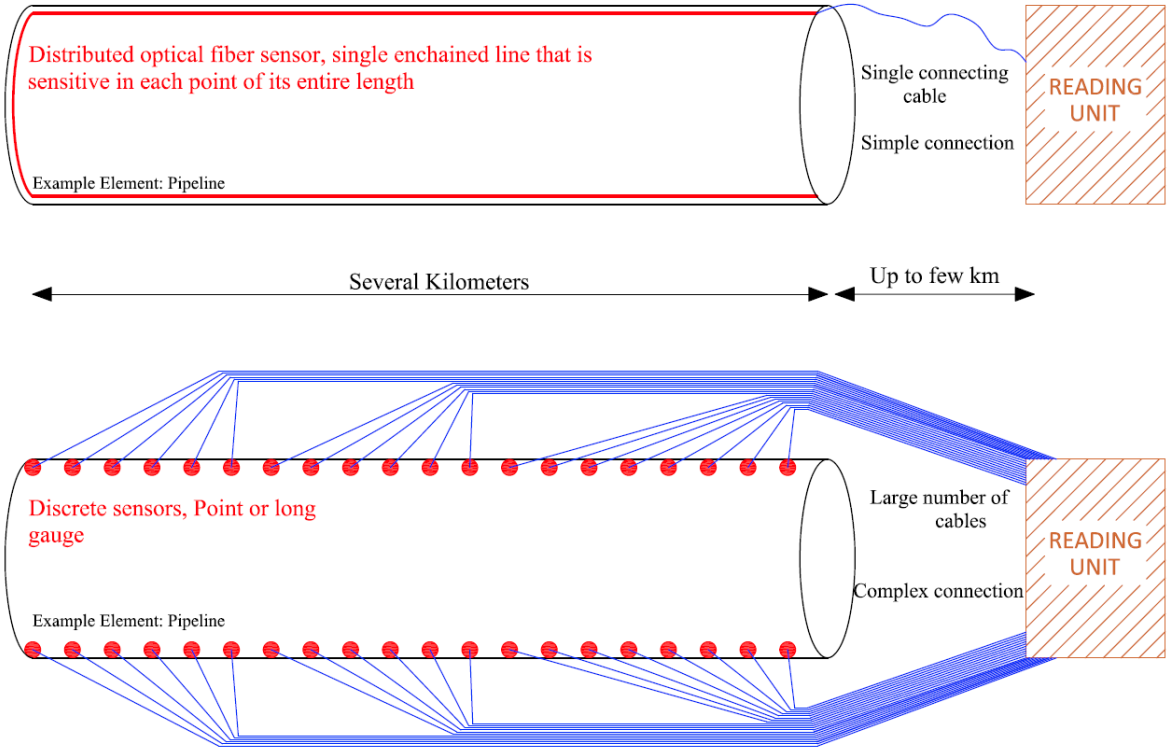

Figure 2.5. Comparison of use of distributed sensor (top) and point sensors (bottom) in large scale structures (Adapted from [46]).

Notwithstanding, quasi-distributed sensing is usually limited to 100 fixed sensing channels in each cable [48], being limited to a spatial resolution based on the FBGs gauge length and spacing.

Given these points, sensing is achieved in DOFS due to the alteration of the scattered signal within the fiber when strain or temperature changes occur in the structural material to which the sensor is externally bonded or embedded to. In essence, is this scattering phenomenon which is the source of distributed optical fiber sensing.

2.5. Scattering in Optical Fiber Sensors

Scattering is the interaction between the light and the medium in which is being propagated, which in the case of DOFS is the optical fiber cable. When an electromagnetic wave is emitted into an optical fiber, its propagation through the medium interacts with the constituent atoms and molecules and the electric field induces a time dependent polarization dipole. This induced dipole generates a secondary electromagnetic wave and this is called light scattering [29].

When the medium where the scattering occurs is homogenous, only a forward scattered beam is propagated. Nonetheless, due to the many variations in its density and composition, an optical fiber is, in reality, an inhomogeneous medium, which means that through the interaction of the emitted light with the fiber, scattering can occur in all directions including the opposite direction of the produced light beam, i.e. generating backscattering. With this, a detailed picture of the local loss distribution or

reflections along the fiber caused by any external event is provided. The location of such defects are simply calculated by the time of flight [49].

This backscattering consists of different spectral components generated by different interaction mechanisms between the propagating light pulse and the optical fiber. These are namely the Rayleigh, Brillouin and Raman components [50], Figure 2.6.

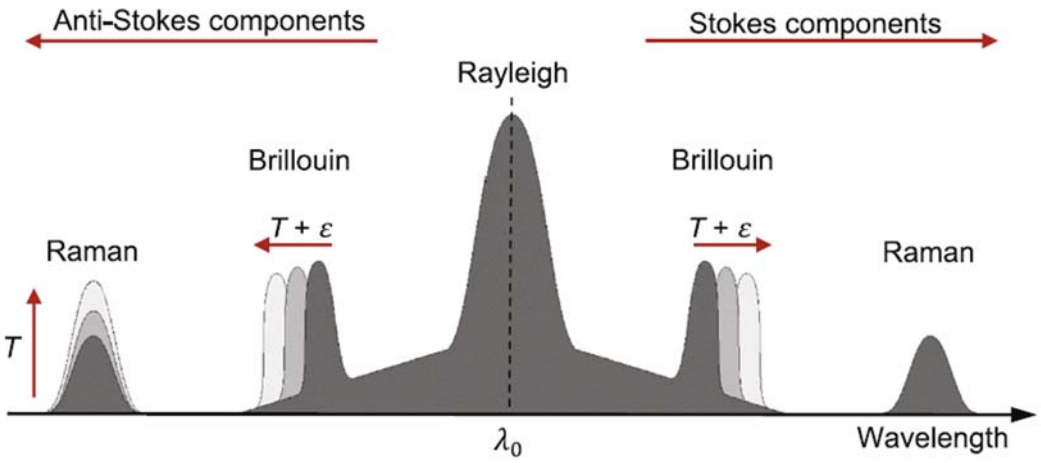

Figure 2.6. Rayleigh, Raman and Brillouin scattering intensity [50]

In this way, when strain and temperature changes are transferred to the optical fiber, the scattered signal within the fiber is modulated by these physical parameters. By measuring the variation of this modulated signal, distributed fiber sensing is achieved.

As seen from Figure 2.6, Raman scattering is greatly dependent of the temperature variation on the fiber but not the strain. In this way, Raman based DOFS have been mostly been used as distributed temperature sensors with some examples in the civil engineering SHM field [51], but mostly used in other type of applications such as art restoration [52] [53], forensics [54] and biomedical applications [55].

On the other hand, Brillouin scattering is inherently dependent on the fiber density, being in this way correlated with any temperature and strain variation. This is the base of all the explored Brillouin based DOFS.

There are two main Brillouin based DOFS techniques that have been used in the past few years. Firstly, there is the Brillouin optical time domain reflectometry (BOTDR) technique, which uses the spontaneous Brillouin scattering and was the first to be used for strain and temperature measurements in civil engineering infrastructure. Then, there is the Brillouin optical time domain analysis (BOTDA) technique, which is based on stimulated Brillouin scattering amplifying the usually very weak Brillouin backscattering through the use of counter propagating lasers [5], [7], [29], [56].

Both BOTDR and BOTDA are characterized for allowing distributed sensing measurements over extensive lengths making them suitable for global monitoring of large-scale structures [57].

Nevertheless, both present a limited spatial resolution of 1 m, which is not ideal for some applications such as damage detection. Nevertheless, Brillouin scattering-based DOFS have been the most studied and practiced in civil engineering structures, largely due to their extended measurement range capability, which goes up to several kilometres.

Finally, the Rayleigh scattering, as a quasi-elastic or linear phenomenon, is by itself independent of almost any external physical field as seen in Figure 2.6. Nonetheless, the Rayleigh backscattered profile of a specific optical fiber is a result of its heterogeneous reflective index (i.e. its imperfections), which is distributed randomly along the entire length of the fiber, establishing a fingerprint of each optical fiber as a result of its manufacturing process [58]. Hence, when subjected to an external stimulus, the Rayleigh backscatter pattern presents a spectral shift that is then used to calculate the strain or temperature variations along the length of the fiber by comparing with its unaltered reference state.

This technique is named Rayleigh based Optical Frequency Domain Reflectometry (OFDR), which has the Optical Backscatter Reflectometer (OBR) as its most popular system. Due to the random fluctuation of the refraction index that gives origin to the Rayleigh scattering, an analogy can be made with the use of fiber optic cable with a series of Bragg gratings with random, yet definable, periods [59], [60]. By scanning the frequency with the OFDR technique, the spectral response of each equivalent FBG is obtained as well as high spatial resolution measurements of strain and temperature variations.

As mentioned in Chapter 1, this later scattering technique, Rayleigh based OFDR, is the focus of the research in this thesis through the use of the OBR system. Moreover, the detailed description of the Optical Time Domain Reflectometry (OTDR) and Optical Frequency Domain Reflectometry (OFDR) techniques is vastly explained in the first part of the published journal article I that is presented in Chapter 4 of the present thesis.

An overall review of the performance of the discussed distributed sensing techniques as reported by different research studies is presented in Table 2.1. The multiplexed FBG sensor technique is also included for comparison.

Table 2.1. Performance review of different Distributed sensing techniques

Sensing Technology	Transducer Type	Sensing Range	Spatial Resolution	Main Measurands
Raman OTDR	Distributed	1 km [61] 37 km [62]	1 cm [61] 17 m [62]	Temperature
BOTDR	Distributed	20–50 km	≈1 m	Temperature and Strain
BOTDA	Distributed	150–200 km [29]	2 cm (2 km) [63] 2 m (150 km) [64]	Temperature and Strain
Rayleigh OFDR/OBR	Distributed	50–70 m [17]	≈1 mm [59]	Temperature and Strain

These type of sensors went then to be used in a wide variety of fields such as oil and gas, industry, safety and security, power and utility and also civil engineering. As seen in Figure 2.7, for Europe alone, as of 2018, only a 13% market share of the optical fiber sensors are headed to the civil engineering field. At the same time, oil and gas is the leading business in optical fiber sensors applications with a 48% market share.

Nevertheless, by 2028, it is expected that the share of the oil & gas and power & utility will relatively decrease, giving space to grow to the other fields, most noticing the civil engineering field which is forecasted do double its share size in the next 10 years [65], Figure 2.7.

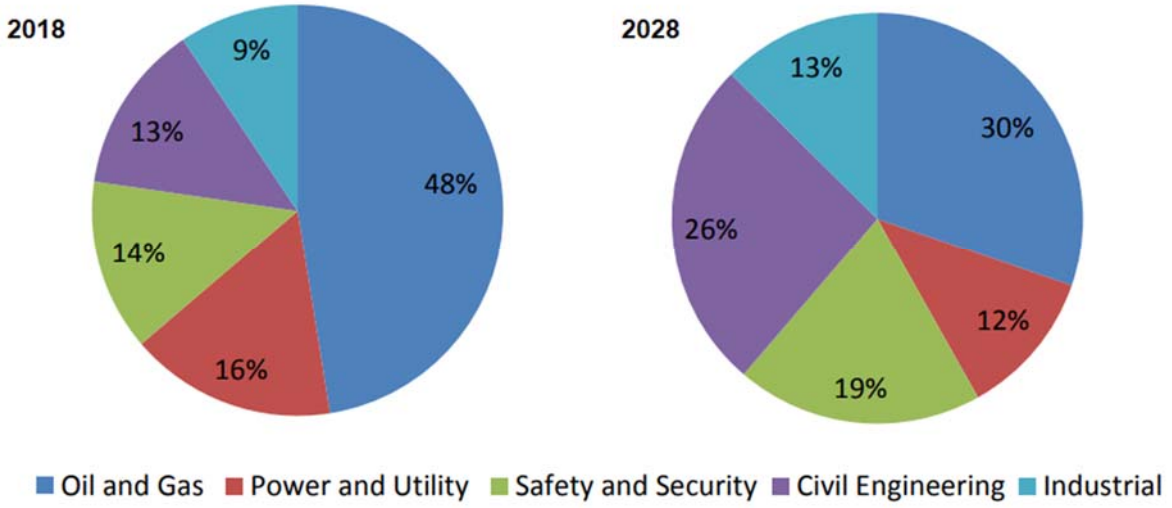

Figure 2.7. Distribution of market share by application in Europe for 2018 and forecast for 2028 (Adapted from [65])

Within this increment of the use of DOFS in civil engineering applications, it is also expected to observe an increase of the share of the Rayleigh based scattering DOFS in the next few years [66], enhancing in this way the relevance of the topic researched in this thesis.

2.6. Civil Engineering Applications with the use of DOFS

This is still a recent and in development technology as it can be observed by the low number of DOFS applications in SHM practice. Nevertheless, different DOFS research in the laboratory environment and applications on different real world civil engineering structures such as bridges, dams, pipelines, slopes and other type of structures were conducted in the last two decades, and are very briefly presented in the following section. This is further developed in the published journal paper I presented in Chapter 4 of this thesis.

2.6.1. DOFS research in laboratory experiments

Due to the aforementioned novelty of this sensing technology, the use of DOFS in experimental laboratory tests is of great interest within the structural engineering field, as it allows the assessment of their feasible uses through the research of its capabilities and limitations.

One of the most active research groups which deals with the topic of DOFS in civil engineering structures is precisely the group where this thesis is conducted within, i.e., UPC-BarcelonaTech's Structural Laboratory. This group's initial interaction with the OBR monitoring technology was conducted in 2009, through a laboratory test where a reinforced concrete slab was instrumented with a 50 m OBR based DOFS attached at the top and bottom faces over four stretches. The evolution of strains was continuously measured (in space and time) during a load test. The obtained results in this test, showcased the ability of the OBR sensing technology to locate emerging cracks that were hardly visible to the naked eye by identifying the strain peaks that surpass the expected concrete tension capacity [67].

The same group, continued the research of this technology by proposing a methodology of cracking damage quantification through the use of DOFS by obtaining an average crack width of the monitored structural element over a characteristic length L. This was successfully conducted for concrete members under bending [68] and shear [69] actions.

A laboratory experiment was conducted by Quiertant et al. where OBR based DOFS where fiber was embedded into a groove of the rebar of a reinforced concrete (RC) member for the measurement of the strain in this element [70]. This is done as a way to reduce the interference of the fiber coating protection in its measurements.

Additionally, Henault et al. performed laboratory experiments where a concrete slab was instrumented with Raman, Brillouin and Rayleigh-based DOFS. The Brillouin scattering based sensor results were limited by their poor accuracy (1 m spatial resolution combined with 20 μm/m) while the Rayleigh ones (OBR sensor) provided very promising results [51]. The Raman based DOFS was used for temperature compensation.

Another group of researchers in Canada, studied the performance of Rayleigh based DOFS when attached to rebars in RC members for the detection of pitting corrosion [71]. In this experiment, polyimide coated fibers were implemented to the rebar elements of embedded reinforced concrete beams under four-point bending tests showing promise for detecting localized corrosion.

More recently, the same research group continued this research with a test where distributed sensing was used to assess the impact of corrosion on bond performance in reinforced concrete with tensile tests on bare rebars and RC members [72]. Here it was seen how the DOFS were able to measure the corrosion effects on the concrete and steel bond as well as locate areas of pitting corrosion that were visually hidden by the surrounding concrete.

Few applications are reported on the assessment of DOFS performance under fatigue loading, especially in the case of Rayleigh scattering based DOFS. Notwithstanding, two reports from LUNA Innovations Incorporated, manufacturers of a commercial OBR system, reported on the superior fatigue performance of DOFS on an experiment where this technology was deployed to fiberglass coupons and subjected to a ± 2000 με and ± 4000 με cyclic load for 1000 cycles each [73] and another where DOFS

were instrumented to wind turbine blades and able to follow the accumulated damage under fatigue [74].

2.6.2. DOFS applications in real world structures

The first applications of DOFS to real case scenarios was mostly conducted with BOTDR technique on the control of slopes, pipelines, tunnels and other large scale structures due to its extensive sensing range capability and where its spatial resolution was sufficient for its monitoring. Nevertheless, with the further conducted research and more widespread use of other DOFS scattering techniques such as the BOTDA and the Rayleigh OFDR techniques, an expanded array of structures has been reported to be instrumented with DOFS and are briefly presented in this section.

Bridges

The instrumentation of DOFS on bridges has unsurprisingly been one of the most appealing areas for the application of these sensors and one of its first successful and most complete applications was conducted on the Götaälv Bridge in Gothenburg, Sweden. This structure presented several cracks in its girders which prompted the responsible traffic authorities to order a continuous monitoring of the structure [30]. A DiTeSt system based on BOTDA technique was successfully implemented and tested on this bridge in 2007-2009 followed by a one-year trial period and intended to work properly for 15 years.

Another Brillouin based DOFS system was implemented in the monitoring of a slab-on-girder bridge on the US Route 54 over the Osage River in Osage Beach and verified by a high-precision total station system. Here a 1.16 km optical fiber circuit was deployed onto the girders for strain measurement and thermal compensation. These experimental strain measured profiles were integrated into vertical displacements, which presented a good agreement with total station measurements [75].

Moreover, Glisic et al 2011 reported on the application on the pedestrian Streicker Bridge at the Princeton University campus where two different optical fiber techniques were applied for almost 4 years [76]. Here, discrete long-gauge fiber FBG sensors were used for the global structural monitoring while a BOTDA system was employed for integrity monitoring. Since these sensors were embedded in the concrete during construction, they were able to capture and measure important observations regarding the early age behaviour of the concrete and initial cracking.

In 2010, Villalba et al implemented a OBR system in a newly built highway viaduct in Barcelona, therefore marking the first time that a distributed sensing method with milimetric spatial resolution was used for the load test of a real, newly built concrete bridge [77].

In 2012, Minardo et al described the use of a portable prototype using the BOTDA technique during the static load test on a 44.40 m steel composite road bridge in Naples, Italy. The deployed system was

able to follow the strain distribution with a spatial resolution of 3 m and a strain resolution of ± 15με [78].

Additionally, the same group reported that same year the application of the same BOTDA system on a one year SHM campaign on the Musmeci concrete bridge in Potenza, Italy. The deployed sensor was attached along one arch of the bridge being able to measure the strain distribution along the structure with a 1 m spatial resolution [79].

Regier & Hoult 2014 deployed OBR based DOFS on the monitoring of a reinforced concrete bridge, The Black River Bridge in Ontario, Canada [80]. The obtained results were validated by other instrumentation such as strain gauges. Additionally, the DOFS acquired data was used to calculate deflections that had a good agreement with measurements collected by displacement transducers sensors.

Dams

As it happens with bridges, also dams are an appellative structural typology for DOFS instrumentation due to their large dimensions. One of the first implementations of Brillouin based DOFS on the monitoring of a dam is reported by Thévenaz et al on the Luzzone dam in the Swiss Alps [81]. Here it was possible to map the temperature distribution of the structure observing how much time it took to cool the central area of the structure that got up to temperatures of 50 ºC that would be otherwise unnoticed. An application of the BOTDA based system, DiTeSt, was reported by Inaudi & Glisic for Plavinu dam in Latvia [82].

As mentioned above, Raman based DOFS are more sensitive to temperature variation than its Brillouin counterpart and therefore, different applications of these sensors on dams have been reported: Birecik gravity dam in Turkey 1997; Shimenzhi arch bridge in Xinjiang, China 2000; Wala dam and Mujib dam in Jordan (2001) [83]. The application of these sensors to the detection of leakage in canals and dikes is also reported in [84] In all of these applications, the acquisition of detailed temperature distributions was possible due to DOFS.

Geotechnical structures

Another field that has seen a great interest in the application of DOFS is the monitoring of geotechnical structures such as slopes. Traditionally, the applied instrumentation is based on discrete sensors what makes it difficult to obtain a global behaviour of the slope. Furthermore, these sensors tend to be incompatible with the deformation of the rock-soil mass turning its application into a pointless effort.

Shi et al successfully tested the instrumentation of a BOTDR based DOFS for slopes. This technique was also studied and deployed on Nanjing Gulou tunnel [85] and Xuanwuhu lake tunnel [86] in China and Royal Mail tunnel at London, U.K [87].

Wu et al also installed BOTDR based sensors for the monitoring of the deformation of soil layers and pore water pressure in a 200 m borehole over almost two years in Suzhou (China) also deploying FBG sensors. From the results, it was possible to observe the unparalleled potential of the application of DOFS for soil subsidence monitoring as it was possible to obtain the strains developed at any depth of the soil layers.

More recently, using BOTDA sensing technology, Zhu et al built a medium sized model of soil nailed slope in laboratory that was then subjected to a surcharge loading test. It was possible to obtain horizontal strain distributions within the slope mass that can be used to define the location of the potential slip surface in the slope [88].

Klar et al evaluated the possibility of deploying both BOTDA and Rayleigh scattering based DOFS for tunnelling induced ground displacements [89]. For this, the authors concluded that, due to the sensors low rigidity, they deformed in accordance with the mentioned ground displacements. With this study, it was also concluded that DOFS technology provided interpretation of results that were only matched by multiple sub-millimetre displacement measurements.

Pipelines

Another field that has seen a significant increase of the interest in the application of the distributed sensing technology is the Oil and Gas industry. The most universally used techniques are based on Brillouin (distributed) and FBG (quasi-distributed) technologies.

An interesting large scale experiment performed on a pipeline is described by Glisic & Oberste-ufer in 2011 [46]. Here, a relative translation with an angle of approximately 50 º was induced by hydraulic jacks between two parts of a 13 m long concrete pipe with an exterior diameter of 30.48 cm and successfully measured with a distributed fiber sensor based on Stimulated Brillouin scattering.

More fruitful applications of Brillouin based DOFS to pipeline monitoring are described by Inaudi & Glisic [82] for a 35 years old gas pipeline near Rimini, Italy and by Lim et al for the deformation monitoring of a non-circular PVC pipe due to the dead weight of its carrying water [90].

Other

Beyond the already discussed applications for DOFS, these sensors can still find its purpose in other fields due to its vast versatility. One example of this is the application of an OBR sensor system for the monitoring of a concrete cooling tower in Spain, Figure 2.8, by Casas et al [91]. After the appearance of two main vertical cracks on this structure this DOFS system was instrumented to monitor

the structural behaviour before and after crack repair extending the lifetime of this structure by presenting the origin of these cracks and the appropriate repair methods.

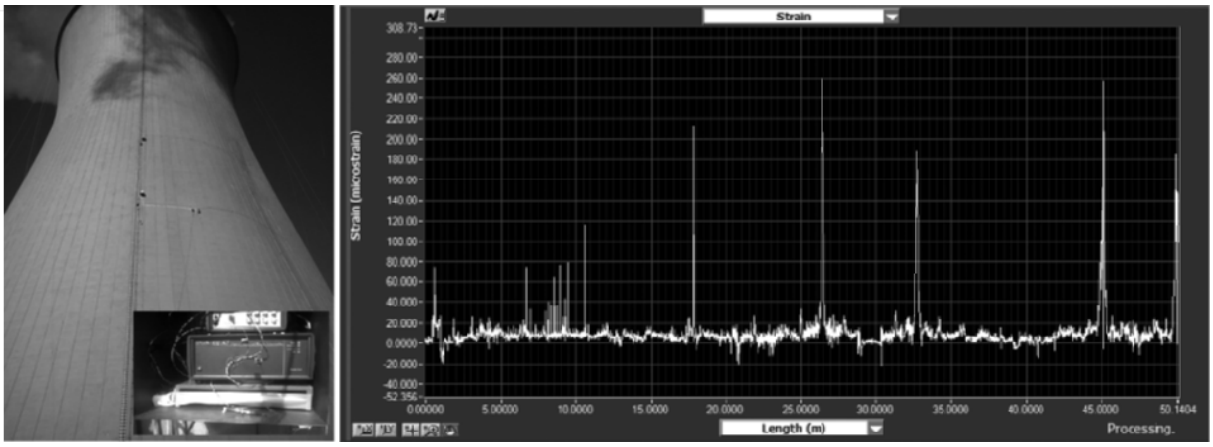

Figure 2.8: Instrumented concrete cooling tower (left); Strain-fiber length on the inside surface of the tower (right) [91]

Another interesting use of DOFS is described by Lan et al in [92] for the monitoring of loss of prestress in concrete beams. For this, they proposed a novel smart strand that combined BOTDA and FBG sensors on a single optical fiber embedding it into a 5 mm diameter fiber-reinforced polymer (FRP) rebar. Different prestressed RC beams were tested with this strand which results were compared with more conventional sensors. The viability of this system was confirmed by showing not only the spatial distribution of prestress loss but also its time history for both construction and in-service phase.

Additionally, historical structures were also subjected to monitoring through the use of this novel technology. Bastianini et al describes in [93] the application of Brillouin based DOFS as a cheap and effective complement monitoring technique on Palazzo Elmi-Pandolfi in Foligno (Italy) that was subjected to retrofitting techniques.

2.7. Lessons learnt and observed needs

In this chapter, a general overview of the state of the art of optical fiber sensing and more specifically its distributed category was described. The content of this chapter is fully developed on the published journal article I, which is presented in Chapter 4 of this thesis. Therefore, parts of the content in this chapter were briefly presented and referred to the mentioned article for a further detailed explanation while presenting other subjects that are not included the mentioned article.

Raman scattering is greatly dependent on the temperature variation and Brillouin scattering based DOFS, such as BOTDR and BOTDA, are able to perform strain and temperature measurements over great lengths reaching several kilometres range. Although this makes these type of scattering DOFS very appealing for the monitoring of large scale structures, their relatively reduced spatial resolution turns these systems not appropriate for several applications such as the case of damage detection and localization. Recent advances have improved said spatial resolution, especially in the case of BOTDA

technique through the use of complex computational algorithms which enable an enhanced performance in damage detection. Notwithstanding, these type of scattering based sensors still present important limitations for this type of monitoring applications.

It is in this context, that Rayleigh based optical frequency domain reflectometry (OFDR) DOFS have been recently developed and considered as a promising DOFS monitoring technique. The systems based in this technique as the OBR system, provide the unique advantage and capability of a remarkably high spatial resolution of 1 mm. These systems techniques are currently limited to a sensing range of 70 m, which already allows for the application of these sensors in a wide variety of structures. Nevertheless, recent developments have been reported to enhance this technique to kilometre range [94]. Moreover, it is believed that with further research and development of Rayleigh scattering technique, the capabilities of Rayleigh based DOFS are going to be greatly enhanced.

In this chapter is also seen that while currently, DOFS systems are relatively more expensive than other monitoring sensors, in practical terms they offer easier and simpler installations and operational processes. Moreover, the operation of these systems can be performed extensively for a multiple number of times and simultaneous diverse applications which decreases the high initial cost of the system. Compared with other technologies, DOFS systems are also very recent. However, with the matureness of this technology, the demand for these systems will greatly increase and with it, diminish its production costs turning these sensors more and more accessible. This is also seen by the forecast, which expects a great increase of DOFS share in the civil engineering market, in its total value and number of applications in the next years.

It is seen the technical viability of DOFS deployment both in laboratory as in the monitoring of real world and in service structures.

Despite observing that different large-scale structures can be globally monitored with Brillouin scattering techniques, as mentioned above, the use of such sensors presents the important limitation of reduced damage detection and localization capabilities. This is not the case for OBR system (Rayleigh OFDR based DOFS) applications as showing great promise in monitoring applications for damage detection, localization and quantification.

Being one of the major concerns related with the use of this technology the strain transfer effectiveness between sensor and substrate material, further research on this topic is necessary.

Moreover, an important challenge is presented in the case of concrete structures due to the roughness of the concrete surface and the heterogeneity of aggregates of several sizes. Cleaning of the grease and additional unwanted particles in the areas were DOFS are intended to be bonded, jointly with a pre-treatment to smooth the surface (brushing) is vital to achieve a good bond between the sensor and the instrumented structure. Additionally, the study and identification of the optimal bonding

adhesive and alternative installation methods for these applications becomes essential for a more widespread use of this technology in current and future concrete structures.

Finally, an important lack of applications is observed regarding the long-term performance of these type of sensors in relation to fatigue loading, especially when dealing with the OBR system. Therefore, this is a point that was addressed and researched in the present thesis.

Chapter 3 – Experimental tests: Results and Discussion

In this chapter, the description of the conducted experimental campaigns within this thesis are presented followed by the general discussion of their results. Therefore, they are displayed both the performed experiments in the laboratory environment and in real world case scenarios. These actions are designed and conducted after the literature review presented in the previous chapter and the assessment of its main takeaways. The contents of this chapter is a summary of the main results obtained, which are fully explored and detailed in the presented articles of Chapter 4 and the Annex of this thesis.

3.1. Introduction

In this chapter, the laboratory experiments planned as a result of the initial literature review are described and discussed. Furthermore, the application of DOFS in two real world structures in the city of Barcelona is outlined. These experiments and results are presented in two of the published journal articles included in Chapter 4 and the two submitted articles included in the annex of the present thesis.

In this way, for sake of redundancy, in this section, the global and general overview of the experiments is presented referring to the corresponding journal articles whenever necessary, while disclosing the obtained results and its main takeaways.

Additionally, as referred in Chapter 1 and 2 of this thesis, this research is focused on the capabilities of Rayleigh OFDR based DOFS (or OBR system). With this in mind, in all the experiments and applications conducted and presented in the following sections, the particular system used to interrogate distributed optical fiber sensor cables was the commercial optical interrogator ODiSI A50 from Luna Innovations Incorporated, Figure 3.1.

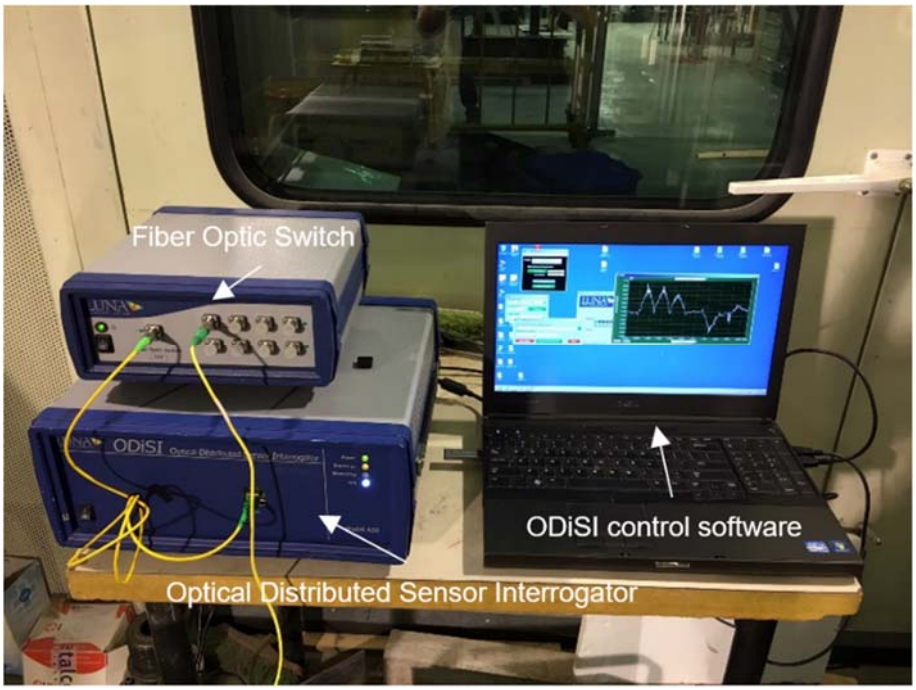

Figure 3.1. Used system for interrogation of DOFS in this research

As observed in Table 3.1, this system has a single scan repeatability of ±2 με, ±0.2 °C and measurement range of ±13,000 με and −50 to 300 °C. Furthermore, this system enables a maximum sensing length of 50 m and user-controlled minimum gauge length and sensor spacing of 1 mm and 0.4 mm respectively [95].

Moreover, in this research, this system is used together with polyimide coated low bend loss fibers which are characterized by having a minimum bend radius of 10 mm and a total sensor diameter of 155 μm, divided by 5 μm for core diameter, 120 μm for the cladding and 15 μm for the coating [96]. Therefore, this is a very thin sensor cable being similar in dimension to a human hair strand, Figure 3.2.

Table 3.1. Properties of used interrogator in this research

Parameter	Specification	Units
Maximum Sensing Length	50	meters
Acquisition rate	2.5	Hz
Minimum Sensor Spacing	0.4	mm
Minimum Gauge Length	1	mm
Wavelength Accuracy	1.5	pm
Strain:		
Range	± 13000	με
Single-scan repeatability	± 2	με
Temperature:		
Range	-50 to 300	℃
Single-scan repeatability	± 0.2	℃

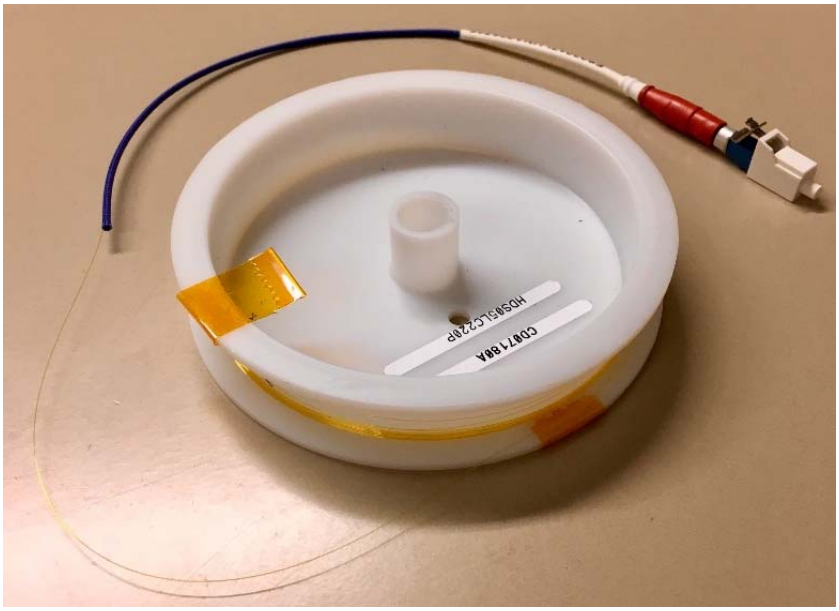

Figure 3.2. DOFS used in this research

3.2. Laboratory tests

After the literature review on the use of DOFS in civil engineering applications, especially of reinforced concrete material, different challenges and uncertainties regarding its application were concluded. In this way, different tasks in form of laboratorial experiments were devised.

3.2.1. First Experimental Campaign

One of this first observed key challenges on the use of DOFS in reinforced concrete structures is related with the compromise between the required accuracy and mechanical protection of the sensor [97].

A relatively thicker coating of the optical fiber sensor generally implies a more robust protection of the sensor to possible external environmental agents while also easing the handling and manipulation of the fiber at the time of installation. However, it also results in a less effective strain-transfer between the material and sensor, clouding and affecting the real strain measurement. The opposite tends to occur when using fibers with thinner or even inexistent coating enhancing the probability of rupturing the fiber when handling it but increasing considerably at the same time the effective strain-transfer between sensor and monitored material.

A few authors have analysed the influence of the coating on the strain transfer between the sensor and the host material for both discrete [28,29] and distributed [100] OFS , through the assessment of the apparent and actual strain profile difference. Depending on the surface material where the sensor is deployed, an optimal bonding can be more difficult to achieve. This is specially the case of applications on reinforced concrete structures. As a consequence of the heterogeneity of this material, due to the aggregates of different sizes and type, which translates to a rough and uneven surface, in order to achieve a desirable bond, a smoothing and cleaning of the original surface is required [31,32].

As observed during the literature review, in order to overcome this challenge, past studies suggested the bonding of the DOFS directly to the rebars of the reinforced concrete element instead of its outside surface [70]. As the fiber is embedded in the element a better protection to the external environmental conditions is provided without the need of a particular thick coating. Nevertheless, the authors in this particular reference mechanized the rebar previously to the deployment of the DOFS, which increases the time of installation and subsequent costs while also having effects in the accuracy of the measurements. Additionally, a relative thick coating was used, not taking advantage in this way of this new improved condition for the fiber durability.

Other research groups, while also using this type of Rayleigh backscattering based DOFS deployed several sensors embedded in the concrete and attached to the rebar in order to detect pitting corrosion and also its impact on the bond performance in reinforced concrete elements [71] [72] [101].

In this way, in this thesis, it was decided to perform an experimental test where the main goal is to further assess the performance and feasibility of deploying a relatively thin polyimide coated low bend loss fiber in the rebar of RC members without previous mechanization. Furthermore, in this case the main goal is not linked to the detection of corrosion induced damage but instead to study the performance of the DOFS when the sensor is crossing a crack that is opening and closing, as this creates a perilous situation for the fiber due to the roughness in the crack lips.

This task is described and discussed in detail in the published journal article II presented in Chapter 4 of the present thesis.

3.2.1.1. *Tensile test on single rebar*

Initially, it was decided to attach the DOFS fiber to a single rebar in order to confirm the feasibility of implementing this thin type of fiber directly to a rebar without its mechanization. Therefore, a tensile test is devised where the polyimide fiber is attached for 75 cm to the longitudinal lateral rib of a single Φ12 (12 mm of diameter) S500 standard rugged steel rebar while using a two-component epoxy as adhesive. The use of this adhesive is based on the previous practiced experience conducted by the research group where this project was included [67], [68].

At the same time, three current electrical strain gauges are deployed equally spaced on the other lateral rib side of the bar (so it wouldn't interfere with the DOFS measurements) for comparison purposes. Afterwards, two load stages of tensile force of 11.3 kN and 22.6 kN are applied to this rebar within the elastic range of the steel, producing 100 and 200 MPa respectively, below the yielding stress level of this material.

With this test, as it is further discussed in Chapter 4, it is observed that it is possible to correctly measure the developed strain along the adhered part of the DOFS to the rebar. The two inputted stress levels are measured by the DOFS and compared accordingly in the point locations where the strain gauges were deployed.

In this way, once the correct performance of these sensors when implemented to the rebar is achieved, the next step is to assess its performance when embedded into concrete, both before and after cracking and also for loading and unloading conditions.

3.2.1.2. *Load test on Reinforced Concrete beams*

Following the previous test, two reinforced concrete beam specimens with a cross-section of 100 mm width and 180 mm height and with a total length of 800 mm are produced. Each of these specimens has only one Φ12 S500 reinforcing bar at the center of the cross-section with a concrete cover of 40 mm. Additionally, a 5.2 m length DOFS is implemented in each specimen initially at its rebar and then, after the hardening of the concrete, to their external outside surface. As in the previous tensile test on the rebar, three strain gauges are deployed uniformly in the rebar for comparison purposes.

These bonded segments are in this way positioned in order to measure simultaneously the strain at the rebar and multiple locations of the concrete surface (for both compression and tension), all of this while using one single sensor. The defined spatial resolution is of 1 cm, therefore measuring 520 different points in each beam, while the sampling acquisition frequency is of 0.2 Hz.

The main difference between the two RC beams is the bonding adhesive used for the instrumentation of the DOFS to the rebar, cyanoacrylate in Beam 1 and two-component epoxy in Beam 2. The expected

cracking load is of 8.86 kN for Beam 1 and 10.15 kN for Beam2. The main goal of these load tests is to load each beam beyond its cracking load and unload again to assess the sensor performance after damage occurrence and further reloading. The setup of these load tests is depicted in Figure 3.3.

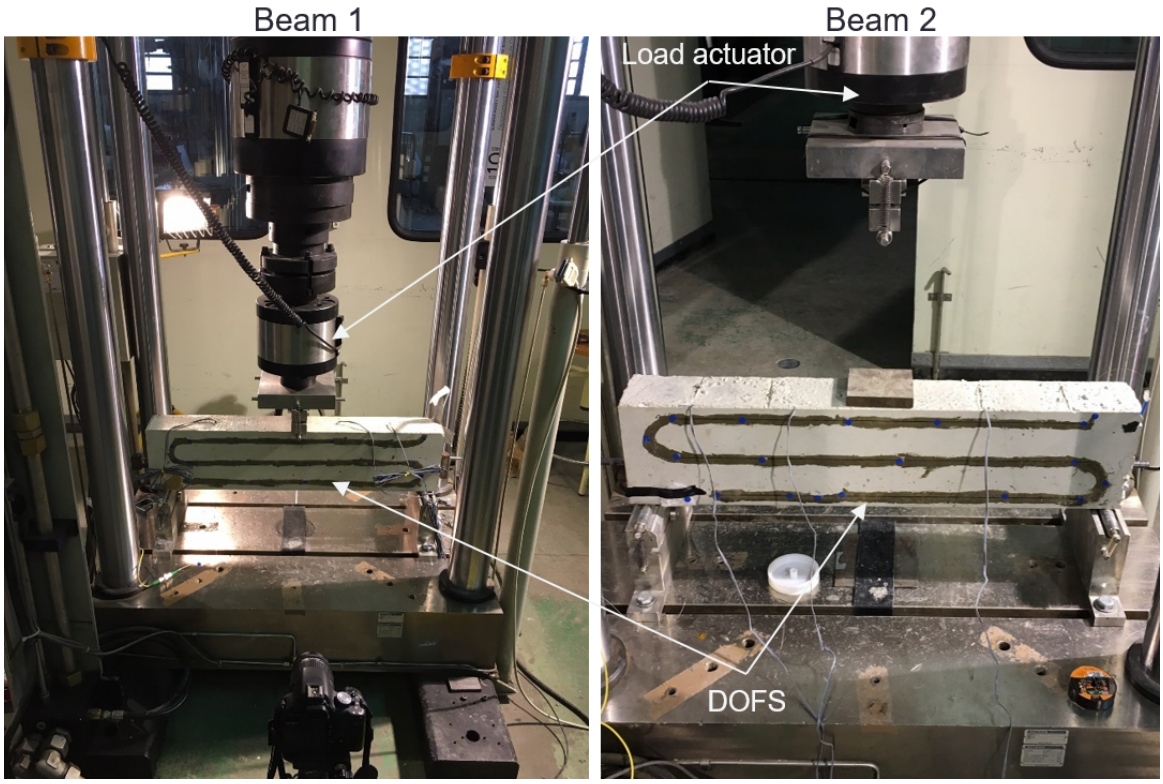

Figure 3.3. Load test setup for Beam 1 (left) and Beam 2 (right)

The DOFS performed very satisfactorily in all segments until the occurrence of cracking by comparison with the strain gauges. In Beam 1, DOFS detect and localize the crack formation for a load of 7.5 kN while it is not visually observable. The same is noticed in Beam 2, where the expected tensile strength is surpassed for a load of 9.2 kN although this crack is not yet detected visually.

When comparing the DOFS segment attached to the rebar (FI) in each specimen, besides the good agreement with the strain gauges it is recognized a better performance of the measurements in Beam 1 (cyanoacrylate bonded) when compared to Beam 2 (epoxy bonded) especially for its initial unloaded stage reading. Moreover, for load levels where cracking had already occurred as detected by the segments bonded externally to the concrete surface, damage is not noticed at the rebar level.

Notwithstanding, in both beams, sometime after the occurrence of damage, at the crack location, the DOFS measurements start showcasing very large and alternative positive and negative peaks. This is observed for Beam 1 until the rupture of the fiber for a load level of 24.3 kN during its second load stage, whereas in Beam 2 this behaviour is noticed for a load level of 17.8 kN, of its first load stage, where, although not broken, the measurements from this fiber are deemed unreliable.

As a consequence, it is necessary to overcome this challenge presented by the inaccurate measurements after cracking at its location and better analyse the obtained data at this stage. In this way, it is proposed to

perform a post-processing routine, where the inaccurate measurements are removed being identified by their inherent spectral shift quality (SSQ) [26], followed by the surface interpolation of the remaining accurate values.

In a simple way, the SSQ is an indicator of the cross-correlation between the baseline measurement and measurement spectra normalized by the maximum expected value, being theoretically between 0 and 1, where 1 corresponds to perfect correlation. The manufacturer suggests the consideration of any measurements with a SSQ below 0.15 unreliable or inaccurate, since when this threshold is reached, it is likely that the strain or temperature change has exceeded the measurable range.

By plotting simultaneously, the measured strain by the DOFS and its associated SSQ values for Beam 1 and Beam 2 during these load tests, it is seen how the locations with a SSQ value below 0.15 and the strain measurements with incomprehensible peaks are highly correlated, Figure 3.4 and Figure 3.5.

This observation of SSQ values dropping during flexural load tests is also reported by other authors [102]. In this case, the authors addressed the situation by considering a SSQ threshold of 0.17 while using nylon-coated fibers adhered on the surface of the concrete due to the proximity of inaccurate values. Additionally, the low SSQ values are found to be close to the crack location in the segments adhered to the surface of the concrete and within a wider area in the rebar segment. This is due to the fact that segments with large strain gradients increase the noise levels of the DOFS measurements [103].

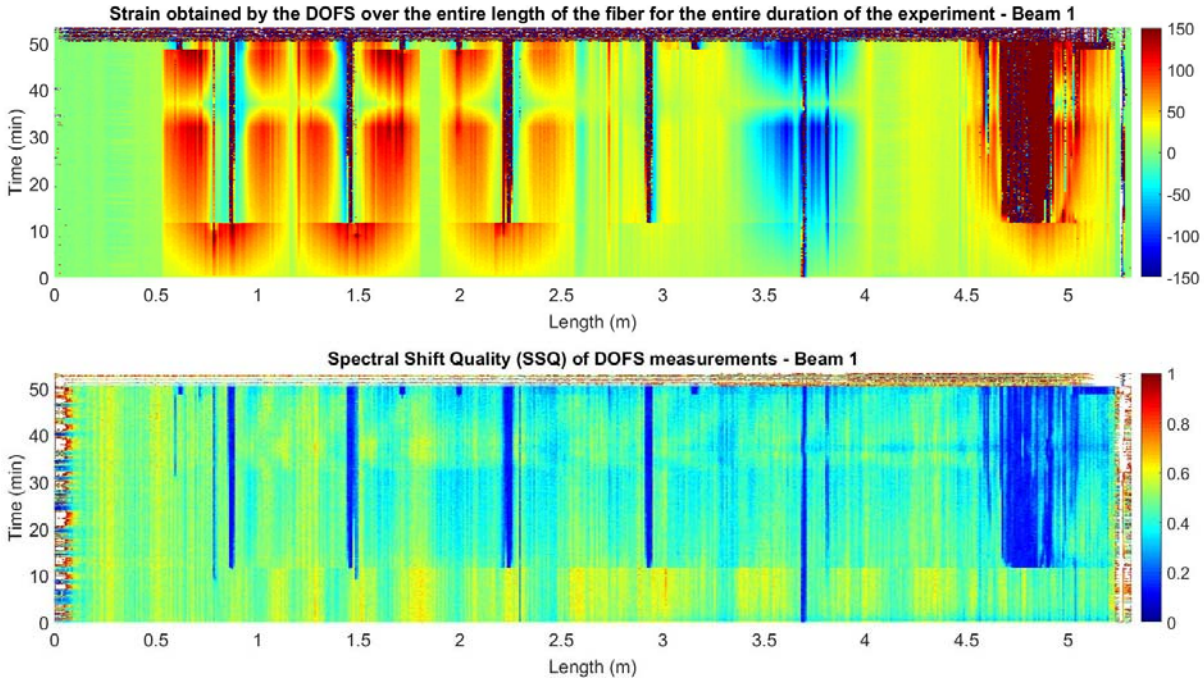

Figure 3.4. Measured strain and SSQ for Beam 1

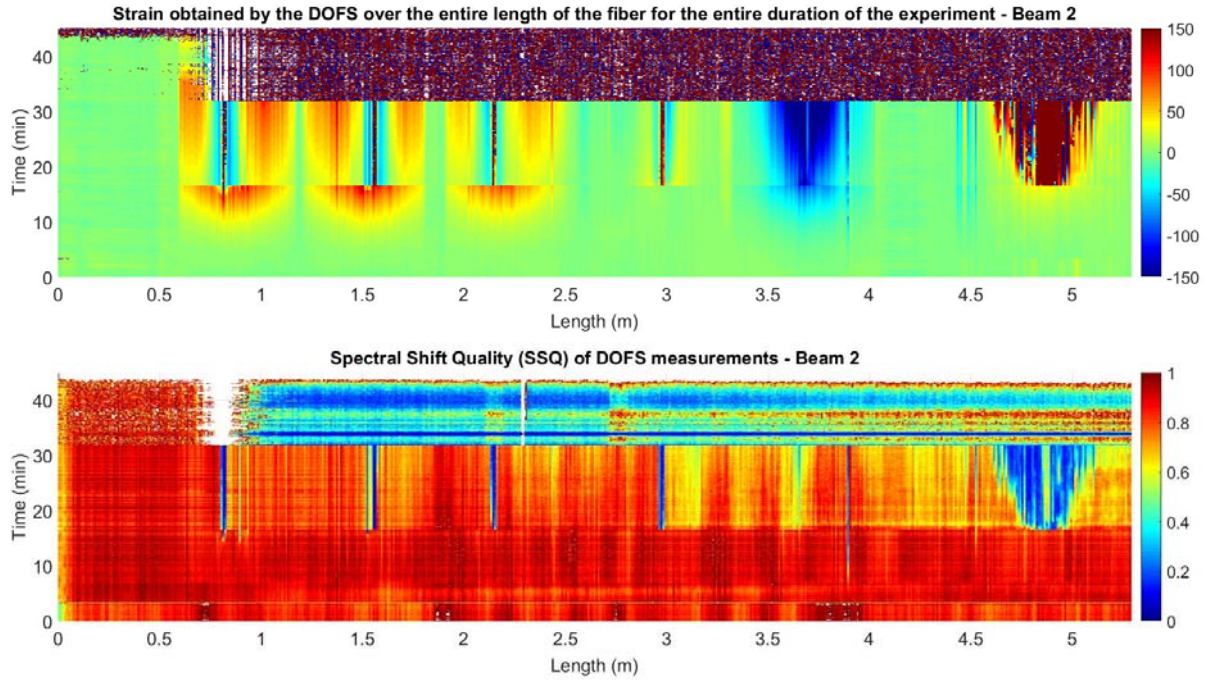

Figure 3.5. Measured strain and SSQ for Beam 2

In the present case, it is observed that considering the recommended threshold of 0.15 as a minimum for the SSQ values, several isolated peaks still prevailed due to the proximity to the values with low SSQ. As a result, it is concluded that for the particular case of the use of a polyimide-coated fiber embedded in the concrete and attached to the rebar, the consideration of a threshold of 0.20 optimally eliminated the aforementioned peaks. Afterwards, a surface interpolation is conducted replacing these eliminated inaccurate values so a better analysis of the behaviour of the beams after cracking is viable.

Despite conducting the same post-processing routine for each beam DOFS data, it is observed that for Beam 2 still some peaks are present. This is thought to be related to the better performance of the cyanoacrylate adhesive when bonded to steel when compared with the use of the epoxy one. Notwithstanding, both beams' data sets, after the replacement of their identified inaccurate values, present a reasonable strain evolution which is compatible with the applied load. This is more noticeable for Beam 1 since, in this case, the sensor performed properly until a later stage of the loading process, further validating the conclusion of the cyanoacrylate as a better bonding adhesive for the implementation of polyimide-coated fibers attached to steel rebars.

After this process, and when comparing the strain values after cracking with what was measured by the strain gauges and with what was visually observed directly on the beam specimens for the corresponding load level a general good agreement is observed for both beams. This is depicted in Figure 3.6 and Figure 3.7.

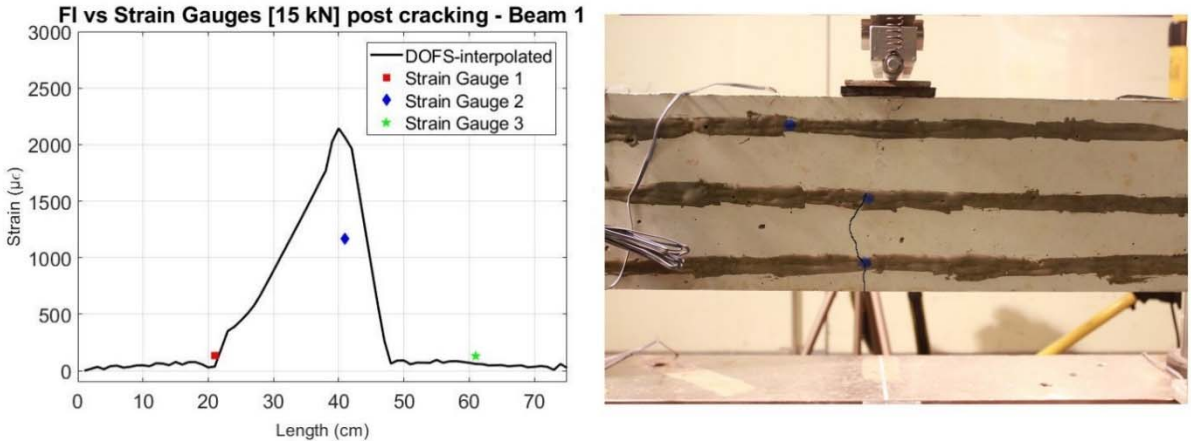

Figure 3.6. Comparison of interpolated values of DOFS with strain gauges at a load level of 15 kN (left) and photo of tested specimen with highlighted crack (right) – Beam 1

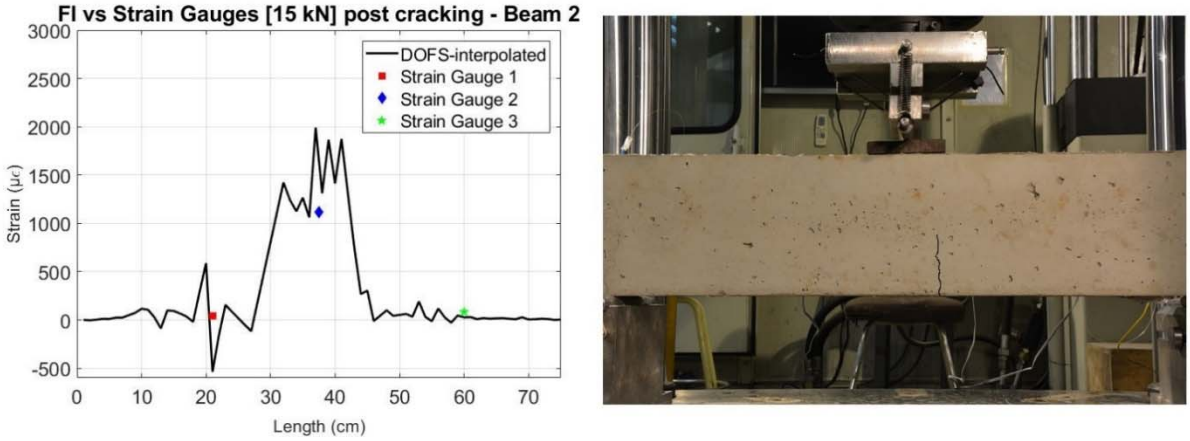

Figure 3.7. Comparison of interpolated values of DOFS with strain gauges at a load level of 15 kN (left) and photo of tested specimen with highlighted crack (right) – Beam 2

Therefore, it is seen thanks to this laboratory test campaign, that despite the drop of the SSQ values of some points of the DOFS after the occurrence of cracking which implied unreliable measurements, due to the distributed capacity of this type of sensor, valuable information was still collected during the cracking stage of the beams using just one single sensor, whereas in other situations multiple discrete sensors would be required.

It is also concluded that the consideration of a minimum SSQ value of 0.20 is necessary in order to obtain reliable information when deploying these polyimide-coated DOFS when adhered into rebars embedded in RC elements. It is also believed that the drop of the SSQ and subsequent appearance of large magnitude peaks, is associated with the sudden and sharp change of stiffness on the beam specimen when the damage reaches the rebar element after the initiation of cracking at the concrete surface.

Finally, it is seen how the cyanoacrylate adhesive bonded segment in the rebar of Beam 1 performed relatively better when compared with the epoxy bonded one in Beam 2. It did not only present smoother readings within the uncracked range as it also worked properly longer until later stages of the applied loading sequence.

In this way, going into this experiment with the intention of analysing the feasibility of deploying a thin coated fiber directly in the rebar element embedded in a RC member without previous mechanization, it is concluded that good results are obtained within the undamaged stage of the specimen and that it can effectively detect and locate the damage formation once it is produced. For the following stage, a post-processing technique is proposed in order to eliminate the identified inaccurate peak values which are originated after damage formation.

This experimental campaign shows, in this way, the feasibility of deploying a single polyimide coated Rayleigh OFDR based DOFS, simultaneously to the rebar and external surface of a reinforced concrete element.

3.2.2. Second Experimental Campaign

In the second experimental campaign, the topic of the influence of different spatial resolution and bonding adhesives are addressed as defined by the initial objectives as described in Chapter 1. This is presented and discussed in detail in the submitted journal article IV which is later outlined in the Annex of the present document.

As mentioned before, in order to obtain the optimal strain transfer between the sensor and the monitored material the topic of its deployment is of considerable importance. In addition to the removal of any grease or dust present in the surface of the host material and the smoothening of the surface, the decision on the adhesive to bond the optical fiber sensor to the surface has to be assessed. This is even, a more pressing issue when applying DOFS without any protective thick coating, such is the case of the deployed fiber in this research.

During the conduction of the literature review, some previous studies were assessed, where the coating influence on the strain transfer on point fiber optic sensors [98], the adhesive spread installation method [99] and the coating strain transfer impact in DOFS [100] are presented. Here, among these studies, it is observed a better performance of the polyimide fiber together with the cyanoacrylate adhesive when bonded to the reinforcement and the combination of nylon fiber with epoxy adhesive when bonded to the concrete.

Moreover, as mentioned in the previous section for the first experimental campaign, all the preceding experience of UPC's structural laboratory research group when deploying DOFS in concrete structures was solely by the use of a commercial epoxy adhesive. Therefore, in this experiment, it is decided to perform a DOFS bonding adhesives performance analysis while expanding the number of compared adhesives.

Additionally, the influence of different spatial resolution inputs in the used DOFS system is assessed. An increased detail provided by an enhanced spatial resolution would be of interest specially for the case of sub-mm crack detection. This is a characteristic unique to Rayleigh backscattering based DOFS as the one used in this research which announces a possible spatial resolution down to 1 mm.

As a consequence, a laboratory experiment is devised where a single 5.2 m polyimide DOFS is attached to the surface of a reinforced concrete beam using four different adhesives: epoxy, cyanoacrylate, polyester and neutral cure silicone and to be tested under a three-point configuration load test.

These adhesives are chosen based on the previous experience of the research group and through what was found during a literature review on this topic. Specifically the three first adhesives: epoxy, cyanoacrylate and polyester are used as advised by the TML strain gauges 2017 catalogue for concrete applications [104]. The used neutral cure silicone however, was a simple commercial one from Ceys brand for general construction applications including concrete.

In previous studies, silicone had only been used as an additional layer of protection of the sensor. Thus, silicone is deployed as a true adhesive in this study for the first time. In this sense, it is important to use a neutral cure silicone in order to not harm the polyimide fiber as it may occur when using an acetoxy cure one.

Furthermore, when deciding the optimal bonding adhesive for sensor implementation in real world scenarios, it is important to have in mind the viscosity and time of curing of each adhesive. In practical cases, most often than not, the surface where sensors are going to be deployed are not horizontal or facing up. For this reason, some adhesives can produce considerable dripping through the action of gravity which weakens the bond. Each of the adhesives selected for this experiment, provides different times of curing and viscosity options that have to be considered carefully depending on each intended application.

The tested reinforced concrete specimen is characterized by having 600 mm longitudinal length with a square cross-section of 150 by 150 mm and reinforced with two longitudinal ϕ12 and four transversal ϕ6 S500 rebars.

The DOFS is bonded to the concrete performing a pattern with four equal segments (each one bonded with aforementioned selected adhesives) on the bottom surface of this beam with the intention of inducing the same strain levels at any moment, allowing the direct comparison between them. For comparison reasons, three 30 mm length strain gauges are also bonded to the bottom surface of the beam, equally spaced between them and parallel to DOFS segments as depicted in Figure 3.8 and Figure 3.9.

As in the previous laboratory campaign, the mechanical properties of the concrete were calculated being that the obtained expected strain tensile capacity was of 104.10 $\mu\varepsilon$ corresponding to an inputted load of around 18 kN. As a result, in order to perform the aforementioned analysis of the influence of different spatial resolutions, it was decided to conduct three separate but identical load cycles with different spatial resolution with a maximum applied load of 11 kN and therefore without inducing cracking. A fourth and final load cycle is then applied inducing cracking and continued until the rupture of either the fiber or beam specimen.

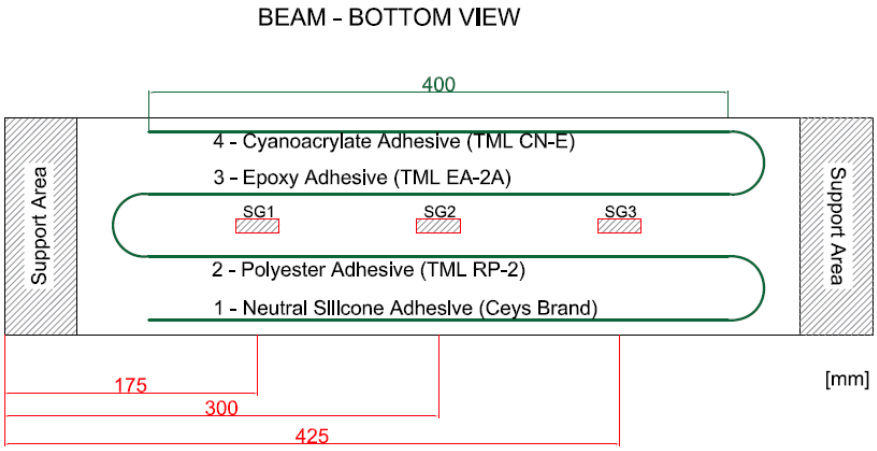

Figure 3.8. Plan of the reinforced concrete beam and its instrumented sensors (DOFS and strain gauges)

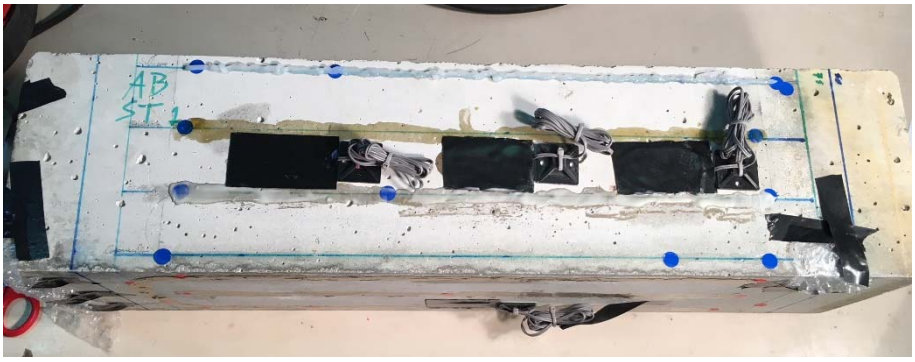

Figure 3.9. Photograph of the bottom surface of the tested beam and its instrumented sensors (DOFS and strain gauges)

3.2.2.1. *Comparison of the spatial resolution input*

Three spatial resolutions of the DOFS measurements are inputted in the first three load cycles: 1 cm, 3 cm and 1 mm, thus representing 520, 174 and 5191 measuring points respectively. The decision of also using a 3 cm spatial resolution is to facilitate the comparison with the strain gauges which were 3 cm long and correspond to the shortest commercially advised strain gauges for concrete applications.

When plotting the measured strain for a specific load level using the three mentioned spatial resolutions (as depicted in the Annex of this thesis) it is observed how the data collected with a 1 mm spatial resolution presents a significantly higher spatial variability when compared with the other two. This is a result of the implicit heterogeneity of the concrete with its different sized aggregates. A significantly smaller but still noticeable variability is also verified for the 1 cm collected data which nevertheless, present a good agreement with the strain gauges' data and the 3 cm spatial resolution measurements.

In this way, it was decided to verify if even using an initially inputted finer spatial resolution (of for example 1 mm and 1 cm), it would be possible to obtain similar results as using a sparser resolution (as to say 3 cm). By conducting a moving average to the originally measured data collected with the 1 mm and 1 cm spatial resolution using a window of 30 and 3 units respectively, it is seen how although significantly

improved the averaged 1 mm data still presents relatively erratic spatial resolution. On the other hand, the averaged 1 cm data fits almost perfectly the one obtained using a 3 cm resolution.

Therefore, it is concluded that no real advantages are accomplished by using a sub-cm spatial resolution. Moreover, the use of 1 cm resolution has showed the capacity of detecting and effectively locating crack formations in previous experiences and being able to measure strain with significantly less spatial variability while allowing to present similar results as a sparser resolution when necessary, being in this way decided to suggest the use of this spatial resolution when using this type of experimental setup.

3.2.2.2. *Comparison of bonding adhesives under elastic behavior*

When assessing the performance of the different used bonding adhesives while not inducing cracking, it is verified that all bonded segments are able to follow correctly the applied load and present a good agreement with the data from the strain gauges.

In fact, at the beam mid-span, where higher strain levels are produced, the higher difference between DOFS bonded segments and the strain gauge at that location is 5.54 με while all others are close or below 2 με which corresponds to the possible strain resolution provided by the used DOFS interrogator system. Moreover, the average difference of the different DOFS segments with the strain gauges' measurements is around 13 % which is in accordance with other tests where a similar DOFS was compared with foil strain gauges at different locations of a wind turbine blade [105].

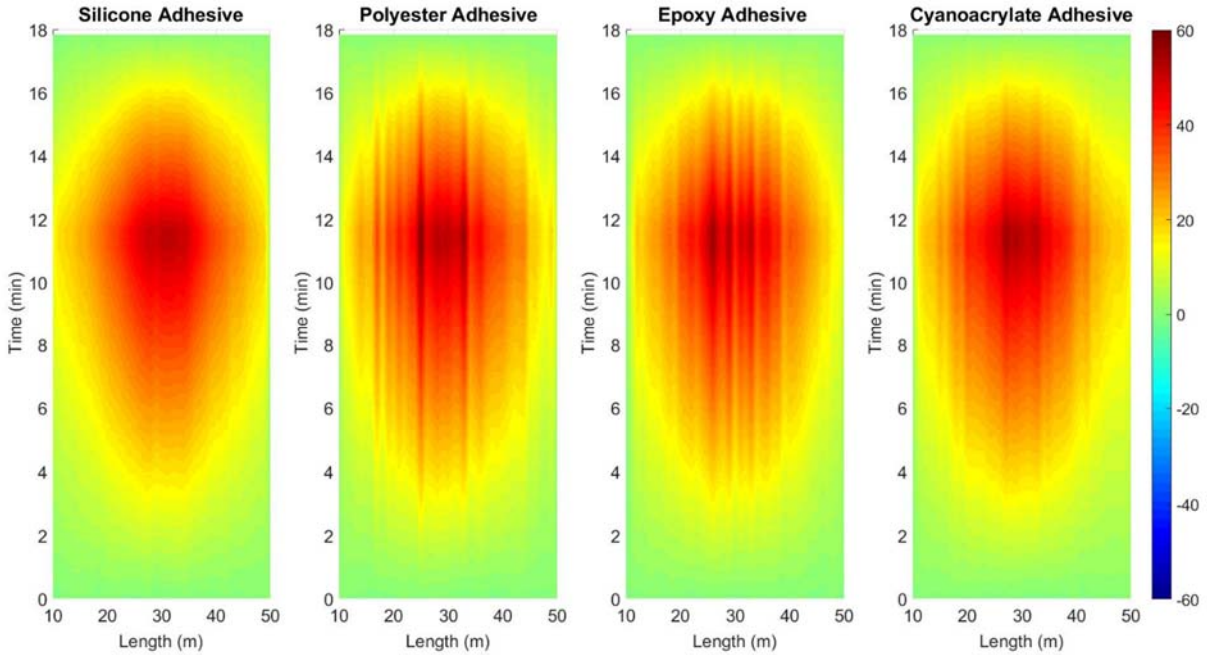

Figure 3.10. Measured strain by the four different bonded segments under elastic range

Additionally, when assessing the measured strain spatial variability achieved by each bonded segment throughout the applied load sequence, is observed how the silicone bonded segment presents smoother and more homogenous readings as seen in Figure 3.10. Although, also corresponding well with the information

measured by the strain gauges at their location, the other used adhesives exhibit a relatively higher spatial variability especially at the point corresponding to the maximum strain value.

3.2.2.3. *Comparison of bonding adhesives when inducing cracking*

Going into the sequence where cracking is reached, here the load is applied initially up to 20 kN, then unloaded and finally loaded again until rupture. In this stage, it is verified that all four different bonded segments are able to effectively detect and locate the crack formation although with different performances. Whereas the polyester, epoxy and cyanoacrylate bonded segments present strain peaks with narrow bases at the location of the crack (around 2 cm), the silicone bonded segment while also presenting a strain peak at the crack location, it has a wider base (around 20 cm). This issue, turns the detection of further cracks formations in this area impractical.

On the other hand, when continuing to assess the performance of each segment after the crack initiation, it is seen, how apart from the silicone bonded segment, all other adhesives present alternating positive and negative strain peaks at the crack locations, where only positive increasing strains corresponding to applied tension should be observed.

Therefore, as in the previous experimental campaign, it is necessary here to consider the SSQ values to each measured strain at any given point and time and assess if they comply with the minimum suggested threshold of 0.15. By doing this, as shown in Figure 3.11, it is seen how all bonded segments present an abrupt and acute change both for their strain measurements as for the corresponding SSQ values. This occurs for a load level of 24.65 kN, slightly after the detection of cracking by the silicone and cyanoacrylate segments.

During this analysis, it is also possible to observe that the low SSQ values which are developed shortly after cracking, are restricted to the narrow segment which corresponds to the crack location for the epoxy, polyester and cyanoacrylate segments. Yet again, the silicone segment presents a wider area with low SSQ values but with strain values that seem to be coherent with what is the expected behaviour in the beam after the crack formation.

In the same way, as it was done in the previous experimental campaign, in an attempt to better assess the DOFS measurements performance after the occurrence of cracking, a post-processing is performed where the DOFS data points with a corresponding SSQ value below 0.15 are removed.

Additionally, since negative values are still remaining after this action, which is not coherent to the expected tension being developed in the bottom surface of the concrete beam, these values are also removed. At the end, a surface interpolation is performed replacing, in this way, the removed and inaccurate data points.

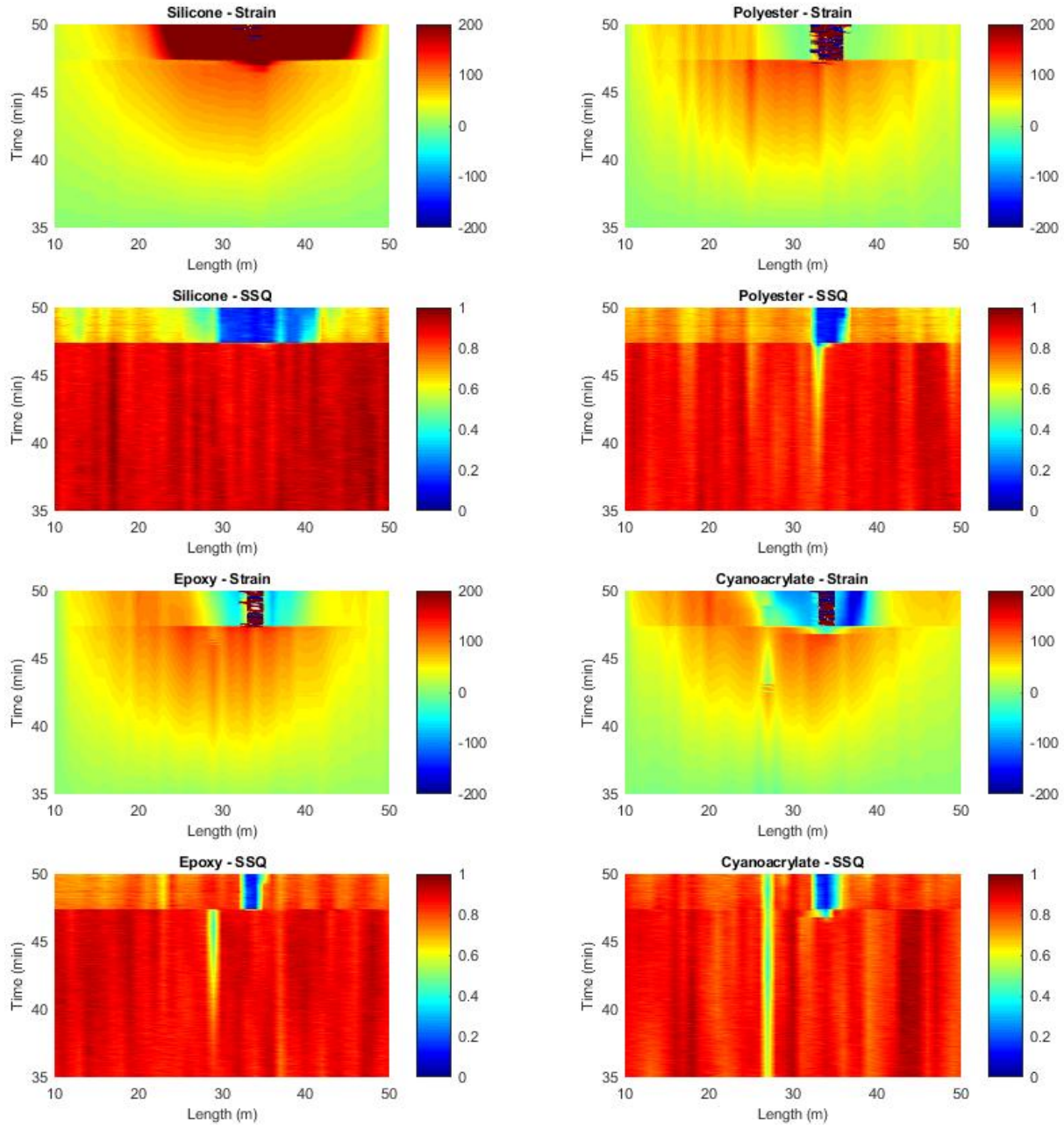

Figure 3.11. Measured strain and corresponding SSQ values for each bonded segment between minute 35 and 50

In this operation, the silicone bonded segment presents the fewer identified inaccurate data points, leading therefore to fewer removed data from the original measurements. Nevertheless, still presenting a significantly wide are of influence for the developed crack, corresponding to almost 2/3 of the total length of the bonded segment. For the other segments, relatively more data is replaced, especially due to the removing of negative strain measurements.

In summary, with this experiment it is observed that the consideration of a spatial resolution of 1 mm doesn't provide real advantages when compared with the use of a 1 cm spatial resolution. Furthermore, during the elastic range of the load test, all bonded segments present a satisfactory agreement with the data

collected by the strain gauges, while the silicone bonded segment depicts a more uniform and smoother performance.

In the stage after cracking, it is observed how all bonded segments are able to detect and locate the crack formation although with different performances. This is followed by a sharp decrease in the associated SSQ values at the location of the crack which is translated to high magnitude peaks. These peaks have a narrow influence length and alternating positive and negative values for the polyester, epoxy and cyanoacrylate segments. The silicone bonded segment doesn't seem to present this high magnitude peaks until very late stages of the test, but has a wider length influence due to the crack formation while always displaying positive strain measurements which is coherent with the load being applied to the specimen.

As a conclusion, it is seen how the neutral cure silicone can be a good option as a bonding adhesive for situations where the quantification of crack damage is not relevant or even where cracking is not foreseen as in prestressed concrete elements. Regarding the other adhesives, it is concluded that they can also be considered for the same situations as suggested for the silicone adhesive, although with a higher spatial variability and more susceptible to the different sized aggregates in the concrete material. In this experiment, these adhesives present the aforementioned high peaks while also displaying negative strain measurements. In previous works, it was described how when using the same setup with an epoxy bonding adhesive the quantification of crack width was obtained without displaying the same problems seen in this case for bigger structural members [68]. It is therefore necessary to further analyse this issue in the future and see the origin of these peaks and subsequent SSQ values decrease after cracking.

3.2.3. Third experimental campaign

This experiment described here is not truly a completely independent campaign from the one detailed in the previous section as it was conducted in the same time period and using a very similar setup. Nonetheless, as the main goals of this experiment diverged from the previous one, it is presented separately here in the same way as conducted in the submitted journal article V which is detailed in this thesis in the Annex section.

In this case, the main objective behind this laboratory experiment is to assess the accuracy and reliability of DOFS measurements over time when monitoring structures over a long-term period. As seen during the conduction of the literature review, very few publications can be found regarding the performance of Rayleigh based OFDR DOFS under fatigue loading.

An engineering note from LUNA Innovations Incorporated [106], described an experiment where a polyimide coated DOFS was instrumented in fiberglass coupons cyclic loads during 1000 cycles showing a superior performance of the DOFS when compared with resistive gauges. Another publication from the same research group reported on the application of similar low-bend-loss fibers embedded in four layers of a carbon fiber spar cap and surface of a 9 m CX-100 wind turbine blade [105]. Here the DOFS were able

to detect accumulated damage in the blade under fatigue loading until failure, while also having a good agreement with also instrumented electric foil gauges. Finally, more recently, the application of an identical DOFS setup was described for the monitoring of the fatigue in a flush step lap joint composite structure, being able to also follow the fatigue damage propagation until failure [107].

As observed, all of these previous conducted studies are focused on other engineering fields and most importantly are applied to composite elements, where the surface characteristics of the material highly affect the fatigue response when compared with concrete elements. Therefore, as established in the objectives of this thesis and described in Chapter 1, here it is proposed to assess the fatigue performance of this technology when applied to reinforced concrete structures.

For this purpose, a laboratory experiment is devised where a fatigue test is performed on reinforced concrete beams instrumented with Rayleigh based DOFS, where the applied load cycles are defined in a way to replicate expected real world conditions for the case of a standard highway bridge. No other work is found on the application to concrete structures under fatigue testing with these type of DOFS setup.

Here, two reinforced concrete beams were produced, beam FA1 and beam FA2, and instrumented with a 5.2 m polyimide coated fiber in each one. As mentioned above, this experiment was conducted in the same time period of the one described in the previous section and in this way, the geometry, mechanical properties of the concrete and general setup of the instrumentation in each beam is in every way equal to what is outlined in section 3.2.2 and depicted in Figure 3.8 and Figure 3.9.

In this way, each beam is instrumented with a DOFS performing four parallel segments in the bottom surface and three strain gauges for comparison purposes. Also in this experiment, the same four different adhesives are used to bond each DOFS segment as conducted in the static test characterized before. The purpose here, is to again assess the performance of each bonding adhesive but now under fatigue conditions. Additionally, a displacement transducer (LVDT) is also used at mid-span in order to follow the deflection in each beam.

When defining the load to input in each load cycle and to replicate the real world conditions, a common reinforced concrete bridge is envisioned with a central span of 15 m and two adjacent spans of 10 m each. The envisioned bridge deck is 10.6 m wide and cross-section depth is 1 m. The description of the bridge is depicted in Figure 4 of the submitted journal article V detailed in this document in the Annex section.

Two different load stages are considered for the stress range of the load cycles. The first and lower inputted stress level corresponds to the actuation of the structures' self-weight and permanent loads. On the other hand, the second and upper inputted stress level corresponds to the addition of the traffic load, represented by a four-axle truck with a load of 120 kN by axle and multiplied by a dynamic factor of 1.3 as described in Fatigue Load Model 3 of EN 1991-2 [108].

Therefore, and in order to reproduce these stress levels in the tested beam specimens in the laboratory, the load cycles ranges from 11.75 kN to 13.73 kN. The cycling load is applied with a frequency of 4 cycles per second with a sinusoidal profile until reaching 2 million cycles (500k seconds) as illustrated in Figure 3.12. This inputted frequency was defined to stimulate as much as possible the real conditions in concrete bridges under traffic and also to facilitate the logistics of such experiment in terms of its duration.

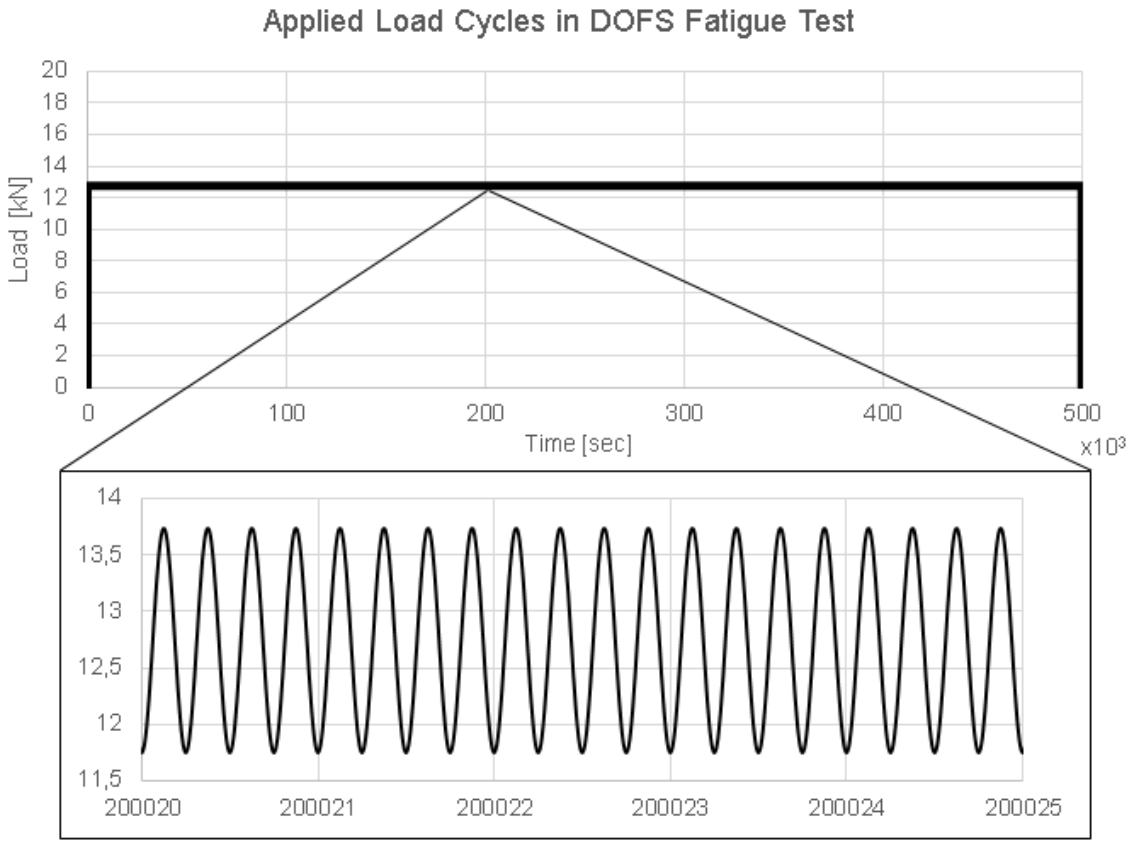

Figure 3.12. Defined load sequence for fatigue cycles

The main difference between the test in each beam is that for beam FA1 the load is applied directly to the beam in an uncracked condition, whereas for beam FA2, the beam is initially loaded statically until a 28 kN load (inducing in this way cracking), unloaded and then finally loaded with the same 2 million cycles as beam FA1. The goal is to assess the fatigue performance in both un-cracked and cracked concrete, simulating the cases where the DOFS will be bonded to prestressed (no cracking) or reinforced (cracking) concrete bridges.

A spatial resolution of 1 cm and sampling acquisition frequency of 0.2 Hz for the DOFS was defined, while using 1 Hz for the strain gauges, LVDT and load cell information. Lastly, due to the extensive duration of the test and the large amount of collected data, the DOFS's measurements were stored for a duration of 5 minutes (1200 load cycles) every 50k cycles.

3.2.3.1. *Beam FA1 results*

In the first tested beam, FA1, due to logistic reasons, the test is intentionally stopped shortly after 1,925,000 cycles which doesn't allow the completion of the total 2 million intended number of cycles. Notwithstanding, the DOFS are able to measure the strain over the number of load cycles and over the bonded length of the DOFS for each adhesive type segment located at the bottom surface of the tested beam with satisfactorily results. It is seen how the different DOFS segments are able to follow the developed strain over the cycling load with different levels of stability.

When plotting the measured strain in the centre of the beam by the DOFS segments and strain gauges while comparing with the LVDT, it is observed how in the first 200k cycles, some unexpected events are taking place. The deflection measured by the linear transducer is progressively increasing for the same applied load range with an amplitude close to 0.02 mm in the first 50 k cycles which suggests an adjustment of beam supports during this period. The strain gauge at this location and the DOFS' segments also reveal some atypical strain readings during this time period. Furthermore, it is also observed how all set of sensors seemed to have been affected by an electrical shut off, which occurred around the 180k cycle mark. Close to the 600k cycles mark it is also seen some atypical readings from SG2, which are then quickly recovered.

However, and more importantly in the context of the research being presented in this thesis, it is seen how between the 100k and the 150k cycle, the measurements from the DOFS segments diverge substantially from what is observed in the strain gauge without any plausible reason, being then sustained and maintained throughout the rest of the test, which results in an average difference between both set of sensors of 20 με. This difference is even observed for the unloaded point of the beam specimen after the conduction of the load test.

By analysing the entire length of the DOFS measurements profile it is noticed that this divergence is also present in segments of the fiber sensor which are not bonded to the beam, thus discarding any possible influence from a mechanical event as seen in Figure 3.13. Moreover, it is also believed that this difference is not a result of any thermal variation since the period between the 100k and 150k cycle mark is too short in order to produce significant temperature variations in the test location (3.5 hours). Additionally, if it would be due to a daily temperature variation, this would be depicted again in the following days' measurements.

From Figure 3.13, it is seen a global divergence in the unbonded segment from the first measurements until the 150k cycle mark. When analysing the following DOFS cycle measurement at the 200k cycle mark, after the occurrence of the electrical shut off at 180k, the aforementioned divergence disappears. Nevertheless, for the remaining bonded parts of the deployed fiber, the following measurements after the 200k cycle mark continue to present the mentioned deviation.

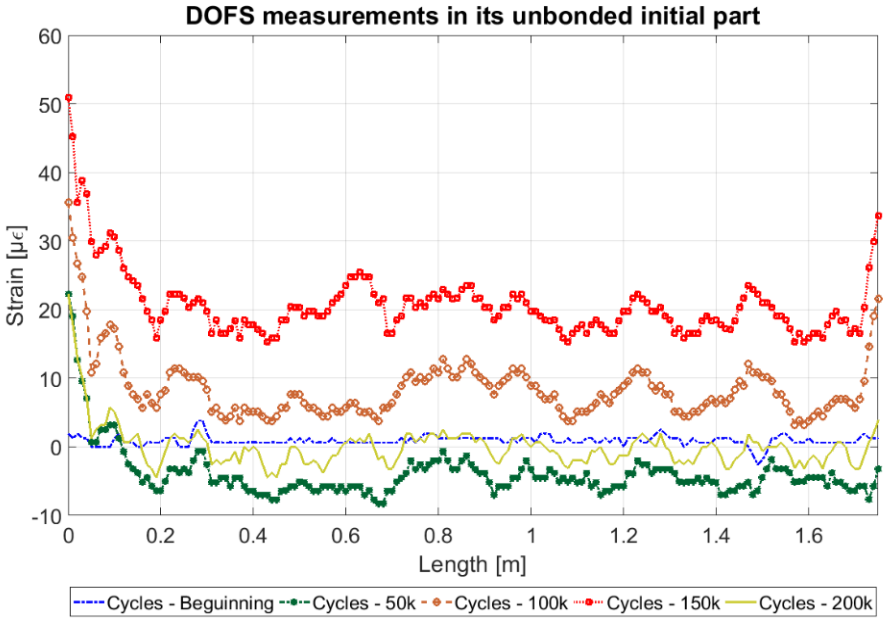

Figure 3.13. Measured strain at the initial unbonded segment of the DOFS for the first 200 k cycles

It is in this way, it may be concluded that this divergence of the measured data observed for the initial unbonded segment of the DOFS before the occurrence of the electrical shut-off at the 180k cycles mark is responsible of the detected difference between the DOFS measurements and the strain gauges throughout the rest of the test. Since this is only verified for the DOFS measurements and any mechanical or thermal event influence is discarded, it is decided to correct this divergence by eliminating this shift on the DOFS measurements. Therefore, the average of the measured values in the initial unbonded segment of the DOFS (between DOFS length coordinate 0.05m and 1.60 m - Figure 3.13) before the occurrence of the electrical shut-off is calculated and its value subtracted to the remaining measured data of the DOFS, thus eliminating the aforementioned shift, as seen in Figure 3.14.

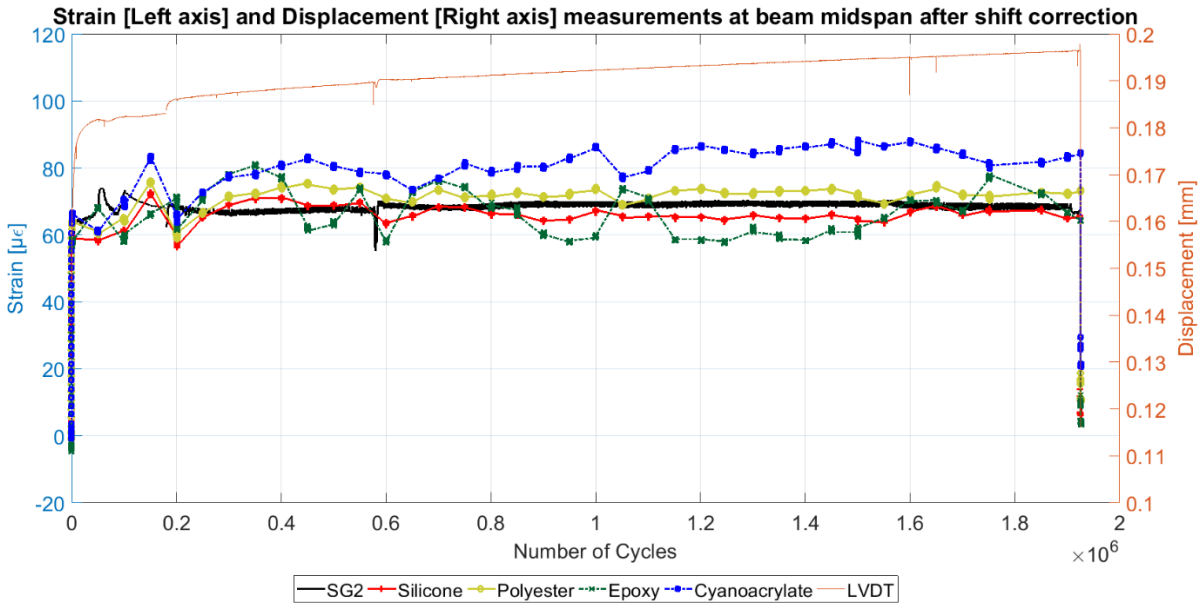

Figure 3.14. Strain and displacement measured at beam FA1 mid-span over the applied load cycles after the shift correction

In Figure 3.14, is possible to observe how the DOFS measurements follow the strain gauge with a better agreement along the number of cycles after the shift correction. In addition, it is important to point out that the applied load frequency is of 4 Hz while the sampling acquisition of the DOFS is of 1 measurement every 5 seconds while being of 1 Hz for the strain gauges.

As a consequence, it is not certain that when storing a DOFS measurement, the obtained strain coincides with the exact same point of the sinusoid profile of the load as the strain gauge, which can justify a maximum amplitude difference in the order of the magnitude of the applied strain range of around 12 με. This is the verified difference between the DOFS and strain gauge measurements. Notwithstanding, as an additional note, it is in this case observed more uniform and constant measurements from the polyester and silicone bonded DOFS segments.

3.2.3.2. *Beam FA2 results*

Going into the results of beam FA2, as it is mentioned above, this specimen is initially and intentionally pre-cracked and only afterwards submitted to the two million load cycles with the same amplitude as beam FA1. Figure 3.15, illustrates the measured strain at the beam midpoint in the initial cracking stage before applying the load cycles. In the same figure, using the right y-axis the applied load is also depicted.

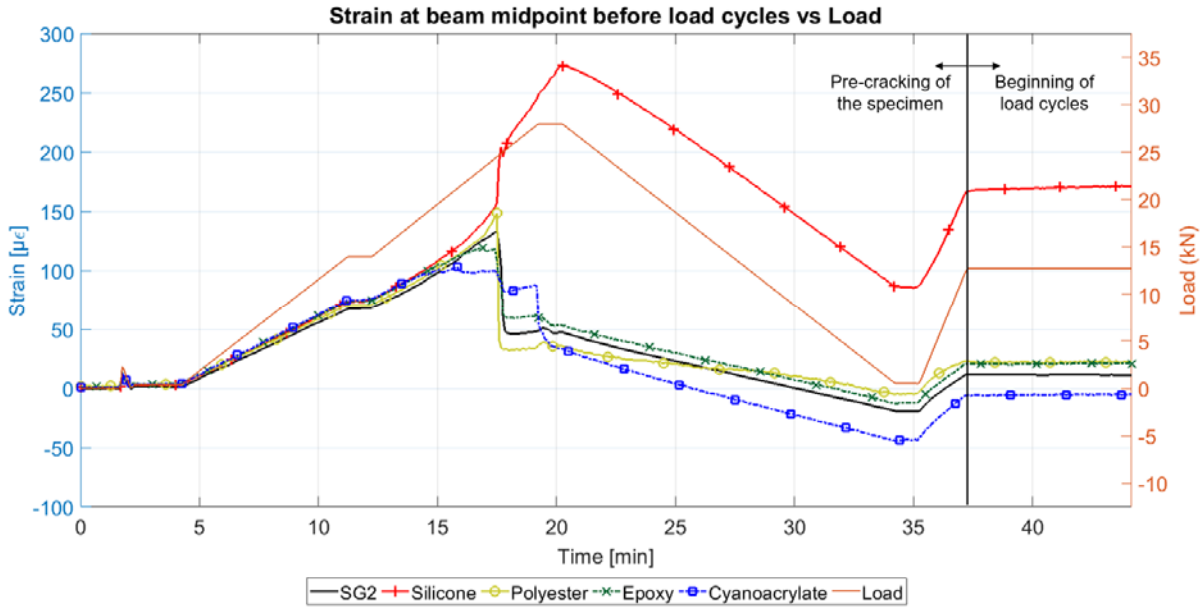

Figure 3.15. Measured strain by DOFS and strain gauge vs applied load in initial cracking stage

Here it is observed that the DOFS measurements present a good agreement with the strain gauge at the same location (SG2) until cracking is initiated. Then, the change of stiffness and subsequent strain redistribution in the element at this location due to cracking is first detected by the cyanoacrylate bonded DOFS segment around minute 15 and then detected by the rest of DOFS segments and SG2 and SG3 at minute 17.5 for a load of 24.67 kN. The developed crack is actually at segment coordinate 36 cm (between SG2 and SG3) as seen in the submitted journal article V in the Annex of this document.

Notwithstanding, after the cracking detection as seen in Figure 3.15, all DOFS bonded segments and strain gauges measurements follow with more or less agreement the applied load until the beginning of the 2 million load cycles application. Nonetheless, it is observed how after the post-cracking stage and unloading stage (minute 35 in the same figure) the strain measurements slightly diverge between the different DOFS segments and the strain gauges, especially observing that the silicone bonded segment, contrary to the other segments and strain gauge, measures an increase in strain. This is due to the different mechanical properties inherent to each adhesive. In the case of the silicone adhesive, due to its relatively low modulus of elasticity, it allows a slight movement of the fiber inside the adhesive, relatively relaxing the part at the crack location and increasing the obtainable measurements at the remaining locations similar to the use of a coarser spatial resolution.

Therefore, since a new load cycles sequence is started after the cracking inducing stage and at his beginning there is an already existing difference between the measured strains by the different sensors, in order to correctly assess the DOFS performance in a cracked element under fatigue, it is decided to reset the sensors measurements at minute 35 (unloaded stage of the beam after cracking).

In this way, when doing the comparison of the measured strain by the DOFS and strain gauge at segment coordinate 17.5 cm (SG1) during the 2 million load cycles after the mentioned reset, Figure 3.16 is obtained. This location is chosen in order to be as far as possible from the crack location so to diminish its influence in the strain measurements.

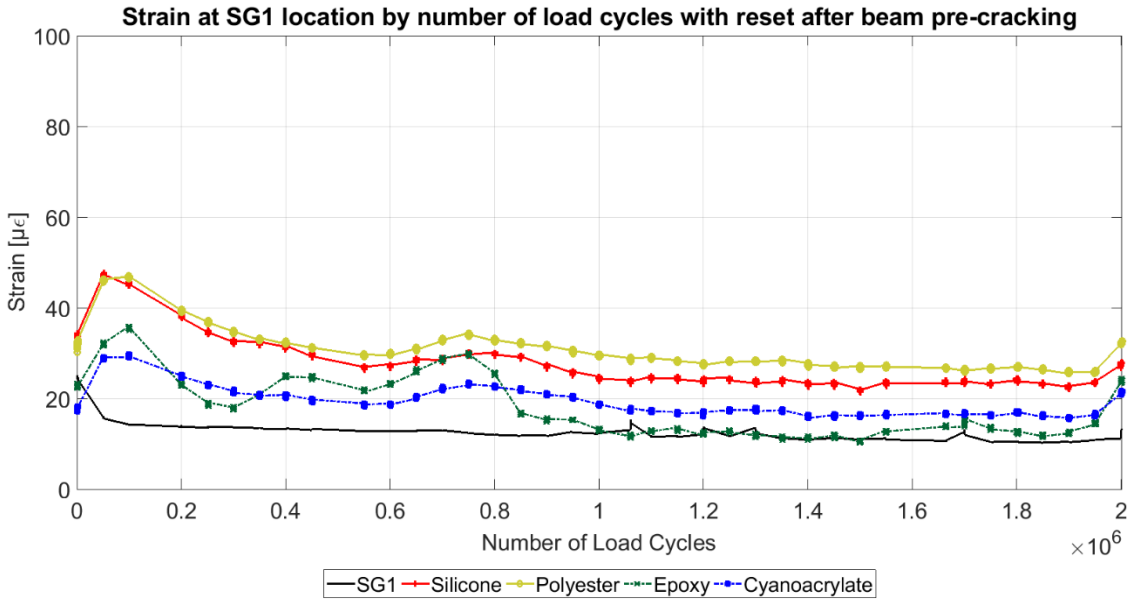

Figure 3.16. Comparison of measured strain by DOFS and SG1 at its location over the applied load cycles

Once again, as seen for beam FA1, the DOFS measurements agree reasonably well with the data measured by the strain gauges. After a small initial deviation within the first measured 50k cycles and despite some subsequent small fluctuations, all segments present a decent stabilization of their measurements. The observed difference between both set of sensors is more relevant for the DOFS using

silicone and polyester and almost negligible for epoxy and cyanoacrylate. Notwithstanding, these differences are, as in the case of beam FA1, related with the system strain resolution (± 2 με), different sampling rates in the acquisition systems and strain range due to the amplitude of the load cycles (12 με).

In conclusion, with this test it is possible to discern positive and encouraging results on the use of this novel technology in real world applications for long-term monitoring periods. The distributed optical fiber technology showcased a good performance under fatigue loading either for the uncracked and cracked scenarios by presenting similar results as the strain gauges' measurements, apart from an easily corrected deviation in beam FA1. Again, this deviation is concluded to be related with a very particular random event and not due to any mechanical or thermal effects in the beam or sensor, validating in this way its correction.

As a result, it is plausible to affirm that fatigue loading doesn't seem to affect the performance of DOFS when obtaining strain profiles along its length. Furthermore, all used bonding adhesives appear to perform well in these conditions with the observed different performances between the deployed adhesives to be almost negligible.

3.3. Real world scenarios applications

During the conduction of this thesis project, it was also possible to assess and interpret the results of the application of this novel technology in two real world existing structures located in Barcelona, Spain. This is an important opportunity to evaluate the feasibility of implementing these type of sensors in real scenarios that present different and new challenges when compared with the case of laboratory experiments in controlled environments.

In these situations, besides the immediate challenge presented by the external environmental agents that can harm and influence the sensors' measurements, a more difficult and defying scenario is present regarding the sensor installation in the structure to be monitored. Due to the fragility of the fiber used in this research, special care has to be taken when handling the fiber in order to not rupture it, which in some construction sites can be demanding.

The cases and results discussed in this section are presented in detail in the published journal article III, fully transcribed in Chapter 4 of the present thesis. Therefore, in the following sections, is presented only a summary of the application of Rayleigh based OFDR DOFS in two rehabilitation works, the first in the Sant Pau Hospital and the second in Sarajevo Bridge, in the city of Barcelona.

3.3.1. Sant Pau Hospital application

The first described application is the one conducted at the historical and UNESCO world heritage site Sant Pau Hospital located in Barcelona. This is one of the most superb and biggest examples of the Catalan architectural modernism movement, which was built between 1902 and 1930 in two phases by the notorious Catalan architect Lluís Domènech i Montaner. After eight decades of use, this complex of buildings ceased

its purpose as a fully functioning hospital in June 2009 and underwent important restoration works in the following years.

During this period, it was observed that in one of the buildings, some threatening cracks were appearing in brick masonry columns on one of its floors. After a structural assessment, it was decided to replace two of those columns by new structural elements made of steel. This procedure implied the installation of a temporary bearing steel structure around the columns to support the load while the masonry element was cut, removed and substituted by the new steel profile columns. Afterwards, the load was transferred from the temporary bearing structure to the new columns.

The floor above these elements that required restoration work, was being used to treat and accommodate recovery drug patients and their relocation was not feasible. As a consequence, it was necessary to perform the replacement of the fault columns while the building was in normal functioning service. For this reason, a structural monitoring scheme was necessary in order to ensure that no harm was being inflicted in the building occupants due to the conducted restoration works.

In this situation, due to the large and continuous area affected by the column removal, the DOFS technology presents a unique advantage when compared to the other conventional sensors used for point/discrete monitoring such as strain gauges and LVDTs. The use of DOFS constitutes a clear more cost-effective solution being able to monitor such large area using just one sensor while a large number of point sensors would be otherwise required.

Therefore, in this procedure it is deployed a 50 m long DOFS, in the upper masonry vaults ceiling, which using a spatial resolution of 1 cm, allows for the monitoring of 5000 different points. Nonetheless, only 38 m of the entire length of the DOFS is adhered to the structure for practicality reasons, using for this bond an epoxy adhesive. The bonded DOFS is depicted in Figure 3.17.

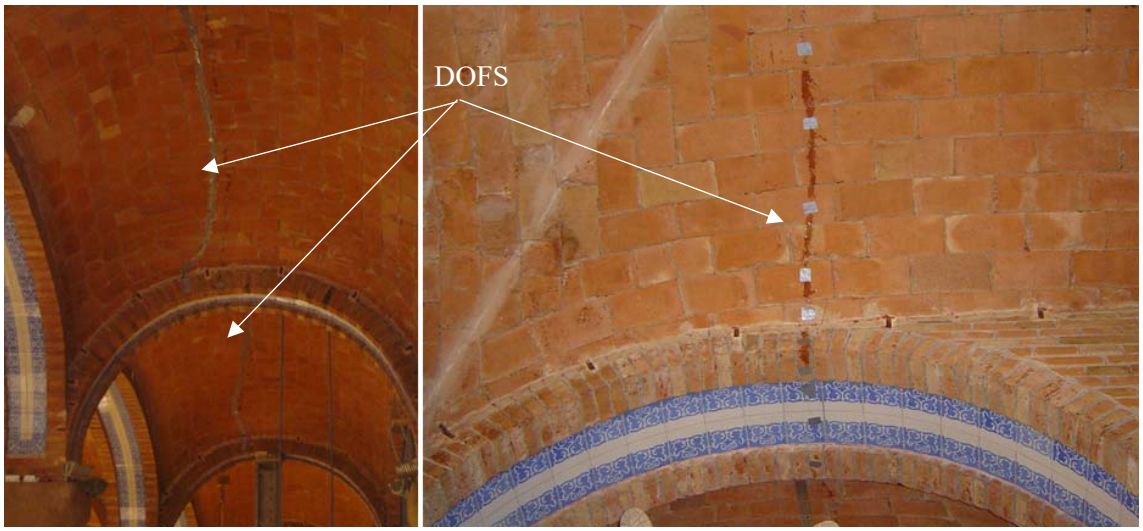

Figure 3.17. Installed DOFS in the masonry vaults of Sant Pau Hospital

The deployed DOFS obtains continuous readings in combined time intervals of: 1 reading per minute, 1 reading per 10 minutes and 1 reading each hour. From all the collected and extensive data, the critical values (maximum and minimum) are analysed and used to generate envelope response graphs, being the main goal of the monitoring system to detect and locate the premature appearance of cracks and their possible subsequent evolution.

The monitoring procedure is conducted along 18 days, where, using just one single sensor, it is possible to separately obtain the evolution of the measured strains in each instrumented masonry vault. Moreover, a more local assessment can be conducted by focusing in shorter lengths extents within specific areas of the DOFS. This demonstrates the great flexibility of this technology in providing both global and local behaviour monitoring. Additionally, it is possible to plot the envelope measured strains at each point along the monitored period in order to better follow the evolution of the conducted works as illustrated in Figure 3.18 for the specific point corresponding to the coordinate 13.05 m in the first monitored vault.

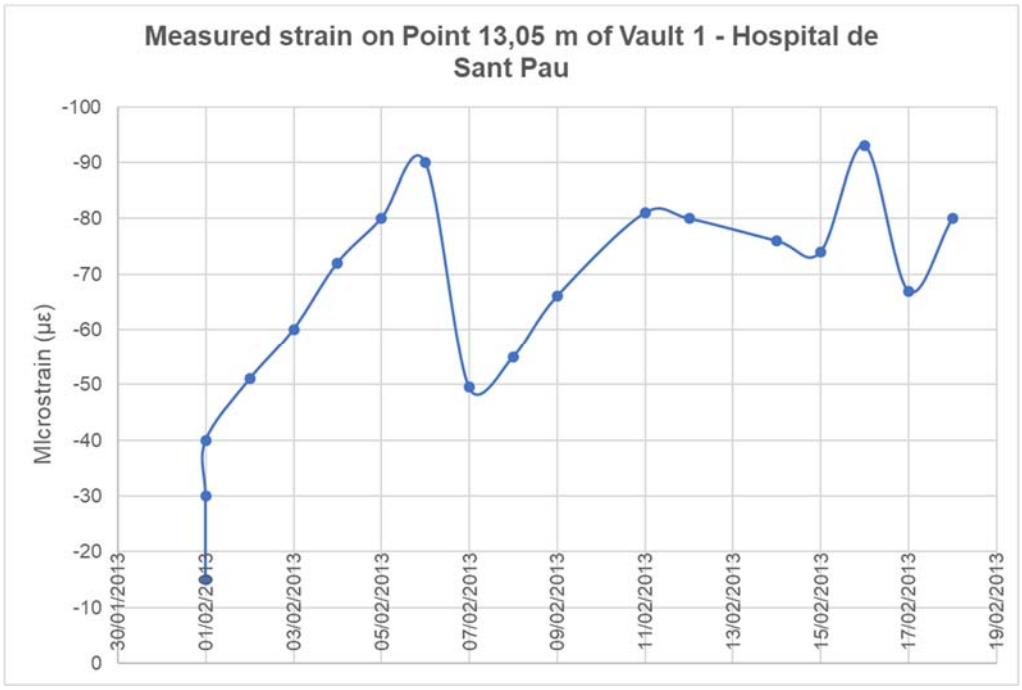

Figure 3.18. Measured strain evolution by DOFS at point 13.05 m

Here it is possible to conclude that the replacing operation caused an increment (in compression) of the strain in the vault in the order of 80 με, which is almost uniform along the whole roof. It is seen how during the entire duration of the rehabilitation works the structural response is under the service limit state since the strain increment generates minimal stresses to the material of 0.14 MPa for a characteristic compressive strength of 3 MPa. Moreover, it is not detected the formation of new cracks.

Furthermore, as seen in Figure 3.18, with the use of this technology it is possible to follow and identify the rehabilitation sequence where the increase of compressive strains is due to the installation of each temporary steel bearing structure while the two observed drop-offs correspond to the transfer of load between those elements and the new steel columns.

In conclusion, due to the implementation of DOFS technology in this historic structure, it is possible to follow the developed strains due to the conducted rehabilitation works and conclude the safety of the structure during this entire procedure while also maintaining the structure in full operation as required by the owner.

3.3.2. Sarajevo Bridge application

The second case where it was possible to instrument a real world structure with Rayleigh OFDR based DOFS was the Sarajevo Bridge. This is a structure located over one of the main roadway entrances of the city of Barcelona, Spain with a high traffic flow during peak hours. It is a two-span bridge with span lengths of 36 and 50 m and where each span is built up by three box-girder prestressed concrete beams connected by an upper reinforced concrete slab.

This structure was subjected to rehabilitation works to enlarge the existing deck while introducing new steel elements in order to increase pedestrian traffic and improve its aesthetics. Due to the high traffic volume of both this structure as its underneath lanes, it was not possible to close the bridge to traffic or place a temporary support beneath the rehabilitated structure. As a result, as in the previous described real world case, it was compulsory to perform the required rehabilitation works while maintaining the structure in its normal service operation and without the possibility of adding a temporary support. Adding the importance of this structure to the city's road network, it was paramount to perform a close monitoring follow up of the induced stresses during and after the execution of the works.

In this way, two 50 m length DOFS (DOFS 1 and DOFS 2) were placed in the internal bottom surface of the box-girder beam most susceptible to be subjected to a larger load increment in the 36 m length span. This is depicted in Figure 3.19. Therefore, the fibers were bonded using an epoxy adhesive, adjusting to the length of the span while the remaining 14 m of the DOFS were left unbonded.

Figure 3.19. Instrumented DOFS sensors in interior of box-girder beam of Sarajevo Bridge

The monitoring period in this application was between June of 2015 and February of 2016 (8 months) and in this way, the DOFS measurements were conducted in chosen days throughout this period, being that

the maximum and minimum measured values in each of those dates was used to generate envelope response graphs. Moreover, it was seen how it was only possible to obtain data alternating between the two deployed DOFS 1 and DOFS 2 for the first 5 months since DOFS 1 was accidentally ruptured during the conduction of works inside the box girder. Hence, the rest of the measurements were solely conducted using DOFS 2.

One important aspect of this application was that due to the vast mentioned duration of the monitoring period, the influence of temperature on the readings had to be considered. Both the refractive index of the backscattered light and the materials which compose the DOFS are dependent of these temperature changes, so a correction of this thermal induced error on the monitoring output is required.

There is the possibility to use two different ways to perform this temperature compensation when using Rayleigh OFDR based DOFS (or OBR) as long as there are segments of the deployed fiber which aren't bonded to the structure and therefore only subjected to the thermal variation induced changes. These techniques are namely the point-to-point thermal compensation and thermal compensation by fiber loop. The first provides a more solid mitigation of the thermal effects, however if not any significant local temperature gradients are expected throughout the fiber cable, both can be used. The two techniques are explained in detail in the published journal article III presented in Chapter 4 of this thesis.

In the case of Sarajevo Bridge application, since 14 m of the fiber were left unbonded in the original spool case, it was therefore only possible to use the second mentioned technique. Here, in order to obtain the pure mechanical strain developed during the monitoring period, it is necessary to subtract from the total and original strain obtained in the bonded part of the fiber, both the effects of the refractive index dependent apparent strain (RIAS) and the coefficient of thermal expansion dependent apparent strain (TEAS). In this way, an average of the spectral shift measured for the entire length of the unbonded segment is calculated and then subtracted to the calculated average of the measured data of the bonded segment.

As mentioned above, by using this thermal compensation by fiber loop, the assumption that the ambient temperature variation is the same along the entire length of the monitored box-girder is made, therefore limiting the use of the DOFS data to a global structural behaviour analysis. However, by dividing the entire deployed DOFS length in different smaller segments this analysis can be improved. As a consequence, five different segments (corresponding to different span adjusting DOFS lengths) are proposed, where a thermal compensation is conducted for each one. In this way, the average and purely mechanical induced strain evolution for each section of the monitored span is obtained as depicted in Figure 3.20 for DOFS 1 and Figure 3.21 for DOFS 2.

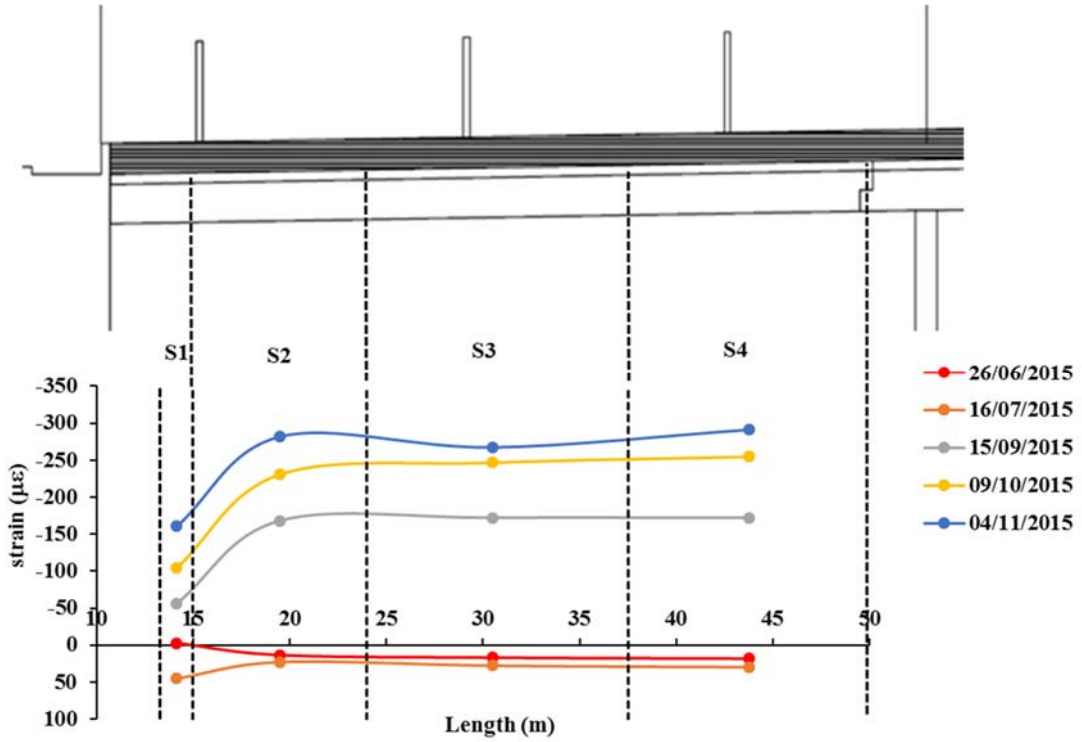

Figure 3.20. Mean mechanical distribution measured by DOFS 1

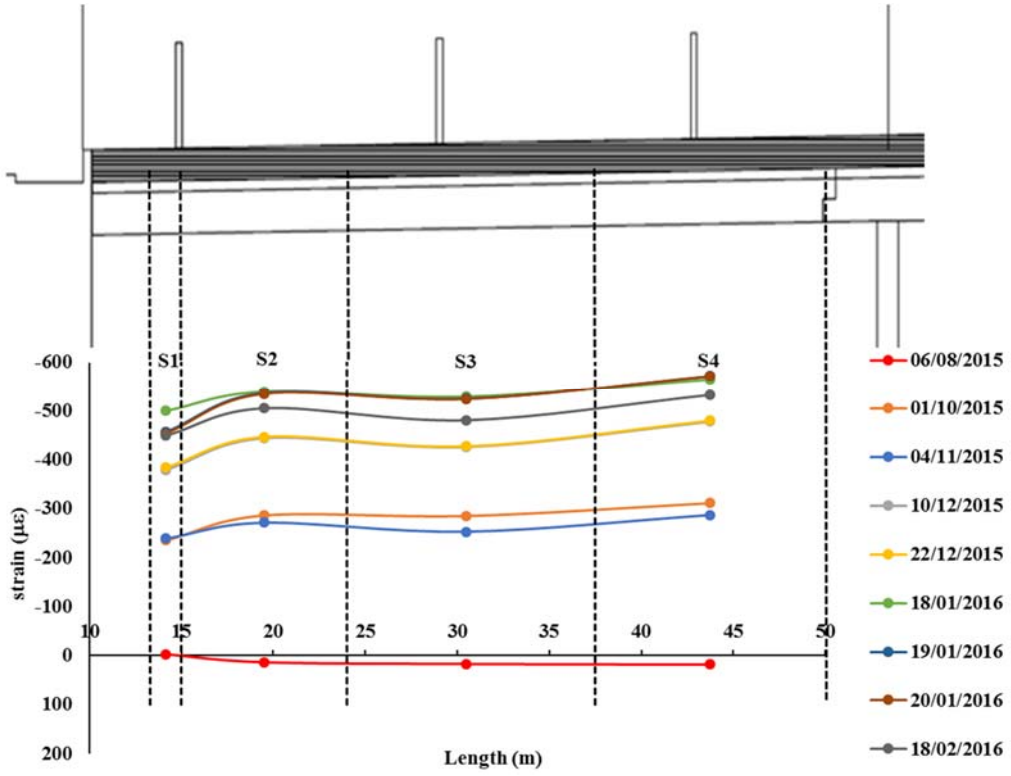

Figure 3.21. Mean mechanical distribution measured by DOFS 2

It should be noted that segment S0 corresponds to the unbonded segment of the DOFS and is not plotted in the mentioned figures.

It is seen that apart from segment S1 which presents a relative lower mechanical strain than the other segments of the DOFS length due to its proximity to the bridge support, the remaining ones present a

uniform mechanical strain distribution. Therefore, it can be concluded that the main responsible for the verified strain variation is the decrease of temperature between summer and winter translated in a uniform shortage of the box-girder.

These two applications of Rayleigh OFDR based DOFS in two real world structures allowed for the verification of the validity of the use of this novel technology in real case scenarios while showcasing these sensors unique advantageous capabilities and its limitations. It is seen how these sensors are able to follow and monitor the structural behaviour in different type of structures with also different type of interventions, while only requiring the use of a relative small number of sensors and simple monitoring systems.

These monitoring processes are able to assess the structure's safety trough the analysis of the developed stresses increment in a continuous way (both in time and space). Furthermore, this is conducted while allowing for the structure to continue to work in its normal service state. Additionally, it is observed the versatility of the use of this technology as two different type of materials (concrete and masonry) were monitored with a good performance of the instrumented DOFS.

In contrast, it is also verified that if a significant protection layer is not provided to the sensors when placed in areas easily accessed by the general public or not trained third party construction workers, the DOFS might be compromised or even ruptured. Also it would be of interest, to attach and perform quasi-simultaneous measurements of more than one DOFS sensor, enhancing the versatility of use of this technology.

All things considered, these real case applications further demonstrated the potential and feasibility of use of OBR based DOFS technology in civil engineering SHM applications by providing valuable and reliable information on the structures condition for the structure's owners and responsible authorities. These described applications, also showcase the first application of this type of technology in a masonry structure, even more so, with such an important historical value and also the first relatively extended continuous in time use on a prestressed concrete structure, which implied the correction due to thermal effects.

Chapter 4 - Published Journal Articles

This chapter reproduces the published journal articles produced in this thesis. Each paper follows its own numbering of sections, figures, tables, equations and references.

Journal Paper I:

A. Barrias, J. Casas, and S. Villalba, "A Review of Distributed Optical Fiber Sensors for Civil Engineering Applications", *Sensors*, vol. 16, no. 5, p. 748, May 2016.

- Area: Instruments & Instrumentation
- Quartile: Q1 (2016)
- JCR Impact Factor: 2.677 (2016)
- Number of cites: 75 (Scopus)

Journal Paper II:

A. Barrias, J. Casas, and S. Villalba, "Embedded distributed optical fiber sensors in reinforced concrete structures: a case study", *Sensors*, vol. 18, no. 4, p. 980, March 2018.

- Area: Instruments & Instrumentation
- Quartile: Q2 (2017)
- JCR Impact Factor: 2.475 (2017)
- Number of cites: - (Scopus)

Journal Paper III:

A. Barrias, G. Rodriguez, J. Casas, and S. Villalba, "Application of Distributed Optical Fiber Sensors for the Health Monitoring of two real structures in Barcelona (Spain)*," Structure and Infrastructure Engineering*, vol. 14, no. 7, p. 967-985, February 2018.

- Area: Civil & Structural Engineering
- Quartile: Q2 (2017)
- JCR Impact Factor: 1.845 (2017)
- Number of cites: 1 (Scopus)

4.1. Journal Article I

A Review of Distributed Optical Fiber Sensors for Civil Engineering Applications

Published in Sensors, vol. 16, no. 5, p. 748, May 2016. doi:10.3390/s16050748

António Barrias [1], Joan R. Casas [1] and Sergi Villalba [2]

[1]Department of Civil and Environmental Engineering, Technical University of Catalonia (UPC), c/ Jordi Girona 1-3, 08034 – Barcelona, Spain

[2]Department of Engineering and Construction Projects, Technical University of Catalonia (UPC), c/ Colom 11, Ed. TR5, 08022 – Terrassa (Barcelona), Spain

Received: 24 March 2016; Accepted: 16 May 2016; Published: 23 May 2016

Abstract: The application of structural health monitoring (SHM) systems to civil engineering structures has been a developing studied and practiced topic, that has allowed for a better understanding of structures' conditions and increasingly lead to a more cost-effective management of those infrastructures. In this field, the use of fiber optic sensors has been studied, discussed and practiced with encouraging results. The possibility of understanding and monitor the distributed behaviour of extensive stretches of critical structures it's an enormous advantage that distributed fiber optic sensing provides to SHM systems. In the past decade, several R & D studies have been performed with the goal of improving the knowledge and developing new techniques associated with the application of distributed optical fiber sensors (DOFS) in order to widen the range of applications of these sensors and also to obtain more correct and reliable data. This paper presents, after a brief introduction to the theoretical background of DOFS, the latest developments related with the improvement of these products by presenting a wide range of laboratory experiments as well as an extended review of their diverse applications in civil engineering structures.

Keywords: fiber optics; structural health monitoring; distributed fiber sensing; time domain reflectometry; frequency domain reflectometry; civil engineering

1. Introduction

1.1. Motivation for SHM

The highway and railway transportation systems are considered to be some of society's critical foundations. In this complex system, bridges and viaducts assume an important role because of their distinct function of joining these networks as their crucial nodes. They face continuously increasing traffic volumes and heavier truck and rail-loads, which degrade the long-term performance of these structures. In the United States alone, over 11% of the nation's 607,380 bridges are deemed structurally deficient and the cost to repair these deficient bridges is estimated to be $76 billion [1]. Well maintained civil infrastructure can substantially increase a country's competitiveness in a global economy and enhance resilience to adverse circumstances. Therefore, a structure, especially in the present days, must be able to reliably produce information regarding any alterations in its structural health condition and communicate it to the responsible operators and decision makers both in a timely way and either automatically or on-demand in order to decrease these costs. To achieve such goals, a modern structure needs to be prepared with a system that includes a "nervous subsystem", a "brain", and "voice lines", which is continuously in operation and able to sense structural conditions [2].

The control and monitoring of the aging process of civil engineering structures is of extreme importance for their quality and safety. Furthermore, there are different external events that can damage a structure. Damage can be defined as alterations that when introduced into a system will have an adverse effect in its current or future performance [3]. The process of employing a damage identification strategy for engineering and aerospace infrastructures is referred to as structural health monitoring (SHM). When dealing with long-term SHM, the goal of the system is to deliver updated information regarding the ability of the structure to continue to serve its intended purpose and function despite the unavoidable effects of the mentioned aging process and the accumulation of damage that results from the operational environment. SHM systems are also able to rapidly assess and screen the structure condition under an accidental or extreme event such as earthquakes, increase of water levels or unexpected loadings. The early detection of structural malfunctions allows the increase of the service life-time of the structure at the same time that decreases the maintenance costs.

The act of damage identification has been around probably, in a qualitative manner, since man started to using tools [3]. Notwithstanding, SHM has been recently a fast-developing area in aerospace and engineering disciplines especially in the civil engineering field. The innovation in the SHM technologies as well as the development of large-scale SHM systems has been a great subject of interest within the engineering and academic communities over the last two decades [4-11]. However, despite its great potential, SHM has not been applied in large scale and in a systematic manner to civil infrastructures. One significant reason for this is the lack of reliable and affordable generic monitoring solutions [12].

1.2. Optical Fiber Technology in SHM of Built Environment

Currently, assessment of buildings, bridges, dams, tunnels and other vital civil engineering infrastructures are carried out by engineers trained in visual inspection, which sometimes can be inaccurate due to differences in their background for safety condition assessment. In order to improve the inspection accuracy and efficiency, optical fiber sensors (OFS) are one of the fastest growing and most promising researched areas, due to their features of durability, stability, small size and insensitivity to external electromagnetic perturbations, which makes them ideal for the long-term health assessment of built environment [13].

Furthermore, the most regularly practiced SHM approaches are based on electric strain sensors, accelerometers, inclinometers, GNSS-based sensors, acoustic emission, wave propagation, *etc*. Nevertheless, all of them present genuine challenges when deployed in real world applications [4]. Different kinds of sensors, embedded or attached to the structure, can be used in SHM systems but only those based on fiber technology provide the ability to accomplish integrated, quasi-distributed, and truly distributed measurements on or even inside the structure, along extensive lengths [2].

Standard monitoring practice is normally based on the choice of a limited and relatively small number of points that are supposed to be illustrative of the structural behaviour [14]. For a large scale structure, the number of point sensors needed to generate complete strain information can grow rapidly. Discrete short-gauge sensors provide useful and interesting data of the structure related with local behaviour but might omit important information in locations where degradation occurs but that is not instrumented. There are ways of covering larger extensions of structures with the application of long-gauge sensors allowing the detection and characterization of phenomenon's that have a global impact on the structure. Notwithstanding, the reliable detection and characterization that occurs far from instrumented areas continues to be challenging since it depends on high-level algorithms whose performance may decrease due to external interferences that can mask the real damage, such as temperature variations, load changes, outliers and missing data in monitoring results [15]. Distributed optical fiber sensors (DOFS) offer an advantage over point sensors for global strain measurements.

The thousands of sensing points that the DOFS provides enables mapping of strain distributions in two or even three dimensions. Thus, real measurements can be used to reveal the global behavior of a structure rather than extrapolation from a few point measurements.

A truly distributed optical sensor is expected to measure temperature, strain and vibration data at any point along an entire fiber through light scattering. The great challenge has been to develop these sensors in a way that they can achieve appropriate sensitivity and spatial resolution [13]. Fortunately, great advances have been made in the last decades in order to improve this area.

Several general state of the art papers of FOS have been published [16–19] and also various where the applications of these sensors on civil engineering structures were reviewed [10,20–22]. A

comprehensive DOFS state of the art paper was presented in [11] where the theoretical background of the most used DOFS techniques was extensively elaborated and where some civil engineering applications, especially focused on bridges, were presented. In the present paper, a broader and wider range of civil engineering applications are presented (geotechnical structures, pipelines, dams, bridges, laboratory experiments) as some other innovative implementations. Furthermore, and finally, a review of the dynamic capabilities of distributed sensing and the most practical challenges associated with the implementation of these sensors are presented.

2. Fiber Optic Sensors

2.1. Introduction

The first reference of fiber optic sensors relates to the flexible endoscopes developed in the first half of the twentieth century. With it came a revolution in the medicine field that continues to the present day [23]. However, the start of the development of modern age of optical fiber sensors started in earnest in 1977 for long distance telecommunications and it has experienced an exponential growth during the last four decades. Sensing applications are a small spin-off from this technology, taking advantage of developments in optoelectronic components and concepts. By 1982, magnetic, acoustic, pressure, temperature, acceleration, gyro, displacement, fluid level, torque, photo acoustic, current, and strain sensors were among the fiber optic sensors already developed and being researched [24] This modern age of fiber optic sensors was possible thanks to the development of extremely low-loss optical fibers in the late 1970s [23].

The fiber optic communications industry has literally revolutionized the telecommunications industry by providing higher-performance, more reliable telecommunication links with ever-decreasing bandwidth cost. As component prices have fallen and quality improvements have been made, the capability of fiber optic sensors to replace the more traditional electric sensors has been improved [25].

There are many inherent advantages related to the application of fiber optic sensors. Among these, it's possible to highlight their resistance to electromagnetic interference, their light weight, small size, high sensitivity, high-temperature performance, immunity to corrosion and large bandwidth.

Initial introduction of this technology into the markets that were directly competing with conventional sensor technology in the last two decades of the past century was relatively slow. This was largely related to the high cost of suitable components. However, this situation has since changed and the projections for the future are tremendously optimistic as can be seen in Figure 1.

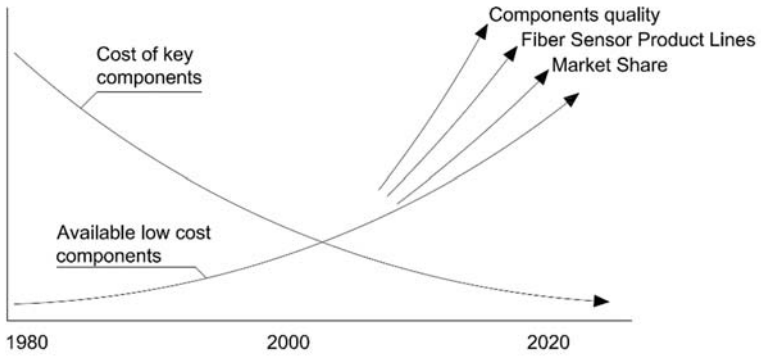

Figure 1. Trends for fiber optic sensors (adapted from [23]).

With the development of each new successful fiber optic product, the cost for existing and newly introduced components continues to drop. By the year 2020 there are many areas where is expected to occur a rapid growth of fiber optics sensors applications. From medical instrumentation, aerospace and industrial applications to structural health monitoring and damage assessment systems in civil structures, the ever-increasing capabilities and lower costs of this technology make it very attractive to end users [23].

Fiber optic sensor based monitoring methods are highly welcome for non-destructive assessment of all types of engineering structures mainly because of the following reasons: they can't be destroyed by lightning strikes, can survive in chemically aggressive environments, they can be integrated into very tight areas of structural components, and finally are able to form sensor chains using a single fiber [26].

2.2. Basics of Fiber Optic Sensors

In a simple way, an optical fiber is a cylindrical symmetric structure that is composed by a central "core" with a diameter between 4 and 600 μm and a uniform refractive index [27]. It's then enclosed by a "cladding" with a relative lower refractive index trapping the light waves being carried in the core by the reflection at the interface between core and cladding Figure 2. In order to provide environmental and mechanical protection to the fiber, this cladding can be covered with an external plastic coating.

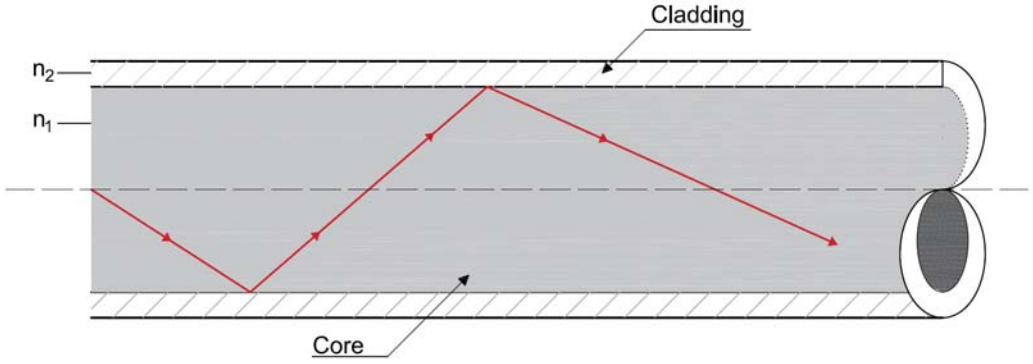

Figure 2. Light guiding and reflection in an optical fiber.

Since the optical fiber is a physical medium it is constantly exposed to external perturbations. In this way, it experiences geometrical and optical changes due to those same perturbations. For communication applications it is preferred to minimize these effects in order to provide a reliable signal transmission and reception. However, in fiber optic sensing, the response to these external induced effects is intentionally enhanced [28]. This change of some of the properties of the guided light can be produced inside or outside (in another medium) of the optical fiber. Therefore, two different types of sensors can be differentiated: extrinsic and intrinsic [29].

In turn, each of these classes of fibers has various subclasses, and even in some cases, sub-subclasses that consist of a large number of fiber sensors. There are different ways to classify optical fiber sensors (OFS) depending of which property is being considered, *i.e.*, modulation and demodulation process, application, measurement points, *etc.* [28]. However, and taking into account the goal of this paper, they can be categorized into three different classes: interferometric sensors, grating-based sensors and distributed sensors [30] (Figure 3). The first two have been widely investigated and used in civil engineering monitoring applications [31–36]. Therefore, the interest of this paper is focused on the latter.

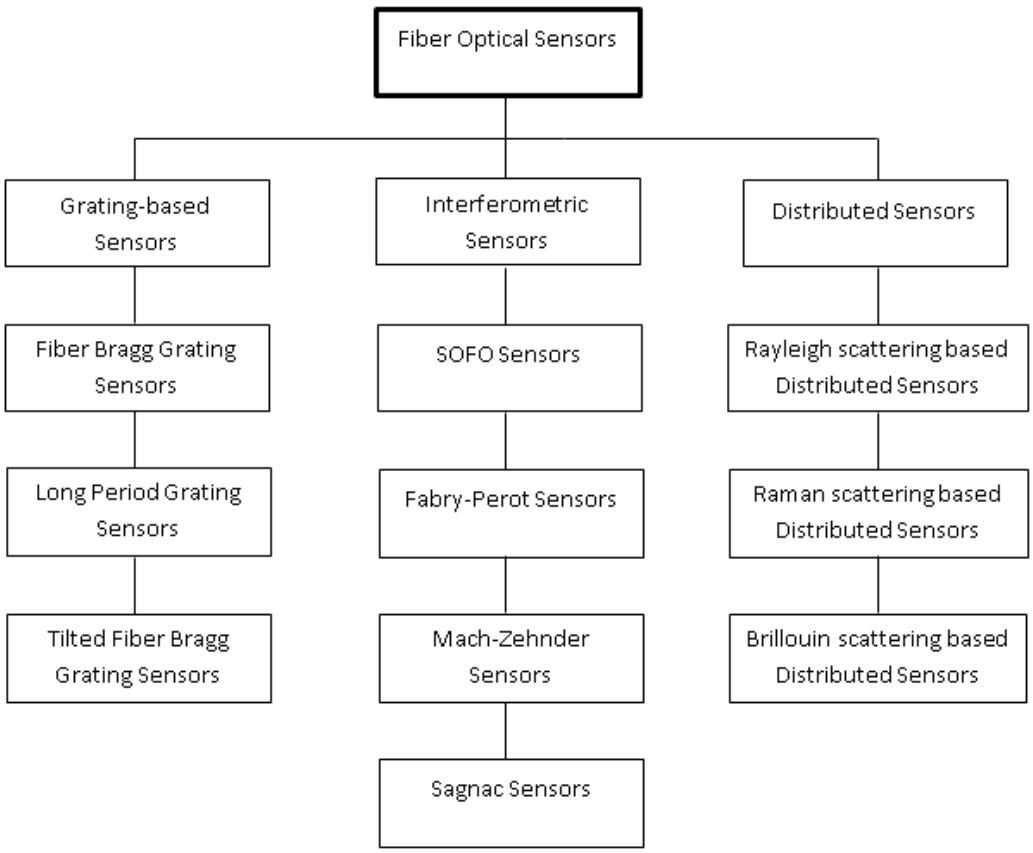

Figure 3. Overview of fiber optic sensor technologies (adapted from [30]).

2.3. Distributed Fiber Optic Sensors

Distributed Optical Fiber Sensors (DOFS) share the same advantages of other OFS. However, they offer the possibility of monitoring variations of one-dimensional structural physical fields along the entire optical fiber in a truly distributed way. Furthermore, an additional benefit regarding distributed sensing is that it only requires a single connection cable in order to communicate the acquired data to the reading unit in opposite of the large number of otherwise required connecting cables when using discrete sensors. This characteristic makes DOFS more cost-effective and at the same time opens a wide range of important applications such as the continuous (in space and time) monitoring of large civil engineering structures.

It should be noted, that distributed sensing can, in a sense, also be achieved through the use of quasi-distributed FBG sensors. In addition, this has been the most popular optic fiber technique for spatial continuous measurements, since 2/3 of the SHM projects which includes fiber sensors, have opted for quasi-distributed FBG [21]. However, in this technique, instead of allowing a continuous monitoring along the fiber path, a finite number of locations are measured. The most effective and used type of quasi-distributed sensors are based on Fiber Bragg gratings by multiplexing many of these sensors in the wavelength domain [37]. Thus, FBG sensing relies on wavelength division multiplexing (WDM) to serve as a quasi-distributed sensor. Using this method usually limits the number of gratings that can be multiplexed to fewer than 100. However, by applying time division multiplexing (TDM) to each wavelength channel and by assigning one central wavelength for each grating an increase in the numbers that can be integrated by these sensors is achieved.

With DOFS technology, the fibers are bonded to the surface or embedded inside the material [2]. When strain and temperature changes are transferred to the optical fiber, the scattered signal within the fiber is modulated by these physical parameters. By measuring the variation of this modulated signal, distributed fiber sensing is achieved.

2.3.1. Scattering in Optical Fibers

Scattering is at the origin of truly distributed fiber optic sensors (DOFS) and it can be defined, in a simple way, as the interaction between the light and an optical medium. Three different scattering processes may occur in a DOFS, namely: Raman, Brillouin and Rayleigh scattering [38].

When an electromagnetic wave is launched into an optical fiber, its propagation through the medium interacts with the constituent atoms and molecules and the electric field induces a time dependent polarization dipole. This induced dipole generates a secondary electromagnetic wave and this is called light scattering [13]. When the medium, where this scattering occurs, is homogenous only a forward scattered beam is allowed. However, the optical fiber is an inhomogeneous medium due to its variations in density and composition and in this way, by the interaction of the light beam with the

fiber, some photons return toward the light source producing backscattering. This back propagating light can be then used to get information about the fiber properties and consequently of the environmental effects to which is subjected to.

Raman scattering is greatly dependent of the temperature of the fiber which has been explored in order to instrument very successful techniques with various applications in different areas [39–41] but also distributed temperature sensors used, for example in the detection of water leakage in dikes [42].

In a similar way, Brillouin scattering is intrinsically dependent on the fiber density, which in its turn is related with temperature and strain being in this way exploited in Brillouin based DOFS [43–48].

On the other hand, Rayleigh scattering, as a quasi-elastic or linear phenomenon, is by itself independent of almost any external physical field. In fact, in Rayleigh-based DOFSs the scattering is used to measure propagation effects, which can include attenuation and gain, phase interference and polarization variation. It is worth mentioning that Raman and Brillouin scattering are also influenced by these propagation effects but since they present a direct relation to the measured parameters, these effects are usually neglected.

Distributed fiber optic sensors can depend on different techniques and principles. For different SHM applications, different DOFSs sensors can be developed and so different techniques are applied. In the next subsections, the most important techniques related to the scope of this document are described.

2.3.2. Time Domain Reflectometry—OTDR

Truly or intrinsic distributed sensing techniques emerged at the beginning of the 1980s when a technique called Optical Time-Domain Reflectometer (OTDR) was created for testing optical cables in the telecommunications industry. In OTDR technique, a short optical pulse is launched into the fiber and then a photo detector processes the amount of light being backscattered as the beam propagates along the fiber. In this process, loss occurs due to the Rayleigh scattering that is a result of the microscopic and random variations of the fiber core refractive index as mentioned before. By monitoring the variations of the intensity of the Rayleigh backscattered signal, the spatial variations in the fiber scattering coefficient are detected or, as it's more commonly called, attenuation [25]. If the optical fiber is not affected by any external phenomenon, this attenuation decays exponentially with time. On the other hand, when the optical fiber under test (FUT) is subject to an external perturbation, attenuation will present a sudden variation localized on the perturbation as shown in Figure 4.

The spatial resolution of an OTDR instrument is the smallest distance between two scatters that can be resolved. For c standing for the velocity of light, n for the refractive index of the fiber and τ for the pulse width, the spatial resolution is given by Equation (1):

$$\Delta Z_{\min} = \frac{c\tau}{2n} \quad (1)$$

For a OTDR instrument with a pulse width of 10 ns, a current fiber refractive index of $n = 1.5$ and the velocity of light as $c = 3 \times 10^8$ m/s, from Equation (1) we obtain a spatial resolution of ≈1 m, which is relatively low, limiting the possible applications of OTDR in SHM. In order to increase this spatial resolution, the pulse width has to be reduced. However, in doing so, a decrease in the launched pulse energy may occur, also decreasing the detected light signal, and in this way, weakening the signal-to-noise ratio. This is problematic, especially for long-range sensing applications, so a basic trade-off between the spatial resolution and the sensing range is inevitable, requiring the optimization of the pulse width and pulse energy based on each application requirements [25].

As mentioned before, Raman and Brillouin scattering have been also used for distributing sensing applications. OTDR based on Raman scattering was developed to sense the ambient temperature during the 1980s.

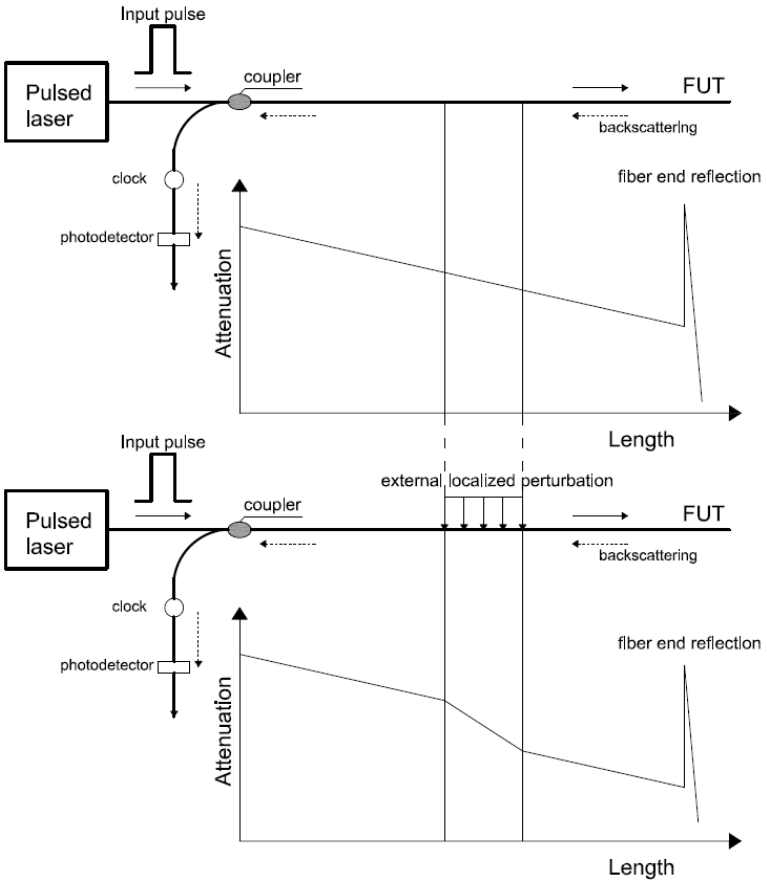

Figure 4. Principle OTDR based on Rayleigh backscattering.

BOTDR and BOTDA

As mentioned above, Brillouin scattering occurs from acoustic vibrations stimulated in the optical fiber [49]. These vibrations produce a counterpropagating wave, called Brillouin scattering wave, which weakens the forward-moving input pulse. To satisfy the requirement of energy conservation, there is a

frequency shift between the Brillouin scattering wave and the original light pulse frequency. This frequency varies for different temperature and longitudinal strain conditions, making it possible to measure strain and temperature distribution based on the Brillouin scattering effect [50]. Brillouin optical time domain reflectometer (BOTDR, Figure 5), is based on the spontaneous Brillouin scattering and was initially introduced as a way to enhance the range of OTDR and with the advantage of monitoring the system from one end of the sensing fiber [51]. Brillouin optical time domain reflectometer (BOTDR) sensors thus mark the beginning of strain and temperature measuring DOFSs.

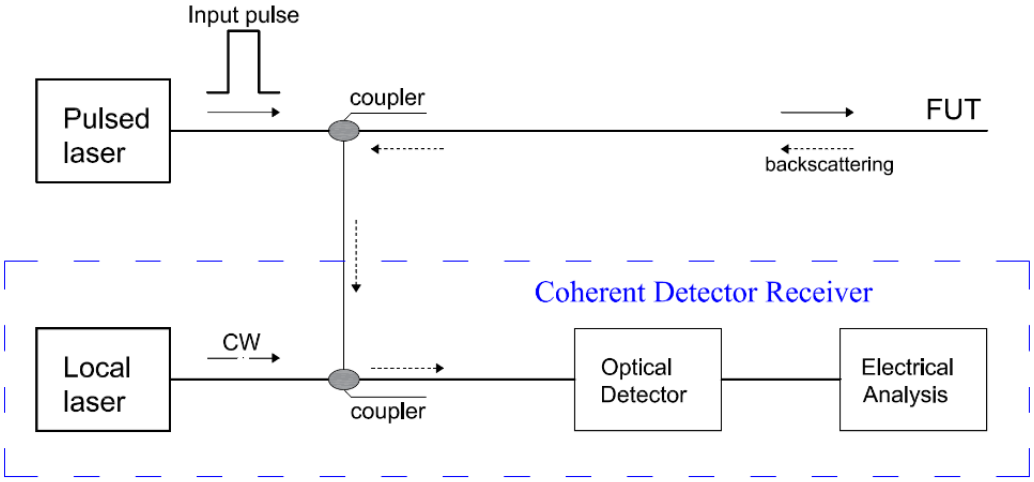

Figure 5. Typical configuration of a BOTDR setup.

On the other hand, Brillouin optical time domain analysis (BOTDA, Figure 6), is based on stimulated Brillouin scattering. This technique uses two counter propagating lasers and takes advantage of Brillouin amplification [13].

A coherent detection technique is necessary to detect the usually very weak counterpropagating Brillouin scattering signal [52]. In this way, the fiber is interrogated with a continuous wave (CW) from one end. Stimulation of the Brillouin scattering process occurs when the frequency difference of the CW signal and the pulse is equal to the Brillouin shift (resonance condition) [22].

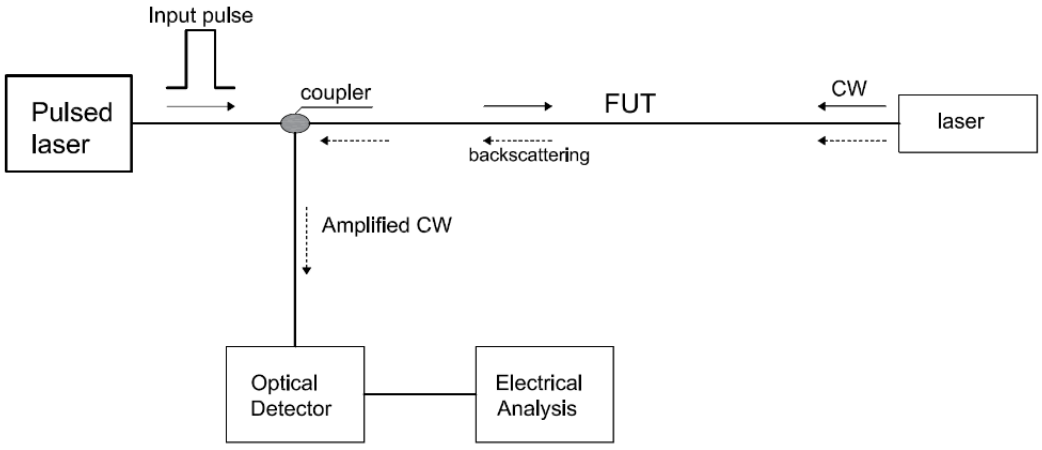

Figure 6. Typical configuration of a BOTDA setup.

The first early works on Brillouin-based DOFS were focused on temperature sensors. Among those works, [43,44,53] can be highlighted. The latter investigated the design of an optimized distributed sensor for temperature measurements based on the Brillouin gain/loss mechanism presenting data from a 51 km system, which was at that date, the longest sensing length reported.

BOTDR is normally capable of long-distance distributed sensing with a sensitivity of 5 με, which is suited for large-scale applications of structural and geotechnical monitoring [54]. However, both BOTDR and BOTDA are limited to a spatial resolution of roughly 1 m and therefore not suitable for a large range of structural monitoring applications. Different techniques have been studied with the intention of improving said resolution [55], such as the Brillouin optical correlation domain analysis (BOCDA) that improves this resolution to the cm level [56–58]. Furthermore, complex and advanced algorithms were studied and developed for several Brillouin backscattering based DOFS applications with the objective of improving its spatial resolution [59,60]. Notwithstanding, Brillouin backscattering based DOFS constitute the most studied and used DOFS systems in civil engineering structure SHM applications.

2.3.3. Frequency Domain Reflectometry

The goal of short spatial resolutions of millimeter scale and cost effective distributed fiber sensors has increased interest in Optical Frequency Domain Reflectometry (OFDR) systems [61–63]. In order to obtain a high spatial resolution with OTDR-based sensors, a very narrow light pulse is required, resulting in a proportionally lower level of the backscattering signal and, at the same time, an increased receiver bandwidth requirement in order to detect such signals [25]. Hence, the noise level is also expected to increase making the detection of small variations in the backscattered signal due to strain and temperature almost impossible. These combined factors make OTDR-based DOFSs with high spatial resolution very expensive systems. In this way, a DOFS with millimeter scale spatial resolution has been developed based on Rayleigh scattering OFDR [64–66]. This is the so called Optical Backscattered Reflectometer (OBR).

Rayleigh scattering originates from the interaction between the electromagnetic wave propagating in the fiber core and silica impurities [42]. In a simple way, the Rayleigh backscatter profile of a determined optical fiber results from its heterogeneous reflective index, which is distributed randomly along the whole length of the fiber. This constitutes as a fingerprint of each optical fiber and is a result of its manufacturing process [67]. When the fiber is subjected to an external stimulus (like strain) the backscatter pattern presents a spectral shift that is then used to calculate the strain changes along the length of the fiber by comparing it with the unaltered (unstrained) reference state.

Instead of reading the intensity of the Rayleigh backscattered signal, OFDR measures the interference fringes of the Rayleigh scattered light from a tunable laser source and a static reference

fiber in frequency domain. By means of the inverse Fourier transformation, the amplitude and phase in frequency domain are converted to the time/spatial domain [22].

Froggatt and Moore described the random fluctuation of the index of refraction that causes Rayleigh scattering as an equivalent FBG [66]. From this perspective, the whole length of the optical fiber is divided in several short sections (in the orders of centimeters) that are equivalent as a weak random FBG with a Swept-wavelength Interferometry (SWI). While the fiber is not perturbed, while random, this equivalent weak FBG is stable in time.

By scanning the frequency with the OFDR technique the spectral response of each equivalent FBG is obtained and in this way, strain and temperature variations with high spatial resolution. This resolution (Δz) is related to the optical frequency sweep range of the tunable laser source (ΔF) as given by Equation (2) where c is the speed of light and n the fiber refractive index:

$$\Delta \mathrm{Z} = \frac{c}{2n\Delta F} \tag{2}$$

The OBR-based DOFSs are excellent for short sensing lengths (<100 m [68-70]). Nonetheless, longer sensing systems are possible at the cost of spatial resolution, and temperature/strain resolution. Koshikiya *et al.*, for instance, reported the detection of high loss points with cm level resolution over 5 km measurement range with high sensitivity and a noise level 23 dB lower than the Rayleigh backscatter [71].

Notwithstanding, the OBR technique, with its high spatial resolution, even if limited to some hundred meters, addresses some applications that aren't easily covered either by Brillouin- or by Raman-based DOFSs [72].

A review of the performance of the discussed distributed sensing techniques as reported by different research studies is presented below in Table 1. The multiplexed FBG sensor technique is also included for comparison.

As already mentioned, Brillouin-based DOFSs are currently the most studied and applied measuring systems in civil structure SHM. This is due to their extended measurement range potential that makes them very useful for application on large structures, such as dams, pipelines, tunnels and long span bridges. Notwithstanding, some applications require a better spatial resolution than that provided by these sensors. The BOTDA sensing technique, through the application of advanced and complex algorithms, can address this point but in the process increases the price of this technology. The OBR technique (Rayleigh OFDR) offers a more cost-effective way of achieving high spatial resolution at the cost of limiting, nonetheless, the sensing range to about 70 m.

Table 1. Performance of distributed and quasi-distributed sensing techniques.

Sensing Technology	Transducer Type	Sensing Range	Spatial Resolution	Main Measurands
Raman OTDR	Distributed	1 km [73] 37 km [74]	1 cm [73] 17 m [74]	Temperature
BOTDR	Distributed	20–50 km	≈1 m	Temperature and Strain
BOTDA	Distributed	150–200 km [13]	2 cm (2 km) [75] 2 m (150 km) [76]	Temperature and Strain
Rayleigh OFDR/OBR	Distributed	50–70 m [11]	≈1 mm [66]	Temperature and Strain
FBG	Quasi-distributed	≈100 channels	2 mm (Bragg length) [21]	Temperature, Strain and Displacement

3. Civil Engineering SHM Applications with DOFS

The great majority of photonic sensing technology applied in the civil engineering area is constituted by discrete sensors such as FBG. This topic has been extensively discussed in different publications in the past decades [20, 77–82]. Taking in account the scope of this state-of-the-art paper, only applications of truly distributed sensing with fiber optics technology are presented.

Nowadays, DOFS sensors are an attractive technology that offers superior performance and advantages when compared with more conventional sensors applied in SHM practice. Despite their apparently high cost, they are ideal for applications where reliability in challenging environments is essential. Furthermore, they offer lower installation and maintenance costs.

However, this is still a recent and developing technology as it can be perceived by the relatively few number of DOFS applications in SHM projects. Notwithstanding, some different DOFSs applications were made in the last two decades in different civil engineering structures such as bridges, dams, tunnels, pipelines and slopes that are presented below. Also, a great amount of work has been done, and discussed below, with the goal of improving these sensors' capabilities by executing different laboratory experiments.

3.1. Laboratory Tests

In order to assure the proper operation of DOFS, one of the most important aspects to consider is the correct transfer of the measurands from the monitored structure to the sensor. Zeng *et al.*, for example, performed a strain measurement of a 1.65 m reinforced concrete beam with a Brillouin scatter-based DOFS where two different installation methods were analysed: fiber embedded in glass fiber reinforced polymer—GFRP—rods and fiber bonded to steel reinforcing bars [45]. Both methods were found to effectively protect the optical fiber strand and measure strain data. On the other hand, Hoult *et al.* performed a series of axial tension tests on steel plates using polyimide and nylon-coated sensing cables [83]. Overall, the polyimide-coated fiber presented a higher accuracy and a better correlation

with the results obtained with electrical strain gauges. However, its measurements seemed erroneous at crack locations. On the other hand, the nylon-coated fiber, although it can be used for crack detection and general deterioration, doesn't offer the same accuracy as the polyimide cable due to the slippage between the nylon coating and inner core.

Furthermore, sometimes, the DOFS protection can interfere in the collection of correct strain measurements. In order to overcome, or at least reduce these problems, and in this way effectively measure the strain of a RC structure after cracking, Quiertant *et al.* tested through a series of experiments the implementation of an OBR interrogation unit paired with fiber optic sensors in rebars with the goal of obtaining strain measurements in reinforced concrete structures made of Ultra High Performance Fiber Reinforced Concrete as seen in Figure 7 [84].

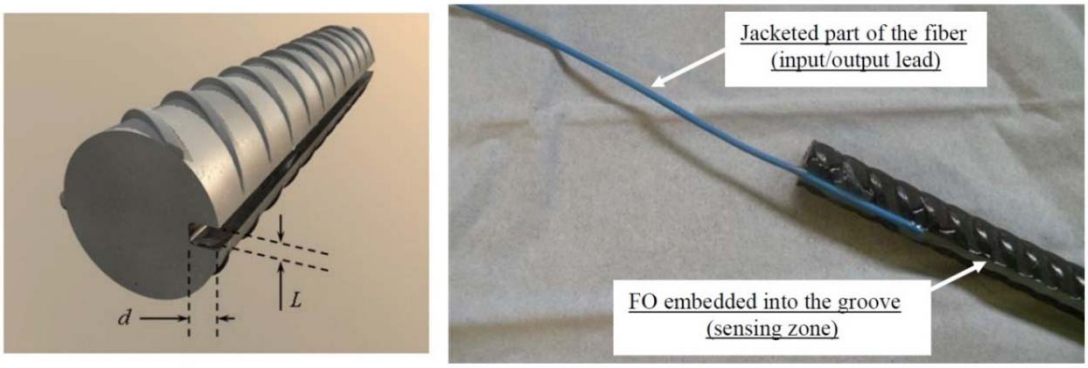

(**a**) (**b**)

Figure 7. Geometry of the groove in the rebar (a) detail view of the end of the bonded zone (b) [84].

The tested parameters of these experiments were the chosen method for the installation of the optical fiber, *i.e.*, an FO bonded on the rebar surface or mounted into a groove, the geometry of the groove and finally the typology of the used optical fiber (subject in its majority to its coating material, ~250 µm diameter polyimide or ~190 µm acrylate coated fiber). It was then found that a fiber optic sensor with a polyimide coating embedded in a groove cut along the rebar presented the best results.

As already mentioned, one of the most sought-out applications for DOFS is the crack detection in RC structures. However, one of the limitations of Brillouin-based DOFS is related to the fact that very significant strain changes that occur over lengths shorter than one-half of the spatial resolution are not detected and measured, making the application of this technology to crack detection very difficult. Deif *et al.* studied the possibility of enhancing the spatial and strain resolutions of distributed BOTDA sensors in order to overcome this issue [85]. A multiple-peak fitting method was applied to extract the strain distributions on the top and bottom surfaces along a RC beam that was subject to a four-point bending configuration. The multi-peak fitting method allowed the spatial resolution of the measurements to be improved from 15 cm (of the sensor) to 5 cm (read-out resolution). However, despite being able to capture damage build-up, the system was unable to detect and precisely locate the formation of cracks, as seen in Figure 8.

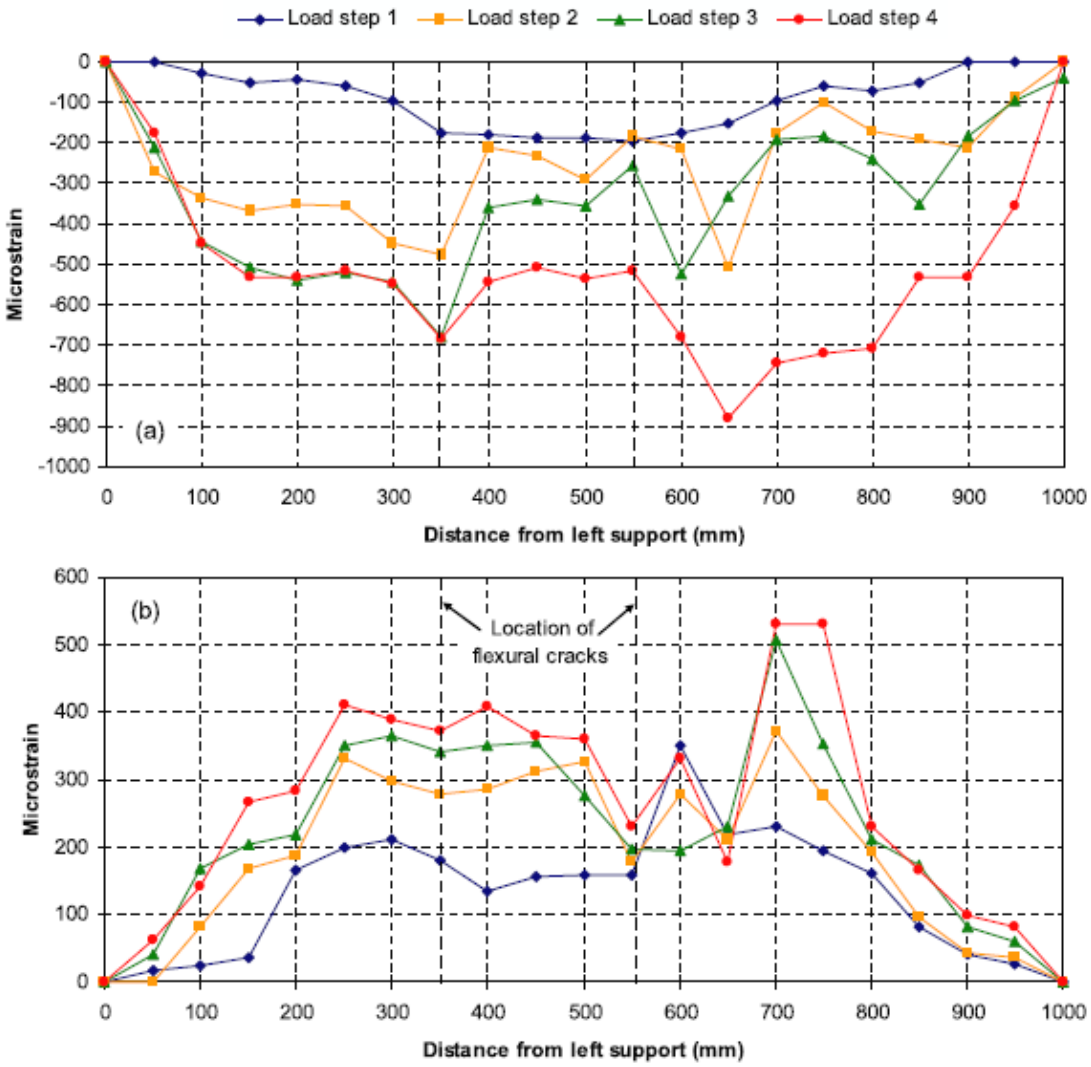

Figure 8. (a) Compressive and (b) tensile strain distributions measured by distributed Brillouin sensors [85].

Glisic and Inaudi also evaluated the performance of the application of an advanced algorithm that was developed to avoid this limitation through several laboratory tests where the distributed temperature and strain monitoring system was based on the changes in Brillouin frequency [14]. For these tests a specific set-up was built and used to tension 10 cm of optical fiber with different previously defined values. All of these simulated crack openings were correctly and successfully detected and localized.

Furthermore, these authors, taking into account the risk of optical fiber breakage when the stress generated by the crack is very high and the fact that this developed algorithm was only suitable if local stress was redistributed over a minimum length of 10 cm, decided to create, at the location of the crack, a mechanism of sensor delamination to ensure that the system would continue to perform even for high strain levels. For this, they paid special attention to the selected adhesive.

This delamination mechanism and selected adhesive were then tested in laboratory with the use of a specific set-up where the DOFS was glued to metallic supports that were given a relative translation movement with the objective of simulating a 0.5 mm crack opening. The obtained test results proved

the delamination mechanism and confirmed the good selection of the adhesive and the performed installation procedures. This demonstrated the capability of the system in detecting and localizing cracks with openings smaller than 0.5 mm. This system was later tested on a pipeline [86] and implemented in the monitoring of a bridge [14,87] with good performance of the implemented crack detection method.

Zhang *et al.* investigated the development of a health monitoring system (HMS, Figure 9), that combined BOTDR and multiplexed FBG techniques with the intention of implementing it on rehabilitated concrete girder bridges [88]. For this, a series of static and dynamic loading tests to a simply supported reinforced concrete T-beam strengthened by externally post-tensioned tendons were executed.

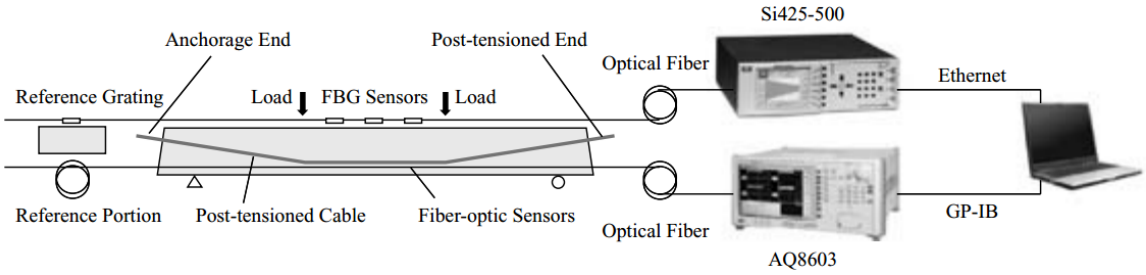

Figure 9. Configuration of the proposed SHM [88].

This developed SHM system proved its great efficiency for operation by correctly identifying the relevant structural state for each loading state.

With the goal of exploring the capabilities of crack detection in concrete elements, without the occurrence of sensor failure and debonding, Villalba and Casas instrumented a concrete slab with OBR-based DOFS, glued to the bottom and upper surfaces, that were subject to a load test [89]. The slab was also instrumented with more conventional electrical sensors, such as embedded strain gauges and LVDTs for comparison purposes. A coating of polymer (polyimide) was used to protect the fiber. This technology was not only able to detect crack openings locations, but also to continue to correctly perform measurements up to load levels producing a crack width in the range of 1 mm. The results obtained in this experiment compared very well with the available data from the other instrumented sensors as well with visual inspection and predicted values of nonlinear FE models [90].

This group also implemented a novel technique in partially prestressed concrete (PPC) beams with OBR sensors in order to detect induced shear cracks. This is of extreme relevance since that contrary to what happens with bending cracking, where the cracks appear orthogonally to the beam axis, in the case of shear action, the inclination of the cracking pattern is previously unknown and may even change depending on the prestressing force and the location along the element [91]. For this, a two-dimensional DOFS grid was proposed that monitored the crack initiation, location, inclination and evolution during a beam load test, as seen in Figure 10.

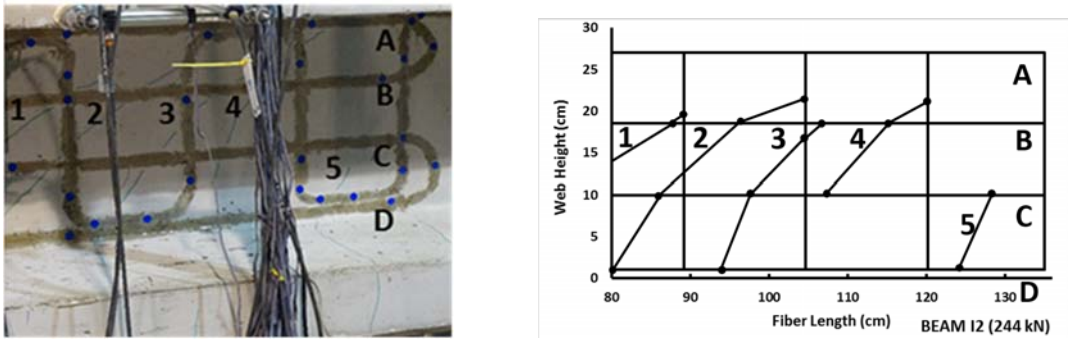

(**a**) (**b**)

Figure 10. Comparison of real shear crack pattern (a) and obtained by OBR system (b) (adapted from [91]).

These results showed good agreement with the visualized cracks and were obtained without requiring prior knowledge of the cracked zone and consequently proved the feasibility of this methodology.

Henault *et al.* conducted laboratory experiments where a concrete slab was instrumented with Raman-, Brillouin- and Rayleigh-based DOFS in order to obtain strain measurements (the Raman sensor was used for temperature compensation). BOTDR sensor results were limited by their poor accuracy (1 m spatial resolution combined with 20 μm/m) while OBR sensors provided very promising results [42]. However, since the applied load induced relatively small strains, temperature variations caused misinterpretations. The implemented DOFS were embedded in the concrete and the influence of the coating and installation process were also studied and highlighted.

The same research group also monitored a 3.4 m long reinforced concrete beam with a 0.25 × 0.5 m^2 rectangular cross section that was subjected to a four-point bending test through the utilization of different Rayleigh scattering-based DOFS (three levels embedded in the concrete and two levels bonded to the external surface of the RC element) that were paired with Vibrating Wire Gauges (VWG) sensors as seen in Figure 11.

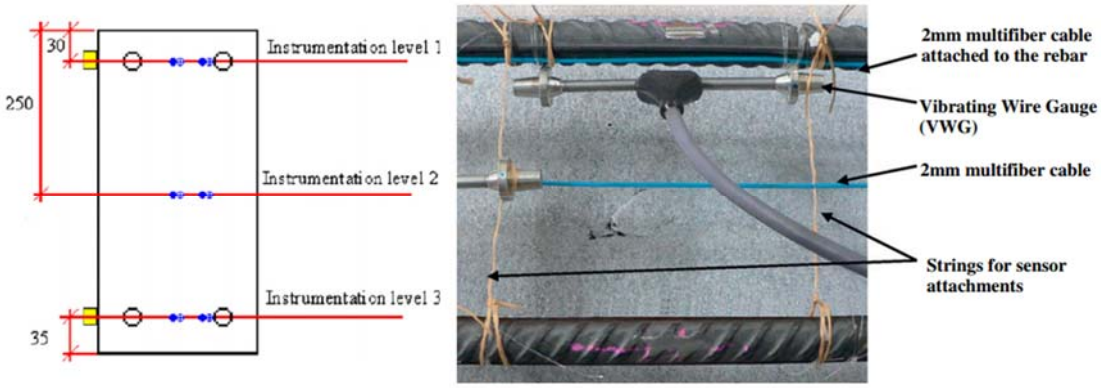

(**a**) (**b**)

Figure 11. (a) details of the cross-sectional instrumentation at mid-span of the beam (dimensions in mm); (b) Picture of the instrumented beam before concrete pouring (adapted from [92]).

The test was divided in two phases. In the first one, the applied load level was below the concrete tensile resistance in order to check the performance of the different applied sensing systems. One interesting conclusion obtained from this part of the test was the much reduced influence of the location of sensors for strain measurement since the results obtained for the embedded (both close and far from the rebar) and the external bonded sensors presented a relatively good agreement both in compression and in tension, as seen in Figure 12.

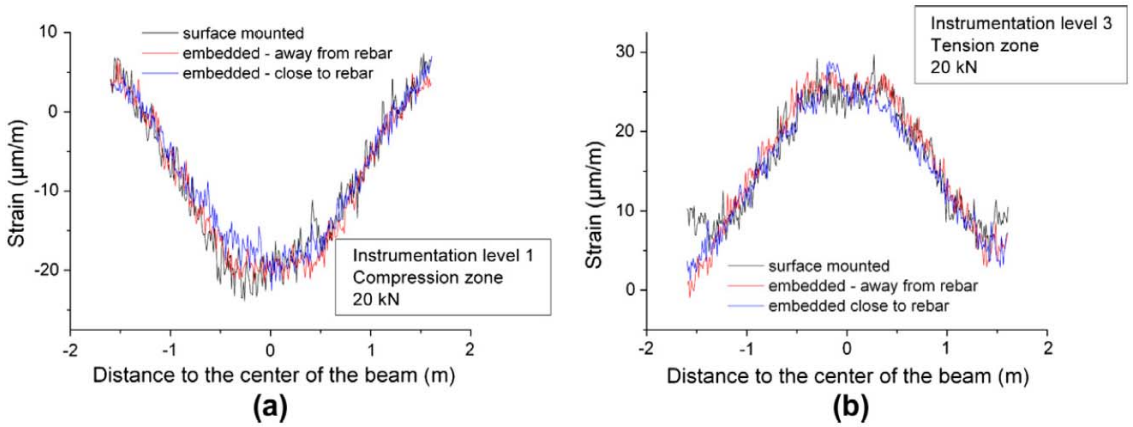

Figure 12. Strain profiles provided by DOFS system for a 20 kN bending load: (a) in the compression zone at instrumentation level 1 and (b) in the tension zone at instrumentation level 3 [92]

In the second phase, the incipient cracks were induced in order to assess the capability of the used DOFS sensors in detecting their location. Despite the fact that the RC specimen was severely damaged at high-load levels, the optical fiber cables didn't present any tensile rupture. As seen in Figure 13, it was possible to detect the location of cracks (even before visual inspection) from the experimental data provided by DOFS and track its evolution.

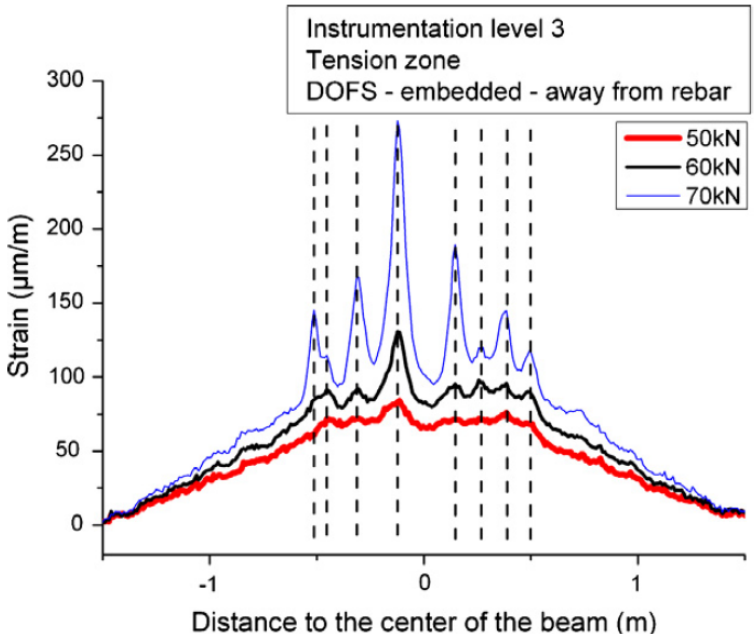

Figure 13. Tensile strain profiles recorded by the Rayleigh scattering based DOFS for various bending loads above 50 kN (adapted from [92]).

The same investigation group developed an algorithm to automatically analyse crack evolution in RC elements [93]. This process provided a precise map of cracks with the evolution of their amplitudes and was tested with a four-point bending test like the one mentioned above.

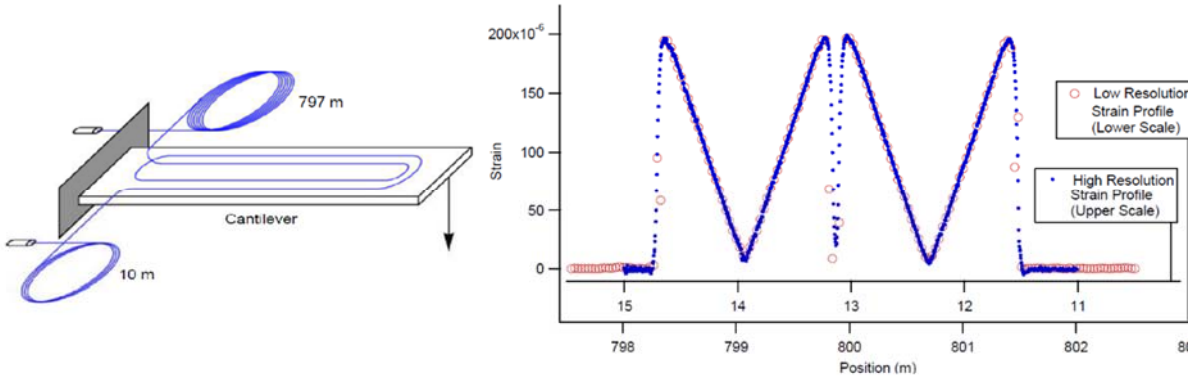

(**a**) (**b**)

Figure 14. (a) Diagram of cantilever beam used for strain measurements. The fiber was adhered to the beam in a double loop and the two ends were spliced to leads of fiber with 10 m and 797 m lengths respectively; (b) Strain on the cantilever as measured from both fiber inputs (adapted from [95]).

One of the referred limitations of Rayleigh-OFDR-based sensing it's the relatively short sensing range in order to obtain high spatial resolution measurements. However, Gifford *et al.* reported high precision measurements with OBR system over a two kilometer extension [94]. The same authors also successfully assessed the strain measurements capabilities of this test for both near (10 m) and long distances (≈1 km) through an experiment carried out on a cantilever beam as shown in Figure 14.

This research group also performed another general test in order to validate the applicability of Rayleigh-OFDR sensors for temperature sensing [95]. This experiment consisted on a resistively heated metal rod that reached temperatures as high as 600 °C and then was subjected to a thermal gradient by dropping water on a localized spot on the rod that was instrumented with gold-coated optical fibers (to ensure fiber integrity at high temperatures) that were isolated in order to be unresponsive to strain Figure 15.

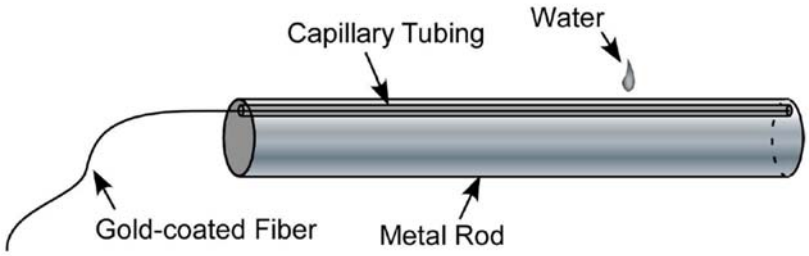

Figure 15. Test article for measuring at high temperatures with a strong thermal gradient [95].

The results, as shown in Figure 16, confirmed the ability to measure temperature with a high spatial resolution with Rayleigh scatter-based DOFS.

Rayleigh backscatter-based DOFS were also reported in an application where localized heating was measured with millimeter spatial resolution [96]. Another successful application of Rayleigh based sensors for temperature measurements is reported by Sang *et al.* [97] in a nuclear reactor. More recently, Sierra-Pérez *et al.* compared the strain measurements of Fiber Bragg Gratings, and OBR- based distributed optical fiber and conventional electrical strain gauges sensors [98]. The two fiber optic technologies were deployed into a 13.5 m wind turbine blade subject to a load test. Several strain gauges were installed at the same locations than the FBGs and in additional places across the structure, as seen in Figure 17.

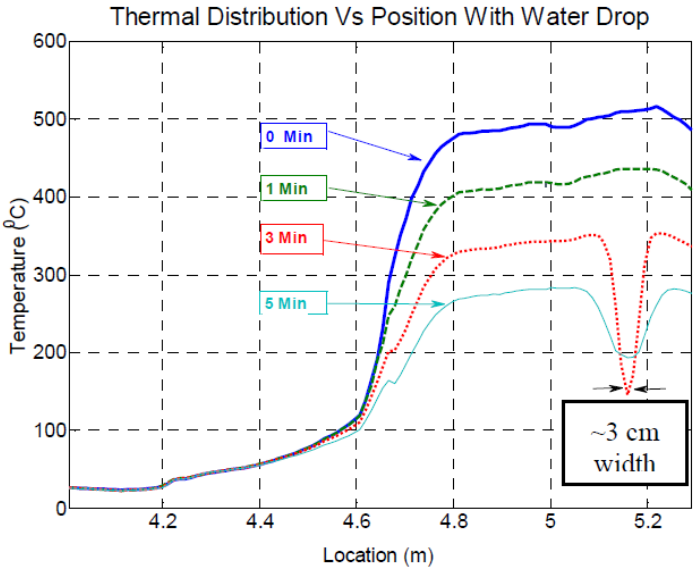

Figure 16. Temperature *vs.* location for fiber in heated metal rod (the fiber enters the rod at about 4.8 m) [95].

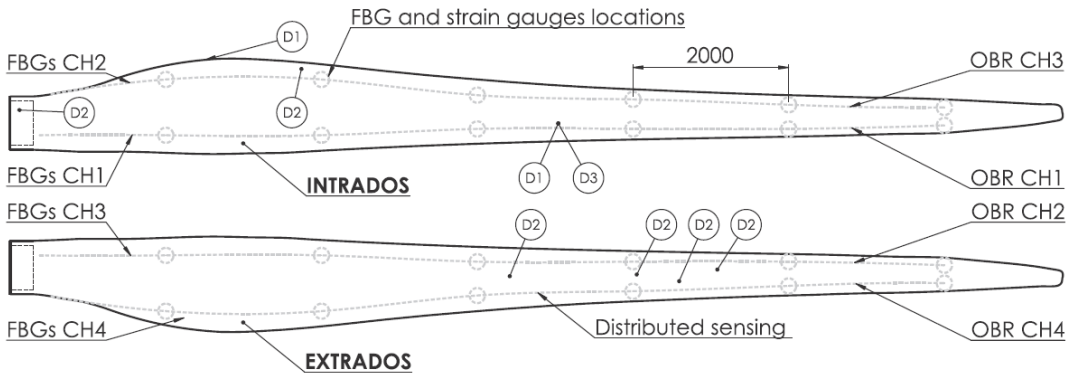

Figure 17. Sensors and damage locations in wind turbine blade. All units in mm [98].

The fiber optics sensors proved to effectively measure strain and correspondent cracks induced during the test as seen in Figure 18.

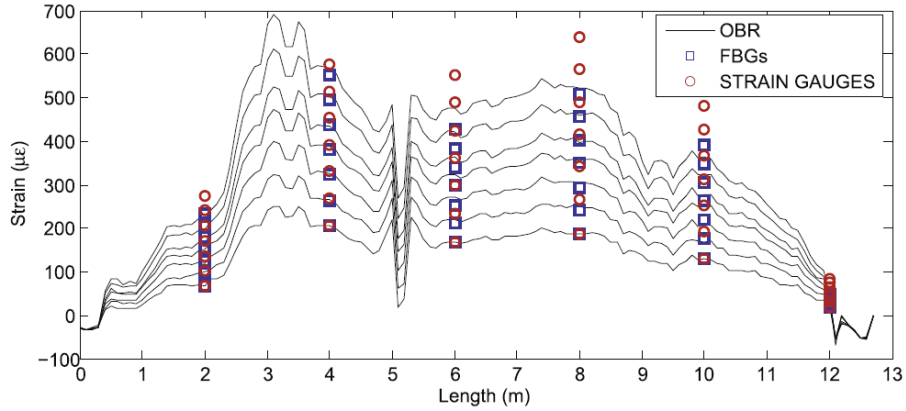

Figure 18. Example of strain profiles for seven load magnitudes gathered with the OBR, the FBGs and the strain gauges [98].

3.2. Geotechnical Structures

Due to its wide range capabilities, DOFS are becoming a very attractive technology for the instrumentation of geotechnical structures. However, when monitoring slope stability, the most common applied sensors are discrete ones such as inclinometers, crack detectors, reinforcement stress detectors and displacement meters. In this way, a global behaviour of the slope is not easily obtained. To make things worse, these instruments are often incompatible with the deformation of the rock-soil mass, and the difficulties associated with installation procedure and bad measurements situations regularly turns the application of these sensors pointless. Shi *et al.* tested the feasibility of the application of a BOTDR-based distributed optical fiber sensing system for slopes as seen in Figure 19 [99].

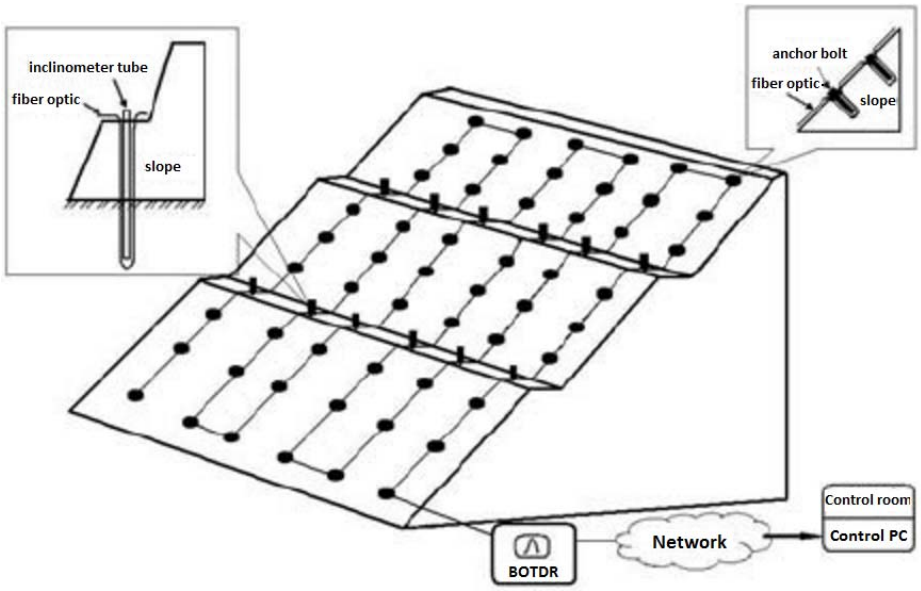

Figure 19. The diagram of BOTDR-based distributed fiber optical sensing monitoring system for slopes [99].

The results are shown in Figure 20 for the period between January and July of 2005 where it's possible to see the increase of strain, especially near the top of the anchor. This trend was related with the slope creep associated with the rainy season.

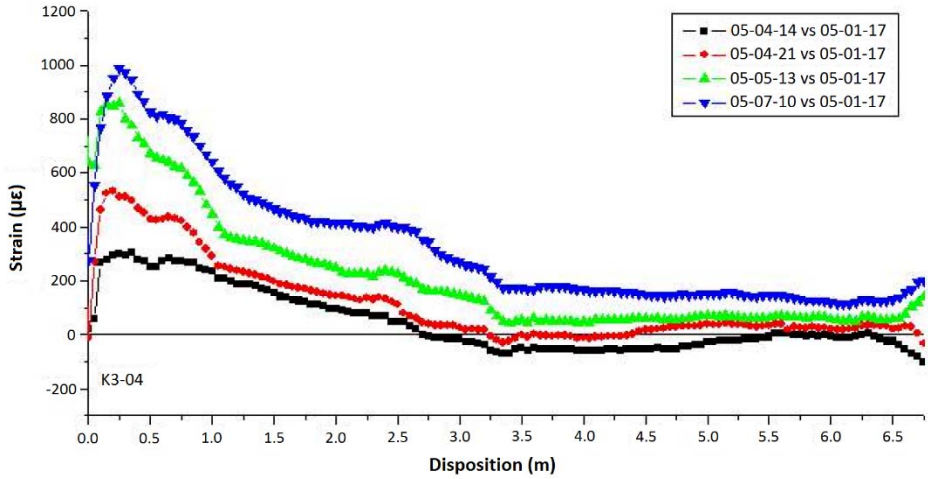

Figure 20. The time history plot of strain distribution along the K3-04 anchor axis [99].

More recently, Zhu *et al.* built a medium-sized model of soil nailed slope in laboratory in order to assess the efficiency of monitoring slope stability problems through the employment of BOTDA sensing technology [100] (Figure 21).

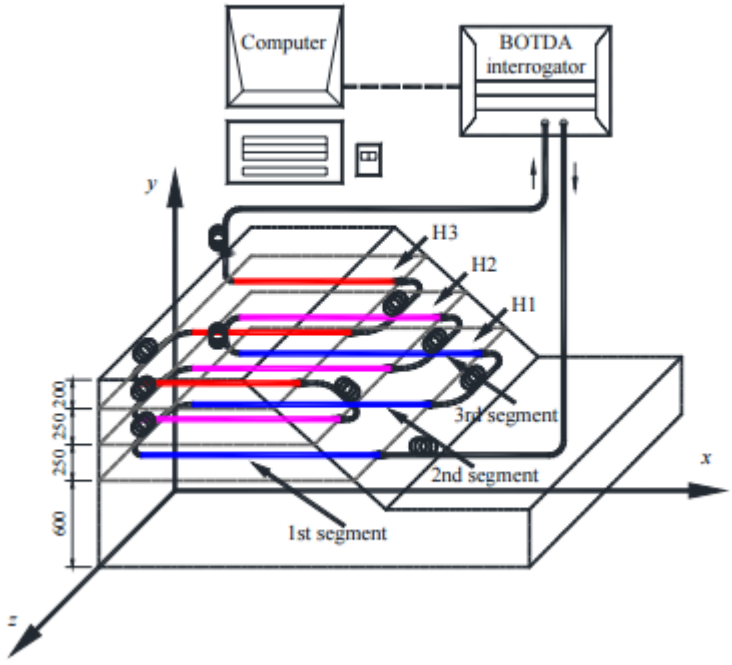

Figure 21. Layout of the BOTDA sensing fiber in the model slope (unit: mm) [100].

The model was subjected to a surcharge loading test. Its results proved the feasibility of measuring horizontal strain distributions within the slope mass that reflect the deformation pattern that can be used to pinpoint the potential slip surface in the slope. Furthermore, it was concluded that the results obtained

by the distributed fiber optic system can be used to estimate the stability conditions of the slope due to an empirical relationship between the characteristic maximum strain and factor of safety of the slope.

Klar *et al.* assessed both BOTDA- and Rayleigh scattering-based DOFS capabilities of monitoring tunneling induced ground displacements [101]. This was based on the idea that a distributed optical fiber within the ground would deform due to the mentioned ground displacements. A detailed study of the soil-fiber interaction was presented by Klar and Linker where it was concluded that the DOFS essentially follows the same displacement of the soil due to its low rigidity [102]. This approach was tested in two different field investigations and it was concluded that both distributed fiber optic technologies provided results that could only be matched by multiple sub-millimeter displacement measurements and are more sensitive than laser-based displacement measurements (Figure 22). However, the authors pointed out the advantages of the OBR system due to its high-spatial resolution and possibility of conducting immediate measurements (less than 5 s) as opposed to BOTDA sensors (10 min).

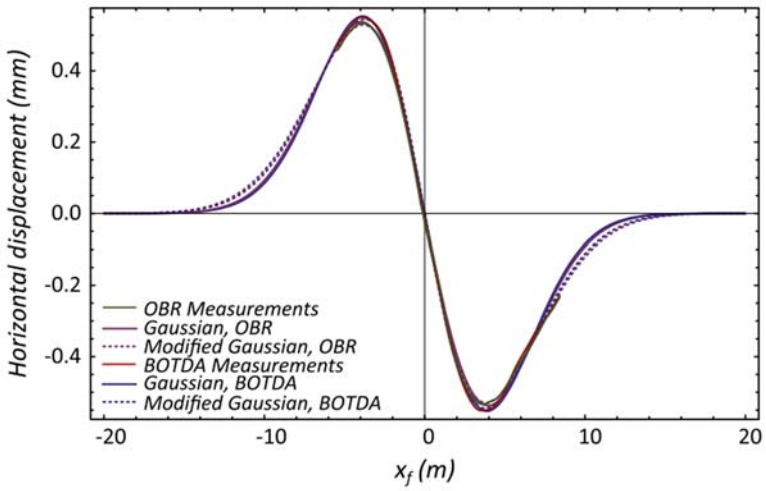

Figure 22. Integrated strain by OBR and BOTDA and best fit model for horizontal displacement from one of the field investigations [101].

The feasibility of applying the BOTDR technology for strain measurement in the Taiwan Strait Tunnel project was tested on the Nanjing Gulou tunnel (Nanjing, China) with good results as reported by Shi *et al.* [103]. This technology was also deployed for the strain measurement of the Xuanwuhu Lake tunnel in Nanjing, China [104], and Royal Mail tunnel at London (UK) [105].

In the framework of a system to detect sinkholes and embedded soil cavities, Lanticq *et al.* compared an OFDR-based strain sensor with a Brillouin-based one [106]. Tests performed on a railway tunnel suggested that the OFDR-based system is more effective owing to its better spatial resolution [72].

Finally, Wu *et al.* applied BOTDR and FBG sensors in order to monitor the deformation of soil layers and pore water pressure in a 200 m borehole over nearly two years in Suzhou, China [107]. Three

different types sensing fibers: polyurethane sheath cable (PSC), metal-reinforced cable (MRC) and 10 m fixed-point cable (FPC) were used, as seen in Figure 23.

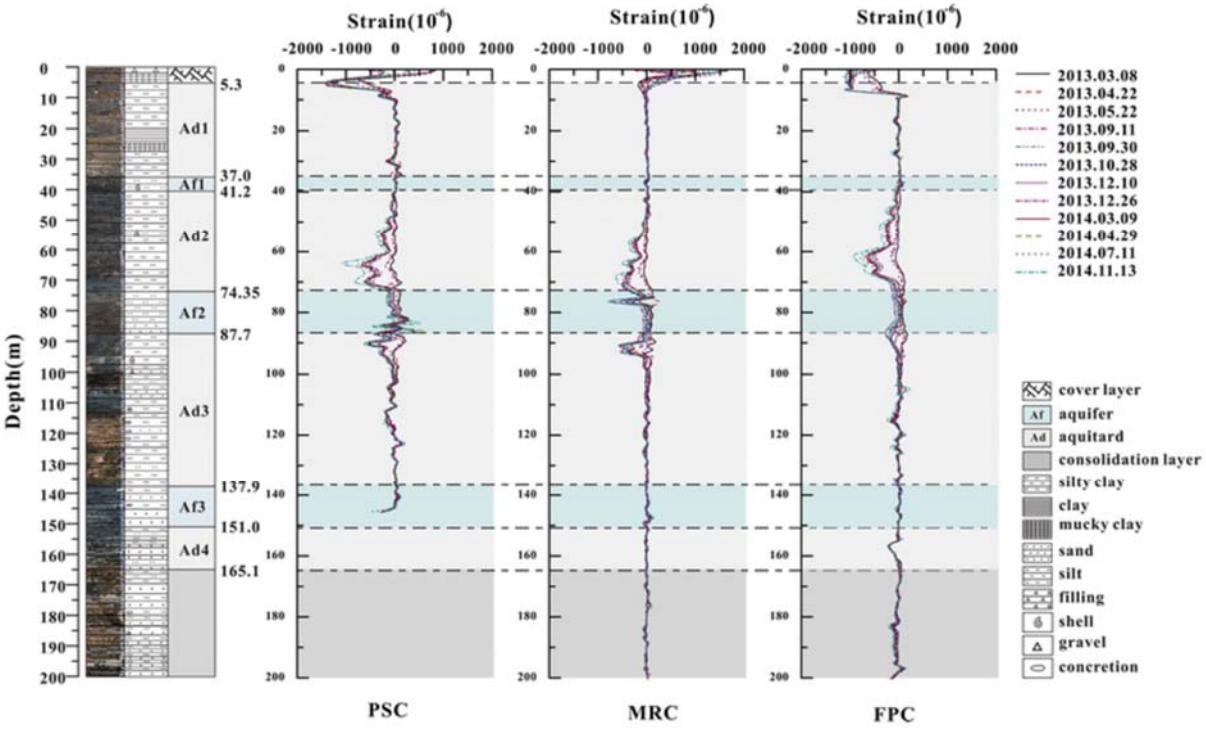

Figure 23. Drill core profile and strain distributions of three cables within 200 m depth [107].

The results showed the incomparable potential of DOFS for soil subsidence monitoring as the strains at any depth of the soil layers were achieved. Regarding the different types of used cables, it was concluded that PSC was unable to monitor land subsidence at deep levels due to its small stiffness. Another borehole strata deformation monitoring with BOTDR-based sensors is also reported in [108].

3.3. Pipelines

The application of distributed sensing technology in the Oil and Gas industry is of great interest and therefore has seen a substantially increase in recent years. Distributed and quasi-distributed techniques based on Brillouin and FBG technologies, respectively, have been the most commonly used [2]. Glisic and Yao performed a large scale test on a pipeline [86]. The main goal of this experiment was to develop a method for the implementation of a distributed fiber-optic system and at the same time provide a reliable way of real-time monitoring of pipelines that were subject to permanent ground displacements induced by earthquakes. In this way, a 13 m long concrete pipe with an exterior diameter of 30.48 cm was instrumented with a distributed fiber sensor based on Stimulated Brillouin scattering, along its length as shown in Figure 24.

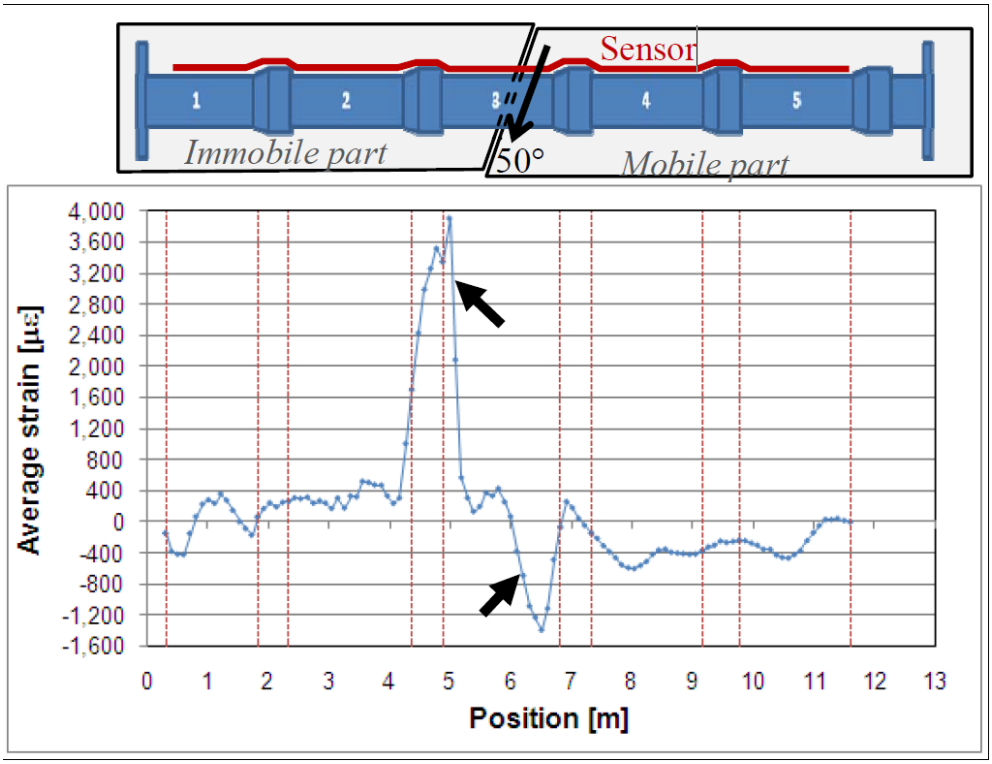

Figure 24. Results of test with detected damage (indicated by arrows) [109].

In this test, a relative translation with an angle of approximately 50° was induced by hydraulic jacks between two parts, an immobile and a mobile part, Figure 24, where it is possible to observe a high tension point near joint number 2 and a high compression one close to joint number 3. These strain changes coincided with locations of damage in the pipeline. These proved the ability of the used system to detect cracks in close-to-real conditions and in real-time [14]. Another successful pipeline Brillouin DOFS monitoring example on a 35 years old gas pipeline near Rimini, Italy is described by Inaudi and Glisic [110]. In addition, Lim *et al.* 2015 were able to monitor the deformation of the cross section of a non-circular PVC pipe due to the dead weight of its carrying water reflected as oscillations in strain measurements made by BOTDA sensors that were deployed helically on the pipe [111].

3.4. Bridges

One of the most appealing areas for the application of DOFS has been naturally the instrumentation of bridges. The Götaälv bridge (Figure 25) in Gothenburg (Sweden), is a 1000 m long bridge composed by a concrete slab poured on nine steel girders that are then supported on more than 50 columns [14,112,113]. The responsible traffic authorities, after the detection of several cracks in the steel girders required a continuous monitoring system for this structure. The capabilities of DOFS proved unique here since there was a great necessity of covering the full length of the structure as a crack could appear virtually at any point or in any girder. Hence, a DOFS system based on Stimulated Brillouin Scattering was successfully implemented and tested in 2007–2009 followed by a one-year trial period [47,114]. Currently, the SHM of this bridge is still ongoing, making it probably the only true long-term implementation of DOFS on a real structure.

Figure 25. Götaälv bridge in Sweden [114].

Another slab-on-girder bridge monitoring with a Brillouin based DOFS is reported in Matta *et al.* [115]. A 1.16 km optical circuit was implemented onto the girders for strain measurement and temperature compensation. The overall response of the girder was successfully measured by the BOTDR system and verified by a high-precision total station system.

A complete and interesting long term monitoring application is described by Glisic *et al.* in [116]. Here DOFS were embedded in the concrete during construction of the Streicker Bridge (a pedestrian bridge located on the Princeton University campus) allowing for the acquisition of important data related with the global performance of the structure, *i.e.*, from the early behaviour of the concrete to the identification of damage, which was unprecedented. These sensors were validated by FBG sensors that were also deployed on this structure.

Bastianini *et al.* compared two different Brillouin sensor installation techniques, near-to-surface fiber (NSF) embedding and "smart" FRP sensor bonding [117]. The two systems were implemented in small reinforced concrete bridges that were in their turn subjected to a diagnostic load test. In the obtained results, it was possible to verify the clear advantages associated with the application of the smart-FRP system related with installation cost, time reduction and performance enhancements. It should be noted that this system was also tested by the same authors as reported in [118] on a historical building where the effectiveness of Brillouin strain monitoring was verified even for reasonably weak strain levels.

In 2010, Villalba *et al.* implemented the OBR system on the bottom surface of the slab of a newly built highway viaduct in Barcelona for its monitoring during the bridge load test, thus marking the first time that a distributed sensing method with millimetric spatial resolution was used for load testing of a real, newly built concrete bridge [119,120].

In order to take advantage of the extended and global range of DOFS and at the same time achieve a high sensitivity, Zhao *et al.*, implemented a multiscale fiber optical sensing network with both FBG- and BOTDA-based sensors [121]. A more comprehensive information of the structure was reported thanks to the DOFS technique by easily obtaining the overall stress condition of the structure.

Regier and Hoult employed DOFS technology in the monitoring system of a reinforced concrete bridge (the Black River Bridge) outside of the town Madoc, Ontario (Canada) [122]. The OBR-based DOFS obtained good results that were validated by other instrumentation such as strain gauges. Furthermore, the results obtained by the distributed fiber optics were then used to calculate deflections that compared well with measurements obtained by displacement transducers sensors. This confirmed that, provided the boundary conditions, measurements of distributed fiber optic sensors can be used to obtain structural deflections. Despite effectiveness of the employed DOFS in locating cracks and the strains related with crack widening during loading, the strain measurement in the locations near the cracks was reported as a challenge due to the fiber robustness properties. Additionally, the subject of temperature compensation was deviated through the acquisition of data over short term periods, however further research was advised for this topic regarding long-term monitoring and also for techniques that would make possible the accurate conversion of strain measurements at a crack to a crack width.

More recently, Rodríguez *et al.*, instrumented one span of a bridge in Barcelona, Spain with an OBR system, glued without protective coating to the inner surface of the slab girder of the bridge, in order to monitor this structure during a deck enlargement rehabilitation, Figure 26. This process was conducted through several months, spanning from summer to winter, so consequently the topic of temperature influence in the measurements was a relevant issue that needed to be addressed [123].

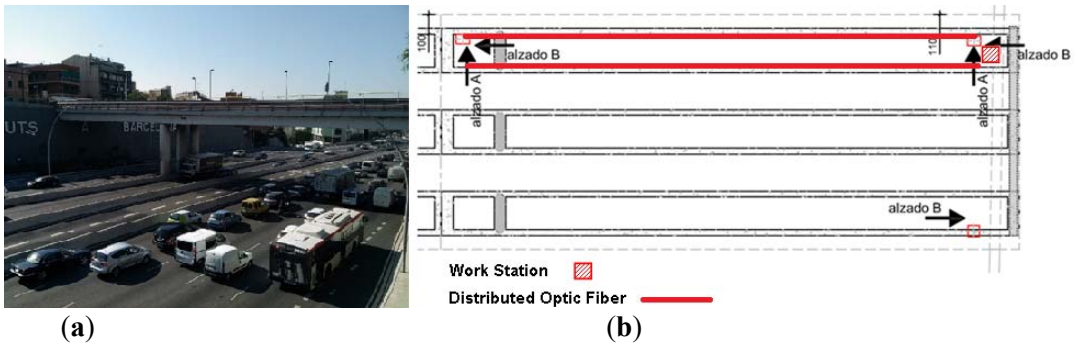

Figure 26. Sarajevo Bridge at Barcelona (a) and general scheme of DOFS monitoring scheme (b) (adapted from [123]).

With this implemented system it was possible to control the strain variation on the deck due to different and various stages of the widening process, ensuring in this way its structural safety.

3.5. Dams

Like bridges, also dams constitute an ideal area of application of DOFS monitoring due to their massive dimensions. Thévenaz et al. was some of the first to assess the implementation of Brillouin distributed fiber optic sensors for the monitoring of a dam [112]. An increase of the power capability of the hydroelectric plant associated with the Luzzone dam in the Swiss Alps was achieved by stacking new 15 m × 10 m concrete slabs for a 3 m thickness. In this way, a DOFS was installed during the

pouring of the concrete in a dense mat geometry in order two provide a 2D temperature distribution of the slab. It was able to observe that after several weeks despite that the outer regions had a relatively stable low temperature, it took a lot of time to cool the central area that reached temperatures of up to 50°C and that otherwise would have gone unnoticed. These measurements proved to be reliable even for the demanding environment present, including snow, dust and great temperature deviations.

Furthermore, the German Federal Ministry of Education and Research started a national research program named "Risk Management of Extreme Flood Events" (RIMAX) due to extreme floods in two large German rivers (the Oder in 1997 and the Elbe in 2002) in order to come up with smart monitoring systems that would be able to detect incipient effects of failure of hydraulic engineering structures. The main idea was to integrate FOS into geosynthetics that would be applied in the stabilization of geotechnical structures such as dams or dikes as seen in Figure 27.

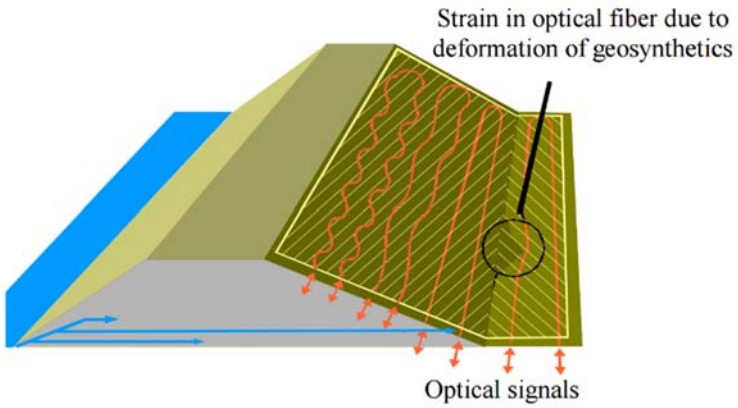

Figure 27. River dike with sensor-based geosynthetics [26].

Another case of dam monitoring using a commercial system named DiTeSt based on BOTDA technology is reported by Inaudi and Glisic for the Plavinu dam in Latvia [124].

3.6. Examples in Other Fields

The most sought out applications of DOFS were reviewed above, nonetheless, this technology, due its remarkable versatility, has found a wide range of potential applications that have been studied and developed in the past years and that are presented below.

For instance, historical buildings play an important role in the cultural heritage of any society; therefore the collection of data about their structural behaviour is paramount in order to maintain such structures. The field of discrete fiber optic sensors has found a wide range of applications in this area. The same has not been observed with DOFS, except for the already briefly mentioned studies mentioned in [118] and [123]. In the latter, they implemented an OBR system during the replacement of two columns, for the monitoring of the adjacent upper slab of Sant Pau Hospital (a UNESCO World Heritage Site, Figure 28) in Barcelona [123]. This system allowed the successful assessment of the structural

stability and safety of the slab by analysing the slab stress redistribution in a distributed and continuous way (both in time and space).

(**a**) (**b**)

Figure 28. Sant Pau Hospital, Barcelona (a) and DOFS installed on the masonry vaults (b) (adapted from [123]).

Monitoring of loss of prestress in concrete beams is of great importance. Lan *et al.* proposed a novel smart steel strand that combined BOTDA and fiber Bragg grating sensors on a single optical fiber by embedding it into a 5 mm diameter fiber-reinforced polymer (FRP) rebar [125] (Figure 29).

For this, they tested several prestressed RC beams simultaneously monitored by BOTDA/R and FBG sensors that were then compared the results with measurements from more conventional sensors. Their results confirmed the viability of the proposed sensing system showing not only the spatial distribution of prestress loss, but also its time history for both construction and in service phase.

Casas *et al.* also reported the monitoring of a cooling tower in Spain with an OBR sensor system [120]. Two main vertical cracks had appeared in this structure and a DOFS system was implemented, glued to the surface of the structure, in order to monitor the structural behaviour before and after crack repair. This allowed the increase of the lifetime of the monitored structure by showing the origin of the main cracks and the means for implementation of the appropriate repair methods.

Furthermore, with the advance of new materials more and more flexible structures are being developed either for civil, mechanical and aerospace applications. These structures are designed for critical loads that are associated with dynamic loading conditions and therefore the monitoring of the distributed shape of flexible components provides important information during design, testing and operation. In this way Lally *et al.* proposed a novel, helically-wound geometry fiber (Figure 30), that uses Rayleigh scattering-based OFDR and is able to measure distributed curvature, twist, longitudinal strain/temperature and 3D shape along its entire length [126]. For more information about the behaviour of this sensor the reading of the corresponding patent is advised [127].

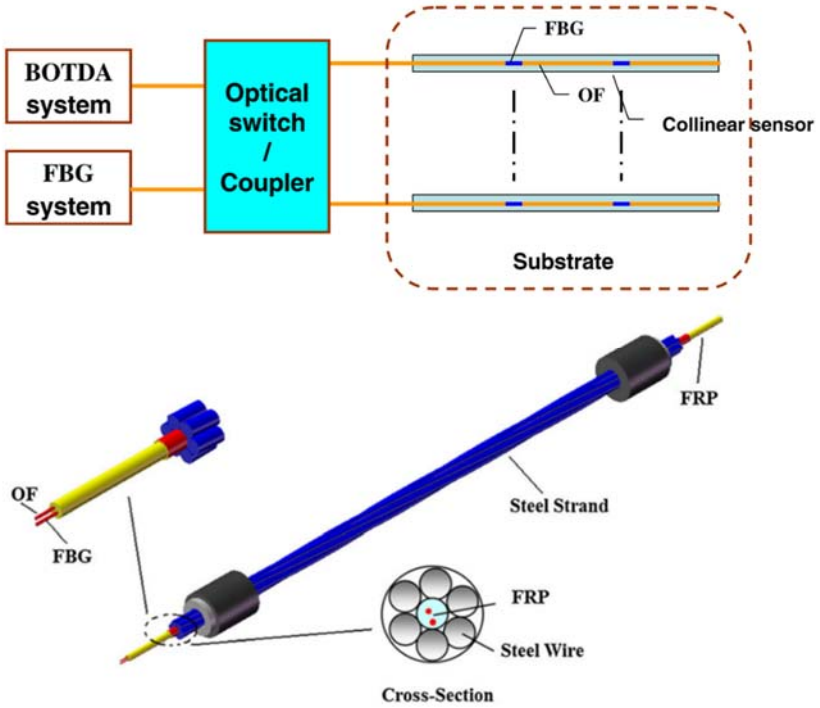

Figure 29. Proposed novel smart steel strand with FBG and BOTDA on a single fiber (adapted from [125]).

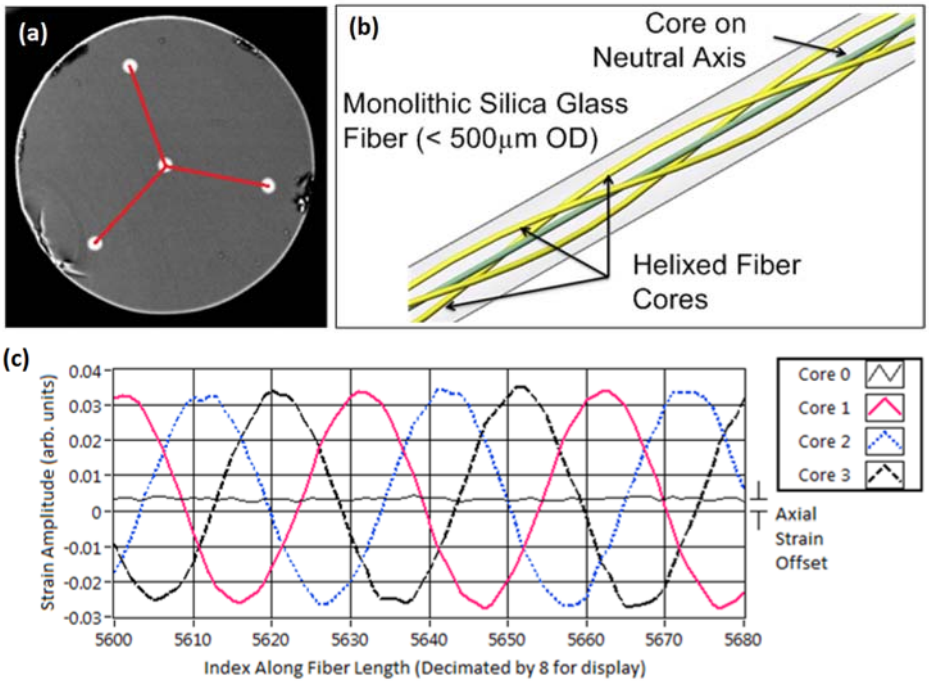

Figure 30. Illustration of shape sensing using helixed multi-core optical fiber: (a) SEM micrograph of shape sensing fiber, sensing triad in red; (b) Illustration of helical cores along length of fiber; (c) Typical four-core strain response to external curvature [126].

To test this new sensor, the authors conducted a laboratory test that consisted on the application of this fiber on a 10 m long flexible structure that would be subject to a 1.4 m translation at one of the ends of this structure as seen on Figure 31 (a).

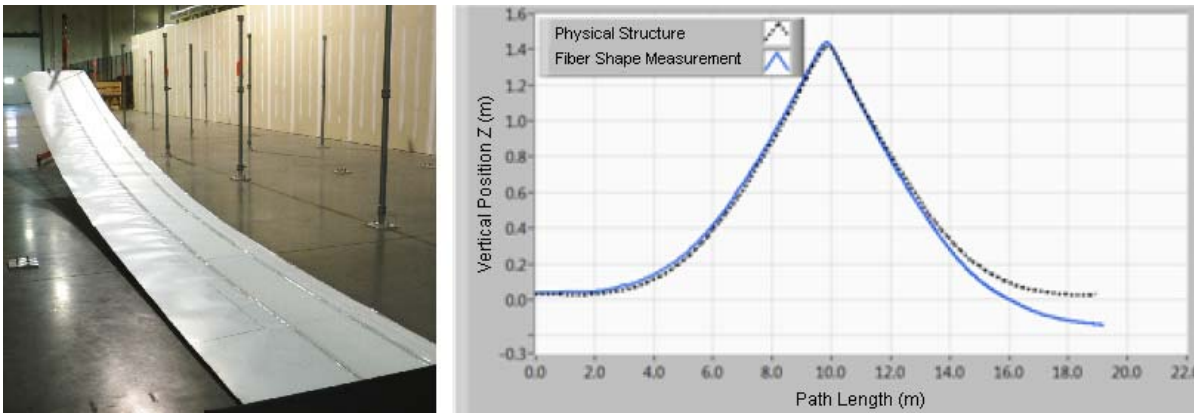

(a) (b)

Figure 31. (a) experimental setup; (b) obtained results (adapted from [126]).

The obtained results (as seen on Figure 31 (b) were very promising, presenting a RMS error of 5.8 cm being that the biggest difference is verified at the end of the fiber due to a systematic error in the measurement of twist. Another tested flexible structure where a sensing fiber was implemented in a convoluted path in opposition to the U-shaped one seen in Figure 31 provided better results regarding this detail.

3.7. Dynamic Capabilities

The capability of dynamic strain response measurements is of great importance for the evaluation of structural fatigue that results from seismic activities and material deterioration [128]. Since the first and most practiced implementations of DOFS were traditionally focused on long range performance, the measurements were then limited mainly to static or quasi-static measurements. Dynamic measurements are more challenging to obtain since they require wide frequency range scanning and large scale averaging to improve weak signals [13]. However, some progress has been made in the past few years in making DOFS technology truly dynamic with sampling rates approaching tens of kHz [48], especially with Brillouin-based techniques [129-134].

The first study, reported by Hotate [135] presented a novel correlation-based continuous-wave technique for high spatial resolution and distributed dynamic strain measurements with stimulated Brillouin scattering sensing. A fully measured dynamic strain from a 5 cm vibrating section was reported with a strain accuracy of about ±38 με at a sampling rate of 8.8 Hz as seen in Figure 32.

Later, Song and Hotate demonstrated 200 Hz distributed sensing (at 1 kHz sampling rate) over a 20 m single fiber measurement with a 10 cm spatial resolution [136] and strain distribution along a 100 m length fiber at 20 Hz sampling rate with 80 cm spatial resolution [137]. Most notably, Minardo et al. performed an experimental modal analysis of a cantilever beam with a BOTDA setup operated at a fixed pump probe frequency shift. This technique allowed the maximum acquisition rate of 108 Hz during the distributed strain measurements of the vibrating beam. The three first bending mode shapes

were obtained with the deployed system and validated by a FEM model analysis [138]. Bao et al. also demonstrated the field application of impact wave detection on a concrete deck excited by the passing of a car at a frequency up to 300 Hz with a BOTDA-based sensor [139].

For Rayleigh scattering-based OTDR, the first reported vibration sensor was achieved through polarization OTDR achieving 10 m spatial resolution and 5 kHz event detection [140] and the best spatial resolution of 0.5 m over 1 km sensing length was achieved with coherent detection of phase OTDR at 8 kHz [141].

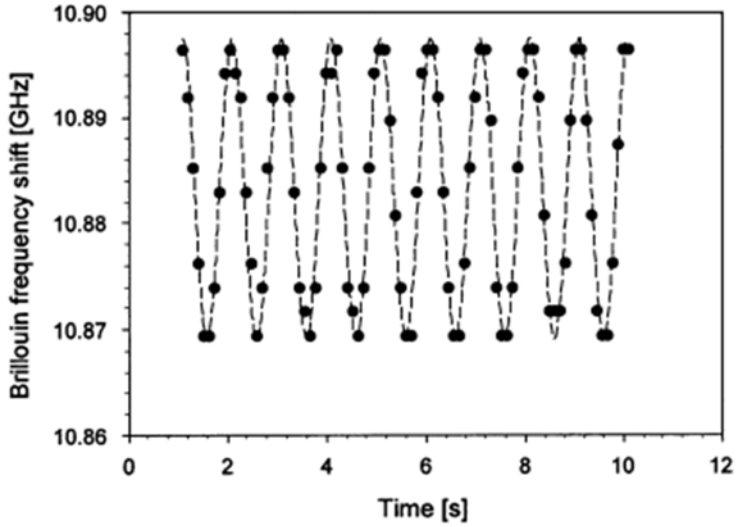

Figure 32. Brillouin frequency shift measured as a function of time, at a sampling rate of 8.8 Hz, when a 1 Hz vibration is applied [135].

Regarding Rayleigh-based OFDR, Zhou et al. performed some experiments in order to investigate the feasibility of distributed dynamic measurements with this technique [142]. The dynamic strain behaviour was induced by wrapping a 20 cm fiber section on a lead zirconate titanate (PZT) tube with a diameter of 3 cm. The measurement of vibration frequency up to 32 Hz with a spatial resolution of 10 cm up to the total length of 17 m was demonstrated [142] as presented in Figure 33.

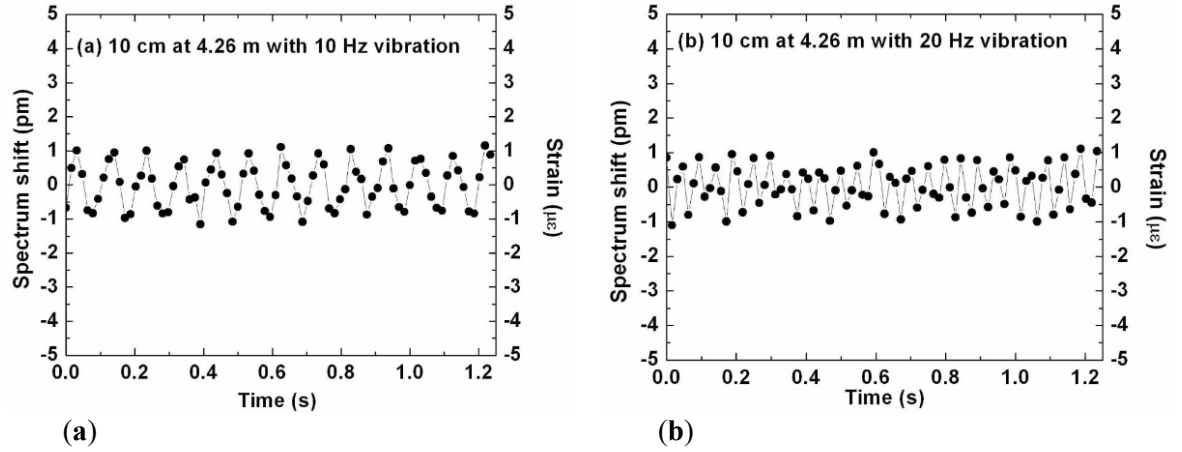

Figure 33. Time-domain Rayleigh backscatter spectrum shift (applied strain) with 10 cm spatial resolution when (a) 10 Hz and, (b) 20 Hz sinusoidal voltage is applied to the PZT tube. [142].

These examples showcase the potential of DOFS application for dynamic measurements in civil engineering structures. Nonetheless, this research topic is still in a very early development stage and more field applications need to be performed.

4. Challenges When Using Distributed Optical Fibers

As happens with any type of monitoring sensing system there are different challenges associated with the application of DOFS systems like the aforementioned limited spatial resolution and monitored length range. However, probably the major practical concern with fiber sensors in SHM of civil engineering structures is to assure that the sensor itself is not damaged during the installation or measurement process. This is not easily achieved due to the great fragility of bare fibers.

As seen in the different applications showcased in this article, a comparison of distinctive coatings and protections for the optical fiber when applied to various structures is of extreme importance [42,83,84,86]. By using a relative thick coating, the process of implementation of the sensor becomes easier and the probability of rupturing the fiber is diminutive, however, the complete stress and strain transfer from the monitored structure to the sensor is not guaranteed. On the other hand, in applications where the coating is very thin or even non-existent, such as the cases of [89,91,120,123], the quality of the measured strains is improved, but at the same time, when applying the sensor to the structure (either embedded or glued to the surface of the structure) a great deal of attention and effort is required in order to not damage the sensor, implying also a strong limitation in long-term applications on exposed structures. This is a compromise that is specific to each implementation and should be carefully considered when planning any DOFS-based monitoring system.

Another concern related with the application of DOFS is the possibility of introducing bending stresses in the fiber during the field installation process, if sufficient care is not taken, which can be very detrimental due to the particularly weak scattering signals.

Additionally, in concrete structures, for bonded applications, the roughness of the concrete surface and the heterogeneity due to the presence of aggregates of several sizes leads to an even greater challenge. Cleaning of the grease and additional unwanted particles in the areas were DOFS are intended to be bonded, jointly with a pre-treatment to smooth the surface (brushing) is vital to achieve a good bond between the sensor and the instrumented structure. Also, when analysing the measured data, low peaks and discontinuities appear due to those same surface irregularities and concrete flaking and spalling so special care should be taken in this step too in order to eliminate false assumptions.

Finally, when taking in account the use of DOFS systems in a damage/deterioration SHM system, it is important to imply a certain amount of redundancy into the sensor network in order to guarantee relevant results even after the failure of one of the sensors.

5. Conclusions

During the past decades, journals and project reports have shown that SHM practice has now become a well-established and mature subject. Furthermore, and within this topic, OFS has suffered an exponentially increase of interest and as a result, several studies and applications have been presented in the past years. However, examples of the distributed potential of this technology are still in a relatively early practice stage. As a result, in the present paper, the topic of distributed fiber optic sensing in SHM practice was widely discussed and reviewed, in particular, the applications in civil engineering structures.

First the concept of SHM and the role of fiber optics sensors were presented. Then the background theory associated with the most used distributed sensing techniques were described and elaborated, being these divided between time domain reflectometry and frequency domain reflectometry. Afterwards a general review of the state-of-the-art applications of different DOFS in geotechnical structures, pipelines, bridges and dams was shown. This was complemented by the state-of-the-art of laboratory works that led to field applications and the most recent researched developments of this technology in various areas. It is worth mentioning that the applications found on this paper only cover the sensor design and basic implementation techniques and performance. For further information regarding each of the applications, the reading of the respective references is advised. Finally, a brief summary of the most relevant challenges associated with the application of DOFS in SHM was presented.

In order to completely establish this technology as a viable solution for civil engineering SHM applications there's still a lot to be studied and developed. The attempt to enhance the resolution of these sensors is something that should be continued in future works in order to create better damage monitoring solutions based on these sensors. Additionally, the identification of the most appropriate coatings and installation methods for each implementation should be further investigated in order to ultimately provide general guidelines for the use of this technology in civil engineering SHM.

As seen in this article, DOFS-based systems can be deployed in different applications which showcase its impressive versatility, but also stress the importance of adapting this system to each solution. The choice of the most appropriate DOFS technique is an obvious result of some parameters such as the size of the structure, spatial resolution, acquisition speed and so forth. While Brillouin-based techniques can easily cover great lengths and therefore acquire global information about a structure, their resolution is not ideal for damage identification. Some attempts to improve this resolution have been made and are presented in this review. However, a more cost-effective technique must be developed in order to achieve high spatial resolution based on Rayleigh OFDR sensing. This is still a recent and developing technology that nevertheless is anticipated to have an important role in structural health monitoring in the near future, if correctly developed and harnessed.

Acknowledgments: The authors want to knowledge the financial support provided by the Spanish Ministry of Economy and Innovation through research projects BIA2013-47290-R, BIA2012-36848 and FEDER (European Regional Development Funds), and also funding from the European Union's Horizon 2020 research and innovation programme under the Marie Sklodowska-Curie grant agreement No. 642453.

Conflicts of Interest: The authors declare no conflict of interest.

References

[1] ASCE. **2013** Report Card for America's Infrastructure. American Society of Civil Engineers. Reston, VA, USA: American Society of Civil Engineers. doi:10.1061/9780784478837.

[2] López-Higuera, J.M.; Cobo, L.R.; Incera, A.Q.; Cobo, A. Fiber optic sensors in structural health monitoring. J. Lightwave Technol. **2011**, 29, 587–608.

[3] Farrar, C.R.; Worden, K. An introduction to structural health monitoring. Philos. Trans. A Math. Phys. Eng. Sci. **2007**, 365, 303–315.

[4] Kudva, J.N.; Marantidis, C.; Gentry, J.D.; Blazic, E. Smart structures concepts for aircraft structural health monitoring. In Proceedings of the 1993 North American Conference on Smart Structures and Materials, Albuquerque, NM, USA, 1–4 February **1993**; pp. 964–971.

[5] Giurgiutiu, V.; Rogers, C.A. Recent advancements in the electromechanical (E/M) impedance method for structural health monitoring and NDE. In Proceedings of the 5th Annual International Symposium on Smart Structures and Materials, San Diego, CA, USA, 1-5 March, **1998**; pp. 536–547.

[6] Sohn, H.; Farrar, C.R.; Hemez, F.M.; Czarnecki, J.J. A Review of Structural Health Review of Structural Health Monitoring Literature 1996–2001; Los Alamos National Laboratory: Los Alamos, NM, USA, **2002**.

[7] Lynch, J.P.; Loh, K.J. A summary review of wireless sensors and sensor networks for structural health monitoring. Shock Vib. Dig. **2006**, 38, 91–130.

[8] Glisic, B.; Inaudi, D.; Casanova, N. SHM process as perceived through 350 projects. In Proceedings of the SPIE Smart Structures and Materials + Nondestructive Evaluation and Health Monitoring, San Diego, CA, USA, 08 April, **2010**; 76480p.

[9] Rice, J.A.; Mechitov, K.; Sim, S.-H.; Nagayama, T.; Jang, S.; Kim, R.; Spencer, B.F., Jr.; Agha, G.; Fujino, Y. Flexible smart sensor framework for autonomous structural health monitoring. Smart Struct. Syst. **2010**, 6, 423–438.

[10] Ye, X.W.; Su, Y.H.; Han, J.P. Structural health monitoring of civil infrastructure using optical fiber sensing technology: A comprehensive review. Sci. World J. 2014, **2014**, 652329.

[11] Rodriguez, G.; Casas, J.R.; Villalba, S. SHM by DOFS in civil engineering: A review. Struct. Monit. Maint. **2015**, 2, 357–382.

[12] Glisic, B.; Hubbell, D.; Sigurdardottir, D.H.; Yao, Y. Damage detection and characterization using long-gauge and distributed fiber optic sensors. Opt. Eng. **2013**, 52, 087101.

[13] Bao, X.; Chen, L. Recent progress in distributed fiber optic sensors. Sensors **2012**, 12, 8601–8639.

[14] Glisic, B.; Inaudi, D. Development of method for in-service crack detection based on distributed fiber optic sensors. Struct. Health Monit. **2012**, 11, 161–171.

[15] Posenato, D.; Lanata, F.; Inaudi, D.; Smith, I.F.C. Model-free data interpretation for continuous monitoring of complex structures. Adv. Eng. Inf. **2008**, 22, 135–144.

[16] Udd, E. An overview of fiber-optic sensors. Rev. Sci. Instrum. **1995**, 66, 4015.

[17] Kersey, A.D. A review of recent developments in fiber optic sensor technology. Opt. Fiber Technol. **1996**, 2, 291–317.

[18] Grattan, K.T.V.; Sun, T. Fiber optic sensor technology: An overview. Sens. Actuators A Phys. **2000**, 82, 40–61.

[19] Lee, B. Review of the present status of optical fiber sensors. Opt. Fiber Technol. **2003**, 9, 57–79.

[20] Li, H.-N.; Li, D.-S.; Song, G.-B. Recent applications of fiber optic sensors to health monitoring in civil engineering. Eng. Struct. **2004**, 26, 1647–1657.

[21] Ferdinand, P. The evolution of optical fiber sensors technologies during the 35 last years and their applications in structure health monitoring. In Proceedings of the 7th European Workshop Structure Health Monitoring (EWSHM), Nantes, France, 8–11 July **2014**.

[22] Leung, C.K.Y.; Wan, K.T.; Inaudi, D.; Bao, X.; Habel, W.; Zhou, Z.; Ou, J.; Ghandehari, M.; Wu, H.C.; Imai, M. Review: Optical fiber sensors for civil engineering applications. Mater. Struct. **2013**, 48, 871–906.

[23] Udd, E.; Spillman, W.B., Jr. Fiber Optic Sensors: An Introduction for Engineers and Scientists, 2nd ed.; John Wiley & Sons: Hoboken, NJ, USA, **2011**.

[24] Giallorenzi, T.G.; Bucaro, J.A.; Dandridge, A.; Sigel, G.H.; Cole, J.H.; Rashleigh, S.C.; Priest, R.G. Optical fiber sensor technology. IEEE Trans. Microw. Theory Tech. **1982**, 30, 472–511.

[25] Yu Francis, T.S.; Shizhuo Yin. Fiber Optic Sensors. **2002**, Marcel Dekker Inc., New York

[26] Habel, W.R.; Krebber, K. Fiber-optic sensor applications in civil and geotechnical engineering. Photonic Sens. **2011**, 1, 268–280.

[27] Gupta, B.D. Fiber Optic Sensors: Principles and Applications; New India Publishing: New Delhi, India, **2006**.

[28] Gholamzadeh, B.; Nabovati, H. Fiber optic sensors. Int. J. Electr. Comput. Energy Electron. Commun. Eng. **2008**, 2, 1107–1117.

[29] Casas, J.R.; Cruz, P.J.S. Fiber optic sensors for bridge monitoring. J. Bridge Eng. **2003**, 8, 362–373.

[30] Guo, H.; Xiao, G.; Mrad, N.; Yao, J. Fiber optic sensors for structural health monitoring of air platforms. Sensors **2011**, 11, 3687–3705.

[31] Peairs, D.M.; Sterner, L.; Flanagan, K.; Kochergin, V. Fiber optic monitoring of structural composites using optical backscatter reflectometry. In Proceeddings of the 41st International SAMPE Technical Conference, Wichita, KS, USA, 19–22 October **2009**; pp. 19–22.

[32] Rodrigues, C.; Felix, C.; Figueiras, J. Fiber-optic-based displacement transducer to measure bridge deflections. Struct. Health Monit. **2010**, 10, 147–156.

[33] Barbosa, C.; Costa, N.; Ferreira, L.A.; Araújo, F.M.; Varum, H.; Costa, A.; Fernandes, C.; Rodrigues, H. Weldable fibre Bragg grating sensors for steel bridge monitoring. Meas. Sci. Technol. **2008**, 19, 125305.

[34] López-Higuera, J.M.; Misas, J.; Incera, A.Q.; Cuenca, J.E. Fiber optic civil structure monitoring system. Opt. Eng. **2005**, 44, 1–10.

[35] Del Grosso, A.; Bergmeister, K.; Inaudi, D.; Santa, U. Monitoring of bridges and concrete structures with fibre optic sensors in Europe. IABSE Symp. Rep. **2001**, 84, 15–22.

[36] Tennyson, R.C.; Mufti, A.A.; Rizkalla, S.; Tadros, G.; Benmokrane, B. Structural Health Monitoring of innovative bridges in Canada with fiber optic sensors. Smart Mater. Struct. **2001**, 10, 560–573.

[37] López-Higuera, J.M. Optical Sensors; Universidad de Cantabria: Cantabria, Spain, **1998**.

[38] Boyd, R. Nonlinear Optics, 3rd ed.; Academic Press: Rochester, NY, USA, **2008**.

[39] Cheng, J.-X.; Xie, X.S. Coherent Anti-Stokes Raman Scattering: Instrumentation, Theory, and Applications. J. Phys. Chem. B **2004**, 108, 827–840.

[40] Abalde-Cela, S.; Aldeanueva-Potel, P.; Mateo-Mateo, C.; Rodríguez-Lorenzo, L.; Alvarez-Puebla, R.A.; Liz-Marzán, L.M. Surface-enhanced Raman scattering biomedical applications of plasmonic colloidal particles. J. R. Soc. Interface **2010**, 7, S435–S450.

[41] Oakley, L.H.; Dinehart, S.A.; Svoboda, S.A.; Wustholz, K.L. Identification of organic materials in historical oil paintings using correlated extractionless surface-enhanced Raman scattering and fluorescence microscopy. Anal. Chem. **2011**, 83, 3986–3989.

[42] Henault, J.-M.; Moreau, G.; Blairon, S.; Salin, J.; Courivaud, J.-R.; Taillade, F.; Merliot, E.; Dubois, J.-P.; Bertrand, J.; Buschaert, S.; et al. Truly distributed optical fiber sensors for structural health monitoring: From the telecommunication optical fiber drawling tower to water leakage detection in dikes and concrete structure strain monitoring. Adv. Civ. Eng. 2010, **2010**, doi:10.1155/2010/930796.

[43] Kurashima, T.; Horiguchi, T.; Tateda, M. Distributed-temperature sensing using stimulated Brillouin scattering in optical silica fibers. Opt. Lett. **1990**, 15, 1038–1040.

[44] Bao, X.; Dhliwayo, J.; Heron, N.; Webb, D.J.; Jackson, D.A. Experimental and theoretical studies on a distributed temperature sensor based on Brillouin scattering. J. Lightwave Technol. **1995**, 13, 1340–1348.

[45] Zeng, X.; Bao, X.; Chhoa, C.Y.; Bremner, T.W.; Brown, A.W.; DeMerchant, M.D.; Ferrier, G.; Kalamkarov, A.L.; Georgiades, A.V. Strain measurement in a concrete beam by use of the Brillouin-scattering-based distributed fiber sensor with single-mode fibers embedded in glass fiber reinforced polymer rods and bonded to steel reinforcing bars.. Appl. Opt. **2002**, 41, 5105–5114.

[46] Bastianini, F.; Matta, F.; Rizzo, A.; Galati, N.; Nanni, A. Overview of recent bridge monitoring applications using distributed Brillouin fiber optic sensors. J. Nondestruct. Test. **2007**, 12, 269–276.

[47] Ravet, F.; Briffod, F.; Glisšć, B.; Nikles, M.; Inaudi, D. Submillimeter crack detection with Brillouin-based fiber-optic sensors. IEEE Sens. J. **2009**, 9, 1391–1396.

[48] Motil, A.; Bergman, A.; Tur, M. State of the art of Brillouin fiber-optic distributed sensing. Opt. Laser Technol. **2015**, 78, 1–23.

[49] Shibata, N.; Waarts, R.G.; Braun, R.P. Brillouin-gain spectra for single-mode fibers having pure-silica, GeO2-doped, and P2O5-doped cores. Opt. Lett. **1987**, 12, 269–271.

[50] Tateda, M.; Horiguchi, T.; Kurashima, T.; Ishihara, K. First measurement of strain distribution along field-installed optical fibers using Brillouin spectroscopy. J. Lightwave Technol. **1990**, 8, 1269–1272.

[51] Shimizu, K.; Horiguchi, T.; Koyamada, Y.; Kurashima, T. Coherent self-heterodyne Brillouin OTDR for measurement of Brillouin frequency shift distribution in optical fibers. J. Lightwave Technol. **1994**, 12, 730–736.

[52] Galindez-Jamioy, C.A.; López-Higuera, J.M. Brillouin Distributed Fiber Sensors: An Overview and Applications. J. Sens. 2012, **2012**, doi:10.1155/2012/204121.

[53] Nikles, M.; Thevenaz, L.; Robert, P.A. Simple distributed temperature sensor based on Brillouin gain spectrum analysis. Proc. SPIE Int. Soc. Opt. Eng. **1994**, 138–141.

[54] Uchida, S.; Levenberg, E.; Klar, A. On-specimen strain measurement with fiber optic distributed sensing. Measurement **2015**, 60, 104–113.

[55] Feng, X.; Zhou, J.; Sun, C.; Zhang, X.; Ansari, F. Theoretical and experimental investigations into crack detection with BOTDR-distributed fiber optic Sensors. J. Eng. Mech. **2013**, 139, 1797–1807.

[56] Hotate, K.; Tanaka, M. Distributed fiber Brillouin strain sensing with 1 cm spatial resolution by correlation-based continuous wave technique. Proc. SPIE Int. Soc. Opt. Eng. **2000**, 4185, 647–650.

[57] Imai, M.; Nakano, R.; Kono, T.; Ichinomiya, T.; Miura, S.; Mure, M. Crack detection application for fiber reinforced concrete using BOCDA-based optical fiber strain sensor. J. Struct. Eng. **2010**, 136, 1001–1008.

[58] Belal, M.; Newson, T.P. A 5 cm spatial resolution temperature compensated distributed strain sensor evaluated using a temperature controlled strain rig. Opt. Lett. **2011**, 36, 4728–4730.

[59] Shen, S.; Wu, Z.; Yang, C.; Wan, C.; Tang, Y.; Wu, G. An improved conjugated beam method for deformation monitoring with a distributed sensitive fiber optic sensor. Struct. Health Monit. **2010**, 9, 361–378.

[60] Zadok, A.; Antman, Y.; Primerov, N.; Denisov, A.; Sancho, J.; Thevenaz, L. Random-access distributed fiber sensing. Laser Photonics Rev. **2012**, 6, L1–L5.

[61] Eickhoff, W.; Ulrich, R. Optical frequency domain reflectometry in single-mode fiber. Appl. Phys. Lett. **1981**, 39, 693–695.

[62] Nakayama, J.; Iizuka, K.; Nielsen, J. Optical fiber fault locator by the step frequency method. Appl. Opt. **1987**, 26, 440–443.

[63] Yu, F.T.S.; Zhang, J.; Yin, S.; Ruffin, P.B. A novel distributed fiber sensor based on the Fourier spectrometer technique. In Proceedings of the OSA Annual Meeting, Dallas, TX, USA, 2–7 October **1994**; p. 50.

[64] Juškaitis, R.; Mamedov, A.M.; Potapov, V.T.; Shatalin, S.V. Distributed interferometric fiber sensor system. Opt. Lett. **1992**, 17, 1623–1625.

[65] Rathod, R.; Pechstedt, R.D.; Jackson, D.A.; Webb, D.J. Distributed temperature-change sensor based on Rayleigh backscattering in an optical fiber. Opt. Lett. **1994**, 19, 593–595.

[66] Froggatt, M.; Moore, J. High-spatial-resolution distributed strain measurement in optical fiber with rayleigh scatter. Appl. Opt. **1998**, 37, 1735–1740.

[67] Grave, J.H.L.; Håheim, M.L.; Echtermeyer, A.T. Measuring changing strain fields in composites with Distributed Fiber-Optic Sensing using the optical backscatter reflectometer. Compos. Part B Eng. **2015**, 74, 138–146.

[68] Soller, B.; Gifford, D.; Wolfe, M.; Froggatt, M. High resolution optical frequency domain reflectometry for characterization of components and assemblies. Opt. Express **2005**, 13, 666–674.

[69] Froggatt, M.; Soller, B.; Gifford, D.; Wolfe, M. Correlation and keying of Rayleigh scatter for loss and temperature sensing in parallel optical networks. In Proceedings of the Optical Fiber Communication Conference, Los Angeles, CA, USA, 23–27 February **2004**; paper PD17.

[70] Froggatt, M.E.; Gifford, D.K.; Kreger, S.T.; Wolfe, M.S.; Soller, B.J. Distributed strain and temperature discrimination in unaltered polarization maintaining fiber. In Optical Fiber Sensors; Optical Society of America **2006**; paper ThC5.

[71] Koshikiya, Y.; Fan, X.; Ito, F. Highly Sensitive Coherent Optical Frequency-domain Reflectometry Employing SSB-modulator with cm-level Spatial Resolution over 5 km. In Proceedings of the 33rd European Conference and Ehxibition of Optical Communication (ECOC), Berlin, Germany, 16–20 September **2007**.

[72] Palmieri, L.; Schenato, L. Distributed optical fiber sensing based on rayleigh scattering. Open Opt. J. **2013**, 7, 104–127.

[73] Tanner, M.G.; Dyer, S.D.; Baek, B.; Hadfield, R.H.; Woo Nam, S. High-resolution single-mode fiber-optic distributed Raman sensor for absolute temperature measurement using superconducting nanowire single-photon detectors. Appl. Phys. Lett. **2011**, 99, 201110.

[74] Park, J.; Bolognini, G.; Lee, D.; Kim, P.; Cho, P.; di Pasquale, F.; Park, N. Raman-based distributed temperature sensor with simplex coding and link optimization. IEEE Photonics Technol. Lett. **2006**, 18, 1879–1881.

[75] Dong, Y.; Zhang, H.; Chen, L.; Bao, X. 2 cm spatial-resolution and 2 km range Brillouin optical fiber sensor using a transient differential pulse pair. Appl. Opt. **2012**, 51, 1229–1235.

[76] Dong, Y.; Chen, L.; Bao, X. Extending the sensing range of Brillouin optical time-domain analysis combining frequency-division multiplexing and in-line EDFAs. J. Lightwave Technol. **2012**, 30, 1161–1167.

[77] Rao, Y.-J. Recent progress in applications of in-fibre Bragg grating sensors. Opt. Lasers Eng. **1999**, 31, 297–324.

[78] Zhou, Z.; Graver, T.W.; Hsu, L.; Ou, J. Techniques of advanced FBG sensors: Fabrication, demodulation, encapsulation, and their application in the structural health monitoring of bridges. Pac. Sci. Rev. **2003**, 5, 116–121.

[79] Chan, T.H.T.; Yu, L.; Tam, H.-Y.; Ni, Y.-Q.; Liu, S.Y.; Chung, W.H.; Cheng, L.K. Fiber Bragg grating sensors for structural health monitoring of Tsing Ma bridge: Background and experimental observation. Eng. Struct. **2006**, 28, 648–659.

[80] Antunes, P.; Lima, H.; Varum, H.; André, P. Optical fiber sensors for static and dynamic health monitoring of civil engineering infrastructures: Abode wall case study. Measurement **2012**, 45, 1695–1705.

[81] Xu, G.Q.; Xiong, D.Y. Applications of fiber Bragg grating sensing technology in engineering. Chin. Opt. **2013**, 6, 306–317.

[82] Miller, J.W.; Mendez, A. Fiber Bragg grating sensors: Market overview and new perspectives. In Fiber Bragg Grating Sensors: Recent Advancements, Industrial Applications and Market Exploitation; Bentham Science Publishers , **2014**; pp. 313–320.

[83] Hoult, N.A.; Ekim, O.; Regier, R. Damage/deterioration detection for steel structures using distributed fiber optic strain sensors. J. Eng. Mech. **2014**, 140, 04014097.

[84] Quiertant, M.; Baby, F.; Khadour, A.; Marchand, P.; Rivillon, P.; Billo, J.; Lapeyrere, R.; Toutlemonde, F.; Simon, A.; Cordier, J. Deformation monitoring of reinforcement bars with a distributed fiber optic sensor for the SHM of reinforced concrete structures. NDE, May 2012; SEATTLE, United States. 10p, **2012**.

[85] Deif, A.; Martín-Pérez, B.; Cousin, B.; Zhang, C.; Bao, X.; Li, W. Detection of cracks in a reinforced concrete beam using distributed Brillouin fibre sensors. Smart Mater. Struct. **2010**, 19, 055014.

[86] Glisic, B.; Yao, Y. Fiber optic method for health assessment of pipelines subjected to earthquake-induced ground movement. Struct. Health Monit. **2012**, 11, 696–711.

[87] Enckell, M.; Glisic, B.; Myrvoll, F.; Bergstrand, B. Evaluation of a large-scale bridge strain, temperature and crack monitoring with distributed fibre optic sensors. J. Civ. Struct. Health Monit. **2011**, 1, 37–46.

[88] Zhang, W.; Gao, J.; Shi, B.; Cui, H.; Zhu, H. Health monitoring of rehabilitated concrete bridges using distributed optical fiber sensing. Comput. Civ. Infrastruct. Eng. **2006**, 21, 411–424.

[89] Villalba, S.; Casas, J.R. Application of optical fiber distributed sensing to health monitoring of concrete structures. Mech. Syst. Signal Process. **2013**, 39, 441–451.

[90] Rodríguez, G.; Casas, J.R.; Villaba, S. Cracking assessment in concrete structures by distributed optical fiber. Smart Mater. Struct. **2015**, 24, 035005.

[91] Rodríguez, G.; Casas, J.R.; Villalba, S.; Barrias, A. Monitoring of shear cracking in partially prestressed concrete beams by distributed optical fiber sensors. In Proceedings of the 8th International Conference on Bridge Maintenance, Safety and Management, IABMAS 2016, São Paulo, Brazil, 26–30 June **2016**.

[92] Henault, J.-M.; Quiertant, M.; Delepine-Lesoille, S.; Salin, J.; Moreau, G.; Taillade, F.; Benzarti, K. Quantitative strain measurement and crack detection in RC structures using a truly distributed fiber optic sensing system. Constr. Build. Mater. **2012**, 37, 916–923.

[93] Buchoud, E.; Henault, J.-M.; D'Urso, G.; Girard, A.; Blairon, S.; Mars, J.; Vrabie, V. Development of an automatic algorithm to analyze the cracks evolution in a reinforced concrete structure from strain measurements performed by an Optical Backscatter Reflectometer. In Proceedings of the 4th Workshop on Civil Structural Health Monitoring, Nov 2012, Berlin, Germany. pp.P10, **2012**.

[94] Gifford, D.K.; Froggatt, M.E.; Wolfe, M.S.; Kreger, S.T.; Soller, B.J. Millimeter resolution reflectometry over two kilometers. In Proceedings of the IEEE Avionics, Fiber-Optics and Photonics Technology Conference, Victoria, BC, USA, 2–5 October **2007**.

[95] Gifford, D.K.; Kreger, S.T.; Sang, A.K.; Froggatt, M.E.; Duncan, R.G.; Wolfe, M.S.; Soller, B.J. Swept-wavelength interferometric interrogation of fiber Rayleigh scatter for distributed sensing applications. Proc. SPIE **2007**, 6770, doi:10.1117/12.734931.

[96] Soller, B.J.; Gifford, D.K.; Wolfe, M.S.; Froggatt, M.E.; Yu, M.H.; Wysocki, P.F. Measurement of localized heating in fiber optic components with millimeter spatial resolution. In Proceedings of the 2006 Optical Fiber Communication Conference and the National Fiber Optic Engineers Conference, Optical Society of America, 5–10 March **2006**; p. 3.

[97] Sang, A.K.; Froggatt, M.E.; Gifford, D.K.; Kreger, S.T.; Dickerson, B.D. One centimeter spatial resolution temperature measurements in a nuclear reactor using rayleigh scatter in optical fiber. IEEE Sens. J. **2008**, 8, 1375–1380.

[98] Sierra-Pérez, J.; Torres-Arredondo, M.A.; Güemes, A. Damage and nonlinearities detection in wind turbine blades based on strain field pattern recognition. FBGs, OBR and strain gauges comparison. Compos. Struct. **2016**, 135, 156–166.

[99] Shi, B.; Sui, H.; Liu, J.; Zhang, D. The BOTDR-based distributed monitoring system for slope engineering. In Proceedings of the 10th IAEG International Congress, Nottingham, UK, 6 – 10 September **2006**; pp. 1–5.

[100] Zhu, H.-H.; Shi, B.; Zhang, J.; Yan, J.-F.; Zhang, C.-C. Distributed fiber optic monitoring and stability analysis of a model slope under surcharge loading. J. Mt. Sci., **2014**, 11, 979–989.

[101] Klar, A.; Dromy, I.; Linker, R. Monitoring tunneling induced ground displacements using distributed fiber-optic sensing. Tunn. Undergr. Space Technol. **2014**, 40, 141–150.

[102] Klar, A.; Linker, R. Feasibility study of automated detection of tunnel excavation by Brillouin optical time domain reflectometry. Tunn. Undergr. Space Technol. **2010**, 25, 575–586.

[103] Shi, B.; Xu, H.; Chen, B.; Zhang, D.; Ding, Y.; Cui, H.; Gao, J. A feasibility study on the application of fiber-optic distributed sensors for strain measurement in the Taiwan Strait Tunnel project. Mar. Georesour. Geotechnol. **2003**, 21, 333–343.

[104] Rajeev, P.; Kodikara, J.; Chiu, W.K.; Kuen, T. Distributed optical fibre sensors and their applications in pipeline monitoring. Key Eng. Mater. **2013**, 558, 424–434.

[105] Gue, C.Y.; Wilcock, M.; Alhaddad, M.M.; Elshafie, M.Z.E.B.; Soga, K.; Mair, R.J. The monitoring of an existing cast iron tunnel with distributed fibre optic sensing (DFOS). J. Civ. Struct. Health Monit. **2015**, 5, 573–586.

[106] Lanticq, V.; Bourgeois, E.; Magnien, P.; Dieleman, L.; Vinceslas, G.; Sang, A.; Delepine-Lesoille, S. Soil-embedded optical fiber sensing cable interrogated by Brillouin optical time-domain reflectometry (B-OTDR) and optical frequency-domain reflectometry (OFDR) for embedded cavity detection and sinkhole warning system. Meas. Sci. Technol. **2009**, 20, 034018.

[107] Wu, J.; Jiang, H.; Su, J.; Shi, B.; Jiang, Y.; Gu, K. Application of distributed fiber optic sensing technique in land subsidence monitoring. J. Civ. Struct. Health Monit. **2015**, 5, 587–597.

[108] Cheng, G.; Shi, B.; Zhu, H.-H.; Zhang, C.-C.; Wu, J.-H. A field study on distributed fiber optic deformation monitoring of overlying strata during coal mining. J. Civ. Struct. Health Monit. **2015**, 5, 553–562.

[109] Glisic, B.; Oberste-ufer, K. Validation Testing of Fiber Optic Method for Buried Pipelines Health Assessment after Earthquake-Induced Ground Movement. In Proceedings of the 2011 NSF Engineering Research and Innovation Conference, Atlanta, GA, USA, 4–7 Jaunary **2011**.

[110] Inaudi, D.; Glisic, B. Distributed fiber optic strain and temperature sensing for structural health monitoring. In Proceedings of the Third International Conference on Bridge Maintenance, Safety and Management, Porto, Portugal, 16–19 July **2006**; pp. 963–964.

[111] Lim, K.; Wong, L.; Chiu, W.K.; Kodikara, J. Distributed fiber optic sensors for monitoring pressure and stiffness changes in out-of-round pipes. Struct. Control Health Monit. **2015**, 23, 303–314.

[112] Thévenaz, L.; Facchini, M.; Fellay, A.; Robert, P.; Inaudi, D.; Dardel, B. Monitoring of large structure using distributed Brillouin fibre sensing. In Proceedings of the 13th International Conference on Optical Fiber Sensors, Kyongju, South Korea, 12 – 16 April **1999**; pp. 5–8.

[113] Glisic, B.; Inaudi, D. Sensing tape for easy integration of optical fiber sensors in composite structures. In Proceedings of the 16th International Conference on Optical Fiber Sensors, Nara, Japan, 13–17 October **2003**; Volume 1, pp. 291–298.

[114] Glišić, B.; Posenato, D.; Inaudi, D. Integrity monitoring of old steel bridge using fiber optic distributed sensors based on Brillouin scattering. In Proceedings of the 14th International Symposium on: Smart Structures and Materials & Nondestructive Evaluation and Health Monitoring, San Diego, CA, USA, 18–22 March **2007**; Volume 6531, p. 65310P-65310P-8.

[115] Matta, F.; Bastianini, F.; Galati, N.; Casadei, P.; Nanni, A. Distributed strain measurement in steel bridge with fiber optic sensors: Validation through diagnostic load test. J. Perform. Constr. Facil. **2008**, 22, 264–273.

[116] Glisic, B.; Chen, J.; Hubbell, D. Streicker Bridge: A comparison between Bragg-grating long-gauge strain and temperature sensors and Brillouin scattering-based distributed strain and temperature sensors. In Proceedings of the SPIE Smart Structures and Materials + Nondestructive Evaluation and Health Monitoring, San Diego, California, USA, 6 -10 March **2011**; p. 79812C.

[117] Bastianini, F.; Rizzo, A.; Galati, N.; Deza, U.; Nanni, A. Discontinuous Brillouin strain monitoring of small concrete bridges: Comparison between near-to-surface and smart FRP fiber installation techniques. Proc. SPIE Int. Soc. Opt. Eng. **2005**, 5765, 612–623.

[118] Bastianini, F.; Corradi, M.; Borri, A.; di Tommaso, A. Retrofit and monitoring of an historical building using 'Smart' CFRP with embedded fibre optic Brillouin sensors. Constr. Build. Mater. **2005**, 19, 525–535.

[119] Villalba, V.; Casas, J.R.; Villalba, S. Application of OBR fiber optic technology in structural health monitoring of Can Fatjó Viaduct (Cerdanyola de Vallés-Spain). In Proceedings of the VI International Conference on Bridge Maintenance, Safety and Management, Lake Maggiore, Italy, 8–12 July **2012**.

[120] Casas, J.; Villalba, S.; Villalba, V. Management and safety of existing concrete structures via optical fiber distributed sensing. In Maintenance and Safety of Aging Infrastructure: Structures and Infrastructures Book Series; CRC Press, **2014**; Volume 10, pp. 217–245.

[121] Zhao, X.; Lu, J.; Han, R.; Kong, X.; Wang, Y.; Li, L. Application of multiscale fiber optical sensing network based on brillouin and fiber bragg grating sensing techniques on concrete structures. Int. J. Distrib. Sens. Netw. 2012, **2012**, doi:10.1155/2012/310797.

[122] Regier, R.; Hoult, N.A. Distributed strain behavior of a reinforced concrete bridge: Case study. J. Bridge Eng. **2014**, 19, doi:10.1061/(ASCE)BE.1943-5592.0000637.

[123] Barrias, A.; Casas, J.R.; Villalba, S.; Rodriguez, G. Health Monitoring of real structures by distributed optical fiber. In Proceedings of the Fifth International Symposium on Life-Cycle Civil Engineering, IALCCE'16, Delft, The Netherlands, 16–19 October **2016**.

[124] Inaudi, D.; Glisic, B. Application of distributed Fiber Optic Sensory for SHM. In Proceeding of the ISHMII-2, Shenzhen, China, 16–18 November **2005**; pp. 163–169.

[125] Lan, C.; Zhou, Z.; Ou, J. Monitoring of structural prestress loss in RC beams by inner distributed Brillouin and fiber Bragg grating sensors on a single optical fiber. Struct. Control Health Monit. **2014**, 21, 317–330.

[126] Lally, E.M.; Reaves, M.; Horrell, E.; Klute, S.; Froggatt, M.E. Fiber optic shape sensing for monitoring of flexible structures. In Proceedings of the SPIE Smart Structures and Materials + Nondestructive Evaluation and Health Monitoring, San Diego, CA, USA, 26 April **2012**; p. 83452Y-83452Y-9.

[127] Froggatt, M.E.; Klein, J.W.; Gifford, D.K.; Kreger, S.T. Optical Position and/or Shape Sensing. U.S. Patent 8,773,650, 8 July **2014**.

[128] Schulz, W.L.; Conte, J.P.; Udd, E. Long-gage fiber optic Bragg grating strain sensors to monitor civil structures. In Proceedings of the SPIE's 8th Annual International Symposium on Smart Structures and Materials, Newport Beach, CA, USA, 30 July **2001**; pp. 56–65.

[129] Sovran, I.; Motil, A.; Tur, M. Frequency-scanning BOTDA with ultimately fast acquisition speed. IEEE Photonics Technol. Lett. **2015**, 27, 1426–1429.

[130] Bernini, R.; Minardo, A.; Zeni, L. Dynamic strain measurement in optical fibers by stimulated Brillouin scattering. Opt. Lett. **2009**, 34, 2613–2615.

[131] Peled, Y.; Yaron, L.; Motil, A.; Tur, M. Distributed and dynamic monitoring of 4km/sec waves using a Brillouin fiber optic strain sensor. In Proceedings of the Fifth European Workshop on Optical Fibre Sensors, Krakow, Poland, 19–22 May **2013**; p. 879434.

[132] Urricelqui, J.; Zornoza, A.; Sagues, M.; Loayssa, A. Dynamic BOTDA measurements based on Brillouin phase-shift and RF demodulation. Opt. Express **2012**, 20, 26942–26949.

[133] Dong, Y.; Ba, D.; Jiang, T.; Zhou, D.; Zhang, H.; Zhu, C.; Lu, Z.; Li, H.; Chen, L.; Bao, X. High-spatial-resolution fast BOTDA for dynamic strain measurement based on differential double-pulse and second-order sideband of modulation. IEEE Photonics J. **2013**, 5, 2600407.

[134] Peled, Y.; Motil, A.; Tur, M. Fast Brillouin optical time domain analysis for dynamic sensing. Opt. Express **2012**, 20, 8584–8591.

[135] Hotate, K.; Ong, S.S.L. Distributed dynamic strain measurement using a correlation-based Brillouin sensing system. IEEE Photonics Technol. Lett. **2003**, 15, 272–274.

[136] Song, K.-Y.; Hotate, K. Distributed fiber strain sensor with 1 kHz sampling rate based on Brillouin optical correlation domain analysis. Opt. East 2007, **2007**, 67700J.

[137] Song, K.Y.; Kishi, M.; He, Z.; Hotate, K. High-repetition-rate distributed Brillouin sensor based on optical correlation-domain analysis with differential frequency modulation. Opt. Lett. **2011**, 36, 2062–2064.

[138] Minardo, A.; Coscetta, A.; Pirozzi, S.; Bernini, R.; Zeni, L. Modal analysis of a cantilever beam by use of Brillouin based distributed dynamic strain measurements. Smart Mater. Struct. **2012**, 21, 125022.

[139] Bao, X.; Zhang, C.; Li, W.; Eisa, M.; El-Gamal, S.; Benmokrane, B. Monitoring the distributed impact wave on a concrete slab due to the traffic based on polarization dependence on stimulated Brillouin scattering. Smart Mater. Struct. **2008**, 17, 015003.

[140] Zhang, Z.; Bao, X. Distributed optical fiber vibration sensor based on spectrum analysis of Polarization-OTDR system. Opt. Express **2008**, 16, 10240–10247.

[141] Qin, Z.; Chen, L.; Bao, X. Wavelet denoising method for improving detection performance of distributed vibration sensor. IEEE Photonics Technol. Lett. **2012**, 24, 542–544.

[142] Zhou, D.-P.; Qin, Z.; Li, W.; Chen, L.; Bao, X. Distributed vibration sensing with time-resolved optical frequency-domain reflectometry. Opt. Express **2012**, 20, 13138–13145.

4.2. Journal Article II

Embedded Distributed Optical Fiber Sensors in Reinforced Concrete Structures— A Case Study

Published in Sensors, vol. 18, no. 4, p. 980, March 2018. doi: 10.3390/s18040980

António Barrias [1], Joan R. Casas [1] and Sergi Villalba [2]

[1]Department of Civil and Environmental Engineering, Technical University of Catalonia (UPC), c/ Jordi Girona 1-3, 08034 – Barcelona, Spain

[2]Department of Engineering and Construction Projects, Technical University of Catalonia (UPC), c/ Colom 11, Ed. TR5, 08022 – Terrassa (Barcelona), Spain

Received: 13 January 2018; Accepted: 22 March 2018; Published: 26 March 2018

Abstract: When using distributed optical fiber sensors (DOFS) on reinforced concrete structures, a compromise must be achieved between the protection requirements and robustness of the sensor deployment and the accuracy of the measurements both in the uncracked and cracked stages and under loading, unloading and reloading processes. With this in mind the authors have carried out an experiment where polyimide-coated DOFS were installed on two concrete beams, both embedded in the rebar elements and also bonded to the concrete surface. The specimens were subjected to a three-point load test where after cracking, they are unloaded and reloaded again to assess the capability of the sensor when applied to a real loading scenarios in concrete structures. Rayleigh Optical Frequency Domain Reflectometry (OFDR) was used as the most suitable technique for crack detection in reinforced concrete elements. To verify the reliability and accuracy of the DOFS measurements, additional strain gauges were also installed at three locations along the rebar. The results show the feasibility of using a thin coated polyimide DOFS directly bonded on the reinforcing bar without the need of indention or mechanization. A proposal for a Spectral Shift Quality (SSQ) threshold is also obtained and proposed for future works when using polyimide-coated DOFS bonded to rebars with cyanoacrylate adhesive.

Keywords: fiber optics; structural health monitoring; distributed fiber sensing; civil engineering; load testing; reinforced concrete; cracking

1. Introduction

1.1. Structural Health Monitoring (SHM)

The decay of the present network of civil engineering infrastructures and the consequent extension of their lifetime period is a highly imperative subject in today's society. Critical infrastructures such as bridges, dams, buildings, tunnels and power plants are inevitably subject to deterioration, which greatly hinders their expected performance with high economic consequences and can even endanger the safety of human lives.

In order to prevent and overcome this circumstance it is essential for infrastructure management owners to correctly maintain and rehabilitate the structural condition of these structures over time. This can be achieved by the installation of a set of sensors that follow the structures' behaviour and detect abnormalities allowing for the identification of damage. This enables a quick and preventive deployment of low-cost minor repairs that can prevent expensive or even irredeemable repairs and/or strengthening. This procedure is known as the Structural Health Monitoring (SHM) practice.

Additionally, this practice is not restricted to outdated or ageing structures. Effectively, when dealing with new and relevant structures the installation of sensors during the construction phase must be well planned and conducted since it provides an immense aid in detecting early stage degradation and damage [1].

Moreover, when deployed correctly, a SHM system provides important quantitative information on the state of the structure, which is simultaneously convenient for the structure's owner and for structural designers by providing important and real world structural behaviour data for future designs.

This topic has been developed and researched with great interest in the last two decades but unfortunately has yet to be applied in a standardized and efficient way since there is still an important lack of reliable and relatively economical SHM civil engineering solutions [2].

1.2. SHM with Distributed Optical Fiber Sensors (DOFS)

Conventionally, the overall condition assessment of a civil structure is carried out by well-trained engineers through visual inspection. This is a very subjective practice, which is dependent on individual experience and background in safety condition assessment. With the initial introduction of SHM systems part of this subjectivity may be eliminated. Nevertheless, the reliability and robustness of a health monitoring system is strongly correlated to the accuracy and robustness of the sensors deployed for each application and the posterior analysis of the gathered data.

In an initial stage and until very recently, the most regularly practiced SHM approaches were based on electrically powered sensors, such as strain gauges, inclinometers, displacement transducers, accelerometers and so on. However, these sensors when applied to real world conditions present significant shortcomings which may hamper the use of the obtained data [3].

In this sense, the use of optical fiber technology has been gaining popularity in the past two decades as one of the most researched topics within SHM sensors. Some inherent advantages, that optical fiber sensors (OFS) present when compared with their electrical based counterparts, are the fact that they are resistant to electromagnetic interference, durability, immunity to corrosion, good performance within large temperature fluctuations and their small size and lightweight [4].

Within these type of sensors, the most popular applications were made through the use of discrete or quasi-distributed Fiber Bragg Grating (FBG) sensors [5] and have been extensively discussed in different publications in past years [6-10].

In addition, standard monitoring practice is generally based in the use of a reduced number of discrete or point sensors which are supposed to be representative of the global structural behaviour [11]. Although the use of discrete sensors delivers interesting data of the monitored specimen related to its local behaviour, relevant information of the global structure's performance might be absent from the acquired data. This is important in several cases, especially in the case of SHM applications deployed in large-scale structures such as bridges, high-rise buildings, tunnels, power plants and dams. Furthermore, in this type of structures, the number of point sensors (and its corresponding connecting cables) required to perform a suitable global monitoring can increase exponentially, which consequently escalates the associated costs and technical challenges for effective deployment.

Moreover, especially for the case of heterogeneous materials such as concrete, the exact prevision of the damage location (normally associated with cracking and corrosion) is practically impossible. Therefore, with the use of discrete sensors there is a higher probability of not detecting the formation of cracks in these structures.

In this context, Distributed Optical Fiber Sensors (DOFS), while sharing the main advantages and capabilities of the aforementioned OFS, offer an additional and exclusive advantage over them as becomes evident in Figures 1 and 2 concerning crack detection capabilities and simplification of multiplexing.

Apart from DOFS technology, the development of other distributed sensing techniques and their use for crack detection on reinforced concrete structures has observed significant progress in recent years, such as the research of smart concrete elements. This are cement-based materials doped with conductive carbon nanoinclusions [12].

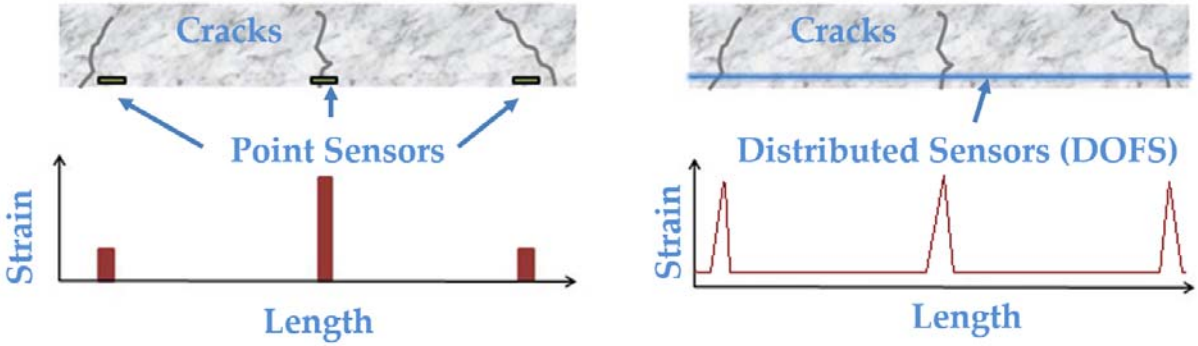

Figure 1. Spatial distribution detection with OFS (left) and DOFS (right).

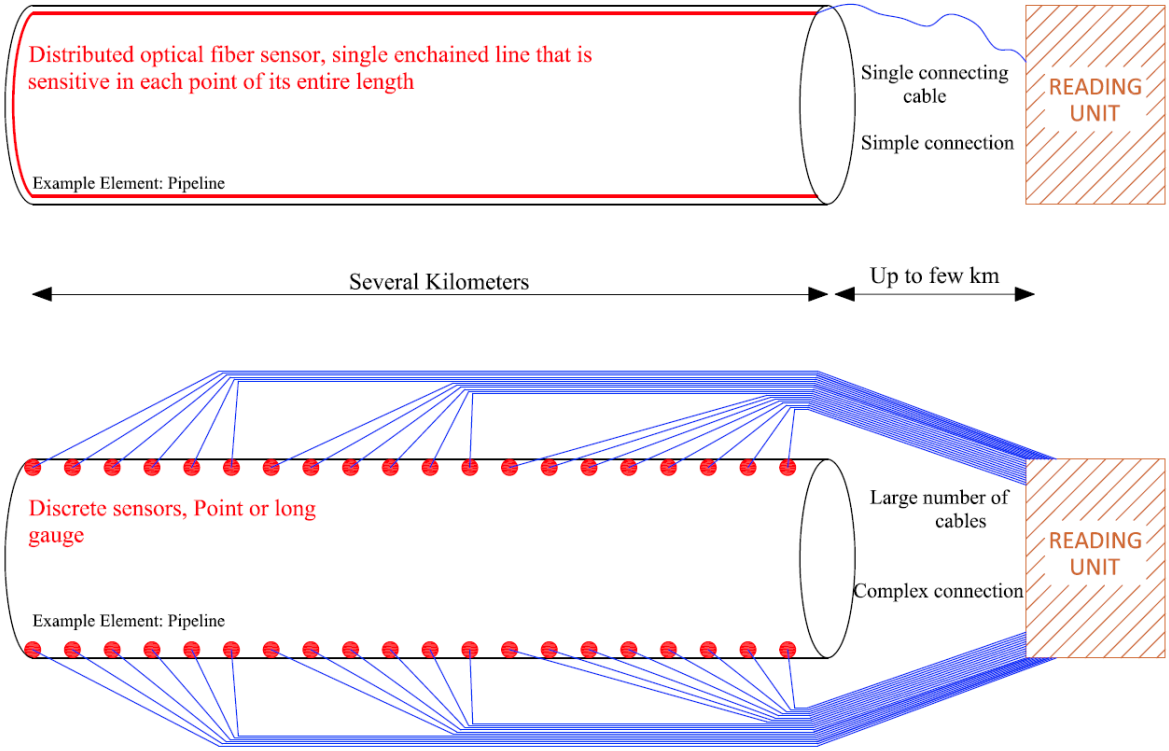

Figure 2. Comparison of use of distributed sensor (top) and point sensors (bottom) in large scale structures (Adapted from) [13]

DOFS are able to measure strain and/or temperature along their entire length by means of light scattering, which allows for the monitoring of virtually every cross-section of the structural element.

Hence, the scattering phenomenon is fundamentally characterized by the interaction between the light emitted and subsequent propagation and the physical medium where this occurs. More so, three different types of scattering processes may occur in a DOF sensor, which are the Raman, Brillouin and Rayleigh scattering, where each presents advantageous or limited capabilities depending on the objectives and specificity of each monitoring solution.

For instance, Raman scattering is characterized by high dependence on temperature which has found some successful applications in the civil engineering field [14] but has mostly been applied in other areas such as art restoration [15] and forensics [16].

In contrast, the Brillouin scattering-based DOFS have been the most studied and practiced in civil engineering structures, mainly due to their extended measurement range capability, which can go up to several kilometers. In this way, these type of sensors have been used to a great extent for long-distance distributed strain and temperature measurements in structural and geotechnical monitoring [17]. However, the achievable spatial resolution of these sensors (around 1 m) without the use of any complex post-processing algorithms is rather limited, which is not ideal for local damage detection and localization.

Nevertheless, important advances and interesting applications have been conducted recently with the use of Brillouin-based scattering DOFS. From research on crack monitoring in concrete pavements [18], surface microcracks detection and monitoring [19], shrinkage induced delamination detection for ultra-high performance concrete (UHPC) [20] and geotechnical engineering applications in the monitoring of the changes of the concrete curing temperature profile of piles [21] and soil slope during infiltration monitoring [22].

Finally, Rayleigh scattering, although limited to a sensing range of around 70 m, provides a substantially higher spatial resolution of 1 mm through the use of the Rayleigh backscattering Optical Frequency Domain Reflectometry (OFDR) [23], which is appropriate for the monitoring of crack formations in concrete structures. A more detailed description of the OFDR sensing mechanism can be consulted in [24].

As a result, this later scattering technique is the one deployed and researched in this study, aimed to the monitoring of reinforced concrete structures, through the use of the commercial optical interrogator ODiSI A from LUNA Technologies (Roanoke, VA, USA), Figure 3. This system has an accuracy and repeatability of ± 2 με, ± 0.2 °C, a measurement range of −50 to 300 °C and ± 13,000 με. Furthermore, this system enables a user-controlled sub-cm spatial resolution and a maximum sensing length of 50 m [25].

With this sensor, strain or temperature measurements are achieved by initially measuring and storing the Rayleigh scatter signature of the optical fiber installed in the structural element and being read by the ODiSI interrogator at an ambient state, constituting in this way the baseline measurement. This interrogator collects in the spectral frequency domain the light backscattered from the fiber sensor. This backscattered spectrum although seemingly random is stable and repeatable thus establishing a fingerprint of the DOFS.

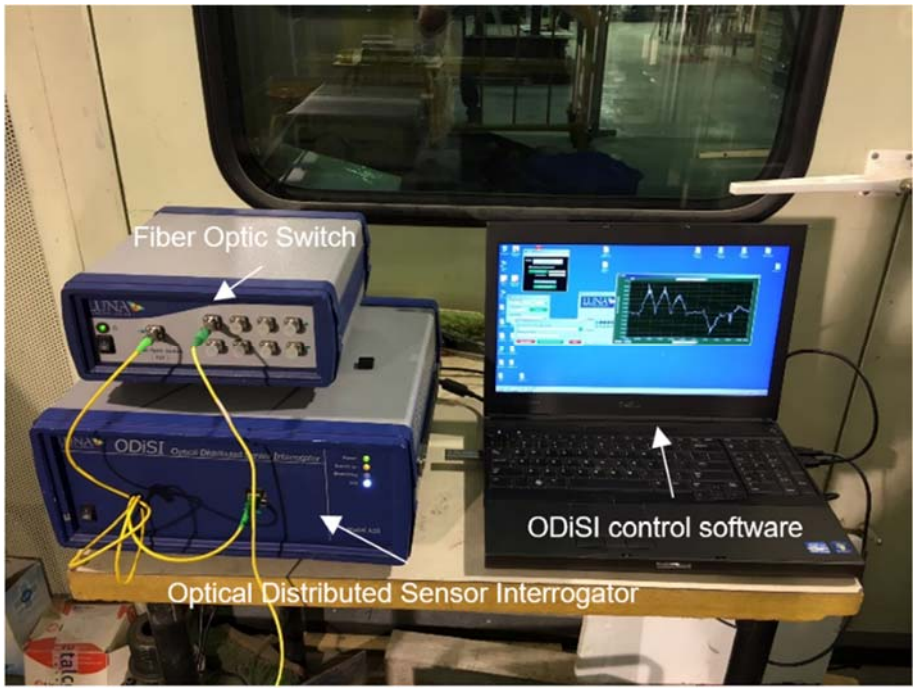

Figure 3. ODiSI A system used in this research case study.

Later, the scatter profile is measured after the variation of strain or temperature at any point along the length of the fiber. These two data sets are then cross correlated at the sensor locations to determine the spectral shift of the scattered light [26]. The shift in the spectrum is directly correlated with the strain or temperature variation which through the use of calibration constants enables the use of this scattering spectral shift as a monitoring sensing technique.

Up to now, some laboratory tests were carried out using also Rayleigh OFDR based DOFS both bonded in the concrete surface and embedded in reinforcing bars into the concrete. However, in all these tests, the application of monotonically increasing load was carried out, as their mean objective was to study the feasibility of assessing corrosion by means of distributed sensing. In the present study, the performance of the sensor bonded to the concrete surface and to the reinforcing bar in cyclic loading in cracked condition is investigated for the first time.

2. Laboratory Experiments

2.1. Motivation

Notwithstanding all the advantages of the use of DOFS-based technology in SHM applications, this is still a relatively recent field of study which requires a significant research and development effort when applied to a complex and heterogeneous material such as reinforced concrete. In this line, one of the key challenges on the use of these sensors is the existing compromise between the accuracy in measuring the strain data from the monitored material and the achievable protection and durability of such a sensor when exposed to the natural environmental conditions in real world applications [27].

When applying these sensors, it is easily understandable that a relatively thicker coating of the fiber itself provides a higher protection, hence, benefiting handling and manipulation at the time of installation, reducing the probability of rupturing, and also providing protection against external disruptive agents during the lifetime period. Nevertheless, the thicker the coating, the greater the effect on the measured data, thus affecting and clouding the real developed strain of the monitored specimen. On the other hand, a thinner coating provides a higher fragility and probability of rupturing when handling it despite the significantly increase of the effectiveness of the strain transfer between sensor and material.

Different studies have been made regarding the coating influence on the strain transfer between the sensor and the host material on both discrete [28,29] and distributed optical fiber sensors [30] by way of assessing the difference between the apparent and actual strain profile. This aspect is even more relevant for applications in reinforced concrete structures. Due to the heterogeneity of the different materials (aggregates of different size and type, cement paste) that constitute the concrete material and the roughness of its surface, a smooth and optimal bonding of the sensor to the material is difficult to achieve. Therefore, a smoothing and cleaning of the original surface is mandatory [31,32].

During the conduction of a comprehensive literature review on the use of Rayleigh OFDR-based DOFS in civil engineering SHM applications, the authors observed some studies where to overcome this mentioned challenge, DOFS were not bonded, as usual, to the surface of the concrete specimen, but rather directly attached to the rebars of a reinforced concrete element [33]. Here the argument is made that the sensor is better protected from environmental conditions during its lifetime due to this implementation method. Notwithstanding, in this case it is still necessary to previously mechanize the rebar where the fiber was to be bonded, what can be a tiresome and cost consuming operation while also having some effect in the accuracy of the results. Moreover, a still relatively thick coating was used, not fully taking advantage of this new improved condition for the fiber durability.

Another group of researchers also using Rayleigh backscattering bonded the fiber directly on the rebars without previous mechanization. The sensor was installed internally in reinforced concrete elements in order to detect pitting corrosion in these elements [34]. Here, polyimide coated fibers were implemented to the rebar elements of embedded reinforced concrete beams under four-point bending tests showing promise for detecting localized corrosion.

Later, this group continued this research with a test where distributed sensing was used to assess the impact of corrosion on bond performance in reinforced concrete [35]. Here, tensile tests were conducted on bare reinforcement and reinforced concrete specimens subjected to accelerated corrosion where polyimide and nylon coated DOFS were implemented to rebars. This technology was able to measure the corrosion effects on the concrete and steel bond as well as locate areas of pitting corrosion that were visually hidden by the surrounding concrete.

These same authors followed this research with an experiment where six reinforced concrete beams under varying levels of corrosion were instrumented with DOFS and tested in three-point bending [36]. The used distributed sensing technology was again able to detect the effect of the corrosion on the loss of bond between the concrete and reinforcement.

Taking this into account, the present paper aims to further analyse the performance and feasibility of deploying a single thin polyimide coated low bend loss fiber (total diameter of core plus coating of 155 μm [37]) to rebar elements without any preliminary mechanization of the steel. However, in the present case, the main objective is not related to the ability of the sensor in the detection of corrosion induced damage, but to examine the performance and feasibility of the DOFS when the sensor is crossing a crack and the crack is opening and closing, what may create a risky scenario for damaging the fiber taking into account the roughness present in the crack lips.

The absence of rebar mechanization simplifies the installation process, decreases the associated costs and increases the reliability of the measurements as almost not coating material is interposed between the reinforcing bar and the DOFS. In a first step, the accuracy of the fiber optic bonded to the rebar is examined and afterwards, the performance of the sensor in measuring the strain in the steel when the rebar is embedded into the concrete is checked for both loading and unloading scenarios that may challenge the fiber integrity and accuracy. Moreover, in this later step, the same optical fiber is used for both the measurements in the rebar as well as the concrete surface.

2.2. Tensile Test on an Isolated Rebar

The objective of this simple test in a single rebar is to observe the performance of the method of bonding the thin coated DOFS directly to the steel without mechanizing it before as done in other experimental works [33]. The fiber optic used in the test is of polyimide type.

2.2.1. Description

A thin-coated polyimide fiber was adhered for nearly 75 cm of its length to the longitudinal lateral rib of a single Φ12 (12 mm of diameter) S500 standard rugged steel rebar through the use a two-component epoxy as the adhesive. In addition, three electrical strain gauges were implemented sparsely on the other side of the rebar (in order to minimize the interference with the DOFS measurements) for comparison purposes. The strain gauge SG2 was positioned at the center of the rebar and the remaining two (SG1 and SG3), 22.5 cm spaced to each side of SG2 (Figure 4).

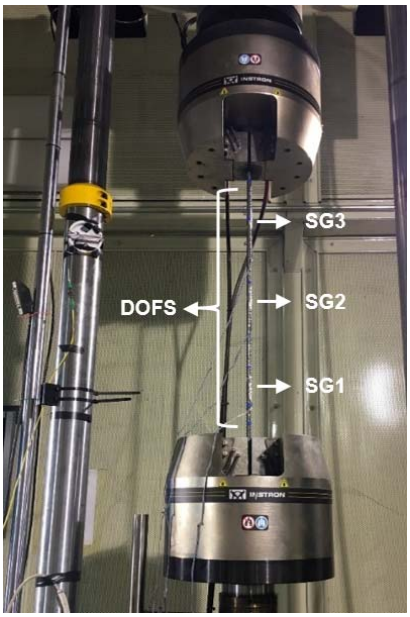

Figure 4. General scheme of the instrumented rebar for the tensile test with the DOFS and the strain gauges.

The induced tensile stress in the rebar was limited to the elastic range of the steel as this rebar had to be used later embedded in the concrete during the three-point bending test. Consequently, two-different load stages were applied to the specimen through the hydraulic press seen in Figure 4. These load stages were of 11.3 kN and 22.6 kN expected to produce tensile stresses of 100 and 200 MPa respectively, thus far below the yielding stress of the steel.

2.2.2. Results

Figure 5 represents the strain measured by the DOFS during this load test. One thing that is important to mention is that the length of the DOFS was 5.2 m, but only the last 0.75 m were adhered to the rebar during this test and this is the part shown in the figure.

The two strain levels produced by the two mentioned load levels are clearly seen in Figure 5. In addition, the distribution of the strain over the entire length of the monitored rebar due to the distributed capability of the DOFS is observable. As expected, according to the cross-sectional area and elasticity modulus of the rebar, these strains are close to 500 με for the first load stage of 11.3 kN and to 1000 με for the second load stage of 22.6 kN.

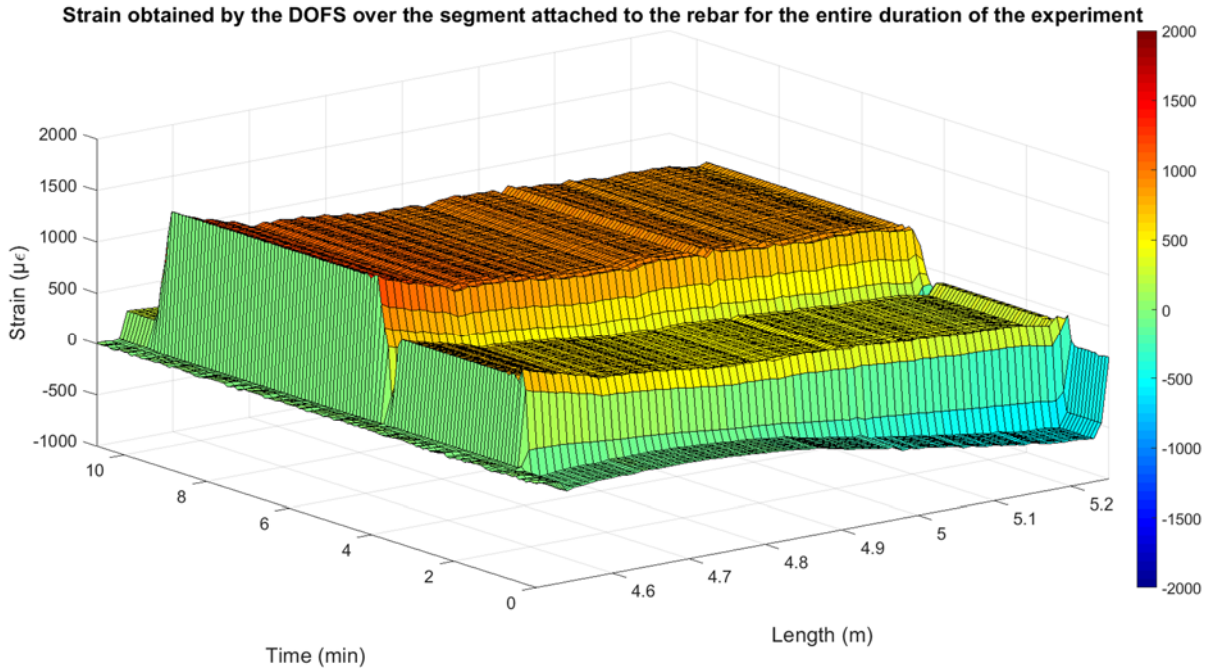

Figure 5. DOFS measured strain for rebar tensile test.

In Figure 6, the strain values measured by the strain gauges over time are compared to the ones obtained by the DOFS at their respective point locations. Here, a good agreement of both set of sensors is observable especially represented at the transition between unloaded and loaded stages.

It is also observable how the strain measured by both sets of sensors is slightly higher on the top part of the rebar compared to the other values measured at lower points. One possible justification for this is the fact that while performing the tensile test, the top jack introduces tensile tension by pulling the top part of the rebar. It is observed that this variation is higher in the DOFS than it is in the deployed strain gauges.

Nonetheless, the obtained results give confidence for the use of DOFS attached directly to the rebar without the need of a previous mechanization of the steel and a thick plastic coating of the fiber. The results clearly show that the DOFS is measuring the actual strain in the steel, as confirmed by the strain gauges, without the need to any further correction due to the interposition of the coating. Once the correct performance of the deployment method in the rebar was checked, the next step was to look at its performance when embedded into concrete, both before and after cracking of the specimen and under loading and unloading conditions.

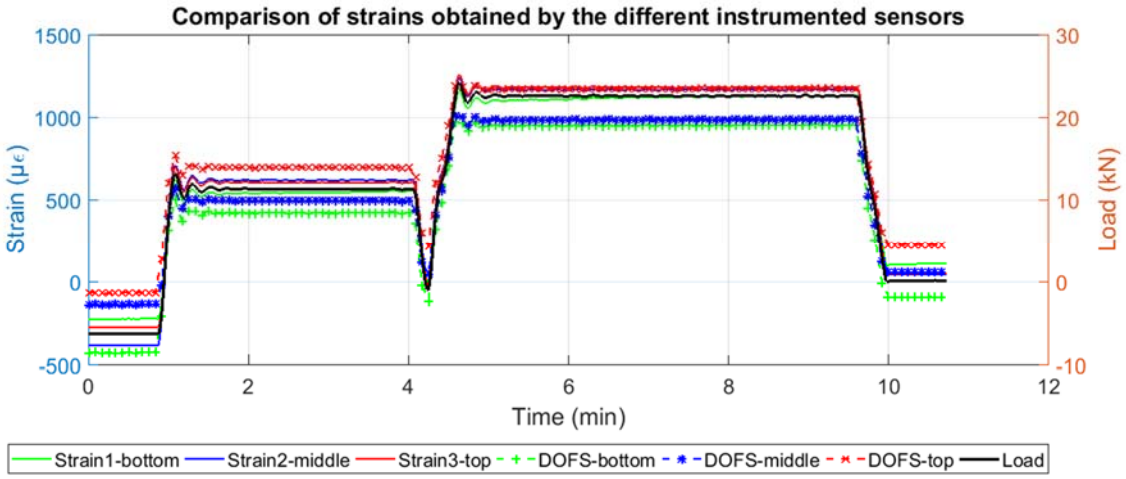

Figure 6. Comparison of strains obtained by the two different sets of deployed sensors.

2.3. Load Test on Reinforced Concrete Beams

As a result, and after evaluating the performance of attaching very thin polyimide coated DOFS directly to a rebar for strain measuring, it was decided to perform a three-point load test on two different reinforced concrete beams specimens represented in Figure 7.

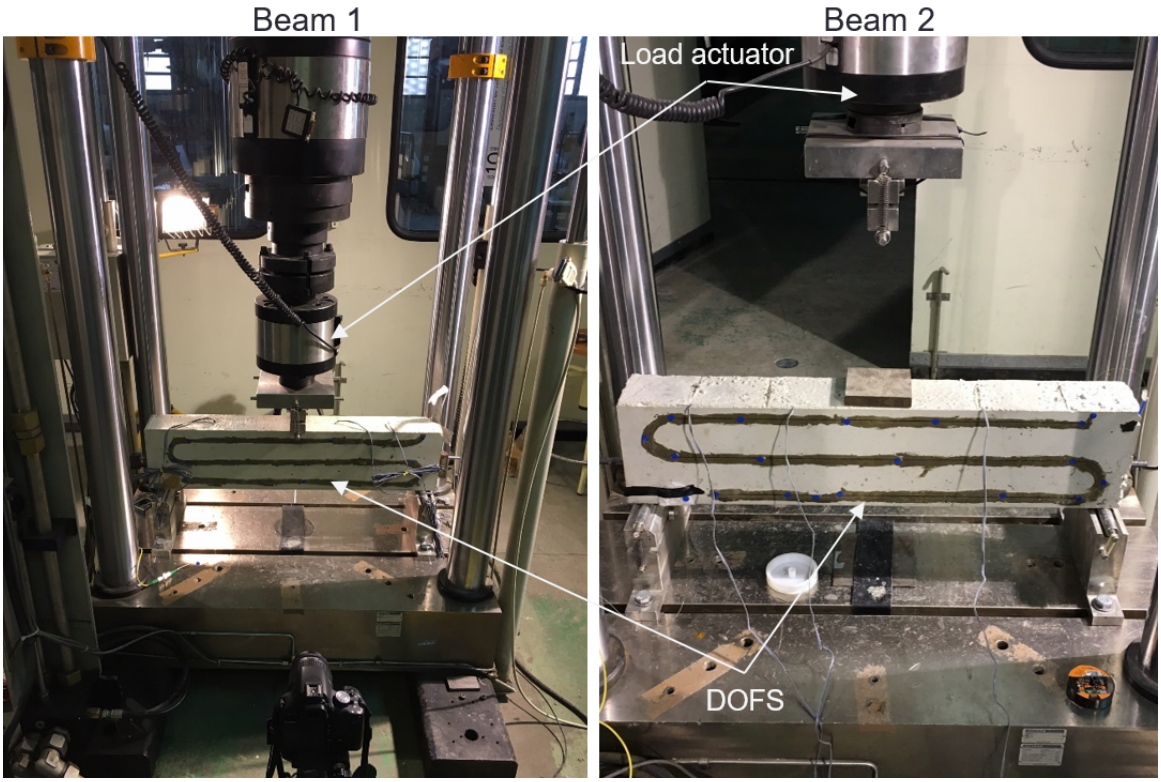

Figure 7. Reinforced concrete beam specimen 1 (left) and 2 (right).

2.3.1. Description

The two reinforced concrete beam specimens present a cross-section of 100 mm width and 180 mm height. The total length was 800 mm. Only one reinforcing bar was deployed at the center of the cross-section and as the rebar used in the tensile test, it was a 900 mm long Φ12 S500 rebar. The concrete

cover was 40 mm. Since both DOFS deployed in this test had a 5.2 m length, it was decided to take advantage of the entire length and install the rest of them at the surface of the concrete after its hardening. These segments and the dimensions of the beams are depicted in Figure 8. The only difference between the two specimens was the bonding material of the fiber to the rebar (cyanoacrylate and two-component epoxy). The same two-component epoxy adhesive is used in both specimens to bond the fiber to the concrete surface.

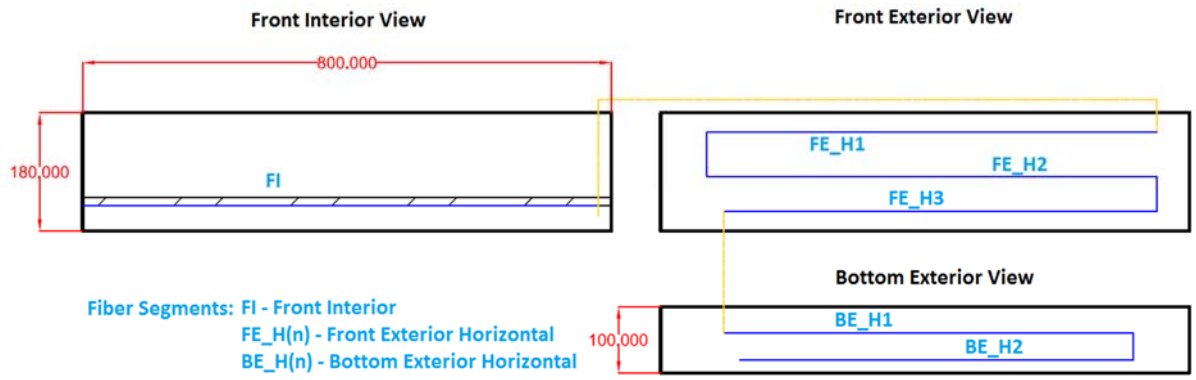

Figure 8. Definition scheme of DOFS deployed on each beam—all dimensions [mm].

With this scheme, it is possible to measure simultaneously the strains both at the rebar and the surface of the concrete using a single sensor. Although the used system allows the user to define sub-cm spatial resolution, it was decided to conduct the measurements of these load tests using a 1 cm spatial resolution, since from other experiences the authors concluded that using a higher spatial resolution provides no practical benefit when applied to concrete structures. This allowed for the measurement of more than 500 different points with each DOFS. The measurements were made with a 5s interval.

For the bonding of the DOFS to the rebar segment, two different adhesives were used in each specimen. In the first beam, a cyanoacrylate adhesive was used whereas in the second beam the installation of the sensor was performed with a two-component epoxy (Figure 9). The idea is to assess which adhesive performed better in these conditions. Finally, as in the case of the tensile rebar test, three strain gauges were installed in the rebar of both specimens for comparison purposes.

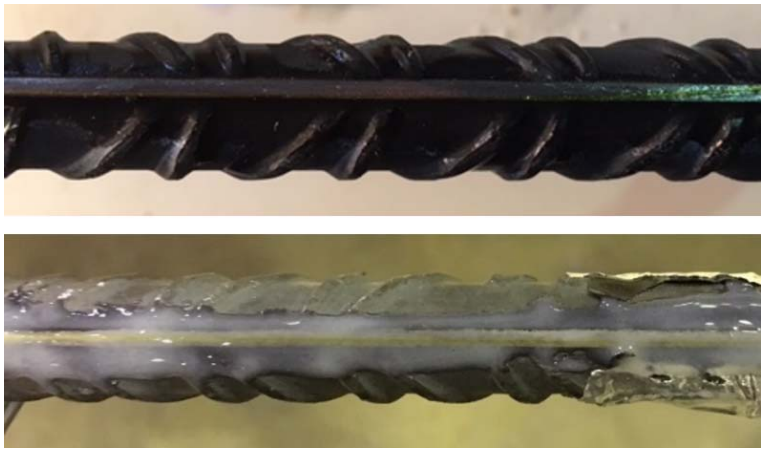

Figure 9. Adhesives on rebar of each beam specimen: cyanoacrylate (Beam 1—top), two-component epoxy (Beam 2—bottom).

Due to the thin coating of the sensors and their subsequent fragility, it was necessary to have great care when pouring the concrete into the moulding where the full set of sensor plus rebar was installed. During concreting, the final part of the fiber not bonded to the rebar was protected with small plastic tubes and fixed to the interior lateral part of the moulding as shown in Figure 7.

After the hardening of the concrete, the remaining length of the fiber was bonded to the surface with the pattern seen in Figures 7 and 8. This scheme was laid out in a way that it was possible to measure compression strains at the top lateral segment (FE-H1); values close to zero at the neutral axis in the middle lateral segment (FE-H2); tension strains at the bottom lateral segment (FE-H3) and the two bottom exterior segments (BE-H1 and BE-H2). For the bonding of the external DOFS segments to the concrete, the two-component epoxy adhesive was used based in successful past experiences of the authors [27,31,32].

With these external segments, it was also expected to detect and follow the evolution of cracking. For this, at the time of pouring the concrete, additional cylindrical samples were also cast. They were later tested at the same dates of the tests in the beam specimens in order to obtain the mechanical properties of the concrete as summarized in Table 1. Here, f_{cm} is the concrete mean compressive strength, f_{ctm} the concrete mean tensile strength, E is elasticity modulus and ε_{fct} the expected maximum tensile strain before concrete cracking. According to these values, the expected cracking load was 8.86 kN in beam 1 and 10.15 kN in beam 2.

Table 1. Mechanical properties of the concrete.

Specimen	f_{cm} (MPa)	f_{ctm}(MPa)	E (GPa)	ε_{fct} (με)
Beam 1	38.41	3.076	28.366	108
Beam 2	44.36	3.523	27.353	129

The goal of the tests was to load the beams up to a load much higher than the cracking load and unload again to observe the performance of the sensor after the occurrence of damage and the further reloading. The loading scheme for each specimen is shown in Figure 10.

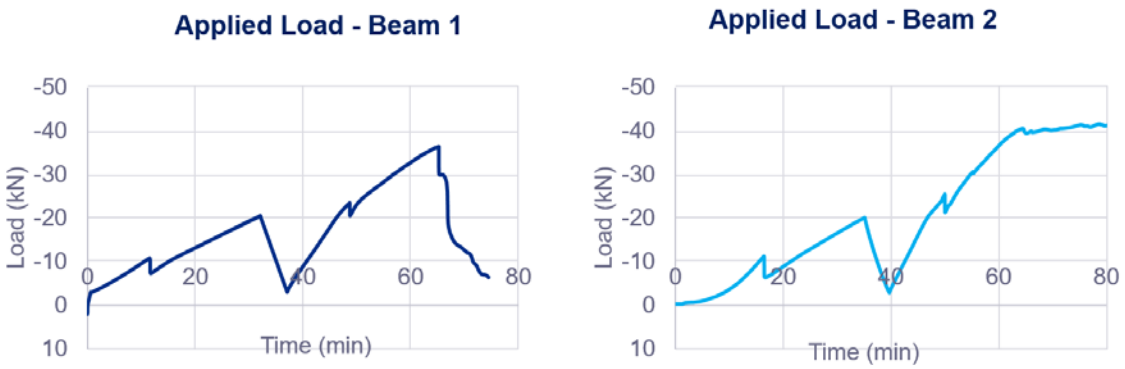

Figure 10. Applied load to each beam specimen.

2.3.2. Results—Beam 1

In this beam, according to the DOFS measurements, the expected concrete tensile strength capacity of 108 με was surpassed for a load of 7.5 kN as seen in Figure 11. However, although being detected by the DOFS, the crack was not yet visually observable. It is not until the load of 10.81 kN which corresponds to minute 11.6 that damage is detected at the segment deployed in the rebar. Moreover, the sensor stopped working around the 51 min mark for a load of 24.3 kN during the second loading stage.

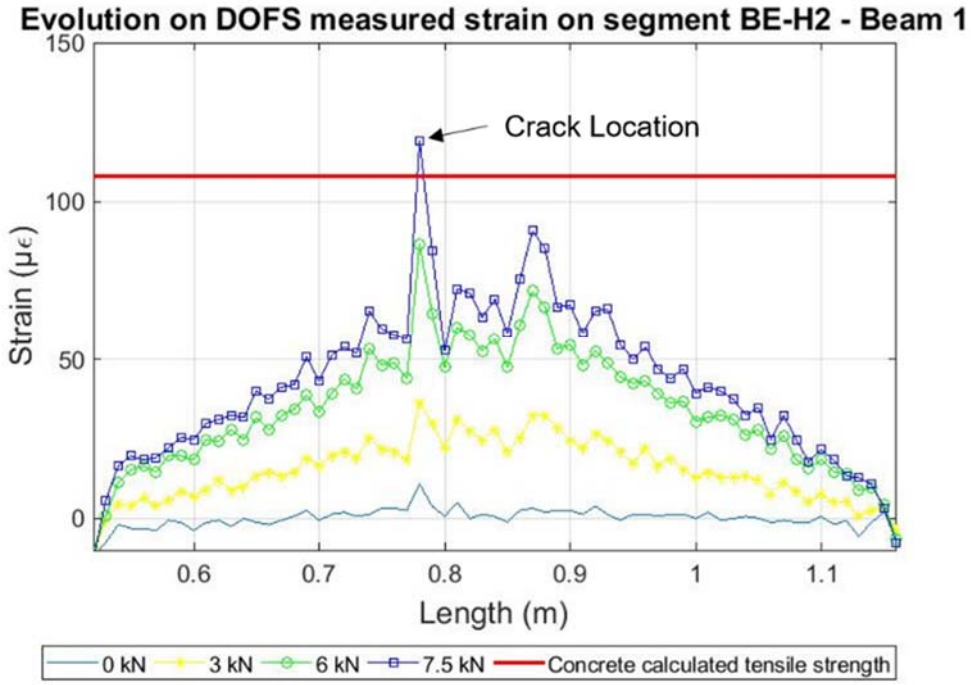

Figure 11. Detection of cracking at the surface of the concrete in beam 1.

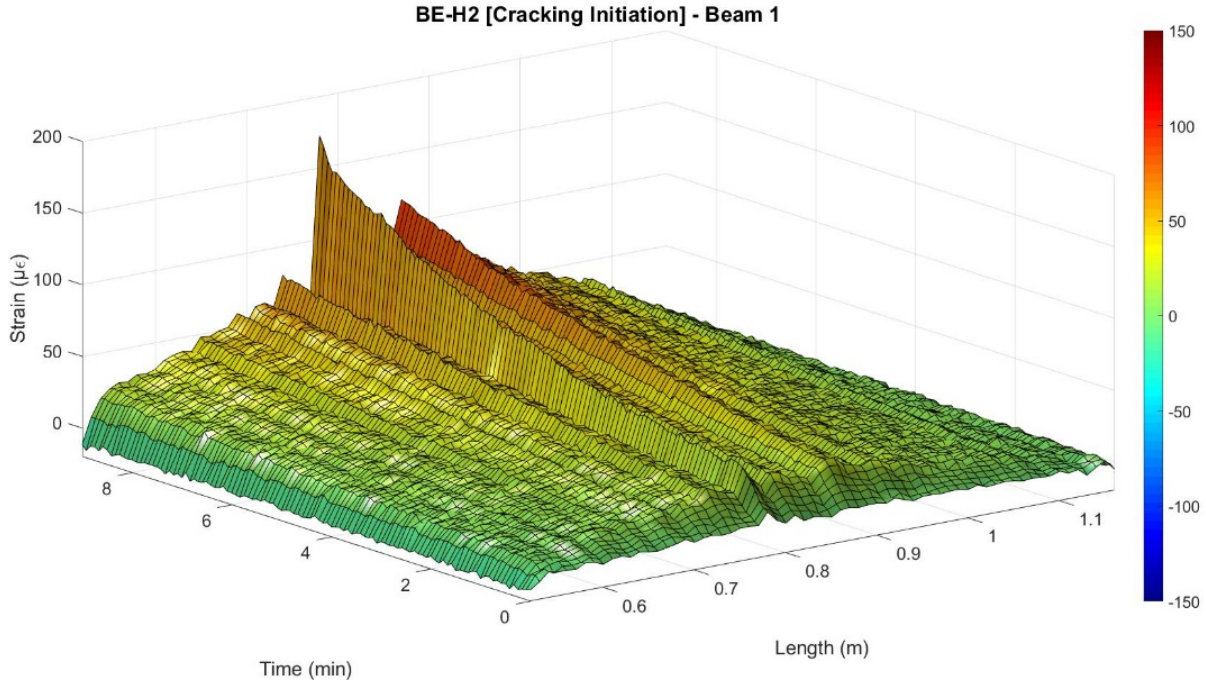

Figure 12. Evolution of strains verified for segment BE-H2 of Beam 1.

Notwithstanding, it was also possible to detect how after the development of cracking the measured values of the DOFS at the location of the crack presented magnitude peaks of either positive or negative values, indicating an invalid measurement. This behaviour after cracking was especially noticeable in the segment attached to the rebar (FI) and will be further discussed in Section 3. However, when analysing each individual segment before the occurrence of cracking, it is possible to observe how the measurements follow smoothly the developed strains as seen in Figure 12.

2.3.3. Results—Beam 2

Here, according to the DOFS measurements, the expected concrete tensile strength of 129 με was surpassed for a load of 9.2 kN as detected by the segments adhered to the bottom surface of the concrete as seen in Figure 13. However, as in Beam 1, it was not until the minute 16.4 that the damage was detected at the rebar for a load of 11.23 kN.

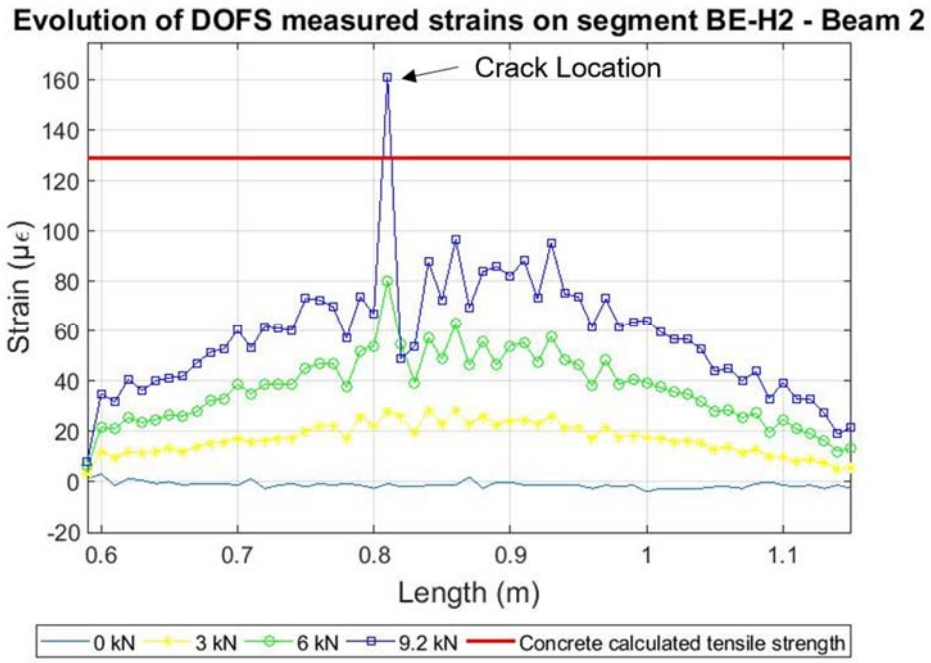

Figure 13. Detection of cracking at the surface of the concrete in beam 2.

Nevertheless, after the development of cracking the DOFS measured strains at the location of the damage show the same alternate positive and negative peaks as obtained in beam 1. Afterwards, the sensor started measuring very inaccurate data starting around the minute 32 for most of the length of the fiber, which corresponded to a load of 17.8 kN until breaking of the sensor close to minute 45. Notwithstanding, for all effects, the fiber sensor was considered unreliable from the minute 32. As before, it is however possible to follow smoothly the evolution of the developed strain along the pre-cracking scenario as seen in Figure 14.

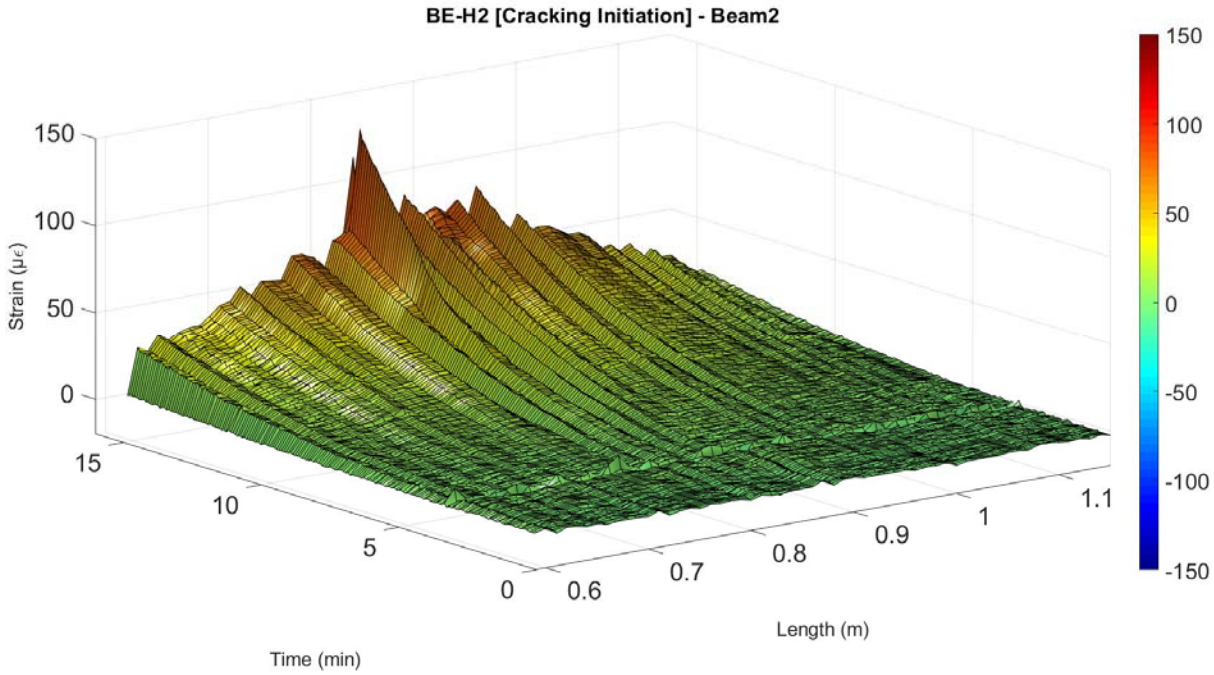

Figure 14. Evolution of strains verified for segment BE-H2 of Beam 2.

2.3.4. Comparison with Strain Gauges

Regarding the segment adhered to the rebar, it is possible to compare the DOFS strains with the ones obtained by the strain gauges. As it is possible to see from Figures 15 and 16, before the development of cracking, a great agreement between the two sets of sensors is achieved. Notwithstanding, it is possible to observe how the measurements in Beam 1 (cyanoacrylate bonded) present an overall smoother reading for the initial unloaded stage when compared with Beam 2 (epoxy bonded).

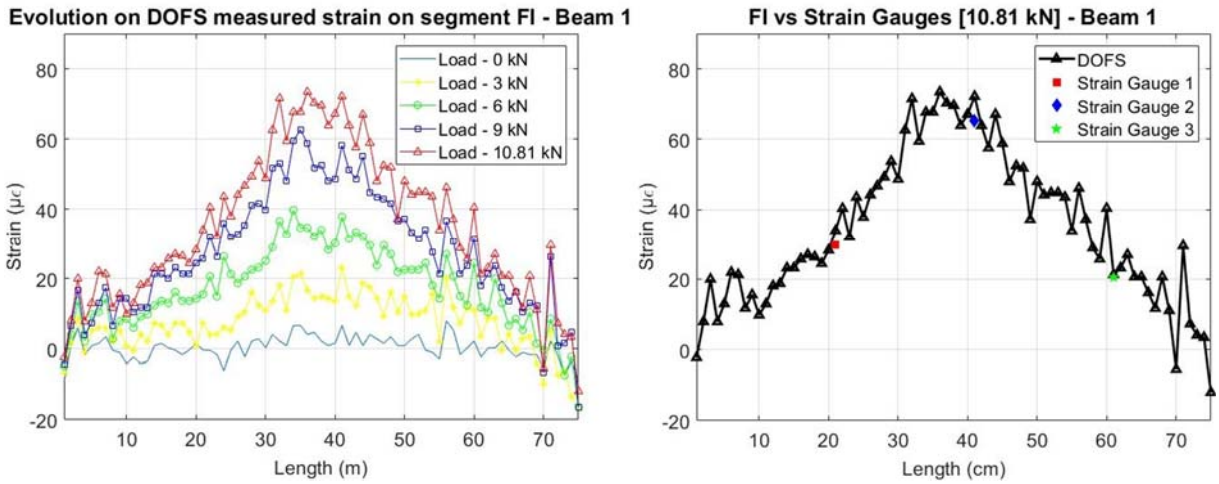

Figure 15. Strains measured by the DOFS on the embedded segment for Beam 1.

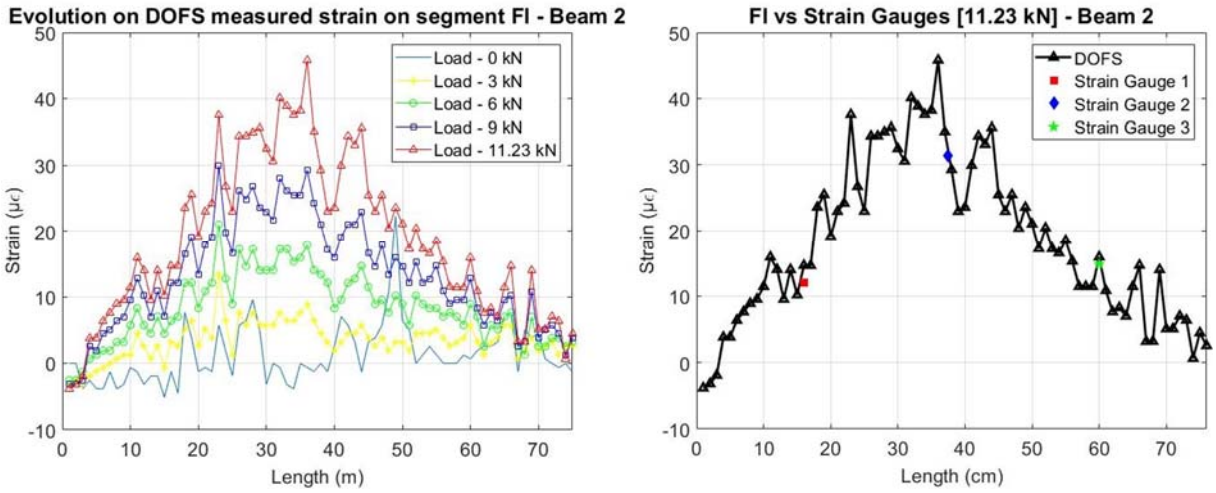

Figure 16. Strains measured by the DOFS on the embedded segment for Beam 2.

In both beams, the two set of sensors measure, as expected, higher strains at mid-span. It is also possible to see, as mentioned before, that for the load levels where cracking has already occurred at the concrete surface, the damage is not yet detected at the rebar level.

After the development of cracking, due to the aforementioned high magnitude peaks observed for the measurements obtained in this segment and also due to the distributed capacity of the DOFS, the comparison of these two set of sensors is hard to achieve and will be only possible after a post-processing of the raw data as presented in Section 3.

As a result, it is necessary to overcome the challenge presented by the inaccurate measurements after the occurrence of cracking in order to better analyse the obtained data in this stage. One possible way to do it is by removing the inaccurate measurements and interpolating based on the remaining accurate values. In order to assess which values are accurate or not, the spectral shift quality (SSQ) of the measured data has to be analysed.

3. Post-Processing

3.1. Spectral Shift Quality — SSQ

When analysing monitored data acquired through the use of optical frequency domain reflectometry (OFDR) based DOFS, such as the ODiSI A system used in this experiment, it is always important to evaluate and assure the Spectral Shift Quality (SSQ) of the obtained measurements.

According to the manufacturer of this data acquisition system (LUNA Technologies), the SSQ is a qualitative measure of the strength of the correlation between the conducted measurement (at any point and time) and the original baseline reflected spectra [26]. This is calculated as shown in the following expression:

$$\text{Spectral Shift Quality } = \frac{\max\left(U_j(\upsilon) \star U_j(\upsilon - \Delta\upsilon_j)\right)}{\Sigma U_j(\upsilon)^2} \tag{3}$$

- $U_j(\upsilon)$ is the baseline spectrum for a given segment of data;
- $Uj(\upsilon - \Delta\upsilon j)$ is the measurement spectrum under a strain or temperature change;
- $\star$ symbol is used to represent the cross-correlation operator.

In this way, the SSQ is the maximum value of the cross-correlation of the baseline measurement and measurement spectra normalized by the maximum expected value. Hence, the value of the SSQ should theoretically be between 0 and 1, where 1 is obtained when a perfect correlation is achieved and 0 when it is uncorrelated. This value can also, in practical terms, be observed to be above the value 1 due to small variations in the laser power.

Therefore, the manufacturer advises to disregard any measurements with a SSQ below 0.15, since when this threshold is reached, it is likely that the strain or temperature change has exceeded the measurable range. This also implies, that the further the damage is developed in the monitored structural element, the lower the SSQ values will be. In this way, when calculating the values SSQ for the measurements obtained in the two beams, Figures 17 and 18 are obtained.

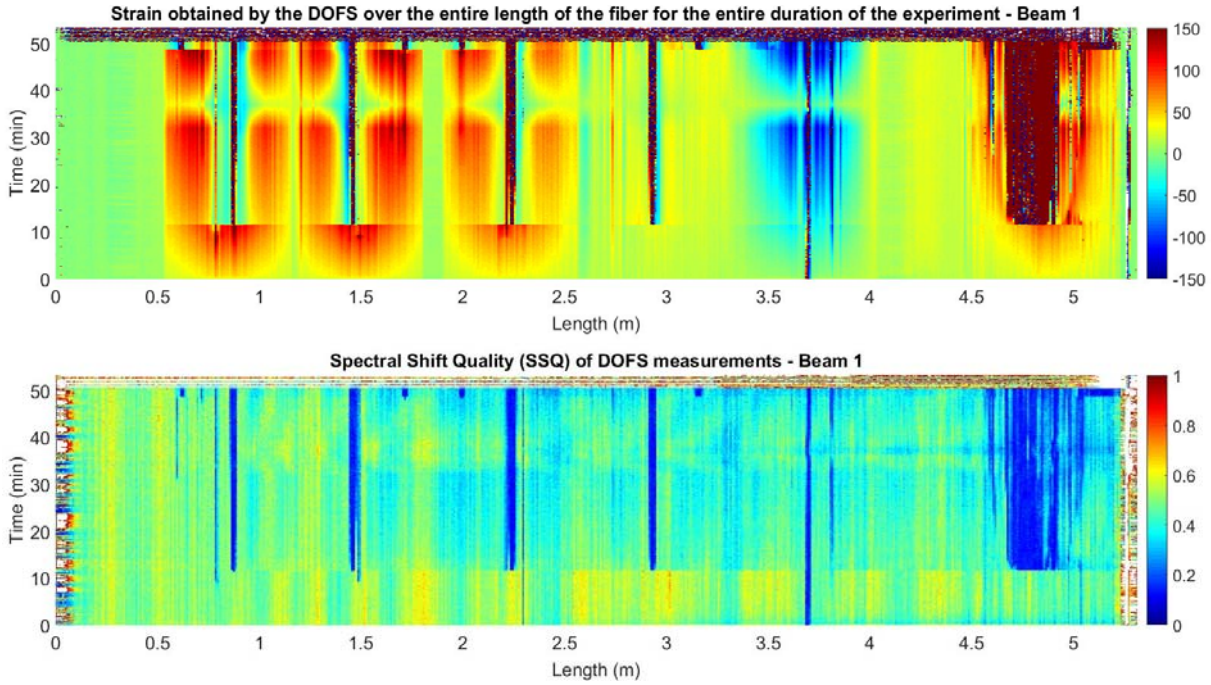

Figure 17. Strain and SSQ for beam 1.

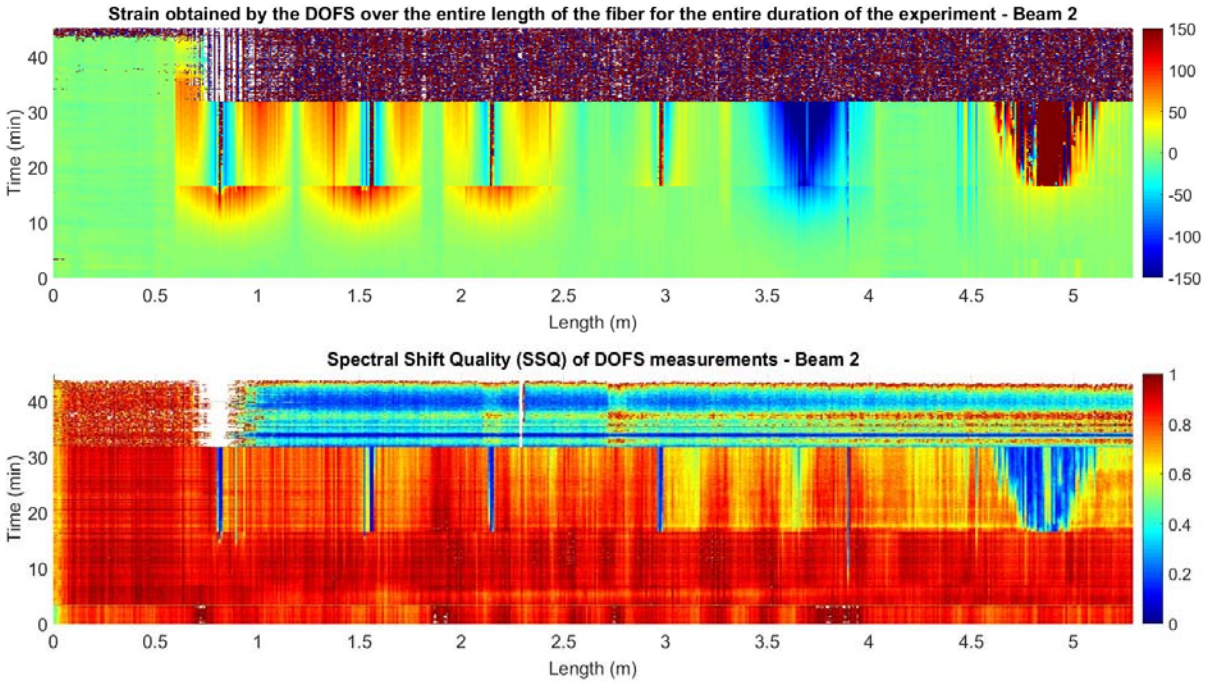

Figure 18. Strain and SSQ for beam 2.

The analysis of Figures 17 and 18 shows how the locations of the values with an SSQ below 0.15 and the strain values with high magnitude peaks are greatly correlated.

This situation of the dropping of the SSQ values during flexural load tests is also reported in [38]. In fact, in this last case the authors refer the consideration of a SSQ threshold of 0.17 while using nylon-coated fibers adhered on the surface of the concrete due to the proximity of inaccurate values.

The low SSQ values are close to the crack location in the segments adhered to the surface of the concrete and within a wider area in the rebar segment. This is explained as segments with large strain gradients increase the noise levels of the DOFS measurements [39].

3.2. Overcoming Drop of SSQ

As mentioned before, in order to feasibly analyse the performance of the fiber sensor in the embedded segment FI after the occurrence of cracking it is necessary to extract all the points with an inaccurate SSQ value. Nevertheless, when performing this task and although the manufacturers' user guide recommends the use of the 0.15 SSQ value as threshold, the authors observed that several isolated peaks still remained in the measured data of segment FI. This is due to the surrounding proximity to the aforementioned values with low SSQ.

Therefore, it was observed that using a threshold of 0.20 these remaining peaks were optimally eliminated. The authors believe that this threshold is subjected to the specific case of the use of a polyimide-coated fiber in the embedded segment in the concrete.

After removing these unreliable data points, it is then possible to interpolate the surface points of the embedded segment in order to better analyse the behaviour of the structural element after cracking.

The result of the elimination of the values with SSQ lower than 0.2 and posterior interpolation in segment FI is shown in Figures 19 and 20 for Beam 1 and Beam 2, respectively.

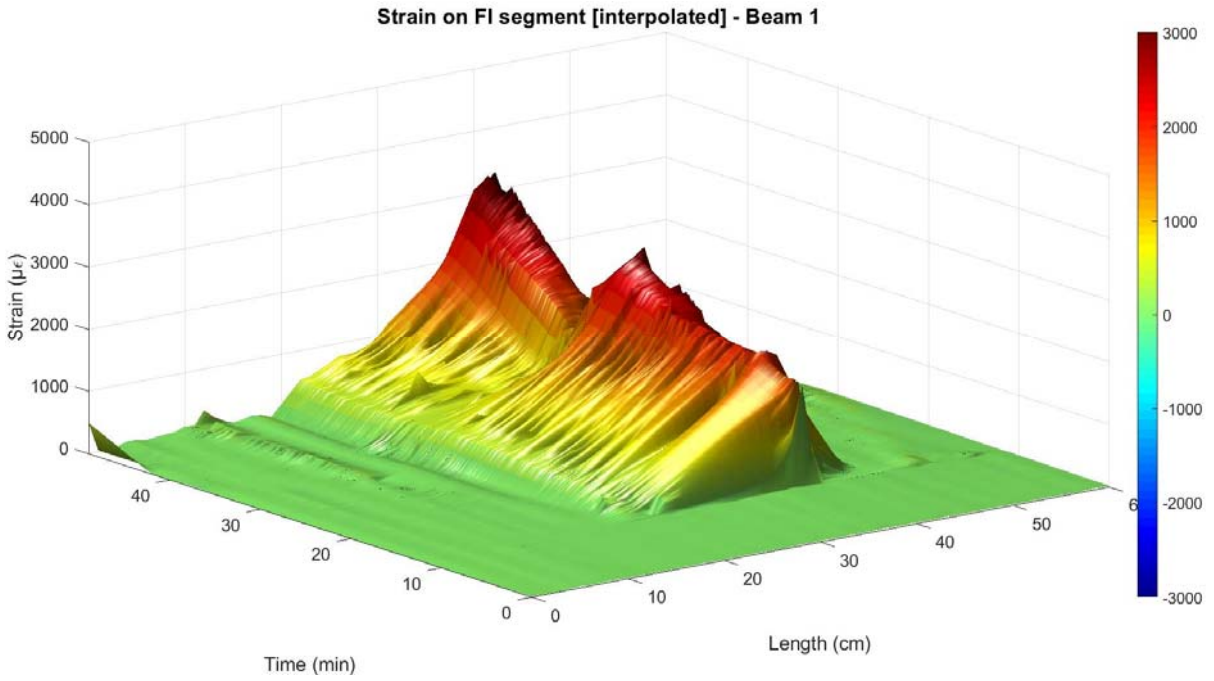

Figure 19. Interpolated measured strain at the embedded segment in Beam 1.

From Figure 20, it is possible to observe that despite the removing of the unreliable values with exactly the same criteria on both beam specimens, after the surface interpolation a reduced number of peaks is still observable for beam 2. This is attributed to the better performance of the cyanoacrylate adhesive as a bonding product when used in the rebar element jointly with a polyimide-coated fiber.

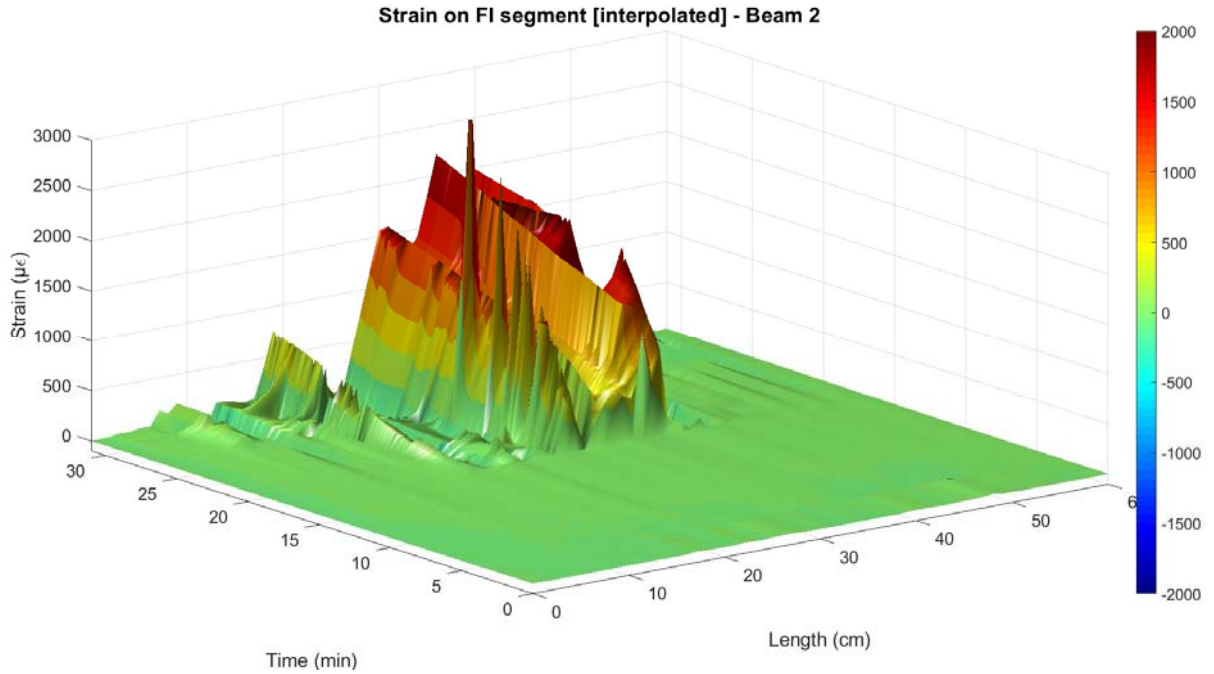

Figure 20. Interpolated measured strain at the embedded segment in Beam 2.

Nevertheless, after this post-processing it is observable how the DOFS data mostly presents strain evolution that is compatible with the applied load. This is especially noticeable in Beam 1 since, as mentioned before, in this specimen the sensor worked properly until a later stage of the loading process. In this specimen and from Figure 19, it is shown how the DOFS interpolated measurements follows the same load cycle of loading, unloading and a new loading until the rupture of the fiber.

The effect of this post-processing is also represented in Figure 21 for the specific load level of 15 kN for both beams. Here, it is observable how the main inaccurate peaks were removed and the interpolated values got closer to what is measured by the strain gauges and what is expected from a three-point load test in a simply supported element.

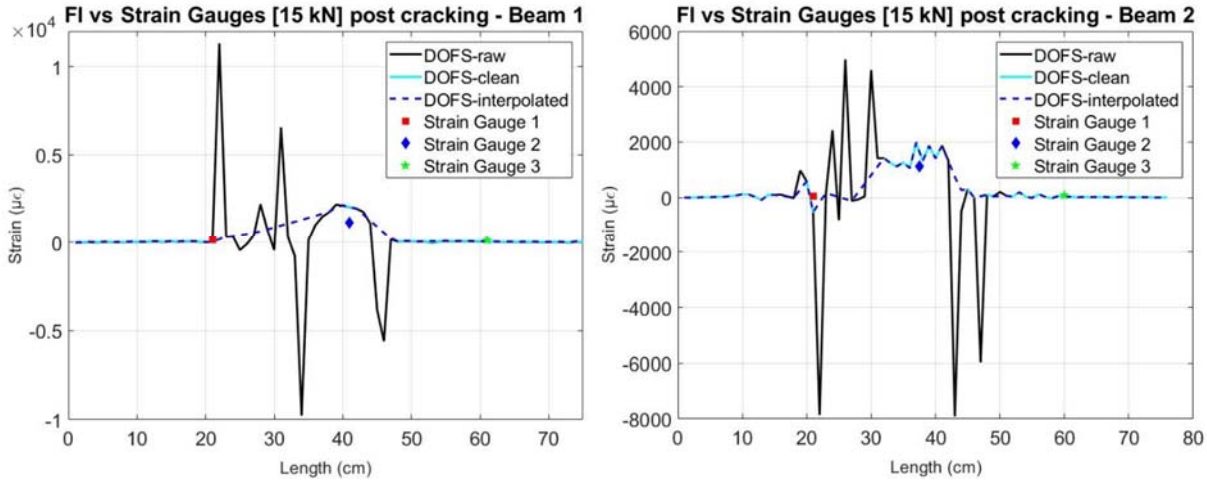

Figure 21. Comparison of the measured values before and after interpolation of the DOFS with the strain gauges for 15 kN—Beam 1 (left) and Beam 2 (right).

3.3. Performance Assessment of the Embedded DOFS

When comparing the values after cracking with those measured by the strain gauges, we can see, in general, a good agreement, as shown in Figures 22 and 23 for a load level of 15 kN. Furthermore, it is observable how the crack observed visually directly on the beam specimens for this load level, agrees with the data obtained by the sensors.

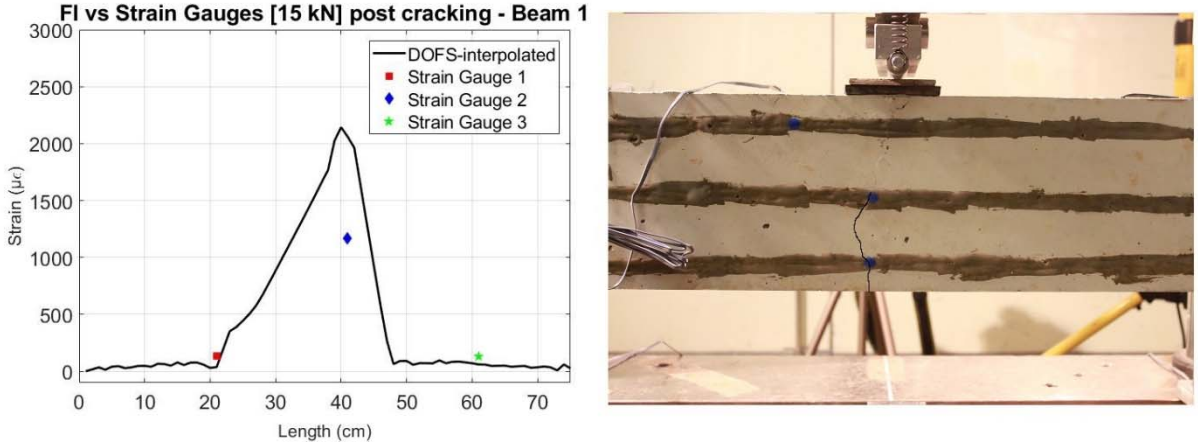

Figure 22. Comparison of interpolated values of DOFS with Strain Gauges for a 15 kN load (left) and photo of beam specimen with highlighted crack (right)—Beam 1.

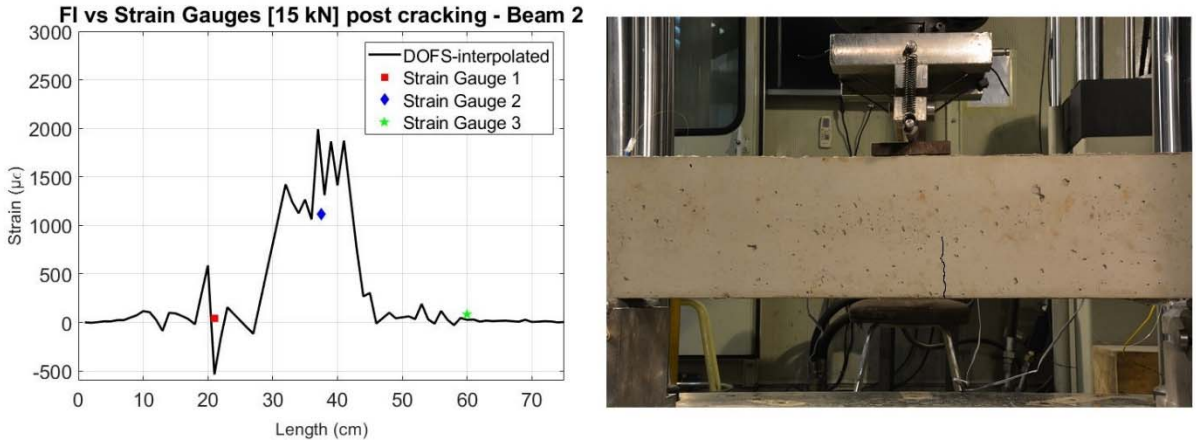

Figure 23. Comparison of interpolated values of DOFS with Strain Gauges for a 15 kN load (left) and photo of beam specimen with highlighted crack (right)—Beam 2.

When comparing the evolution of the strain data obtained by the DOFS at the mid-span point of the rebar and the strain gauge 2 (also located close to the center) with the applied load, Figures 24 and 25 are obtained.

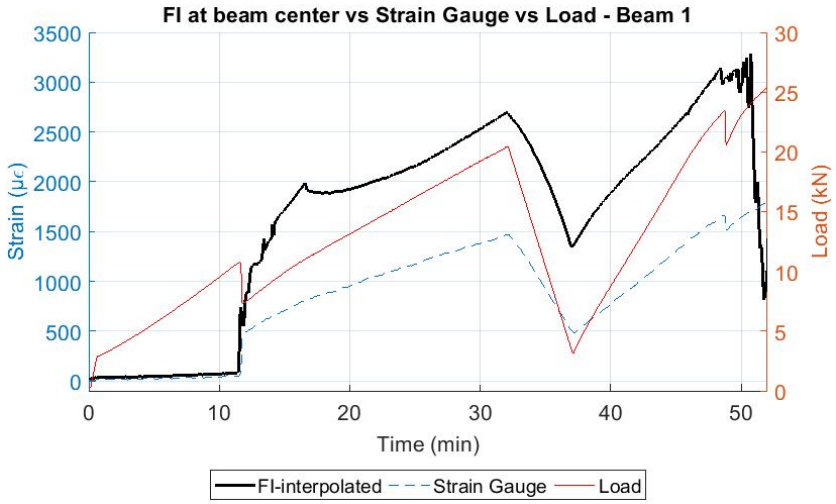

Figure 24. Comparison of DOFS with strain gauge and the applied load—Beam 1.

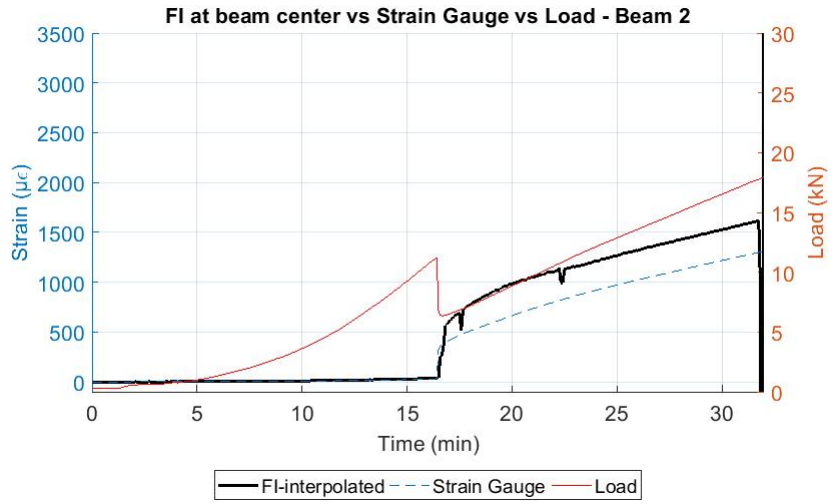

Figure 25. Comparison of DOFS with strain gauge and the applied load—Beam 2.

In these figures, it is possible to see how the strain in the rebar increases significantly only when load levels reach the cracking load and how the DOFS measurements follow the same trend as the strain gauge according to the applied load. The difference in the values measured by the DOFS and the strain gauge are explained by two facts: first, the location of the strain gauge does not match exactly the point where the DOFS measurement is represented and, second, as the fiber and the strain gauge are bonded on opposite parts of the rebar, then a local bending effect in the rebar itself may derive on a local compression and local tension to be added to the general tension in the rebar due to the global bending induced by the vertical applied load. It is again observable, how the fiber in beam 1 was able to perform longer until rupturing around minute 51 for a load of 24.3 kN while on beam 2, the fiber ruptured around minute 32 for a load of 17.8 kN.

Despite the challenge presented by the reduction of the SSQ values associated to some points of the DOFS after the occurrence of cracking to levels that implied unreliable measurements, due to the distributed capacities of this sensor technology, it is still possible to gather relevant information corresponding to the cracked behaviour of the concrete beams. This is obtained using only one single sensor, where in other scenarios, multiple discrete sensors would be required.

4. Conclusions

In this paper, a new method of implementation of Rayleigh OFDR-based DOFS in reinforced concrete structures in both uncracked and cracked scenarios is discussed. With the intention of increasing the accuracy of the sensor measurements and to increase its protection to external environmental effects, a thin polyimide-coated distributed sensor was bonded directly to a reinforcing steel bar without any previous mechanization.

This implementation technique was first tested in an isolated S500 steel rebar during a simple tensile load test within the elastic range of this material. Comparing with the results coming from the strain gauges, it was observed how the DOFS provided reliable measurements for the entire length of bonding and duration of the test.

Afterwards, a three-point load test with a loading and unloading sequence after cracking was conducted in two similar reinforced concrete beams, where a 5.2 m DOFS was simultaneously deployed in the rebar and, after the hardening of the concrete, bonded to the outer surface of the beam through different segments intended to measure different structural patterns. Strain gauges were also used for comparison purposes. The only difference between the two beam specimens was the adhesive, cyanoacrylate for beam 1 and a two-component epoxy for beam 2. This adhesive was also used to bond the same DOFS to the concrete surface. The main findings of this study are the following:

1. The optic fiber bonded to the rebar and crossing the cracks delivered good results even in the case of loading and unloading of the specimen, what may create some disturbances in the fiber surrounding the lips of the crack due to the roughness and heterogeneity of the concrete material.

2. The distributed optical fiber sensors were able to detect and locate the formation of cracking at the surface of the concrete and to reflect how while this cracking had already occurred at the concrete surface, this damage was not detected in the rebar element until a later load stage.
3. After a certain load which corresponded to a significant stiffness change in the beam specimens and the detection of damage at the rebar element, some measurements at the location of the damage started to present unreliable data values. This was especially noticeable for the rebar-adhered DOFS segment (FI). This is associated with a decrease of the spectral shift quality (SSQ) values at these point locations.
4. The results show that a minimum spectral shift quality (SSQ) of 0.20 is necessary to get reliable results when embedded polyimide-coated DOFS are used in the reinforcing bars. By now, the only recommendations in this sense were the one by the system acquisition manufacturers' users guide which refers DOFS data points with SSQ values below 0.15 to be unreliable, and that of Brault et al. [38] which considers SSQ values below 0.17 as unreliable when using nylon-coated fibers bonded to concrete surfaces. In any case, further research is planned on the preventive decrease of the SSQ values by analysing the conditions causing this effect circumstance and the optimal way to avoid them. The proposed threshold of 0.20 for the SSQ value should be also verified in further tests using polyimide-coated DOFS.
5. A method is presented to overcome the low SSQ values with an interpolation post-processing routine that enables a better interpretation of the measurements in later steps of the load test.
6. A better performance was observed when using cyanoacrylate adhesive in the reinforcing steel compared to a two-component epoxy in the case that polyimide-coated DOFS are used. Not only did the embedded cyanoacrylate bonded segment presented smoother data within the uncracked range, but an enhanced performance during a longer time and load level was achieved too.
7. The tests have shown the feasibility of deploying a single polyimide coated Rayleigh OFDR based DOFS, simultaneously to the rebar and external surface of a reinforced concrete beam. This results in a simpler and more economic experimental set-up.

Acknowledgments: The authors want to knowledge the financial support provided by the European Union's Horizon 2020 research and innovation programme under the Marie Sklodowska-Curie grant agreement No. 642453.

Author Contributions: António Barrias and Joan R. Casas conceived and designed the experiments; António Barrias performed the experiments with the aid of Sergi Villalba in the implementation step of the DOFS to the specimens and the interrogator software configuration; António Barrias and Joan R.

Casas analyzed the data; Sergi Villalba contributed with the ODiSI A interrogator for the conduction of the experiment; António Barrias and Joan R. Casas wrote the paper.

Conflicts of Interest: The authors declare no conflict of interest.

References

[1] Leung, C.K.; Wan, K.T.; Inaudi, D.; Bao, X.; Habel, W.; Zhou, Z.; Ou, J.; Ghandehari, M.; Wu, H.C.; Imai, M. Review: Optical fiber sensors for civil engineering applications. *Mater. Struct.* **2013**, *48*, 871–906.

[2] Glisic, B.; Hubbell, D.; Sigurdardottir, D.H.; Yao, Y. Damage detection and characterization using long-gauge and distributed fiber optic sensors. Opt. Eng. **2013**, 52, 87101.

[3] Kudva, J.N.; Marantidis, C.; Gentry, J.D.; Blazic, E. Smart structures concepts for aircraft structural health monitoring. In Proceedings of the North American Conference on Smart Structures and Materials, Albuquerque, NM, USA, 1–4 February **1993**, pp. 964–971.

[4] Bao, X.; Chen, L. Recent progress in distributed fiber optic sensors. Sensors **2012**, 12, 8601–8639.

[5] Ferdinand, P. The Evolution of Optical Fiber Sensors Technologies during the 35 Last Years and Their Applications in Structure Health Monitoring. In Proceedings of the EWSHM-7th European Workshop on Structural Health Monitoring, Nantes, France, 9 July **2014**.

[6] Li, H.N.; Li, D.S.; Song, G.B. Recent applications of fiber optic sensors to health monitoring in civil engineering. Eng. Struct. **2004**, 26, 1647–1657.

[7] Chan, T.H.; Yu, L.; Tam, H.Y.; Ni, Y.Q.; Liu, S.Y.; Chung, W.H.; Cheng, L.K. Fiber Bragg grating sensors for structural health monitoring of Tsing Ma bridge: Background and experimental observation. Eng. Struct. **2006**, 28, 648–659.

[8] Xu, G.Q.; Xiong, D.Y. Applications of fiber Bragg grating sensing technology in engineering. Chin. Opt. **2013**, 6, 306–317.

[9] Miller, J.W.; Mendez, A. Fiber Bragg Grating Sensors: Market Overview and New Perspectives. Fiber Bragg Grating Sens. Recent Adv. Ind. Appl. Mark. Exploit. **2014**, 8, 313–320.

[10] Fanelli, P.; Biscarini, C.; Jannelli, E.; Ubertini, F.; Ubertini, S. Structural health monitoring of cylindrical bodies under impulsive hydrodynamic loading by distributed FBG strain measurements. Meas. Sci. Technol. **2017**, 28, 24006.

[11] Glisic, B.; Inaudi, D. Development of method for in-service crack detection based on distributed fiber optic sensors. Struct. Health Monit. **2012**, 11, 161–171.

[12] García-Macías, E.; D'Alessandro, A.; Castro-Triguero, R.; Pérez-Mira, D.; Ubertini, F. Micromechanics modeling of the uniaxial strain-sensing property of carbon nanotube cement-matrix composites for SHM applications. Compos. Struct. **2017**, 163, 195–215.

[13] Glisic, B.; Oberste-ufer, K. Validation Testing of Fiber Optic Method for Buried Pipelines Health Assessment after Earthquake-Induced Ground Movement. In Proceedings of the 2011 NSF Engineering Research and Innovation Conference, Atlanta, GA, USA, 4–7 January **2011**.

[14] Henault, J.M.; Moreau, G.; Blairon, S.; Salin, J.; Courivaud, J.R.; Taillade, F.; Merliot, E.; Dubois, J.P.; Bertrand, J.; Buschaert, S.; et al. Truly Distributed Optical Fiber Sensors for Structural Health Monitoring: From the Telecommunication Optical Fiber Drawling Tower to Water Leakage Detection in Dikes and Concrete Structure Strain Monitoring. Adv. Civ. Eng. 2010, **2010**, 1–13.

[15] Mayhew, H.E.; Frano, K.A.; Svoboda, S.A.; Wustholz, K.L. Using Raman Spectroscopy and Surface-Enhanced Raman Scattering To Identify Colorants in Art: An Experiment for an Upper-Division Chemistry Laboratory. J. Chem. Educ. **2014**, 92, 148–152.

[16] Muehlethaler, C.; Leona, M.; Lombardi, J.R. Review of surface enhanced Raman scattering applications in forensic science. Anal. Chem. **2015**, 88, 152–169.

[17] Uchida, S.; Levenberg, E.; Klar, A. On-specimen strain measurement with fiber optic distributed sensing. Measurement **2015**, 60, 104–113.

[18] Bao, Y.; Tang, F.; Chen, Y.; Meng, W.; Huang, Y.; Chen, G. Concrete pavement monitoring with PPP-BOTDA distributed strain and crack sensors. Smart Struct. Syst. **2016**, 18, 405–423.

[19] Meng, D.; Ansari, F. Interference and differentiation of the neighboring surface microcracks in distributed sensing with PPP-BOTDA. Appl. Opt. **2016**, 55, 9782–9790.

[20] Bao, Y.; Valipour, M.; Meng, W.; Khayat, K.H.; Chen, G. Distributed fiber optic sensor-enhanced detection and prediction of shrinkage-induced delamination of ultra-high-performance concrete overlay. Smart Mater. Struct. **2017**, 26, 85009.

[21] Rui, Y.; Kechavarzi, C.; O'Leary, F.; Barker, C.; Nicholson, D.; Soga, K. Integrity Testing of Pile Cover Using Distributed Fibre Optic Sensing. Sensors **2017**, 17, 2949.

[22] Yan, J.; Shi, B.; Ansari, F.; Zhu, H.; Song, Z.; Nazarian, E. Analysis of the strain process of soil slope model during infiltration using BOTDA. Bull. Eng. Geol. Environ. **2017**, 76, 947–959.

[23] Güemes, A.; Fernández-López, A.; Soller, B. Optical Fiber Distributed Sensing—Physical Principles and Applications. Struct. Health Monit. **2010**, 9, 233–245.

[24] Barrias, A.; Casas, J.; Villalba, S. A Review of Distributed Optical Fiber Sensors for Civil Engineering Applications. Sensors **2016**, 16, 748.

[25] LUNA. Fiber Optic Sensing. Available online: https://lunainc.com/wp-content/uploads/2012/08/3567_Luna_Sensing_Brochure_FINAL_111414.pdf (accessed on 22 February **2018**).

[26] LUNA. ODiSI-A Users Guide. Available online: http://lunainc.com/wp-content/uploads/2014/05/ODiSI-A-Users-Guidev1.2.pdf (accessed on 6 October **2014**).

[27] Barrias, A.; Rodriguez, G.; Casas, J.R.; Villalba, S. Application of distributed optical fiber sensors for the health monitoring of two real structures in Barcelona. Struct. Infrastruct. Eng. **2018**, doi:10.1080/15732479.2018.1438479.

[28] Ansari, F.; Libo, Y. Mechanics of bond and interface shear transfer in optical fiber sensors. J. Eng. Mech. **1998**, 124, 385–394.

[29] Wan, K.T.; Leung, C.K.Y.; Olson, N.G. Investigation of the strain transfer for surface-attached optical fiber strain sensors. Smart Mater. Struct. **2008**, 17, 35037.

[30] Henault, J.M.; Salin, J.; Moreau, G.; Quiertant, M.; Taillade, F.; Benzarti, K.; Delepine-Lesoille, S. Analysis of the strain transfer mechanism between a truly distributed optical fiber sensor and the surrounding medium. In Concrete Repair, Rehabilitation and Retrofitting III, Proceedings of the 3rd International Conference on Concrete Repair, Rehabilitation and Retrofitting, ICCRRR-3, Cape Town, South Africa, 3–5 September **2012**; Taylor & Francis Group: London, UK, 2012; p. 266.

[31] Rodriguez, G.; Casas, J.R.; Villalba, S. Cracking assessment in concrete structures by distributed optical fiber. Smart Mater. Struct. **2015**, 24, 35005.

[32] Villalba, S.; Casas, J.R. Application of optical fiber distributed sensing to health monitoring of concrete structures. Mech. Syst. Signal Process. **2012**, 39, 441–451.

[33] Quiertant, M.; Baby, F.; Khadour, A.; Marchand, P.; Rivillon, P.; Billo, J.; Lapeyrere, R.; Toutlemonde, F.; Simon, A.; Cordier, J.; Renaud, J.C. Deformation monitoring of reinforcement bars with a distributed fiber optic sensor for the SHM of reinforced concrete structures. In Proceedings of the NDE, Seattle, WA, USA, May **2012**; p. 10.

[34] Regier, R.; Hoult, N.A. Concrete deterioration detection using distributed sensors. Proc. Inst. Civ. Eng. Build. **2015**, 168, 118–126.

[35] Davis, M.; Hoult, N.A.; Scott, A. Distributed strain sensing to determine the impact of corrosion on bond performance in reinforced concrete. Constr. Build. Mater. **2016**, 114, 481–491.

[36] Davis, M.; Hoult, N.A.; Scott, A. Distributed strain sensing to assess corroded RC beams. Eng. Struct. **2017**, 140, 473–482.

[37] LUNA. High-Definition Fiber Optic Strain Sensors. Available online: https://lunainc.com/wpcontent/uploads/2016/10/Sensors_DataSheet_Template_final_092216.pdf (accessed on 9 November **2016**).

[38] Brault, A.; Nurmi, S.; Hoult, N.A. Distributed Deflection Measurement of Reinforced Concrete Elements Using Fibre Optic Sensors. In Proceedings of the International Association for Bridge and Structural Engineering (IABSE) Symposium, Vancouver, BC, Canada, 22 September **2017**; pp. 1461–1469.

[39] Kreger, S.T.; Gifford, D.K.; Froggatt, M.E.; Soller, B.J.; Wolfe, M.S. High resolution distributed strain or temperature measurements in single-and multi-mode fiber using swept-wavelength interferometry. In Optical Fiber Sensors, OSA Technical Digest (CD) (Optical Society of America, **2006**), paper ThE42.

4.3. Journal Article III

Application of Distributed Optical Fiber Sensors for the Health Monitoring of two real structures in Barcelona (Spain)

Published in Structure and Infrastructure Engineering, vol. 14, 2018 – Issue 7, p. 967-985, February 2018. doi: 10.1080/15732479.2018.1438479

António Barrias [1], Gerardo Rodriguez [1], Joan R. Casas [1] and Sergi Villalba [2]

[1]Department of Civil and Environmental Engineering, Technical University of Catalonia (UPC), c/ Jordi Girona 1-3, 08034 – Barcelona, Spain

[2]Department of Engineering and Construction Projects, Technical University of Catalonia (UPC), c/ Colom 11, Ed. TR5, 08022 – Terrassa (Barcelona), Spain

Received: 24 March 2017; Accepted: 12 July 2017; Published: 23 February 2018

Abstract: The versatility and easy installation of Distributed Optical Fiber Sensors (DOFS) compared with traditional monitoring systems is an important characteristic to consider when facing the Structural Health Monitoring (SHM) of real world structures. The DOFS used in this study provide continuous (in space) strain data along the optical fiber with high spatial resolution. The main issues and results of two different existing structures monitored with DOFS, are described in this paper. The main SHM results of the rehabilitation of an historical building used as hospital and the enlargement of a prestressed concrete bridge are presented. The results are obtained using a novel DOFS based on an Optical Backscattered Reflectometry (OBR) technique. The application of the optical fiber monitoring system to two different materials (masonry and concrete) provides also important insights on the great possibilities of this technique when monitoring existing structures. In fact, the influence in strain transfer between the DOFS and the bonding surface is one of the principal effects that should be considered in the application of the OBR technique to real structures. Also, and because structural surfaces generally present considerable roughness, the procedure to attach the optical fiber to the two monitored structures is described.

Keywords: SHM, optical fiber, DOFS, Rayleigh backscatter, OBR,

1. Introduction

Civil engineering infrastructure has an extremely important role in the comfort, security and competitiveness of any society, enabling it to function properly. These structures however, are subjected to several events that deteriorate and compromise their structural integrity throughout their service lifetime. These events may adversely affect the future performance of infrastructures. In order to maintain and ensure the wellbeing of their users, it is paramount that the occurrence of damage in infrastructures is well followed and even predicted and controlled, enabling a fast action of condition screening that can minimize the adverse effects and inherent repair costs. Implementing such damage identification strategy for civil engineering infrastructure (as well as aerospace and mechanical engineering infrastructures) is indicated as Structural Health Monitoring (SHM) [1].

This has been one of the most studied and researched fields in the past two decades within the engineering and academic communities due to its vital importance and potential to allow better decision making by infrastructure owners and agencies. Nevertheless, there is still a lot of work to be done in order to practice SHM strategies in a large scale and in a systematic manner to civil infrastructures due to the current lack of reliable and inexpensive generic monitoring solutions [2].

Traditionally, the assessment of the condition of buildings, bridges, tunnels and other vital civil engineering infrastructures, is carried out through periodical visual inspections by trained engineers, which sometimes can result in inaccurate evaluations due to the wide range of the background for safety condition assessment associated with each inspector.

The use of sensor-based monitoring systems improves SHM practices by improving their efficiency and accuracy, being here where the use of optical fiber sensors offers unmatched features. As it was already presented in various research papers [3], [4], optical fiber sensors (OFS) present several advantages when compared to the more traditional and used electrical ones. Some of their most appealing characteristics are related with their immunity to electromagnetic interferences and corrosion, long term reliability and small size and weight [5], [6]. More specifically, the use of long-gauge fiber optic sensors combined with other standard sensors as accelerometers have shown their applicability in the damage detection in the case of a laboratory experiment. The use of fiber-optic sensors allows to overcome the difficulties associated with the traditional dynamic measurement methods, such as the limitations in the number and in the locations of the monitoring devices [7], [8].

Distributed Optical Fiber Sensors (DOFS) share the same advantages of discrete optical fiber sensors. However, contrary to the other sensors, they offer the possibility of monitoring variations of one-dimensional structural physical fields along the entire optical fiber in a truly distributed way. In this way, virtually every cross-section of the structure is instrumented. Furthermore, an additional benefit associated with distributed sensing is that it only requires a single connection cable in order to communicate the acquired data to the reading unit in opposition to the large number of otherwise

required connecting cables when using discrete sensors. Hence, the installation and operation of distributed sensors is more simple and cost-effective [9].

The use of DOFS has opened new possibilities in structural tests and SHM due to its capabilities and versatility. There are three different processes of scattering that can be explored in a DOFS: Brillouin, Raman and Rayleigh scattering. Each scattering based technique has advantages and limitations, which makes that the decision to use any of them is directly correlated to its intended particular application.

The Raman scattering is significantly dependent of temperature effects. For this reason, only some applications in civil engineering, as distributed temperature sensors in the detection of water leakage in dams and dikes, have been performed [10]. Notwithstanding, this scattering technique has been used in a greater extent in the art restoration [11] and forensic fields [12].

On the other hand, the Brillouin scattering based DOFS have found an extensive use in a wide range of applications to infrastructures, which makes it the most practiced technique in civil engineering SHM. This is due to its inherent characteristics which enables the use of this technique based sensors for long-distance distributed strain and temperature sensing which is favourable for large-scale applications of structural and geotechnical monitoring [13]. Nevertheless, its spatial resolution is considerably limited (around 1 m) which consequently makes it not suitable for applications where damage detection is intended and in this way a higher spatial resolution is required. Some attempts have been made in order to improve this resolution to the level of centimeters [14], [15] which implies, however, greater computational and production costs.

The Optical Backscatter Reflectometry (OBR) is based on the Rayleigh backscattering Optical Frequency Domain Reflectometry (OFDR) which enables it to obtain strain and temperature measurements with high spatial resolution [16], [17]. Although this implies also a limitation in terms of sensing length of around 70 m [18], this technique allows the potential monitoring of different types of structures where it is possible to detect and locate, not only the premature emergence of cracks, but also their evolution and behaviour.

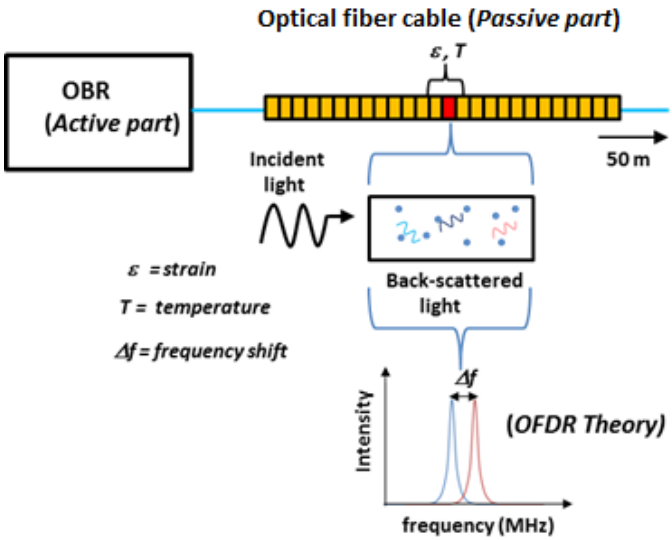

Figure 1. Measuring process by OBR system

The OBR technique, Figure 1, is composed by an active part which sends a laser light through an optical fiber, and a passive part, where the light is reflected by the intrinsic variations along the fiber length [19]. This pattern of the reflections and the corresponding time of flight of the light is measured and stored, acting as a unique fingerprint for each fiber. When an external stimulus (like strain or temperature variation) happens, a temporal and spectral shift in the local Rayleigh backscatter pattern occurs. This new reflection pattern is then stored and compared with the original one providing through cross-correlation the variation and evolution of generated strains along the entire length of the fiber due to this external stimulus [20].

This process uses the swept wavelength interferometry (SWI) to measure the Rayleigh backscatter as a function of length in an optical fiber with millimetre spatial resolution. More information on this system characteristics is also available in [21] and [22]. Numerous works presenting information regarding the study of the potential of these sensors have been published in the last decade [21]-[24], but very few showcase their application to real world structures. In this work, a step forward the application in the field is discussed as the application to two real structures is presented.

2. Application to existing structures

Although nowadays, there are others OBR systems with more setup functions and possibilities to measure using different types of fibers, the OBR model used in both cases of this study is limited to use a silica (glass) single mode fibers with a core diameter of 2 mm and a thin coating of polymer (polyimide) to protect it against scratches and environmental attack. Initially, this OBR system was created to measure strains and temperature variations in new components of aircraft and automobiles. Either at aircraft, automobile or civil structural monitoring, the principal reason to use a practically nude fiber is to optimally transfer the possible strain variation from the host material to the fiber core. Furthermore, although it is true that packaged fibers allow an easier manipulation and better protection

of the fiber, an extra analysis of the strain transfer between the host material and the fiber is required to obtain the real strain variation in the monitored structure [25], [26].

The OBR manufactures have provided a basic guide to DOFS installation [109]. This guide is focused in implementing the DOFS onto a relatively smooth metallic or plastic surfaces at short lengths. In this way, for the implementation of these sensors in more fragile and rough materials, such as the ones showcased in this paper (masonry and concrete) the authors relied in other previous experiences where DOFS were installed in this type of materials [28], [29].

Firstly, and in general form, a DOFS route was planned in order to measure strain at the locations and the directions of interest. The elected surfaces were prepared to develop a suitable bond area. These areas were cleaned with alcohol and wipes to free them from grease and facilitate the DOFS adhesion to the monitoring surface. The DOFS comes from the manufacturer rolled on a spool.

In general, the DOFS is strong in tension but weak in shear, therefore care needs to be taken in the installation to avoid its rupture. To prevent this, a carefully unwind of the DOFS from the spool is recommended followed by the attachment only using small adhesives dots, spaced at a maximum distance of 1 m, to hold the DOFS in the planned route without any previous layer of adhesive on the monitoring surface. A view of this step of the sensor installation in the Sarajevo bridge, is shown in the Figure 2.

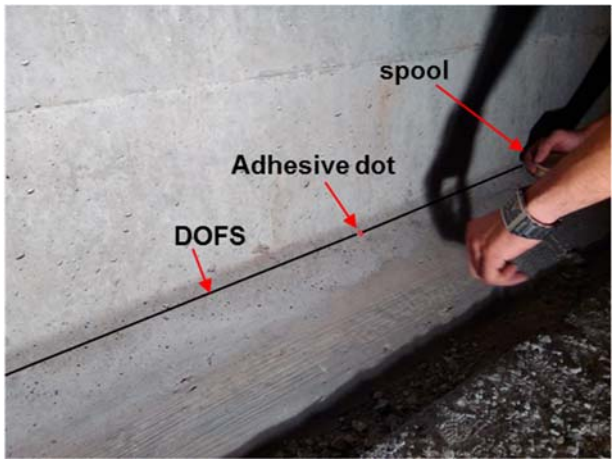

Figure 2. Unwind of the DOFS onto the chosen area of monitoring

Once the DOFS is laid on the structure's surface, the final step is to apply the epoxy adhesive to the DOFS and cure. A commercial glue as epoxy or cyanoacrylate could be applied to the bond area. About this, some authors [30], have shown that the installation of DOFS with of epoxy adhesives in concrete, produces better measures than using cyanoacrylate adhesives.

Therefore, a commercial bicomponent epoxy adhesive was applied to the bond area. A small brush to cover was used to cover the DOFS with epoxy avoiding to apply adhesive in excess [21]. The bond thickness, amount of epoxy between the fiber and the surface, should be minimized to ensure that the fiber is truly resting on the surface of the monitored structure as shown in Figure 3, [27].

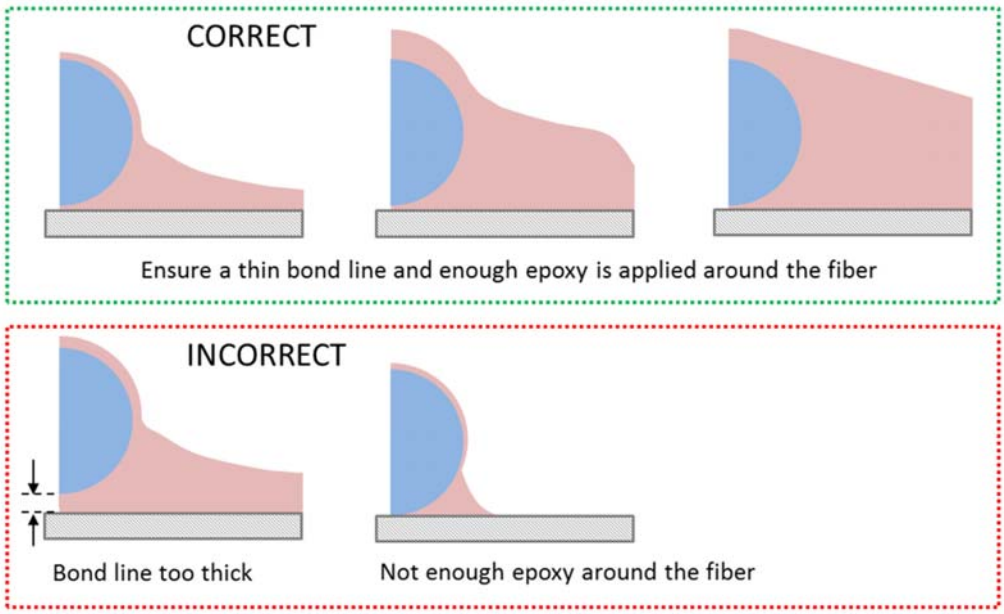

Figure 3. Adhesive application around the DOFS, [109]

A general aspect of the sensor installation in the Sarajevo bridge is shown in Figure 4.

Figure 4. Final aspect of the sensor installation in Sarajevo Bridge

2.1. Sant Pau Hospital

This historical building and UNESCO world heritage site in Barcelona is an exquisite example of the Catalan architectural modernism movement (Figure 5). After many years in operation, some parts of the building presented some causes of concern related to its structural behaviour since some cracks were appearing in some brick masonry columns in one of the floors.

Figure 5. Sant Pau Hospital at Barcelona, Spain

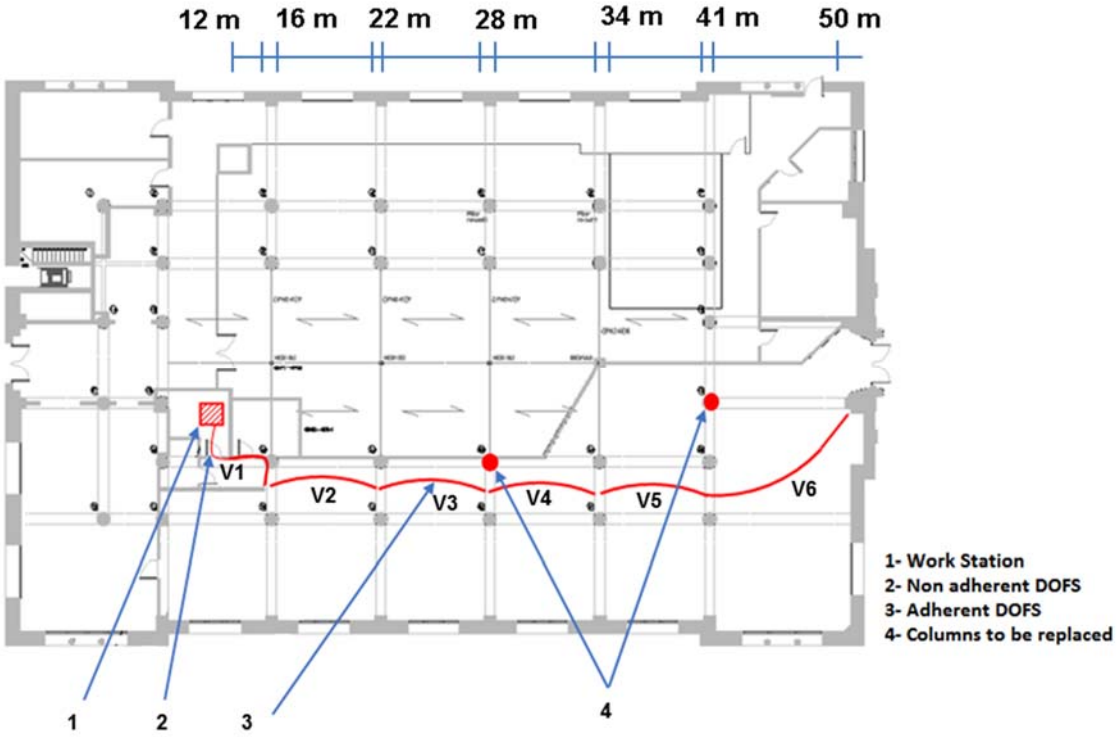

Figure 6. DOFS monitoring scheme. Plan view of the building

After a complete structural assessment, it was decided to replace two of those columns that were assessed to be working unsatisfactorily (represented as red circles in Figure 6) by new columns with

steel as main structural material. The floor above was being used to accommodate recovery drug patients and their relocation during the restoration works was not an option. Therefore, it was mandatory to carry out the replacement/strengthening work with the building in full service. For this reason, a full structural monitoring was deemed as necessary during the rehabilitation works.

The replacement procedure consisted on implementing a steel structure surrounding the column to be replaced, just to transfer the load from the masonry column to this temporary bearing steel structure (see Figure 7 and Figure 9). Afterwards, the masonry columns were cut and removed (see Figure 8) and then replaced by definitive steel columns. The load was further transferred from the temporary bearing steel structure to the new column. These new members were then covered and protected with masonry elements in order to preserve the same architecture pattern as the remaining columns (see Figure 10).

Figure 7. Preparation of columns to be replaced in this procedure

Figure 8. Cutting procedure of the columns

Figure 9. Temporary steel frame installed close to the columns to be replaced

Figure 10. Final works. Implementation of steel profiles and following encapsulation

Because of this challenging process, that had to maintain the hospital in full operation, it was decided to implement a system that could monitor continuously (both in time and space) the structural behaviour during the column replacement process. In this way, any deviation from a normal structural performance could be detected, the warning processed and the posterior operations decided.

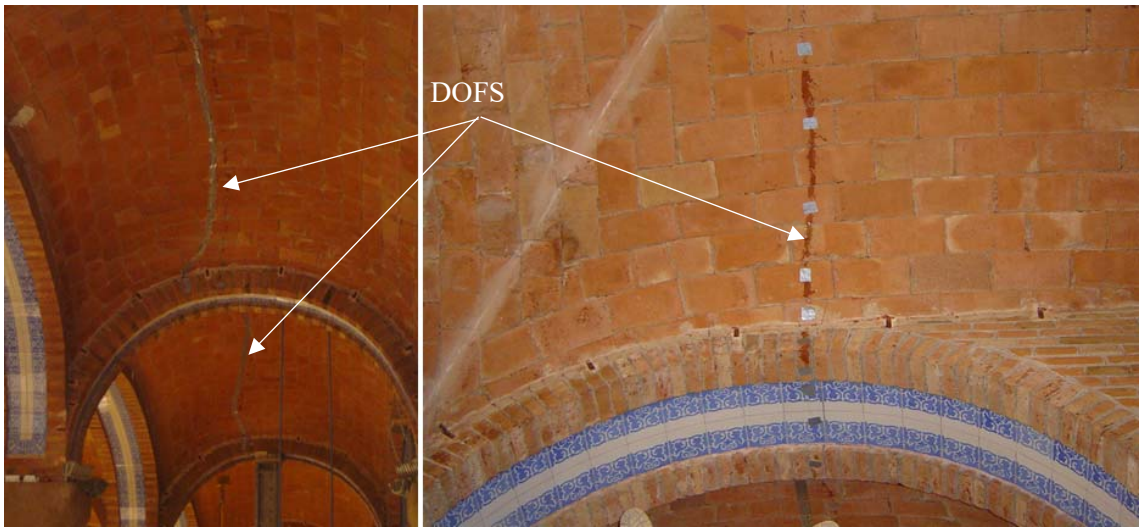

Figure 11. DOFS installed on the masonry vaults

The continuous monitoring in space of the whole affected area because of the column removal could be hardly achievable by using conventional sensors that are normally used for discrete monitoring (strain gauges, LVDT). Thus, in order to analyse and monitor the correct stress distribution of the slab supported by the columns during the replacement process in a cost-effective and in a truly distributed way, a DOFS was deployed. Otherwise, a large and unaffordable number of sensors would be required.

The DOFS monitoring system was placed in a strategically zone sensible to the evolution of movements and crack forming and widening, as seen on Figure 6and Figure 11.

In this application, a single 50 m long sensor was deployed enabling the performance of the SWI technique with 5000 points being interrogated and the signal from the sensor recorded simultaneously with a spatial resolution of 1 cm. Nevertheless, for practicality reasons not the entire length of the fiber is adhered to the structure (see Figure 6) and only around 38 m of fiber was bonded to the structure.

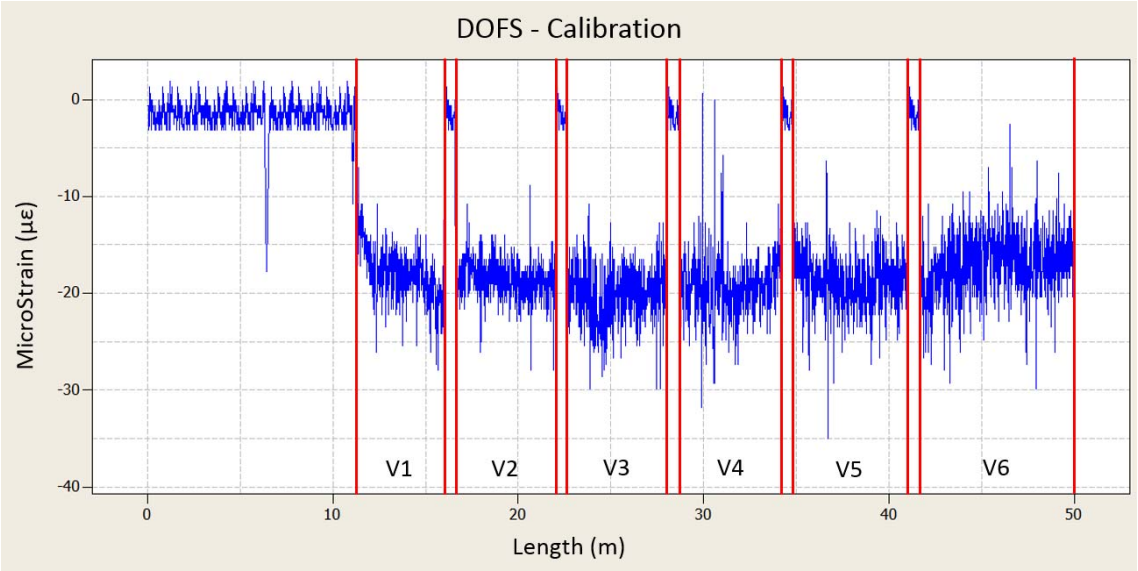

Figure 12. DOFS initial calibration

Previously to start the measuring under construction works, it was necessary to obtain an initial calibration of the system as shown in Figure 12. This provided the zero point from where the strains were measured. From the results presented in Figure 12, two clearly bands are highlighted. A first one where the strain is practically null (microstrain in the order of 0-5 με) and a second one, where nonzero values with an average of 20 με are obtained. The first 12 m of the fiber (necessary length required to reach the first monitored arch) corresponds to one of the areas where the fiber is not attached to masonry structure. Then, in the corresponding sections around 16, 22, 28, 34 and 41 meters, also a null strain is recorded in a zone of around 60 cm. This corresponds to the transition zone between low arches vaults where the fiber is also not bonded (see Figure 11).

The information acquired by the DOFS corresponds to continuous readings obtained in combined time intervals of: 1 reading per minute, 1 reading per 10 minutes and 1 reading each hour. From this extensive data, the critical values (maximum and minimum) are analysed and used to generate the envelope response graphs.

2.1.1. Results

The main objective of this deployed monitoring system was the detection and location of the premature appearance of cracks as well as their posterior evolution.

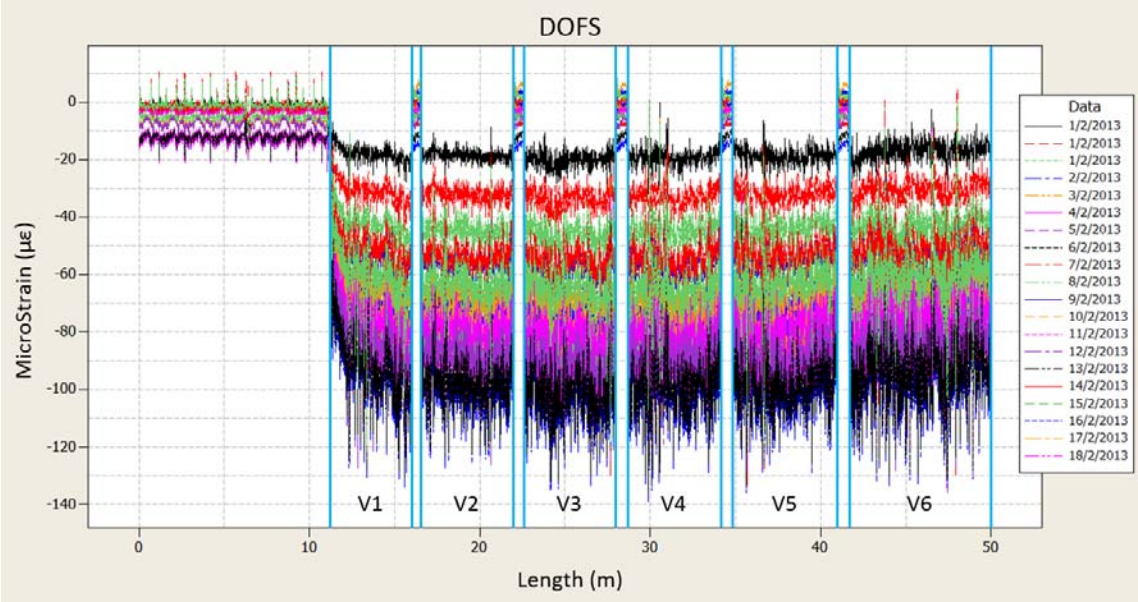

Figure 13. DOFS measurements for the whole length of the fiber during different days of the columns replacement

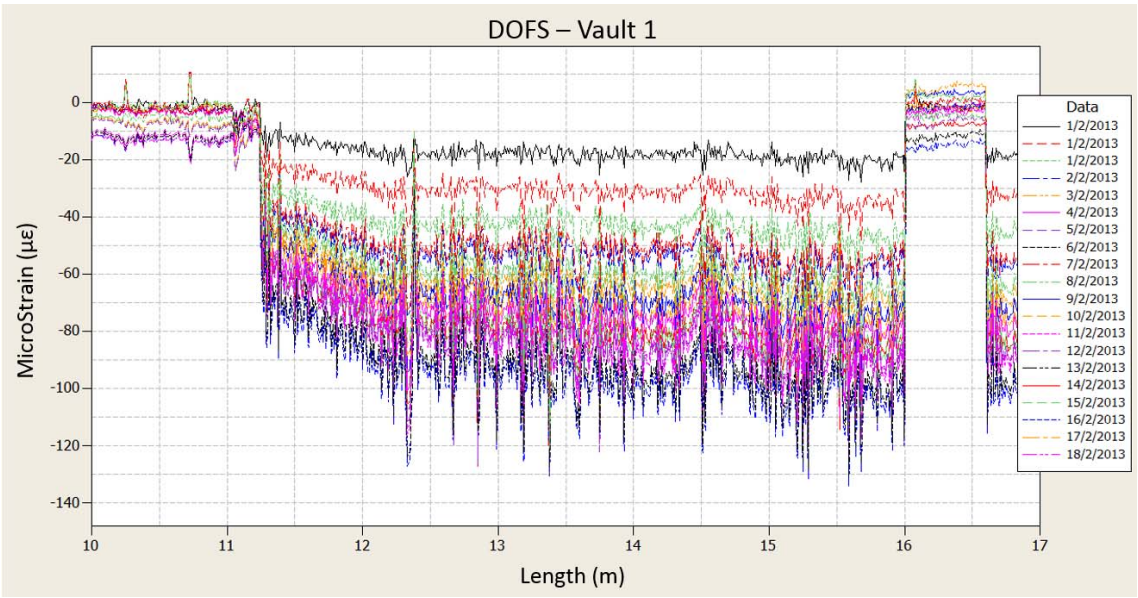

Figure 14. DOFS measured data for the instrumented vault V1

Figure 13 shows the superposition of measurement plots obtained in the days between the 1st and 18th of February of 2013. In this figure, the obtained strain along the entire length of the fiber is displayed. Here it is possible to observe the evolution of the measured strains in each of the instrumented masonry vaults for the total monitoring period. Due to the distributed capacity of this technology, it is possible to analyse separately this evolution for each vault as seen in Figure 14. Nevertheless, in order to enhance and clarify the evolution of strain with time and length, it is advisable to further zoom the window of analysis as seen in Figure 15 for a zoomed section of 10 cm. Furthermore, measurements at each point versus time can be plotted to better follow the evolution of works as seen in Figure 16.

From this analysis, the range of deformation after the initial calibration was obtained. The range of strain change for the period that corresponds to the replacement of the first column (1st of February of 2013) is of 20-40 με. After the replacement of the second column, an increase of the strain was observed with a maximum value of 100 με. Since, it is necessary to subtract the initial calibration value of 20 με to this value, it is possible to conclude that the replacing operation caused an increment of the strain in the vault in the order of 80 με, almost uniform along the whole roof. The objective of the operation was that during the removal of the old column and placement of the new one, the state of the strains in the vaults would not change significantly (thanks to the temporary steel frame) and also that any small change would be as uniform as possible in the whole roof. The observed increment in strain and its uniformity along the different vaults is in agreement to what was desired and predicted.

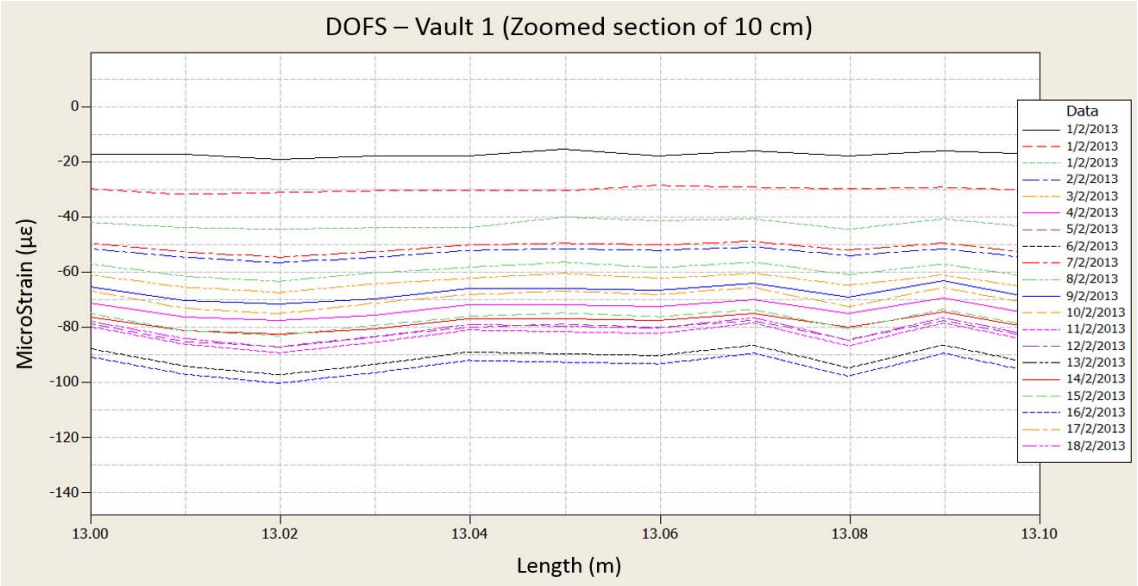

Figure 15. DOFS measurements for a 10 cm stretch of V1

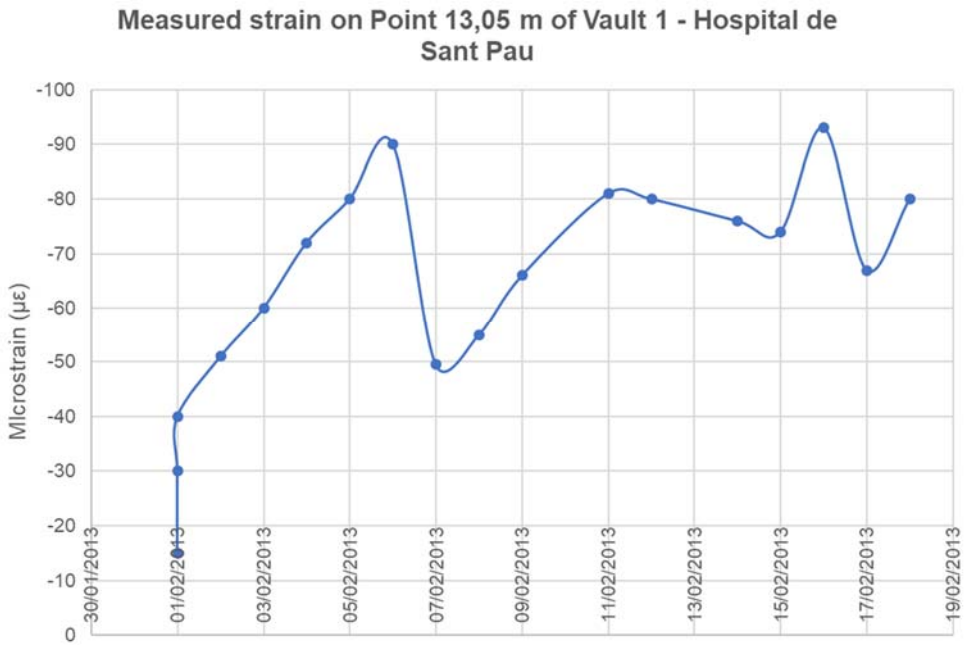

Figure 16. DOFS measurement for point 13.05 m of Vault 1

At every moment of the monitoring period, the structural response is under the service limit state since the strain increment generates minimal stresses to the material. According to the constitutive equations of the material, and specifically the stress-strain diagrams for the masonry, assuming an elastic and linear behaviour (acceptable for the obtained strain increment), the material has an increase of 0.14 MPa, for a characteristic compressive strength of 3 MPa and a Young modulus in service of 1.8 GPa as measured in the laboratory in samples cored from the removed pier.

Additionally, there was no evidence of the emergence of new cracks, either through visual inspection or from the obtained information acquired through the DOFS based monitoring system. As seen in Figure 13 and Figure 14, the observed peaks present small values without showing significant jumps in the measured strain, that would represent the formation of a crack at that location.

By analysing the evolution of strain at one point over time, Figure 16, it is possible to observe the increase of compressive strains due to the implementation of the external metallic supports and the two drop-offs that correspond to the transfer of load between these and the columns replacement.

Finally, it is worth mentioning that in the last readings shown in Figure 15 and Figure 16 (17^{th} and 18^{th} of February), is observed a recovery in the strain of 20 με, that perceives a certain turnaround and stabilization that was maintained throughout subsequent obtained readings. Therefore, it was concluded that the stresses in the masonry were stabilized without relevant modification in its structural response induced by the columns replacement. The replacement operation was carried out successfully and with the hospital in full operation as required by the owner.

In this application, due to the relatively controlled temperature environment and the fact that the monitoring period was only of a few days, it was not necessary to take into account the temperature effects in the strain data. This is not the case in the application described in the next section.

2.2. Sarajevo Bridge

Figure 17. Sarajevo Bridge in Barcelona, Spain

This bridge is located at one of the main entrances of the city of Barcelona, Spain (Figure 17). It is a simply-supported two span bridge with span-lengths of 36 and 50 m (Figure 18). Each span consists of three box-girder prestressed concrete beams connected by an upper reinforced concrete slab (Figure 19).

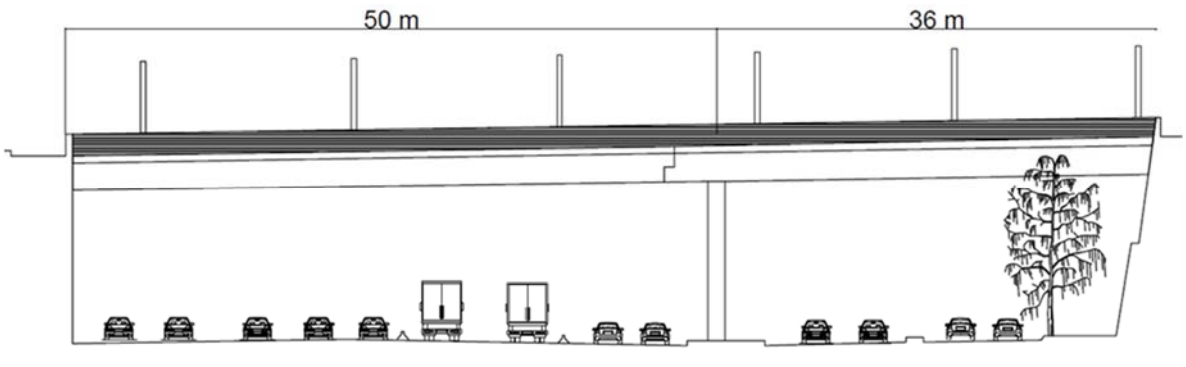

Figure 18. Side view of Sarajevo bridge

Figure 19. Bottom perspective of the bridge slab's box-girders

In order to further increase pedestrian traffic and capacity as well as bridge aesthetics, it was decided to enlarge the deck. This procedure also involved the addition of overhead metal protections for the pedestrians.

The construction works started on summer of 2015. Since the bridge is located at one of the main entrances of the city and due to its high traffic volume, closing the bridge to perform this deck widening was not an option. Also, it was not possible to close any of the existing traffic lanes underneath to place a temporary support due to the high volume of traffic entering the city in the rush hours. As a result of the change in the load pattern of the bridge, the absence of temporary support as well as the critical importance of the bridge in the Barcelona network, it was not wise to carry out the works without a close follow-up of the stresses induced in the material during the widening operation.

In this way, it was decided to carry out the monitoring to detect major changes in the structural behaviour of the bridge and obtain information to assess the structural safety during and at the end of the construction work. DOFS were decided to monitor as much length of the bridge as possible. (Figure 20 and Figure 21). The sensors were placed in the areas more sensible to possible stress increments and cracking. For this reason, and since the beam on Barcelona's side was the part of the structure where a larger load increment was planned (due to an increase length of 2.30 m overhang), it was decided to instrument this beam (Figure 21).

Figure 20. Deployed OBR system

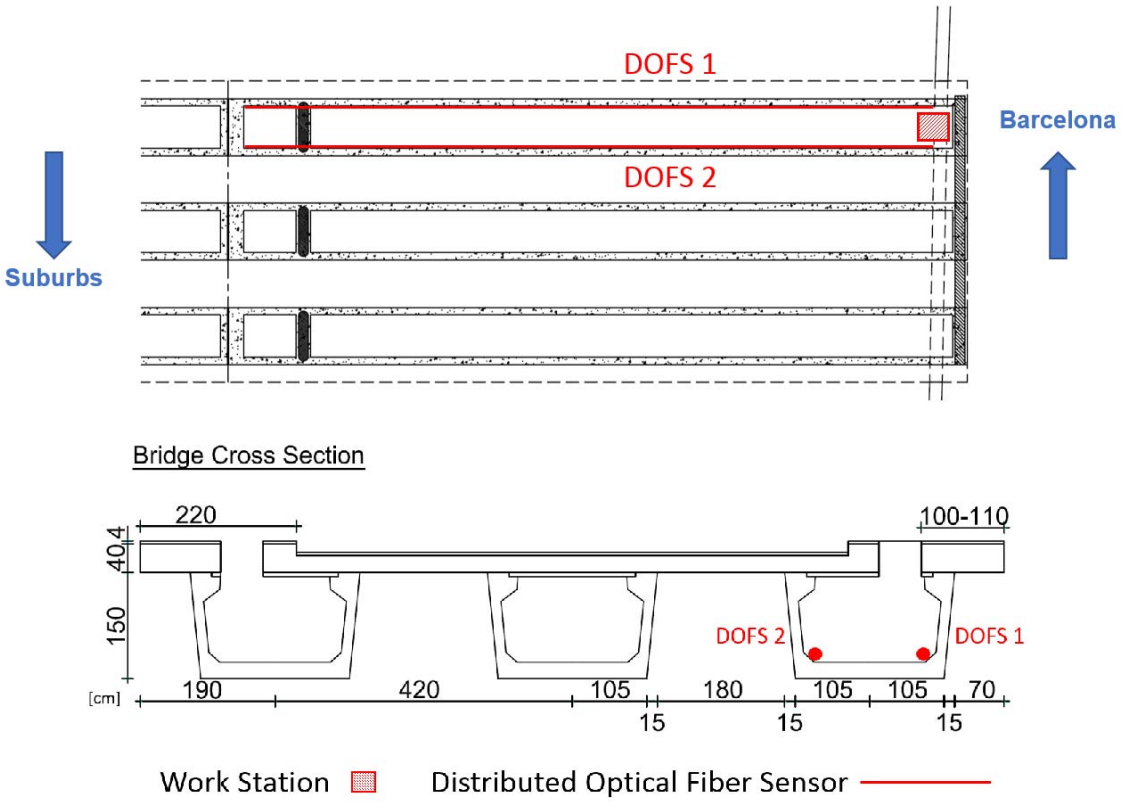

Figure 21. General scheme of DOFS monitoring

As seen in Figure 20 and Figure 21, DOFS were placed inside the box girder allowing for a better protection of the sensors and an easier access for their installation and operation.

The type of sensors as well as the installation procedure were similar to those described for the Hospital de Sant Pau. Due to the anticipated long duration of the monitoring period, the correct and careful implementation of these sensors assumes an even greater importance since any potential rupture or misuse of the fiber may compromise its performance. In this way, the use of two sensors instead of one also provides a desirable redundancy level.

2.2.1. First Results

The results obtained with both 50 m of optical fibers (36 m of which were bonded to the structure, adjusting to the span length) are analysed. Consequently, SWI was performed in a way that 3600 points were interrogated simultaneously with a spatial resolution of 1 cm. The information acquired by the DOFS corresponds to continuous readings obtained in 1 reading each 5 minutes. From this large amount of data, the critical values (maximum and minimum) are analysed and used to generate envelope response graphs.

Table 1. Summary of the monitoring events

Date	Description
29/06/2015	2 hrs 30 min measurement – DOFS 1 only
16/07/2015	3 hrs 20 min measurement – DOFS 1 only
06/08/2015	7 hrs measurement – DOFS 2 only
15/09/2015	7 hrs measurement – DOFS 1 only
01/10/2015	5 hrs measurement – DOFS 2 only
02/10/2015	1 hrs 30 min measurement – DOFS 2 only*
09/10/2015	5 hrs 30 min measurement – DOFS 1 only
04/11/2015	4 hrs measurement – DOFS 1** and DOFS 2
10/12/2015	6 hrs 30 min measurement – DOFS 2 only
22/12/2015	3 hrs measurement – DOFS 2 only
18/01/2016	5 hrs 40 min measurement – DOFS 2 only
19/01/2016	2 hrs 30 min measurement – DOFS 2 only
20/01/2016	3 hrs measurement – DOFS 2 only
18/02/2016	7 hrs 40 min measurement – DOFS 2 only

* The short measurement duration was due to the rupture of the cable that provided electrical power to the monitoring system

** Measuring of a single 5 minutes' event with DOFS 1

Different events corresponding to different days were monitored as seen in Table 1. The data collected between June 29 and November 4 of 2015 was made in an alternate way between DOFS 1 and DOFS 2. However, starting from December 10 until the last measurement only data from DOFS 2 was collected since the sensor DOFS 1 ceased to work properly. After this event, a visual inspection was conducted on the instrumented area of the beam and it was possible to conclude, that some works carried out inside the box girder could have broken DOFS 1. Notwithstanding, the rest of the measurements were proceeded by the data provided by DOFS 2.

Figure 22. DOFS 1 and 2 readings evolution for the monitoring period interval

In Figure 22, is plotted the evolution of the strains measured by the DOFS 1 and 2. It is important to point out, that this comparison is made with measurements from different days taking care of selecting readings within the similar time interval period in order to mitigate the influence of daily time dependent phenomenon.

It is detected by both deployed fibers the increase of compression strain. This was a result of the construction works being done in this time window, such as the removing of asphalt layers (see Figure 23) and some bridge equipment in the first stages of the procedure and naturally the effect of the temperature variation from summer to winter.

Figure 23. Bridge's load stage comparison between July (left) and September (right) of 2015

Furthermore, due to this relatively long monitoring period, the temperature variation not only affects the structure's behaviour but also the readings of the DOFS. Both the refractive index of the backscattered light and the materials which compose these sensors are dependent of these temperature changes, so a compensation of its effect on the monitoring output is required, as it is normally conducted in these type of applications, such as the case of discrete FBG sensors equipped with temperature sensors [31].

In order to take into account these effects, in terms of spectral shift, the thermal output, Δv_T can be expressed as:

$$\Delta v_T = \Delta v_n + \Delta v_S \quad (1)$$

Where Δv_n represents the refractive index-dependent spectral shift and Δv_S is the coefficient of thermal expansion-dependent spectral shift.

There are two different ways to perform this thermal induced error compensation for measurements performed by OBR based DOFS where the thermal conditions are variable and where non-adhered segments of the DOFS are present [32]: point-to-point thermal compensation and thermal compensation by fiber loop.

2.2.2. Point-to-point thermal compensation

This thermal compensation method can be used in the situation where significant temperature gradients are expected throughout the entire active length of the DOFS. Here, an unbonded fiber segment is implemented beside the bonded fiber segment, floating in a tube. Therefore, the output of this unbonded segment is only dependent of the temperature variation and can be used to perform a point-to-point compensation of the mechanical strain measurements of the bonded fiber as represented in Figure 24.

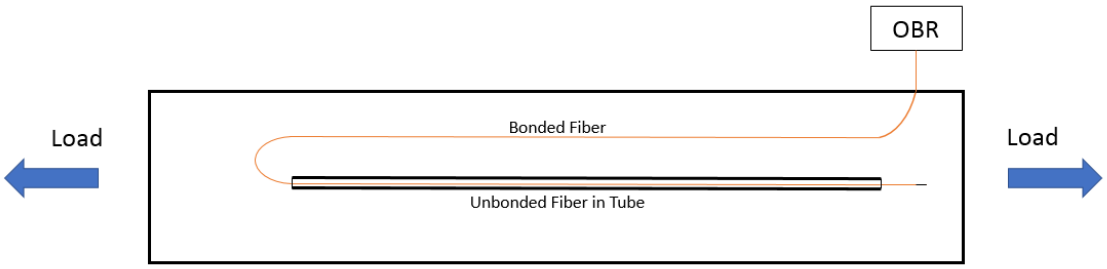

Figure 24. Point-to-point thermal compensation method scheme

In this way, Equation (2) can be formulated, where in order to obtain the mechanical strain in point *i* of the bonded fiber segment, it is necessary to subtract the thermal effects outputs from the unbonded segment of the fiber in point *i* to the total strain measured in point *i* of the bonded segment.

$$\varepsilon_{L_i} = \left(\Delta\nu_{B_i} \times k_\varepsilon\right) - \left(\left(k_{nT} \times \Delta\nu_{U_i} \times k_\varepsilon\right) + \left(\Delta\nu_{U_i} \times k_T \times \alpha_S\right)\right) \quad (2)$$

where,

$\Delta\nu_B$= Spectral shift in bonded segment;

$\Delta\nu_U$= Spectral shift in unbonded segment;

$k_{nT} = \frac{dn}{dT}$ effect – approximately 0.95;

k_ε = Fiber strain conversion factor – approximately -6.67 με/GHz

k_T = Fiber temperature conversion factor – approximately -0.801 ºC/GHz

α_S = Substrate coefficient of thermal expansion – $10x10^{-6}$ for concrete

2.2.3. Thermal compensation by fiber loop

For the situation where there are not significant local temperature gradients throughout the length of the optical fiber, this method can be used for compensation. In this case, a relatively short fiber loop can be created by leaving a small part of the sensor lying down on the monitored structural element without bonding it, as represented in Figure 25.

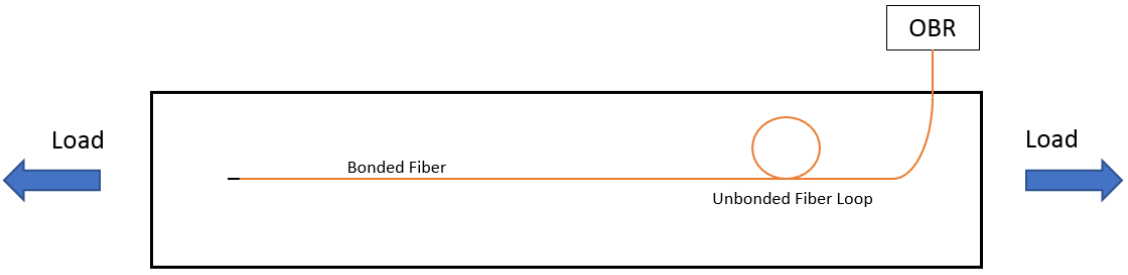

Figure 25. Fiber loop thermal compensation method scheme

With this method, in order to obtain the pure mechanical strain generated during the monitoring period, it is necessary to subtract from the strain obtained in the bonded part of the fiber both the effects of the refractive index dependent apparent strain and the coefficient of thermal expansion dependent apparent strain. For the rest of this text the first is designated by RIAS (refractive index apparent strain) and the second by TEAS (thermal expansion apparent strain).

This compensation can be described mathematically by the same expression described before (2), with the only difference being that while in point to point thermal compensation, the spectral shift of the unbonded segment is subtracted in each measured point to the correspondent point of the bonded segment counterpart, in the thermal compensation by fiber loop, an average of the spectral shift measured for the entire length of the unbonded segment is calculated and then subtracted to the calculated average of the measured data of the bonded segment.

This was the method adopted in this real-world monitoring application, by the use of the unbonded loop segment of the fiber located at the end, inside the beam, as seen in Figure 26.

Figure 26. Unbonded loop of the DOFS

Since the strain measured by the first 14 meters of the fiber that are not bonded is exclusively dependent from the temperature variations, one may obtain from its measurements the information to calculate RIAS and TEAS.

The values obtained in this temperature compensation process are presented in Table 2 and 3. The results of Figure 23 were updated to the ones shown in Figure 27 and Figure 28.

Table 2. Temperature compensation for DOFS 1

DOFS 1				
Date	**με (mean) bonded fiber**	**RIAS με (mean)**	**TEAS με (mean)**	**Mechanical με (mean)**
29/06/2015	11	-1	1	11
16/07/2015	16	90	-114	40
15/09/2015	-89	-321	405	-173
09/10/2015	-136	-444	561	-253
04/11/2015	-153	-574	726	-304

Table 3. Temperature compensation for DOFS 2

DOFS 2				
Date	**με (mean) bonded fiber**	**RIAS με (mean)**	**TEAS με (mean)**	**Mechanical με (mean)**
06/08/2015	0.23	-6.00	7.58	-1.35
01/10/2015	-152	-568	718	-302
04/11/2015	-117	-630	796	-283
10/12/2015	-209	-976	1234	-467
20/12/2015	-202	-953	1205	-454
18/01/2016	-270	-1112	1406	-563
19/01/2016	-252	-1143	1445	-554
20/01/2016	-253	-1160	1466	-559
18/02/2016	-219	-1070	1356	-502

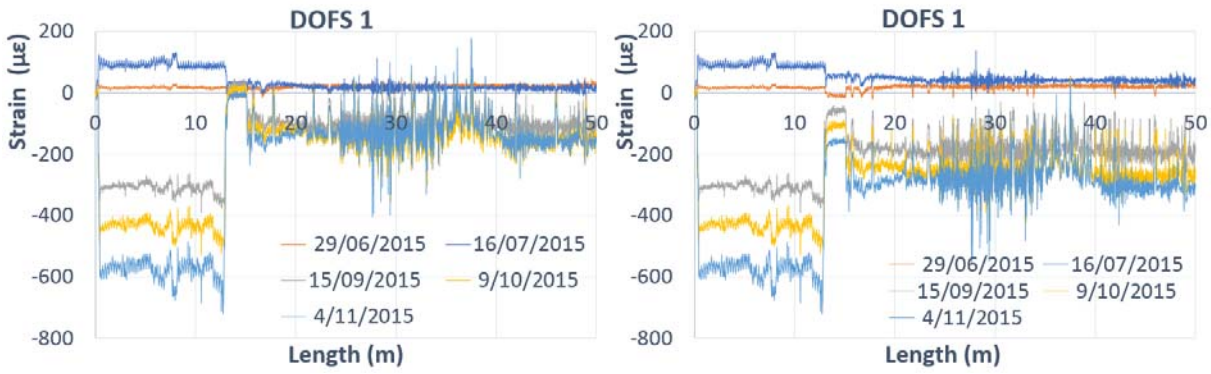

Figure 27. Comparison of DOFS 1 readings before (left) and after temperature compensation (right)

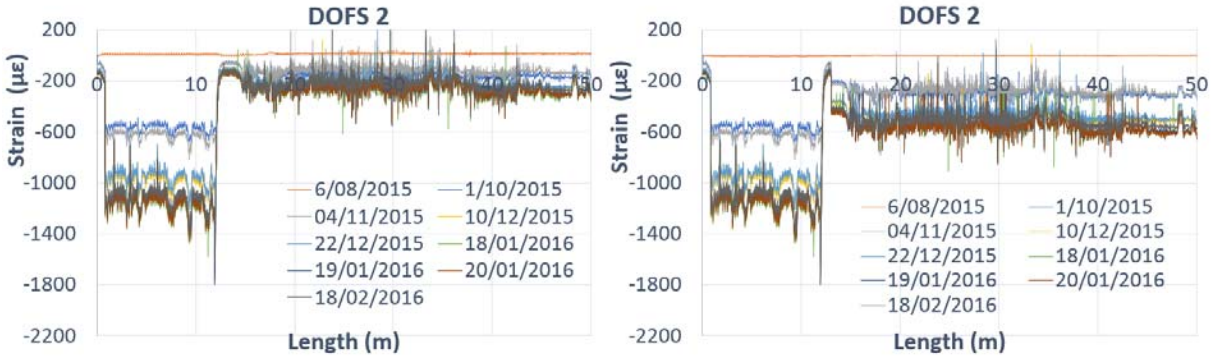

Figure 28. Comparison of DOFS 2 readings before (left) and after temperature compensation (right)

From these results, the effect of the general unloading that the bridge suffered due to the removal of the slabs, pavement and the milling of the agglomerate, when compared to the loading values at the time of calibration and the structure's shrinkage behaviour induced by the decrease of temperature, is further evidenced. Furthermore, this continuous increase of compression of the bottom part of the monitored span is also explained by a higher induced load on the adjacent span compared to the one applied to the instrumented span, as seen in the photograph taken in January observed in Figure 29.

Figure 29. Photograph of the load increase on the non-instrumented span of the bridge taken in January 2016

Regarding the stresses analysis, and from the longitudinal deformation modulus of concrete E_c, it is possible to observe and conclude that, despite the variation of strain, excessive stresses are not induced to the concrete during the construction works.

In this way, from DOFS 1 the biggest strain variation was observed for -304 με which corresponds to a stress change of 11.42 MPa. Regarding the measurements of DOFS 2, the biggest variation was detected in January for -563 με that is equivalent to a stress increase of 21.16 MPa.

Consequently, it is possible to conclude that these observed stress increments did not induce significant changes in the bridge structural behaviour since they are permissible and acceptable for this type of bridge, enhanced by the fact that these variations are of compressive nature.

The peaks and discontinuities in the data measured by the DOFS are representative of the joints between the prefabricated beams where the distributed optical fiber suffers from lack of bonding and other locations where due to the roughness or small cavities present near the surface, as a result of the heterogeneity of the concrete itself, the full and proper bonding between the sensor and the structural surface was not completely achieved, as seen in Figure 30. To not be confused with the emergence of new cracks, the peaks, although presenting variations in their magnitude, remain stable in terms of their location. These variations of magnitude in their turn are a consequence of possible vibrations which are transmitted from the operational loads.

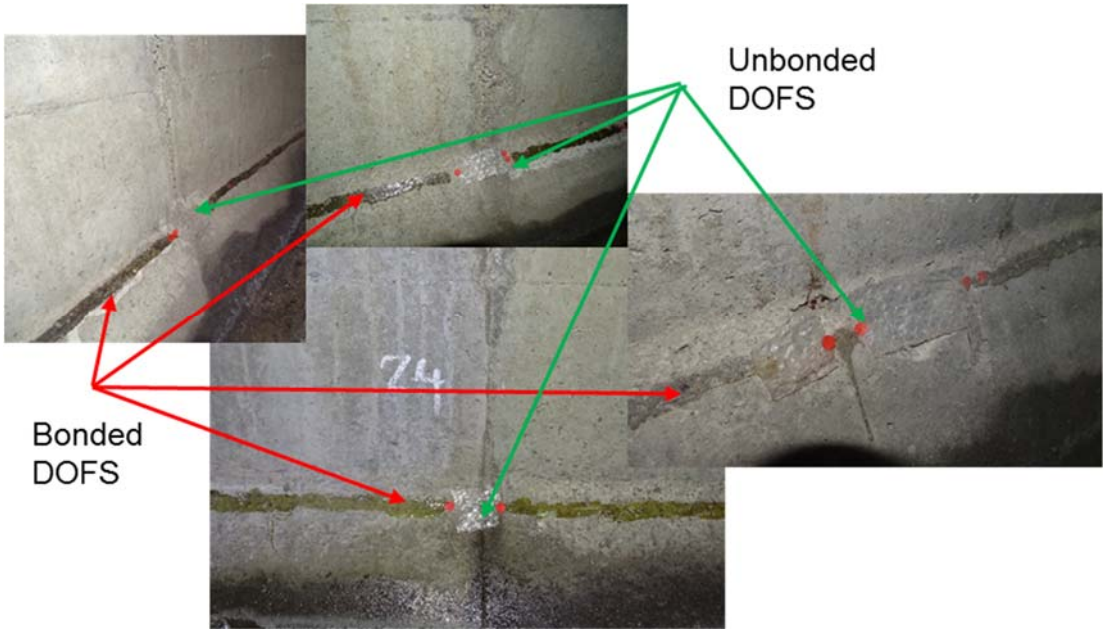

Figure 30. Some examples of unbonded points of the DOFS in the Sarajevo bridge application

The fact that the temperature compensation was made using the average of the entire length of the deployed fiber limits the obtained measurements to a more global structural behaviour analysis, where it is assumed that the ambient temperature is the same all along the box-girder. This could be corrected by the use of the other mentioned thermal compensation method (point-to-point measurement

compensation) or the use of two or more thermometers in different locations of the DOFS to have a measure of the ambient temperature along the deployed fiber.

Notwithstanding, with the results obtained from the method adopted in this application it is possible to improve the results. This is achieved by dividing the entire length of the DOFS in different segments. In this way, it is proposed to divide the sensor in 5 different sections – S0, S1, S2, S3 and S4 – where a local temperature compensation is performed in the same way as explained before for the entire length of the sensor. For both deployed fibers the length of each segment is characterized as described in Table 4.

Table 4. Segment Length Definition for Extended Temperature Compensation

Segment ID	Length (m)
S0	0.5-12.7
S1	13.3-15.0
S2	15.0-24.0
S3	24.0-37.5
S4	37.5-50.0

The mechanical strain measured for each section is represented in Table 5 and Table 6 for the different periods of observation.

Table 5. Section localized temperature compensation for DOFS 1 (microstrain)

Segment ID	29/06/2015	16/07/2015	15/09/2015	09/10/2015	04/11/2015
S0	10.4	113.5	-389.3	-546.3	-670.7
S1	-2.8	45.3	-56.1	-104.1	-160.4
S2	13.4	23.0	-168.3	-230.8	-281.8
S3	17.0	27.8	-172.1	-246.5	-267.2
S4	18.2	29.9	-172.3	-254.5	-291.1

Table 6. Section localized temperature compensation for DOFS 2 (microstrain)

Segment ID	06/08/2015	01/10/2015	04/11/2015	10/12/2015	22/12/2015	18/01/2016	19/01/2016	20/01/2016	18/02/2016
S0	14.1	-707.7	-771.0	-1168.5	-1177.5	-1393.4	-1383.2	-1397.4	-1353.6
S1	5.5	-235.0	-238.7	-379.1	-383.6	-499.5	-456.2	-453.5	-448.8
S2	17.1	-286.0	-271.2	-443.8	-446.2	-539.0	-536.5	-534.8	-504.8
S3	19.8	-284.9	-253.0	-425.6	-426.9	-528.7	-524.4	-524.1	-480.4
S4	20.7	-311.1	-287.0	-477.4	-479.3	-565.2	-571.7	-571.6	-532.3

Due to the presence of the peaks, the strain is possibly masked and its real distribution along the instrumented box-girder is not clear. To observe a better strain distribution, a spatially averaging only of the mechanical strains for S1, S2, S3 and S4 segments was performed and plotted in Figure 31 and Figure 32. These are the values also present in Tables 5 and 6.

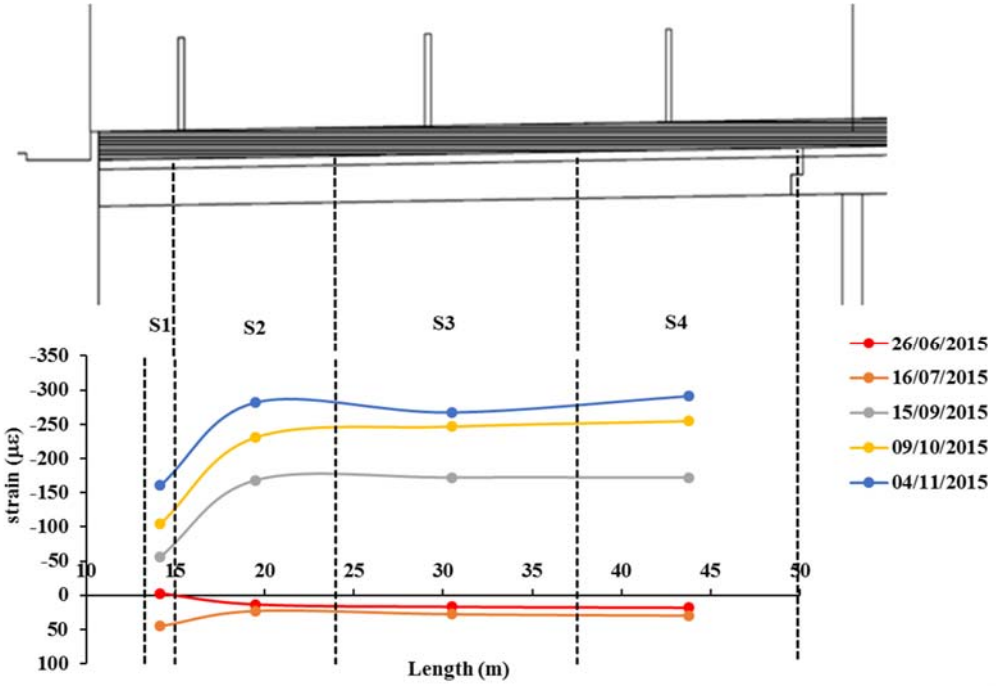

Figure 31. Mean mechanical distribution for DOFS1

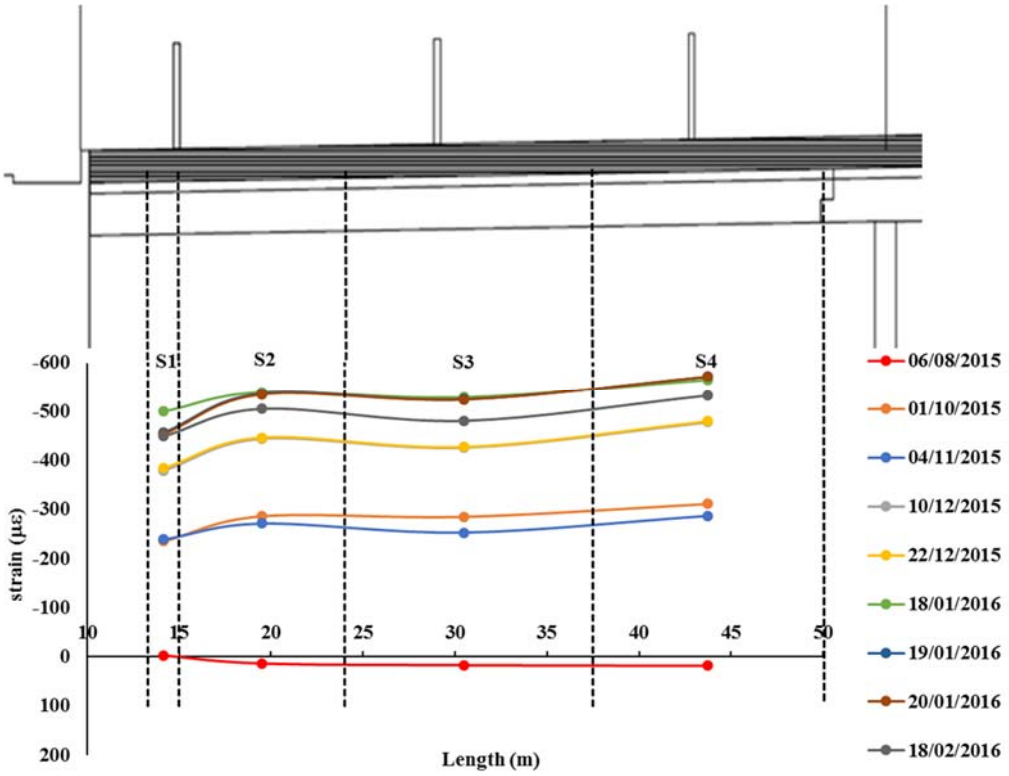

Figure 32. Mean mechanical distribution for DOFS2

In segment S1, mean mechanical strain values lower than those generally present in the rest of the DOFS length can be shown. This decrease is due to the influence of the support system (elastomeric bearings) on the bridge kinematics. The mean mechanical strain distribution is almost uniform in the rest of the box-girder. This means that the applied forces in the deck that could produce variations of strain along the bottom part of the bridge were very small at the time of measuring the sensors, being therefore the strain mainly due to the uniform shortage of the box-girder associated to the decrease of temperature from summer to winter. Note that the difference in strain between August and February in the order of 500 microstrain (Figure 32) is very much plausible for a bridge like this and the climate in Barcelona.

This is also perceived and validated by analysing Figure 33 which plots the evolution of the average strain at each section over time for both instrumented DOFS.

In Figure 33, as expected, the increase of compressive strains is observed from the summer to the winter period. It is also possible to observe some specific and short-term variations that correspond to the global effect of introduction and withdrawal of construction equipment to the deck and the variation of the applied load that is inherent to the deck widening procedure.

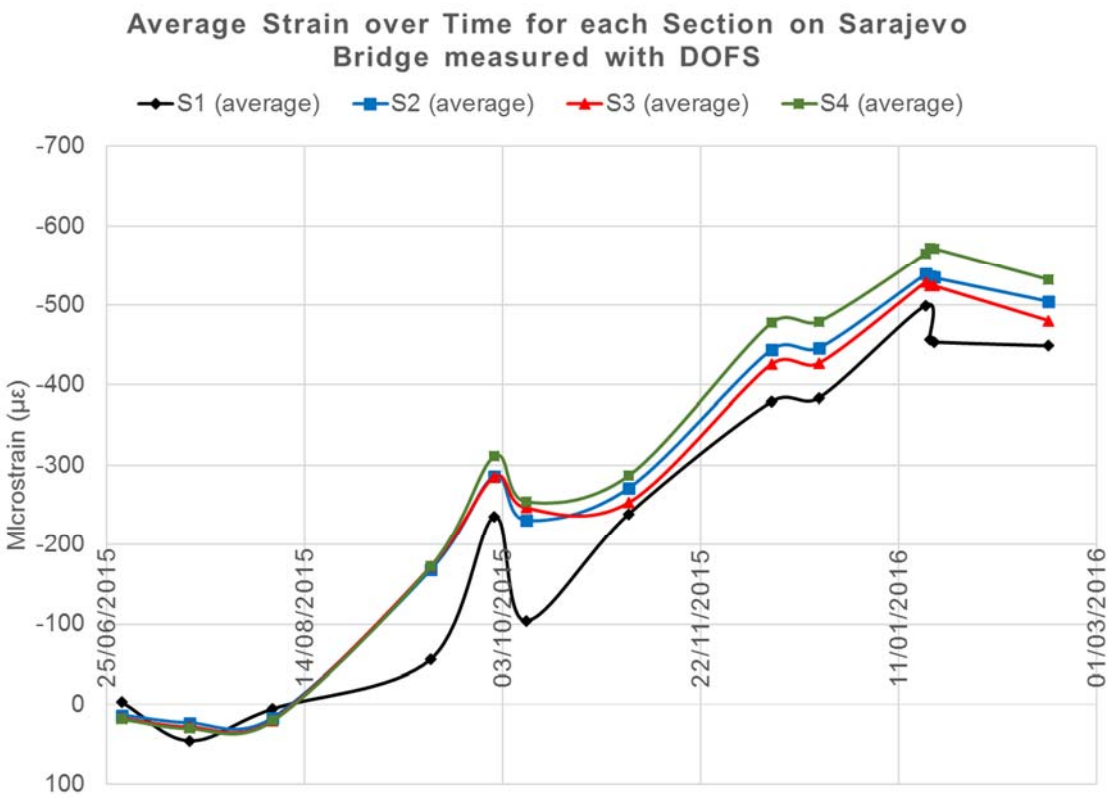

Figure 33. Evolution of average strain measured at each section over time

Some photos of the final stage of the structure after the completion of the aforementioned procedure can be seen in Figure 34.

Figure 34. Sarajevo bridge after the completion of the rehabilitation works

3. Conclusions

In this paper, the successful application of distributed fiber optic sensors, DOFS, on the structural health monitoring of two real structures was presented.

Due to their particularities, each one of these structures underwent changes in their structural behaviour without, nevertheless, ceasing to serve their purpose, i.e. accommodating patients in the case of the Sant Pau Hospital and the passage of vehicles and pedestrians in the case of Sarajevo bridge.

In this way, with the application of the DOFS technology it was possible to follow and monitor the structural behaviour in these structures during the different operations executed with the use of a relative small number of sensors and simple monitoring systems. With the DOFS readings at different dates, it was possible to easily detect the stresses increments in each structure and in this way, assess their actual safety. If anomalous changes were detected with the instrumentation, automatically the works would stop and necessary corrective measures would be taken. Furthermore, the evolution of strain variation along an extensive length of structure was achieved with a relatively simple and easy installation of only one sensor and one connection to a reading terminal.

Also, in this paper, two different types of applications were shown with two different types of structural materials (masonry and concrete), which showcases the versatility allowed by this technology and the feasibility to correctly bond the fiber to those materials.

Notwithstanding, there are still some improvements to be made regarding the application and use of the DOFS technology in real world scenarios. For example, it would have been interesting to obtain data from the two different fibers deployed on Sarajevo bridge in a quasi-simultaneous way in order to better evaluate the effects of transversal bending and torsion. This is a limitation imposed by the particular OBR system used in these applications.

Furthermore, the compromise between the protection coating of the sensors and their strain accuracy should be carefully assessed before its implementation in any real-world scenario structure. As seen in this document, when the location of the sensor might be accessed and handled during the monitoring period, the probability of its rupture is increased if not a considerable thick coating is used. However, in the situation where it is believed that the DOFS is located away from such events, the use of a thin coating is advised in order to allow for an increased accuracy.

In conclusion, this paper showcased the first application of OBR based DOFS technology in a masonry structure (at least that the authors are aware of), specially, with such an important historical value. Furthermore, it reports the first application of this technology for the monitoring of a real structure during a relatively extended period of time (in the case of Sarajevo bridge) where the topic of the thermal effects compensation on the sensor had to be addressed in a non-controlled environment.

All of this serving as practical evidence for designers and rehabilitation engineers of the potential, advantages and disadvantages of the use of this sensing technology.

Nevertheless, with the results obtained in this work, the OBR theory associated with DOFS proved its reliability in SHM of civil engineering applications and continues to showcase the promising future of monitoring systems based on this technology.

Acknowledgements: This project has received funding from the European Union's Horizon 2020 research and innovation programme under the Marie Sklodowska-Curie grant agreement No. 642453. The authors acknowledge the funds received from the Spanish Ministry of Economy and Competitiveness and the FEDER funds through the research grant BIA2013-47290-R and are also grateful to Vicente Alegre Heitzmann CEO of COTCA SA for his useful cooperation and by providing the ODiSI-A fiber Optic Sensing System. Furthermore, we would also like to thank the owners BIMSA (Barcelona d'Infraestructures Municipals) and the Fundació Privada de l'Hospital de la Santa Creu i Sant Pau for allowing the use of their buildings and public structures in this research.

References

[1] C. R. Farrar and K. Worden, "An introduction to structural health monitoring.," Philos. Trans. A. Math. Phys. Eng. Sci., vol. 365, no. 1851, pp. 303–315, **2007**.

[2] B. Glisic, D. Hubbell, D. H. Sigurdardottir, and Y. Yao, "Damage detection and characterization using long-gauge and distributed fiber optic sensors," Opt. Eng., vol. 52, p. 87101, **2013**.

[3] J. R. Casas and P. J. S. Cruz, "Fiber Optic Sensors for Bridge Monitoring," J. Bridg. Eng., vol. 8, no. 6, pp. 362–373, **2003**.

[4] X. W. Ye, Y. H. Su, and J. P. Han, "Structural Health Monitoring of Civil Infrastructure Using Optical Fiber Sensing Technology: A Comprehensive Review.," Sci. World J., vol. 2014, p. 652329, **2014**.

[5] J. M. Lopez-Higuera, L. Rodriguez Cobo, A. Quintela Incera, and A. Cobo, "Fiber Optic Sensors in Structural Health Monitoring," J. Light. Technol., vol. 29, no. 4, pp. 587–608, **2011**.

[6] M. D. Todd, G. A. Johnson, and S. T. Vohra, "Deployment of a fiber Bragg grating-based measurement system in a structural health monitoring application," Smart Mater. Struct., vol. 10, no. 3, p. 534, **2001**.

[7] S. Casciati, M. Domaneschi, and D. Inaudi, "Damage assessment from SOFO dynamic measurements," in 17th International Conference on Optical Fibre Sensors, **2005**, vol. 5855, pp. 1048–1052.

[8] S. Casciati, M. Domaneschi, and D. Inaudi, "Local damage detection from dynamic SOFO experimental data," in Smart Structures and Materials 2005: Sensors and Smart Structures Technologies for Civil, Mechanical, and Aerospace Systems, **2005**, vol. 5765, pp. 591–600.

[9] B. Glisic and D. Inaudi, "Development of method for in-service crack detection based on distributed fiber optic sensors," Struct. Heal. Monit., vol. 11, no. 2, pp. 161–171, Mar. **2012**.

[10] J.-M. Henault, G. Moreau, S. Blairon, J. Salin, J.-R. Courivaud, F. Taillade, E. Merliot, J.-P. Dubois, J. Bertrand, S. Buschaert, S. Mayer, and S. Delepine-Lesoille, "Truly Distributed Optical Fiber Sensors for Structural Health Monitoring: From the Telecommunication Optical Fiber Drawling Tower to Water Leakage Detection in Dikes and Concrete Structure Strain Monitoring," Adv. Civ. Eng., vol. 2010, pp. 1–13, **2010**.

[11] H. E. Mayhew, K. A. Frano, S. A. Svoboda, and K. L. Wustholz, "Using Raman Spectroscopy and Surface-Enhanced Raman Scattering To Identify Colorants in Art: An Experiment for an Upper-Division Chemistry Laboratory," J. Chem. Educ., vol. 92, no. 1, pp. 148–152, **2014**.

[12] C. Muehlethaler, M. Leona, and J. R. Lombardi, "Review of surface enhanced Raman scattering applications in forensic science," Anal. Chem., vol. 88, no. 1, pp. 152–169, **2015**.

[13] S. Uchida, E. Levenberg, and A. Klar, "On-specimen strain measurement with fiber optic distributed sensing," Measurement, vol. 60, pp. 104–113, **2015**.

[14] M. Belal and T. P. Newson, "A 5 cm spatial resolution temperature compensated distributed strain sensor evaluated using a temperature controlled strain rig," Opt. Lett., vol. 36, no. 24, pp. 4728–4730, **2011**.

[15] S. Shen, Z. Wu, C. Yang, C. Wan, Y. Tang, and G. Wu, "An improved conjugated beam method for deformation monitoring with a distributed sensitive fiber optic sensor," Struct. Heal. Monit., vol. 9, no. 4, pp. 361–378, **2010**.

[16] A. Güemes, Fernández-López;, and B. Soller, "Optical Fiber Distributed Sensing – Physical Principles and Applications," Struct. Heal. Monit., **2010**.

[17] G. Rodriguez, J. R. Casas, and S. Villalba, "Assessing Cracking Characteristics of Concrete Structures by Distributed Optical Fiber and Non-Linear Finite Element Modelling To cite this version :," in 7th European Workshop on Structural Health Monitoring, **2014**.

[18] LUNA, "Optical Backscatter Reflectometer (Model OBR 4600). [Online]," **2012**. [Online]. Available: http://lunainc.com/wp-content/uploads/%0A2012/11/NEW-OBR4600_Data-Sheet_Rev-04.pdf. [Accessed: 01-Feb-2017].

[19] D. Samiec, "Distributed fibre-optic temperature and strain measurement with extremely high spatial resolution," Photonik Int., **2012**.

[20] J. H. L. Grave, M. L. Håheim, and A. T. Echtermeyer, "Measuring changing strain fields in composites with Distributed Fiber- Optic Sensing using the optical backscatter reflectometer," Compos. Part B, vol. 74, pp. 138–146, **2015**.

[21] G. Rodríguez, J. R. Casas, and S. Villalba, "SHM by DOFS in civil engineering: a review," Structural Monitoring and Maintenance, vol. 2, no. 4, p.357-382, **2015**.

[22] A. Barrias, J. Casas, and S. Villalba, "A Review of Distributed Optical Fiber Sensors for Civil Engineering Applications," Sensors, vol. 16, no. 5, p. 748, May **2016**.

[23] G. Rodriguez, J. R. Casas, and S. Villalba, "Cracking assessment in concrete structures by distributed optical fiber," Smart Mater. Struct., vol. 24, no. 3, p. 35005, **2015**.

[24] L. Palmieri and L. Schenato, "Distributed Optical Fiber Sensing Based on Rayleigh Scattering," Open Opt. J., vol. 7, no. 1, pp. 104–127, **2013**.

[25] K. T. Wan, C. K. Y. Leung, and N. G. Olson, "Investigation of the strain transfer for surface-attached optical fiber strain sensors," Smart Mater. Struct., vol. 17, no. 3, p. 35037, **2008**.

[26] A. Billon, J.-M. Henault, M. Quiertant, F. Taillade, A. Khadour, R.-P. Martin, and K. Benzarti, "Quantitative strain measurements with distributed fiber optic systems: Qualification of a sensing cable bonded to the surface of a concrete structure," 7th Eur. Work. Struct. Heal. Monit. EWSHM 2014 - 2nd Eur. Conf. Progn. Heal. Manag. Soc., **2014**.

[27] Luna Innovations Incorporated, "ODiSI Fiber Optic Sensor Installation Guide," **2017**.

[28] S. Villalba and J. R. Casas, "Application of optical fiber distributed sensing to health monitoring of concrete structures," Mech. Syst. Signal Process., vol. 39, no. 1, pp. 441–451, **2012**.

[29] V. Villalba, J. R. Casas, and S. Villalba, "Application of OBR fiber optic technology in structural health monitoring of Can Fatjó Viaduct (Cerdanyola de Vallés-Spain)," in VI International Conference on Bridge Maintenance, Safety and Management, **2012**.

[30] R. Regier and N. a. Hoult, "Distributed Strain Behavior of a Reinforced Concrete Bridge: Case Study," J. Bridg. Eng., vol. 19, no. 12, p. 05014007, **2014**.

[31] M. Domaneschi, D. Sigurdardottir, and B. Glišić, "Damage detection on output-only monitoring of dynamic curvature in composite decks," Struct. Monit. Maint., vol. 4, no. 1, pp. 1–15, **2017**.

[32] Luna Innovations Incorporated, "Distributed Fiber Optic Sensing: Temperature Compensation of Strain Measurement Contents," **2014**.

Chapter 5 - Conclusions

In this chapter, a review of the actions conducted in this thesis are presented while enhancing the main obtained results and its conclusions. Additionally, are presented lines of further research on the use of DOFS in civil engineering applications that were identified during the conduction of the presented research.

5.1. Conclusions

In this doctoral thesis it was proposed to research and assess the performance of distributed optical fiber sensing, more specifically the case of the OBR system, in the structural health monitoring of bridges and large scale structures. As explained in this document, this is a relatively recent technology that has demonstrated great promise for monitoring applications in a wide range of fields. Notwithstanding, due to its novelty, its use is still far from being conducted in a more systematic and efficient way in civil engineering infrastructures as a result of the still present uncertainties and lack of knowledge when dealing with this technology in this field. Being this especially true and relevant for the case of the application to concrete structures. As a consequence, this thesis pretended to continue and further analyse this topic following the initial applications using the OBR system as a monitoring tool in concrete structures.

Therefore, with the previous goal in mind, the thesis was divided in three parts. The first and initial part was the conduction of a thorough and global review of the information regarding the general topic of optical fiber sensors (OFS) and its differentiation in several categories with the goal of analysing their main differences and their possible field of application. Additionally, the further segmentation of the different types of DOFS and their individual particularities were conducted. Finally, in this first part, an overall review of the previous conducted applications of this technology in civil engineering applications both in the laboratory environment as in real world scenarios was performed while assessing the main reported limitations and capabilities of the system.

Here it was concluded about the further maturity on the understanding and use of several point sensors, especially FBGs, which is translated into a broader and larger number of applications of this type of sensors in civil engineering structures. This also included the assessment of a large number of examples where multiplexed FBG sensors are deployed conforming in this way quasi-distributed system.

Furthermore, it was seen how among the distributed optical fiber sensors, the Raman scattering is highly dependent on the temperature variation and therefore been mostly used as distributed temperature sensor with some observed applications in civil engineering infrastructures such as pipelines and dams. Moreover, due to the extended sensing range capabilities of Brillouin scattering based DOFS such as BOTDR and BOTDA, these type of sensors have been until now the most applied and instrumented type of sensors in large scale civil engineering infrastructures. Nevertheless, as a result of its relatively reduced spatial resolution, they present important limitations for damage detection and localization.

On the other hand, despite presenting a shorter sensing range when compared with the former DOFS technique based sensors, Rayleigh based optical frequency domain reflectometry (OFDR) DOFS, such as the OBR system, present the unique advantage of conducting strain distributed

measurements with a spatial resolution as high as 1 mm. Consequently, making this DOFS technique the most promising and adequate choice for civil engineering SHM applications where damage detection, localization and quantification are desired.

Furthermore, it was observed and concluded the extreme importance on the decision of the used fiber coating and bonding adhesives and overall protection in the performance of DOFS. This being consequence of their influence in the strain transfer effectiveness between the sensors and substrate material of the monitored structure. In the case of concrete structures, this achieved an even greater importance due to the inherent heterogeneity and surface roughness of this material. Therefore, the further research for the identification of the optimal bonding adhesive and alternative installation methods for these applications was deemed essential for a more reliable use of the DOFS technology in concrete structures. Additionally, an important lack of application examples regarding the long-term reliability and performance monitoring applications based on the OBR system was observed.

As a result of the work conducted in this first part of the thesis, one journal publication was achieved [110].

In the second part, considering what was observed in the literature review, different laboratory experimental campaigns were devised where multiple aspects of the instrumentation of DOFS technology in civil engineering applications was assessed and scrutinized. Here, as stipulated in the goals of this thesis, the study of new implementation methods, comparison and performance analysis of different bonding adhesives and spatial resolution were performed through the conduction of load tests in reinforced concrete beam elements instrumented with OBR DOFS technology. The long-term reliability of this sensing typology was assessed through the conduction of a fatigue load test on additional reinforced concrete beams.

The main conclusions is the proposal of a new methodology of implementation of Rayleigh OFDR based DOFS in reinforced concrete structures for both uncracked and cracked conditions. While having in mind the goal of improving the accuracy and at the same time guarantee the protection of these sensors from external environmental effects, a polyimide coated DOFS was directly instrumented in the steel rebar without previous mechanization and compared with the results provided by traditional strain gauges.

From this experience it was concluded how the deployed sensors performed well in uncracked conditions and how the measured data agreed almost perfectly with the one measured by the strain gauges. The proposed methodology allowed for the detection and localization of the developed crack and it was concluded that the use of cyanoacrylate adhesive for the bonding of the DOFS to the rebar element provided better results when compared with the use of epoxy.

Nevertheless, it was verified how after a certain load level following the formation and detection of cracking both at the surface and rebar levels, a significant change of stiffness in the elements seemed

to give origin to unreliable data values at the location of the crack, being more noticeable in the DOFS segment adhered to the rebar. This was associated to the decrease of the spectral shift quality (SSQ) values at those point locations. Therefore, a post-processing method was proposed in order to overcome this issue and enabling the plausible assessment of the DOFS measured data after cracking. As a conclusion, the consideration of a minimum SSQ threshold of 0.20 obtained the most reliable results in this particular case. Therefore, with this experiment it was displayed the feasibility of deploying such implementation method of a DOFS system for the monitoring of a RC beam. It is concluded, that this implementation method can be of interest in several type of applications such as in the case of prestressed concrete members while providing an additional protection to sensor regarding external environmental effects.

Also in this second part of the thesis, while assessing different spatial resolution values, it was seen how despite theoretically more promising, the use of a 1 mm spatial resolution didn't enhance the measured results at all. Moreover, it was seen that after performing a moving average to this resolution set in order to directly compare it to the other coarser resolutions, no significant improvements were obtained. This was not the case when using a spatial resolution of 1 cm, which proved to be more versatile while being able to perform solid damage characterization as seen in previous applications on concrete elements. Therefore, this spatial resolution of 1 cm is considered suitable and recommended for future applications using this system.

Additionally, when comparing the performance of the different deployed bonding adhesives (silicone, polyester, epoxy and cyanoacrylate) it was seen how for uncracked conditions, all segments agreed well with the data measured by the strain gauges although with a relative smoother and more uniform data measurement by the silicone bonded segment. In this way concluding that in applications where cracking is not expected, the use of any of this adhesives provides reliable results albeit a slightly better performance by the silicone adhesive.

Notwithstanding, for cracked conditions scenarios, it was observed how the different bonded segments performed relatively differently under the same load stages. For instance, despite always presenting strain measurements coherent with the applied load, the silicone bonded segment displayed a significantly wider area of influence produced by the developed crack similar to the use of a system with a coarser spatial resolution, therefore constituting a significant limitation of this adhesive in these type of situations. The other deployed adhesives on the other hand, displayed significantly narrower peaks derived from cracking but started to produce more erratic measurements at the location of the damage. Notwithstanding, due to the existence of previous works where for instance the epoxy adhesive performed better after the production of cracking in bigger RC elements, further similar experiments could be conducted in order to validate the findings of this particular experiment.

As a conclusion, the decision on the optimal bonding adhesive goes in hand with the objectives and performance preferences of the instrumented application in cracked scenarios. As seen in this research, the use of silicone adhesive provides measurements, which seem to be less influenced by the decrease of the associated spectral shift quality values and therefore provide coherent information for further stages of the load but presenting less spatially accurate measurements. The other researched adhesives, especially the cyanoacrylate, provide more precise spatially data but are limited earlier to the effect of the decrease of the SSQ values.

Still within this second part of the thesis, when assessing the long-term reliability of Rayleigh OFDR based DOFS in concrete elements through the conduction of fatigue tests to two RC elements, it can be concluded that for the uncracked state of the tested specimen, the DOFS measurements agreed reasonably well with the ones obtained by the also deployed strain gauges for the entire duration of the test. DOFS measurements presented a good stability along the number of cycles and no malfunction due to fatigue effects were observed. Therefore, concluding the applicability of deploying DOFS for long-term monitoring periods in real world structures as far as the environmental effects will not affect the correct performance of the bonding material and/or the optical fiber itself.

The activities conducted within this second part of the thesis gave origin to the production of one already published journal article [111], and two currently under revision.

Finally, the third part of this thesis was related to the successful application of the OBR system technology in two real world structures in Barcelona (Spain). The OBR was applied to a historical masonry building (Sant Pau hospital) during the conduction of important retrofitting works and to a prestressed concrete bridge (Sarajevo bridge in Barcelona) during the widening and rehabilitation actions. Both experiences showcased the feasibility of using this technology in real world applications.

The main conclusion is that the use of this monitoring system, through the use of a minimal number of fiber sensors, allowed for the correct surveillance and following-up of the developed strain variations on both structures, while allowing these to continue to be in service during the conduction of the referred works. Furthermore, it was concluded how this technology is able to provide useful data information for different structural material applications (masonry and concrete).

Lastly, the relatively long monitoring period conducted on the Sarajevo bridge structure proved that even the challenge presented by the important seasonal temperature variations on the sensor are able to be corrected and in this way not interfere in the correct assessment of the real mechanical strain variations produced on the monitored structure.

The work carried out in this third part of the thesis allowed for the production of an already published journal article [97]

As a final conclusion, the work performed in this doctoral thesis, continued the solid basis found during the literature review on the use of the OBR system for the monitoring of concrete structures and further researched ways of reducing the uncertainty behind the use of these sensors. This was done by proposing novel implementation techniques, assessing and comparing the performance of different bonding adhesives under uncracked and cracked scenarios both for static and dynamic tests and assessing the long-term reliability of DOFS measurements by means of fatigue tests.

5.2. Future Developments

As a result of the novelty of the researched topic in its application for monitoring systems in concrete structures it was also seen how further developments are still necessary and recommended for a more confident use of these sensors.

Within the observed limitations and aspects of improvement, the ones identified as more relevant are presented here.

1. For instance, an important field of further development on the use of DOFS in concrete structures is the necessity of identifying the possible causes of the decrease of the SSQ values, which is associated with the appearance of unreliable data measurements at the location of developed damage. Moreover, an identification of possible measures that would avoid this event would greatly benefit the performance of this technology in monitoring applications.
2. Additionally, the performance of a similar fatigue test but on larger RC beam specimens and with also higher induced stress ranges would be of interest. This would enable a more robust and accurate comparison of the data measured by the DOFS with the other instrumented sensors as the strain levels measured in the experiment conducted in this thesis were relatively small. Furthermore, a relevant enhancement of the results could be obtained with a lower frequency of the inputted cycling load. This would allow for the sampling rate of the DOFS acquisition system to follow the load profile of the cyclic load.
3. In the same direction, a further test using multiple bonding adhesives (including the ones researched in this thesis) in larger RC members would be of great interest in order to obtain a more resolute conclusion on the performance of each adhesive, more notably for the stage after the development of damage.
4. In addition, the post-processing stage of the measured data should also be further developed and enhanced. Currently, apart from the possibility of visualizing in a software window the measured strain during the conduction of any application, it is necessary to wait after the conduction of each measurement period to convert the spectral shift into strain or temperature, which takes considerable time. Moreover, the .txt files are then necessary to be converted manually by the user into Excel or Matlab format for a more convenient handling of the measured data. The development of a software add-on that would convert the measured spectral shift into strain/temperature data almost

simultaneously to the conduction of the measurements and storing them in multiple file formats would also be of great interest for a more widespread and reliable use of these sensors.

5.3. References

[1] P. Gerland, A. E. Raftery, H. Ševčíková, N. Li, D. Gu, T. Spoorenberg, L. Alkema, B. K. Fosdick, J. Chunn, and N. Lalic, "World population stabilization unlikely this century," *Science (80-.).*, vol. 346, no. 6206, pp. 234–237, **2014**.

[2] ASCE, "Infrastructure report card," *ASCE News*, vol. 53, no. September 2017, pp. 1–36, **2017**.

[3] U. N. U. I. H. D. Programme, *Inclusive Wealth Report 2014*. Cambridge University Press, **2015**.

[4] Centre for Research on the Epidemiology of Disasters (CRED), "Natural disasters in 2017: Lower mortality, higher cost," **2018**.

[5] J. M. Lopez-Higuera, L. Rodriguez Cobo, A. Quintela Incera, and A. Cobo, "Fiber Optic Sensors in Structural Health Monitoring," *J. Light. Technol.*, vol. 29, no. 4, pp. 587–608, **2011**.

[6] Y. L. Xu and Y. Xia, Structural health monitoring of long-span suspension bridges. CRC Press, **2011**.

[7] C. K. Y. Leung, K. T. Wan, D. Inaudi, X. Bao, W. Habel, Z. Zhou, J. Ou, M. Ghandehari, H. C. Wu, and M. Imai, "Review: optical fiber sensors for civil engineering applications," *Mater. Struct.*, vol. 48, no. 4, pp. 871–906, **2013**.

[8] D. S. Carder, "Observed vibrations of bridges," *Bull. Seismol. Soc. Am.*, vol. 27, no. 4, pp. 267–303, **1937**.

[9] C. R. Farrar and K. Worden, "An introduction to structural health monitoring.," *Philos. Trans. A. Math. Phys. Eng. Sci.*, vol. 365, no. 1851, pp. 303–315, **2007**.

[10] J. N. Kudva, C. Marantidis, J. D. Gentry, and E. Blazic, "Smart structures concepts for aircraft structural health monitoring," in *1993 North American Conference on Smart Structures and Materials*, **1993**, pp. 964–971.

[11] V. Giurgiutiu and C. A. Rogers, "Recent advancements in the electromechanical (E/M) impedance method for structural health monitoring and NDE," in *5th Annual International Symposium on Smart Structures and Materials*, **1998**, pp. 536–547.

[12] H. Sohn, C. R. Farrar, F. M. Hemez, and J. J. Czarnecki, "A Review of Structural Health Review of Structural Health Monitoring Literature 1996-2001.," Los Alamos National Laboratory, **2002**.

[13] J. P. Lynch and K. J. Loh, "A summary review of wireless sensors and sensor networks for structural health monitoring," *Shock Vib. Dig.*, vol. 38, no. 2, pp. 91–130, **2006**.

[14] B. Glisic, D. Inaudi, and N. Casanova, "SHM process as perceived through 350 projects," in *SPIE Smart Structures and Materials+ Nondestructive Evaluation and Health Monitoring*, **2010**, p. 76480P–76480P.

[15] J. A. Rice, K. Mechitov, S.-H. Sim, T. Nagayama, S. Jang, R. Kim, B. F. Spencer Jr, G. Agha, and Y. Fujino, "Flexible smart sensor framework for autonomous structural health monitoring," *Smart Struct. Syst.*, vol. 6, no. 5–6, pp. 423–438, **2010**.

[16] X. W. Ye, Y. H. Su, and J. P. Han, "Structural Health Monitoring of Civil Infrastructure Using Optical Fiber Sensing Technology: A Comprehensive Review.," *Sci. World J.*, vol. 2014, p. 652329, **2014**.

[17] G. Rodriguez, J. R. . Casas, and S. Villalba, "SHM by DOFS in civil engineering: a review," *Struct. Monit. Maint.*, vol. 2, no. 4, pp. 357–382, Dec. **2015**.

[18] B. Glisic, D. Hubbell, D. H. Sigurdardottir, and Y. Yao, "Damage detection and characterization using long-gauge and distributed fiber optic sensors," *Opt. Eng.*, vol. 52, p. 87101, **2013**.

[19] A. Lep, R. Ianoschi, and A. Neagu, "Gnss technology for structural health monitoring," no. 4, **2011**.

[20] A. Nair and C. S. Cai, "Acoustic emission monitoring of bridges: Review and case studies," *Eng. Struct.*, vol. 32, no. 6, pp. 1704–1714, **2010**.

[21] T. Khuc and F. N. Catbas, "Vision-Based for Bridge Structural Health Monitoring and Identification," in *SMAR 2015 - Third Conference on Smart Monitoring, Assessment and Rehabilitation of Civil Structures*, **2015**.

[22] S. Chen, D. F Laefer, and E. Mangina, "State of technology review of civilian UAVs," *Recent Patents Eng.*, vol. 10, no. 3, pp. 160–174, **2016**.

[23] P. Psimoulis, I. Peppa, L. Bonenberg, S. Ince, and X. Meng, "Combination of GPS and RTS measurements for the monitoring of semi-static and dynamic motion of pedestrian bridge," in *Proceedings of 3rd Joint International Symposium on Deformation Monitoring, Vienna, Austria*, **2016**.

[24] S.-H. Sim, J. Li, H. Jo, J.-W. Park, S. Cho, B. F. Spencer Jr, and H.-J. Jung, "A wireless smart sensor network for automated monitoring of cable tension," *Smart Mater. Struct.*, vol. 23, no. 2, p. 25006, **2013**.

[25] X. W. Ye, Y. Q. Ni, T. T. Wai, K. Y. Wong, X. M. Zhang, and F. Xu, "A vision-based system for dynamic displacement measurement of long-span bridges: algorithm and verification," *Smart Struct. Syst.*, vol. 12, no. 3–4, pp. 363–379, **2013**.

[26] Luna Innovations Incorporated, "ODiSI-A Users Guide," Blacksburg, VA, **2013**.

[27] G. Chen, H. Mu, D. Pommerenke, and J. L. Drewniak, "Damage detection of reinforced concrete beams with novel distributed crack/strain sensors," *Struct. Heal. Monit.*, vol. 3, no. 3, pp. 225–243, **2004**.

[28] Y. Yao, S. E. Tung, and B. Glisic, "Crack detection and characterization techniques—An overview," *Struct. Control Heal. Monit.*, vol. 21, no. 12, pp. 1387–1413, **2014**.

[29] X. Bao and L. Chen, "Recent progress in distributed fiber optic sensors," *Sensors (Basel)*, vol. 12, no. 7, pp. 8601–8639, **2012**.

[30] B. Glisic and D. Inaudi, "Development of method for in-service crack detection based on distributed fiber optic sensors," *Struct. Heal. Monit.*, vol. 11, no. 2, pp. 161–171, Mar. **2012**.

[31] D. Posenato, F. Lanata, D. Inaudi, and I. F. C. Smith, "Model-free data interpretation for continuous monitoring of complex structures," *Adv. Eng. Informatics*, vol. 22, no. 1, pp. 135–144, **2008**.

[32] J. Hecht, *City of light: the story of fiber optics*. Oxford University Press on Demand, **2004**.

[33] E. Udd and W. B. Spillman Jr, *Fiber optic sensors: an introduction for engineers and scientists*, Second Edi. Hoboken, New Jersey: John Wiley & Sons, **2011**.

[34] A. Rogers, "Distributed optical-fibre sensing," *Meas. Sci. Technol.*, vol. 10, no. 8, p. R75, **1999**.

[35] C. D. Butter and G. B. Hocker, "Fiber optics strain gauge," *Appl. Opt.*, vol. 17, no. 18, pp. 2867–2869, **1978**.

[36] T. G. Giallorenzi, J. A. Bucaro, A. Dandridge, G. H. Sigel, J. H. Cole, S. C. Rashleigh, and R. G. Priest, "Optical Fiber Sensor Technology," *IEEE Trans. Microw. Theory Tech.*, vol. 30, no. 4, pp. 472–511, **1982**.

[37] F. T. S. Yu and S. Yin, *Fiber Optic Sensors*, vol. 76. **2002**.

[38] B. Gholamzadeh and H. Nabovati, "Fiber Optic Sensors," *Int. J. Electr. Comput. Energ. Electron. Commun. Eng.*, vol. 2, no. 6, pp. 1107–1117, **2008**.

[39] H. Guo, G. Xiao, N. Mrad, and J. Yao, "Fiber Optic Sensors for Structural Health Monitoring of Air Platforms," *Sensors*, vol. 11, no. 12, pp. 3687–3705, Mar. **2011**.

[40] D. M. Peairs, L. Sterner, K. Flanagan, and V. Kochergin, "Fiber Optic Monitoring of Structural Composites using Optical Backscatter Reflectometry," in *Proceeddings of the 41st International SAMPE Technical Conference*, **2009**, no. November, pp. 19–22.

[41] C. Rodrigues, C. Felix, and J. Figueiras, "Fiber-optic-based displacement transducer to measure bridge deflections," *Struct. Heal. Monit.*, vol. 10, no. 2, pp. 147–156, **2010**.

[42] C. Barbosa, N. Costa, L. a Ferreira, F. M. Araújo, H. Varum, A. Costa, C. Fernandes, and H. Rodrigues, "Weldable fibre Bragg grating sensors for steel bridge monitoring," *Meas. Sci. Technol.*, vol. 19, no. 12, p. 125305, **2008**.

[43] J. M. López-Higuera, J. Misas, A. Q. Incera, and J. E. Cuenca, "Fiber optic civil structure monitoring system," *Opt. Eng.*, vol. 44, no. 4 artigo nº 44401, pp. 1–10, **2005**.

[44] A. Del Grosso, K. Bergmeister, D. Inaudi, and U. Santa, "Monitoring of bridges and concrete structures with fibre optic sensors in Europe," *IABSE Symp. Reports*, vol. 84, no. 6, pp. 15–22, **2001**.

[45] R. C. Tennyson et al, "Structural Health Monitoring of innovative bridges in Canada with fiber optic sensors," *Smart Mater. Struct.*, vol. 10, no. 3, pp. 560–573, **2001**.

[46] B. Glisic and K. Oberste-ufer, "Validation Testing of Fiber Optic Method for Buried Pipelines Health Assessment after Earthquake-Induced Ground Movement," in *Proccedings of 2011 NSF Engineering Research and Innovation Conference*, **2011**.

[47] P. Ferdinand, "The Evolution of Optical Fiber Sensors Technologies During the 35 Last Years and Their Applications in Structure Health Monitoring," in *EWSHM-7th European Workshop on Structural Health Monitoring*, **2014**.

[48] J. M. López-Higuera, *Optical Sensors*. Cantabria, Spain: Universidad de Cantabria, **1998**.

[49] A. Güemes and J. Sierra, "Fiber Optic Sensors," in *New trends in structural health monitoring*, Springer, **2013**, pp. 265–316.

[50] J. Sierra-Pérez, M. A. Torres-Arredondo, and A. Güemes, "Damage and nonlinearities detection in wind turbine blades based on strain field pattern recognition. FBGs, OBR and strain gauges comparison," *Compos. Struct.*, vol. 135, pp. 156–166, Jan. **2016**.

[51] J.-M. Henault, G. Moreau, S. Blairon, J. Salin, J.-R. Courivaud, F. Taillade, E. Merliot, J.-P. Dubois, J. Bertrand, S. Buschaert, S. Mayer, and S. Delepine-Lesoille, "Truly Distributed Optical Fiber Sensors for Structural Health Monitoring: From the Telecommunication Optical Fiber Drawling Tower to Water Leakage Detection in Dikes and Concrete Structure Strain Monitoring," *Adv. Civ. Eng.*, vol. 2010, pp. 1–13, **2010**.

[52] H. E. Mayhew, K. A. Frano, S. A. Svoboda, and K. L. Wustholz, "Using Raman Spectroscopy and Surface-Enhanced Raman Scattering To Identify Colorants in Art: An Experiment for an Upper-Division Chemistry Laboratory," *J. Chem. Educ.*, vol. 92, no. 1, pp. 148–152, **2014**.

[53] L. H. . Oakley, S. A. . Dinehart, S. A. . Svoboda, and K. L. Wustholz, "Identification of Organic Materials in Historical Oil Paintings Using Correlated Extractionless Surface-Enhanced Raman Scattering and Fluorescence Microscopy," *Anal. Chemestry*, no. 83, pp. 3986–3989, **2011**.

[54] C. Muehlethaler, M. Leona, and J. R. Lombardi, "Review of surface enhanced Raman scattering applications in forensic science," *Anal. Chem.*, vol. 88, no. 1, pp. 152–169, **2015**.

[55] S. Abalde-Cela, P. Aldeanueva-Potel, C. Mateo-Mateo, L. Rodríguez-Lorenzo, R. A. . Alvarez-Puebla, and L. M. Liz-Marzán, "Surface-enhanced Raman scattering biomedical applications of plasmonic colloidal particles," *J. R. Soc. Interface*, no. 7, pp. S435–S450, **2010**.

[56] C. A. Galindez-Jamioy and J. M. López-Higuera, "Brillouin Distributed Fiber Sensors: An Overview and Applications," *J. Sensors*, vol. 2012, pp. 1–17, **2012**.

[57] S. Uchida, E. Levenberg, and A. Klar, "On-specimen strain measurement with fiber optic distributed sensing," *Measurement*, vol. 60, pp. 104–113, **2015**.

[58] J. H. L. Grave, M. L. Håheim, and A. T. Echtermeyer, "Measuring changing strain fields in composites with Distributed Fiber-Optic Sensing using the optical backscatter reflectometer," *Compos. Part B Eng.*, vol. 74, pp. 138–146, **2015**.

[59] M. Froggatt and J. Moore, "High-spatial-resolution distributed strain measurement in optical fiber with rayleigh scatter.," *Appl. Opt.*, vol. 37, no. 10, pp. 1735–40, **1998**.

[60] N. a. Hoult, O. Ekim, and R. Regier, "Damage/Deterioration Detection for Steel Structures Using Distributed Fiber Optic Strain Sensors," *J. Eng. Mech.*, vol. 140, no. 1, p. 04014097, **2014**.

[61] M. G. Tanner, S. D. Dyer, B. Baek, R. H. Hadfield, and S. Woo Nam, "High-resolution single-mode fiber-optic distributed Raman sensor for absolute temperature measurement using superconducting nanowire single-photon detectors," *Appl. Phys. Lett.*, vol. 99, no. 20, p. 201110, **2011**.

[62] J. Park, G. Bolognini, D. Lee, P. Kim, P. Cho, F. Di Pasquale, and N. Park, "Raman-based distributed temperature sensor with simplex coding and link optimization," *Photonics Technol. Lett. IEEE*, vol. 18, no. 17, pp. 1879–1881, **2006**.

[63] Y. Dong, H. Zhang, L. Chen, and X. Bao, "2 cm spatial-resolution and 2 km range Brillouin optical fiber sensor using a transient differential pulse pair," *Appl. Opt.*, vol. 51, no. 9, pp. 1229–1235, **2012**.

[64] Y. Dong, L. Chen, and X. Bao, "Extending the sensing range of Brillouin optical time-domain analysis combining frequency-division multiplexing and in-line EDFAs," *J. Light. Technol.*, vol. 30, no. 8, pp. 1161–1167, **2012**.

[65] Visiongain, "Distributed Fibre Optic Sensing (DFOS) Market Report **2018**-2028."

[66] L. W. V. LLC, "2018 Distributed and Single Point Fiber Optic Sensing Systems Forecast - A Photonic Sensor Consortium Market Survey Report," **2018**.

[67] S. Villalba and J. R. Casas, "Application of optical fiber distributed sensing to health monitoring of concrete structures," *Mech. Syst. Signal Process.*, vol. 39, no. 1, pp. 441–451, **2012**.

[68] G. Rodriguez, J. R. Casas, and S. Villalba, "Cracking assessment in concrete structures by distributed optical fiber," *Smart Mater. Struct.*, vol. 24, no. 3, p. 35005, **2015**.

[69] G. Rodríguez, J. R. . Casas, S. Villalba, and A. Barrias, "Monitoring of shear cracking in partially prestressed concrete beams by distributed optical fiber sensors," in *Proceedings 8th International Conference on Bridge Maintenance, Safety and Management, IABMAS 2016*, **2016**.

[70] M. Quiertant, F. Baby, A. Khadour, P. Marchand, P. Rivillon, J. Billo, R. Lapeyrere, F. Toutlemonde, A. Simon, and J. Cordier, "Deformation monitoring of reinforcement bars with a distributed fiber optic sensor for the SHM of reinforced concrete structures," in *NDE*, **2012**, p. 10p.

[71] R. Regier and N. A. Hoult, "Concrete deterioration detection using distributed sensors," *Proc. Inst. Civ. Eng. Build.*, vol. 168, no. 2, pp. 118–126, **2015**.

[72] M. Davis, N. A. Hoult, and A. Scott, "Distributed strain sensing to determine the impact of corrosion on bond performance in reinforced concrete," *Constr. Build. Mater.*, vol. 114, pp. 481–491, **2016**.

[73] N. A. A. Rahim, M. A. Thoreson, T. Gorney, N. Garg, D. K. Gifford, M. E. Froggatt, and A. K. Sang, "Superior fatigue characteristics of fiber optic strain sensors," **2013**.

[74] J. R. Pedrazzani, S. M. Klute, D. K. Gifford, A. K. Sang, and M. E. Froggatt, "Embedded and surface mounted fiber optic sensors detect manufacturing defects and accumulated damage as a wind turbine blade is cycled to failure," **2012**.

[75] F. Matta, F. Bastianini, N. Galati, P. Casadei, and A. Nanni, "Distributed Strain Measurement in Steel Bridge with Fiber Optic Sensors: Validation through Diagnostic Load Test," *J. Perform. Constr. Facil.*, vol. 22, no. 4, pp. 264–273, **2008**.

[76] B. Glisic, J. Chen, and D. Hubbell, "Streicker Bridge: A comparison between Bragg-grating long-gauge strain and temperature sensors and Brillouin scattering-based distributed strain and temperature sensors," in *SPIE Smart Structures and Materials+ Nondestructive Evaluation and Health Monitoring*, **2011**, p. 79812C–79812C.

[77] V. Villalba, J. R. Casas, and S. Villalba, "Application of OBR fiber optic technology in structural health monitoring of Can Fatjó Viaduct (Cerdanyola de Vallés-Spain)," in *VI International Conference on Bridge Maintenance, Safety and Management*, **2012**.

[78] A. Minardo, R. Bernini, L. Amato, and L. Zeni, "Bridge monitoring using Brillouin fiber-optic sensors," *IEEE Sens. J.*, vol. 12, no. 1, pp. 145–150, **2012**.

[79] A. Minardo, G. Persichetti, G. Testa, L. Zeni, and R. Bernini, "Long term structural health monitoring by Brillouin fibre-optic sensing: A real case," *J. Geophys. Eng.*, vol. 9, no. 4, p. S64, **2012**.

[80] R. Regier and N. a. Hoult, "Distributed Strain Behavior of a Reinforced Concrete Bridge: Case Study," *J. Bridg. Eng.*, vol. 19, no. 12, p. 05014007, **2014**.

[81] L. Thévenaz, M. Facchini, A. Fellay, P. Robert, D. Inaudi, and B. Dardel, "Monitoring of large structure using distributed Brillouin fibre sensing," *Int. Conf. Opt. Fiber Sensors*, pp. 5–8, **1999**.

[82] D. Inaudi and B. Glisic, "Application of distributed Fiber Optic Sensory for SHM," in *Proceeding of the ISHMII-2*, **2005**, pp. 163–169.

[83] M. Aufleger, M. Conrad, T. Strobl, A. I. H. Malkawi, and Y. Duan, "Distributed Fibre Optic Temperature Measurements in RCC-Dams in Jordan and China," in *RCC Dams-Roller Compacted Concrete Dams: Proceedings of the IV International Symposium on Roller Compacted Concrete Dams*, **2003**, p. 401.

[84] K. Radzicki and S. Bonelli, "Physical and parametric monitoring of leakages in earthdams using analysis of fibre optic distributed temperature measurements with IRFTA model," in *24th International Congress on Large Dam*, **2012**.

[85] B. Shi, H. Xu, B. Chen, D. Zhang, Y. Ding, H. Cui, and J. Gao, "A feasibility study on the application of fiber-optic distributed sensors for strain measurement in the Taiwan Strait Tunnel project," *Mar. Georesources Geotechnol.*, vol. 21, no. 3–4, pp. 333–343, **2003**.

[86] P. Rajeev, J. Kodikara, W. K. Chiu, and T. Kuen, "Distributed Optical Fibre Sensors and their Applications in Pipeline Monitoring," *Key Eng. Mater.*, vol. 558, pp. 424–434, **2013**.

[87] C. Y. Gue, M. Wilcock, M. M. Alhaddad, M. Z. E. B. Elshafie, K. Soga, and R. J. Mair, "The monitoring of an existing cast iron tunnel with distributed fibre optic sensing (DFOS)," *J. Civ. Struct. Heal. Monit.*, vol. 5, no. 5, pp. 573–586, **2015**.

[88] H.-H. Zhu, B. Shi, J. Zhang, J.-F. Yan, and C.-C. Zhang, "Distributed fiber optic monitoring and stability analysis of a model slope under surcharge loading," *J. Mt. Sci.*, vol. 11, no. 4, pp. 979–989, Jul. **2014**.

[89] A. Klar, I. Dromy, and R. Linker, "Monitoring tunneling induced ground displacements using distributed fiber-optic sensing," *Tunn. Undergr. Sp. Technol.*, vol. 40, pp. 141–150, **2014**.

[90] K. Lim, L. Wong, W. K. Chiu, and J. Kodikara, "Distributed fiber optic sensors for monitoring pressure and stiffness changes in out-of-round pipes," *Struct. Control Heal. Monit.*, vol. 23, no. 2, pp. 303–314, **2015**.

[91] J. Casas, S. Villalba, and V. Villalba, "Management and Safety of Existing Concrete Structures via Optical Fiber Distributed Sensing," in *Maintenance and Safety of Aging Infrastructure: Structures and Infrastructures Book Series, vol 10*, **2014**, pp. 217–245.

[92] C. Lan, Z. Zhou, and J. Ou, "Monitoring of structural prestress loss in RC beams by inner distributed Brillouin and fiber Bragg grating sensors on a single optical fiber," *Struct. Control Heal. Monit.*, vol. 21, pp. 317–330, **2014**.

[93] F. Bastianini, M. Corradi, A. Borri, and A. di Tommaso, "Retrofit and monitoring of an historical building using 'Smart' CFRP with embedded fibre optic Brillouin sensors," *Constr. Build. Mater.*, vol. 19, no. 7, pp. 525–535, **2005**.

[94] Luna Innovations Incorporated, "OBR 4600 Data Sheet," Roanoke, VA, USA, **2018**.

[95] Luna Innovations Incorporated, "ODiSI A Data Sheet," Roanoke, VA, USA, **2013**.

[96] Luna Innovations Incorporated, "High-Definition Fiber Optic Strain Sensors." **2016**.

[97] A. Barrias, G. Rodriguez, J. R. Casas, and S. Villalba, "Application of distributed optical fiber sensors for the health monitoring of two real structures in Barcelona," *Struct. Infrastruct. Eng.*, **2018**.

[98] F. Ansari and Y. Libo, "Mechanics of bond and interface shear transfer in optical fiber sensors," *J. Eng. Mech.*, vol. 124, no. 4, pp. 385–394, **1998**.

[99] K. T. Wan, C. K. Y. Leung, and N. G. Olson, "Investigation of the strain transfer for surface-attached optical fiber strain sensors," *Smart Mater. Struct.*, vol. 17, no. 3, p. 35037, **2008**.

[100] J. M. Henault, J. Salin, G. Moreau, M. Quiertant, F. Taillade, K. Benzarti, and S. Delepine-Lesoille, "Analysis of the strain transfer mechanism between a truly distributed optical fiber sensor and the surrounding medium," in *Concrete Repair, Rehabilitation and Retrofitting III: 3rd International Conference on Concrete Repair, Rehabilitation and Retrofitting, ICCRRR-3, 3-5 September 2012, Cape Town, South Africa*, **2012**, p. 266.

[101] M. Davis, N. A. Hoult, and A. Scott, "Distributed strain sensing to assess corroded RC beams," *Eng. Struct.*, vol. 140, pp. 473–482, **2017**.

[102] A. Brault, S. Nurmi, and N. A. Hoult, "Distributed Deflection Measurement of Reinforced Concrete Elements Using Fibre Optic Sensors," in *IABSE Symposium Report*, **2017**, vol. 109, no. 43, pp. 1461–1469.

[103] S. T. Kreger, D. K. Gifford, M. E. Froggatt, B. J. Soller, and M. S. Wolfe, "High resolution distributed strain or temperature measurements in single-and multi-mode fiber using swept-wavelength interferometry," in *Optical Fiber Sensors*, **2006**, p. ThE42.

[104] TML, "TML STRAIN GAUGES 2017." Tokyo Sokki Kenkyujo Co., Ltd., **2017**.

[105] J. R. Pedrazzani, S. M. Klute, D. K. Gifford, A. K. Sang, and M. E. Froggatt, "Embedded and surface mounted fiber optic sensors detect manufacturing defects and accumulated damage as a wind turbine blade is cycled to failure," *Luna Innov. Inc*, **2012**.

[106] N. A. A. Rahim, M. A. Thoreson, T. Gorney, N. Garg, D. K. Gifford, M. E. Froggatt, and A. K. Sang, "Superior fatigue characteristics of fiber optic strain sensors," Roanoke, VA, USA, **2013**.

[107] L. Wong, N. Chowdhury, J. Wang, W. K. Chiu, and J. Kodikara, "Fatigue damage monitoring of a composite step lap joint using distributed optical fibre sensors," *Materials (Basel).*, vol. 9, no. 5, p. 374, **2016**.

[108] CEN (European Committee For Standardization), "EN 1991-2." **2002**.

[109] Luna Innovations Incorporated, "ODiSI Fiber Optic Sensor Installation Guide," **2017**.

[110] A. Barrias, J. Casas, and S. Villalba, "A Review of Distributed Optical Fiber Sensors for Civil Engineering Applications," *Sensors*, vol. 16, no. 5, p. 748, May **2016**.

[111] A. Barrias, R. J. Casas, and S. Villalba, "Embedded Distributed Optical Fiber Sensors in Reinforced Concrete Structures—A Case Study," *Sensors* , vol. 18, no. 4. **2018**.

Annex – Other Submitted Journal Articles

This chapter reproduces two additional journal articles produced within this thesis that are currently under revision. Since these documents, at the moment of writing this thesis document, were not published yet, they cannot be considered as part of the official compendium of publications. Nevertheless, these documents present relevant findings in the scope of the present thesis and discuss important aspects presented in previous sections.
As before, each paper follows its own numbering of sections, figures, tables, equations and references.

Journal Paper IV:

A. Barrias, J. Casas, and S. Villalba, "Distributed optical fiber sensors in concrete structures: Performance of bonding adhesives and influence of spatial resolution",

Submitted to Structural Control Health Monitoring in July 2018

Journal Paper V:

A. Barrias, J. Casas, and S. Villalba, "Fatigue performance of distributed optical fiber sensors in reinforced concrete elements",

Submitted to Smart Structures and Systems in August 2018

Journal Article IV

Distributed optical fiber sensors in concrete structures: Performance of bonding adhesives and influence of spatial resolution

Submitted to Structural Control Health Monitoring in July 2018

António Barrias [1], Joan R. Casas [1] and Sergi Villalba [2]

[1]Department of Civil and Environmental Engineering, Technical University of Catalonia (UPC), c/ Jordi Girona 1-3, 08034 – Barcelona, Spain

[2]Department of Engineering and Construction Projects, Technical University of Catalonia (UPC), c/ Colom 11, Ed. TR5, 08022 – Terrassa (Barcelona), Spain

Abstract: In this paper, the authors conducted an experiment where a reinforced concrete beam was instrumented with a 5-meter-long polyimide single DOFS performing four equal segments externally bonded to the bottom surface of the element, using for each segment a different type of adhesive. Three strain gauges were also used for comparison purposes. This beam was then loaded, producing expected equal levels of strain in each of the fiber segments for a more direct comparison of the different adhesives performance. The effect of alternating the spatial resolution is also analysed. In this exercise, additionally to the comparison with the other instrumented sensors it is also important the consideration and analysis of the associated Spectral Shift Quality (SSQ) values of the DOFS measurements.

Keywords: Distributed optical fiber sensors, Rayleigh backscatter, structural health monitoring, sensor bonding, reinforced concrete

1. Introduction

The maintenance and safety of infrastructures is of great importance for the overall well-functioning of the modern society. All civil engineering infrastructures are subject to natural hazardous and ordinary mechanical resistance decay and deterioration through its lifetime. Therefore, the accessible and immediate maintenance of such infrastructures is of paramount importance for the safety of its users and the economic competitiveness of any region.

It is in this context that the research and development of viable and robust Structural Health Monitoring (SHM) techniques in the past decades has become an important tool for the increase of the service life of these infrastructures. The early and correct detection of the damage in these infrastructures derives on great economical savings, a better structural maintenance and an improved assessment of the structural safety.

Within SHM applications, the use of optical fiber sensors (OFS) has been a popular topic of research and practice in the last two decades. This is due to their distinctive properties that offer significant advantages when compared with the more conventionally used electric sensors. OFS are immune to electromagnetic interference presenting measurements with lesser noise. These sensors perform also well under a wide range of temperature variations and since they are chemically inert, they are also free from corrosion. Lastly, OFS are generally small and lightweight, which facilitates the transport and installation of such sensors in a wide range of application scenarios. The use of these sensors has been well documented and practiced particularly through the use of Fiber Bragg Grating sensors [1].

On the other hand, the particular study and use of distributed optical fiber sensors (DOFS) is a relatively more recent topic of research within civil engineering infrastructures SHM. At the same time that these sensors provide the same advantages of the aforementioned optical fiber sensors, with the additional clear advantage of being able of acquiring strain and/or temperature information for longer extensions of the monitored structural components on which they are deployed and with very high spatial resolution [2].

This advantage is of great convenience and importance for the monitoring of concrete structures where the exact location of the possible crack formations is unknown beforehand and in this way, might be missed with the use of point or discrete sensors if not positioned at that particular location. With the use of distributed sensing, virtually every cross-section along the length of the fiber sensor is being monitored.

Furthermore, with the use of DOFS a larger area of the structure may be monitored with the use of up to one single sensor, which only requires one connecting cable, thus enabling a simpler and more economical monitoring system.

Previous work has displayed the promising capabilities of this technology on the monitoring of civil engineering infrastructures [3]-[8].

Nevertheless, as mentioned before, this is still a relatively new approach of this technology in the application on civil engineering infrastructures, which still presents substantial uncertainties regarding its use. Therefore, a continuous and deeper research of this topic is of vital importance for an eventually more systematically and regular use in SHM applications.

2. Distributed optical fiber sensing (DOFS)

When using DOFS technology, the optical fiber cables can be bonded to the surface or embedded inside the material. When strain and temperature variations occur, these changes are transferred from the monitored material to the sensor which variates the scattered signal being reflected inside the fiber. As mentioned before, the use of DOFS, provide additional advantages when compared with the use of their discrete or point sensors counterpart. However, these advantages are also strongly correlated with the specific use of each of the scattering techniques, which enables distributed sensing.

Scattering is at the origin of distributed optical fiber sensing and is defined by the interaction between the light and the optical medium. From this interaction three different scattering processes occur, where each can be used for different applications due to their inherent particularities. These scattering processes are the Raman, Brillouin and Rayleigh scattering [2].

Raman scattering is highly dependent of temperature variations, which has led to some applications in civil engineering SHM but has been more typically used in other fields [5].

Brillouin scattering based DOFS on the other hand have been the most studied and used DOFS systems in civil engineering SHM applications due to their large-scale capability, which can go up to the kilometre range. Nonetheless, as this technique has been mostly used employing optical time domain reflectometry (OTDR) it presents a relatively low spatial resolution of roughly one meter, which is not ideal for crack detection and other applications.

On the contrary, the optical frequency domain reflectometry (OFDR) systems, which are based in the Rayleigh scattering, offer a spatial resolution as high as one millimetre, which makes it ideal for crack detection and localization although currently limited to a monitoring length of 70 m. This is achieved through the use of swept wavelength interferometry (SWI) to measure the Rayleigh backscatter as a function of length.

The Rayleigh backscatter, for any given fiber as a function of distance, is a random but static property working as an individual fingerprint for each specific cable. External stimulus to the fiber such as strain or temperature variations induce shifts in the locally reflected spectrum and in this way facilitating distributed strain or temperature sensing with a high spatial resolution [9].

In this way, in the present study it is used the ODiSI A model from LUNA technologies which is an optical backscattered reflectometry (OBR) system based on the Rayleigh OFDR, Figure 1. This system allows the acquisition of distributed strain and temperature measurements with sub-cm spatial resolution and a ±2 με and ±0.2 ºC resolution. The maximum sensing length is of 50 m and the strain measurement range is of ±13000 με [10].

More detailed information of this technology and the theoretical background of distributed optical fiber sensing can be consulted in [2].

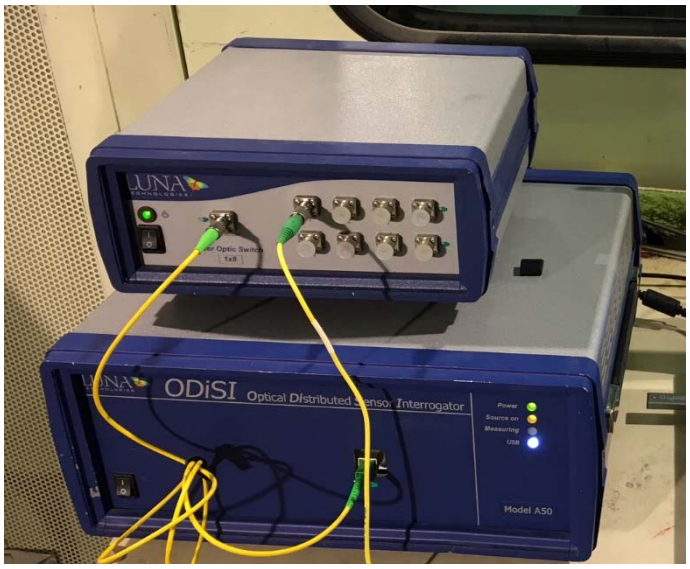

Figure 1. ODiSI A system used in the laboratory test campaign

3. DOFS adhesive bonding performance analysis

Despite the significant increase in interest on the study and practice of SHM applications through the use of DOFS, due to its relatively novelty, a considerable lack of knowledge is still present regarding the choice of the optimal bonding adhesive, especially in its use when deploying these sensors in reinforced concrete structures.

In order to assure a reliable monitoring of the strain data in the substrate, an optimal strain transfer between the sensor and the monitored material must be achieved, therefore the topic of its deployment is of considerable importance. In addition to the removal of any grease or dust present in the surface of the host material and the smoothening of the surface, the decision on the adhesive to bond the optical fiber sensor to the surface has to be assessed and considered. This is even a more critical issue when applying DOFS without any protective thick coating, such as the case of the deployed fiber in this research, Figure 2. Here, it was used a polyimide coated fiber that had a combined total diameter of core, cladding and coating of 155 μm [11], being that the coating only contributed with 15 μm for this diameter. The use of this specific fiber, is by itself, related with the objective of reducing the influence of the sensor coating material in the strain accuracy of the DOFS measurements.

Figure 2. DOFS type deployed in the experimental campaign

There have been some studies where the coating influence on the strain transfer on point fiber optic sensors [12], the adhesive spread installation method [13] and the coating strain transfer impact in DOFS [14] were analysed.

Moreover, one particular study [15], analysed among other things the performance of the use of cyanoacrylate and epoxy adhesives together with both nylon and polyimide DOFS when attached to the surface of the concrete and when attached to the reinforcement of the same structural elements. In this case, the results displayed a better performance of the polyimide fiber deployed together with the cyanoacrylate adhesive when bonded to the reinforcement and the combination of nylon fiber with the epoxy adhesive when bonded to the concrete.

Furthermore, in the authors personal experience, a combined use of epoxy adhesive with polyimide fiber when bonded to the concrete surface had offered promising results in different experiments [3], [5], [16].

Consequently, in the present paper, the authors decided to conduct a test where a single 5 m polyimide DOFS is attached to the surface of a reinforced concrete beam using four adhesives: epoxy, cyanoacrylate, polyester and neutral cure silicone, Figure 3.

These adhesives were selected based on the previous experience of the authors and through what was found during a literature review on this topic. Namely, the three first adhesives: epoxy, cyanoacrylate and polyester were ordered as advised by the TML strain gauges 2017 catalogue for concrete applications [17]. On the other hand, the used neutral cure silicone, was a simple commercial one from Ceys brand for general construction applications where concrete was included.

Figure 3. Adhesives deployed in this experimental campaign, from left to right: Epoxy, Cyanoacrylate, Polyester, Neutral Cure Silicone

It is important to mention that to the author's knowledge, the use of silicone in this type applications had only been performed before as an additional layer of protection of the sensor for the case of embedded implementations. In this case, for the first time the silicone is deployed primarily as an adhesive. In this sense, it is important to use a neutral cure silicone in order to not harm the polyimide fiber as it may occur when using an acetoxy cure one.

Finally, it has to be also referred that in practical terms it is important to have in consideration the viscosity and time of curing of each adhesive. In real world scenarios, it is often the case where the surface where the sensor is going to be instrumented is not horizontal or facing up. Therefore, for these situations it is important to deploy a very fast curing adhesive that allows for an also fast bonding. Moreover, the chosen adhesive should also have a high viscosity that prevents its dripping along the member which would weaken the bond. Each one of the chosen adhesives for this experiment provides different times of curing and viscosity options that have to be considered carefully depending on each intended application.

4. Experimental setup

As mentioned before, the main goal of this experimental campaign was to assess the performance of different adhesives for the bonding of DOFS to concrete elements during a three-point load test.

A 60x15x15 [cm] reinforced concrete beam, Figure 4, was used. Furthermore, as observed in Figure, this structural element had two longitudinal ϕ12 and four ϕ6 S500 rebars.

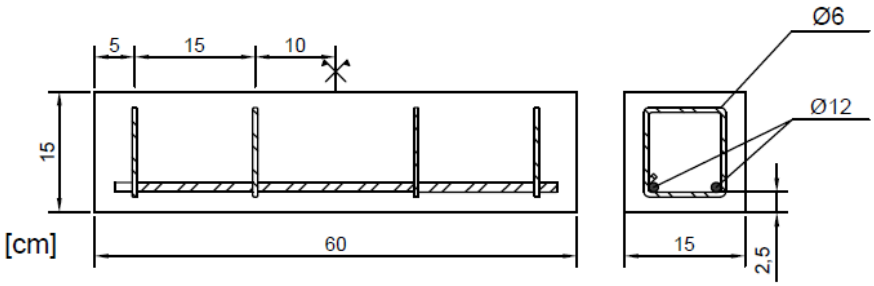

Figure 4. Tested beam definition scheme

A 5.2 m long DOFS was bonded to this concrete by providing a pattern with four different equal segments on the bottom surface of the beam. This was done with the intention to submit them to the same strains (in tension) and therefore they would be directly and immediately comparable.

Additionally, three 30 mm length strain gauges were also bonded to the centre of the bottom surface of the concrete beam with equal distance between them: SG1, SG2 and SG3. These sensors are later used for comparison purposes with the data obtained by the DOFS, Figure 5. The deployment of the instrumented sensors on the reinforced concrete beam with the information of the adhesive used in each DOFS segment is presented in Figure 5. A photo of the specimen is also seen in Figure 6.

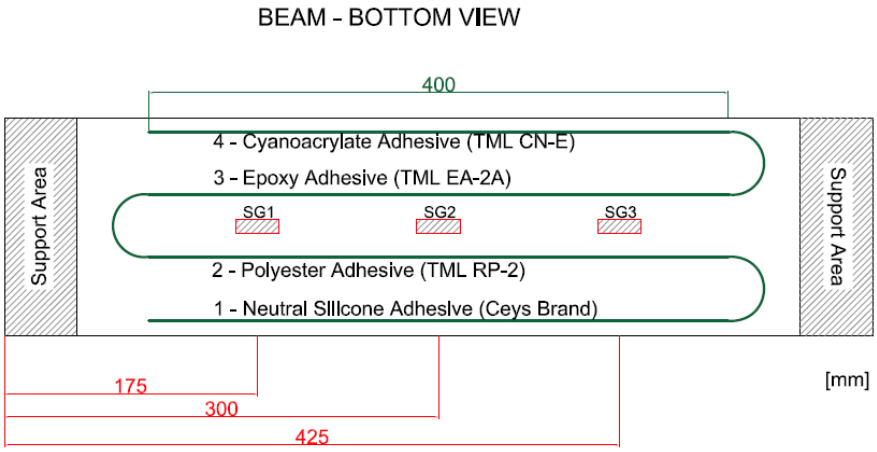

Figure 5. Plan of the reinforced concrete beam instrumented sensors

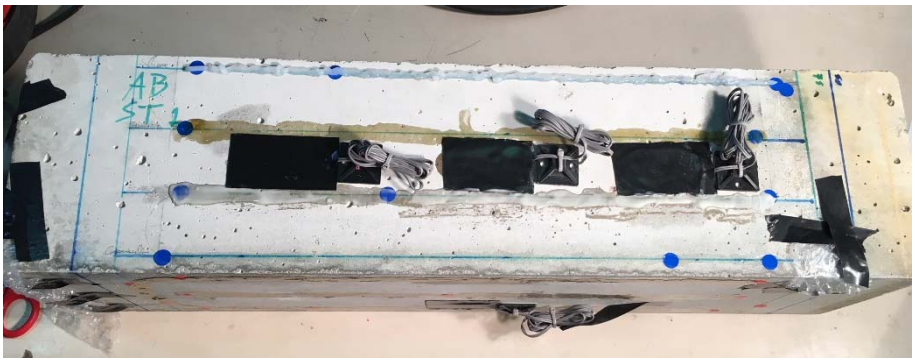

Figure 6. View of the sensors (DOFS and strain gauges) instrumented in the bottom surface of the tested beam

In this way, the global setup of the three-point load test on this beam can be seen in Figure 7.

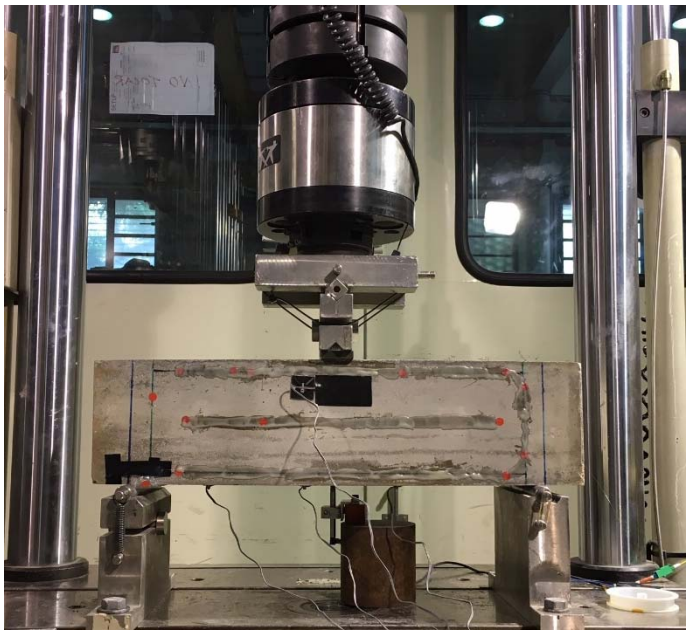

Figure 7. View of the loading arrangement (the DOFS segments considered in the analysis are the ones on the bottom surface of the beam)

At the time of pouring the concrete, additional cylindrical samples were also produced. Afterwards, close to the date of the test, these samples were tested in order to calculate the material properties of the used concrete. Therefore, the mean compressive strength (f_{cm}), the mean tensile strength (f_{ctm}) and the mean Young modulus (E_c) were obtained. Consequently, with this information, it is also possible to calculate the strain level expected to initiate the formation of cracking at the concrete (ε_{ct}). These properties are described in Table 1.

Table 1. Concrete material properties

Properties	f_{cm} **[MPa]**	f_{ctm} **[MPa]**	E_c **[MPa]**	ε_{ct} **[με]**
Specimen	48.027	3.944	37886.64	104.10

An additional point of interest in this study was the assessment of the influence of different spatial resolution used in the DOFS system. Here the objective was to observe if a milimetric spatial resolution would improve significantly the strain monitoring on concrete members compared with a resolution in the centimetre level. It is important to mention that milimetric spatial resolution level implies ten times the amount of acquired data. Furthermore, due to the heterogeneity of the concrete material and its aggregate sizes, this aspect is of interest for the application of DOFS based monitoring systems in this material.

In this way, it was decided to initially perform three separate but identical load cycles where a different spatial resolution was used. The maximum applied load in these cycles was only 11 kN, therefore not inducing cracking in the concrete.

Afterwards, a final load was applied inducing cracking and continuing until failure of either the specimen or the DOFS. The test sequence is defined in Table 2and Figure 8.

Table 2. Test cycle description

Test cycle number	Spatial Resolution	Sampling Rate
1	1 cm	0.2 Hz
2	3 cm	
3	1 mm	
4-rupture	1 cm	

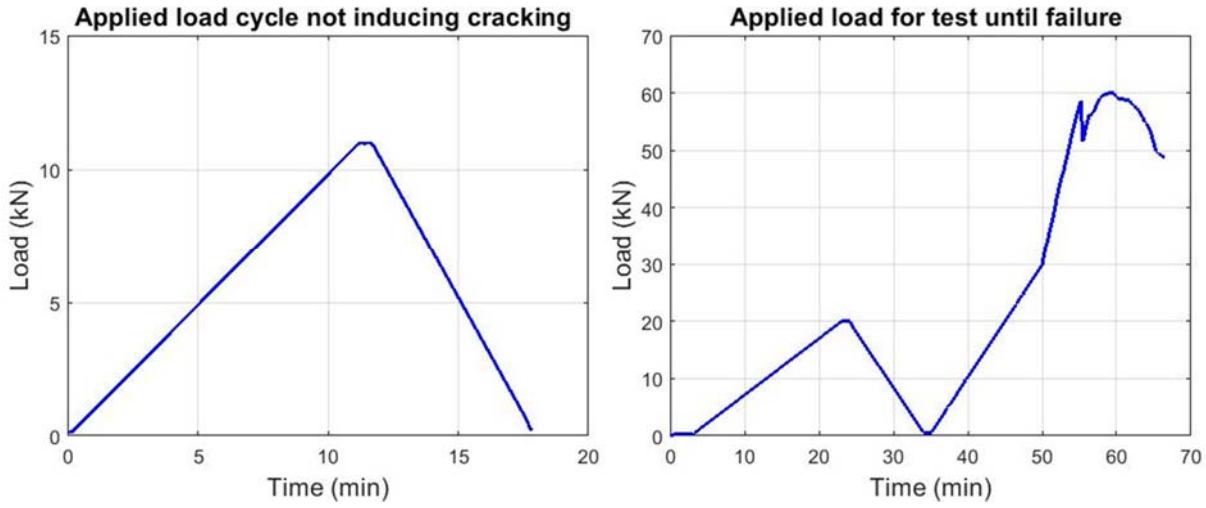

Figure 8. Load cycle applied for tests 1 to 3 (left) and test 4 – rupture (right)

5. Results

The data from both the DOFS and the strain gauges was post processed and analysed. The DOFS handling software allows the storage of the data in three different formats, namely: its raw spectral shift form, directly converted to strain/temperature using the manufacturer calibrated constant factors and finally in its associated Spectral Shift Quality (SSQ) matrix. This last one is of significant importance in order to assess the performance of the fiber during the test, especially after the occurrence of damage (cracking).

5.1. Comparison of spatial resolution input

As described in Table 2, it was decided to input three different spatial resolutions of the DOFS measurements in the first three load cycles applied to the tested specimen: 1 cm, 3 cm and 1 mm. The 3 cm spatial resolution is justified by the minimum length of the available strain gauges recommended in concrete measurements. Thus, 520 points, 174 points and 5191 points of the DOFS were measured in the first, second and third load test cycle respectively.

In Figure 9, the obtained strain measurements for the different used adhesives and inputted spatial resolutions for a load of 11 kN are displayed. The results from the strain gauges is also displayed for comparison.

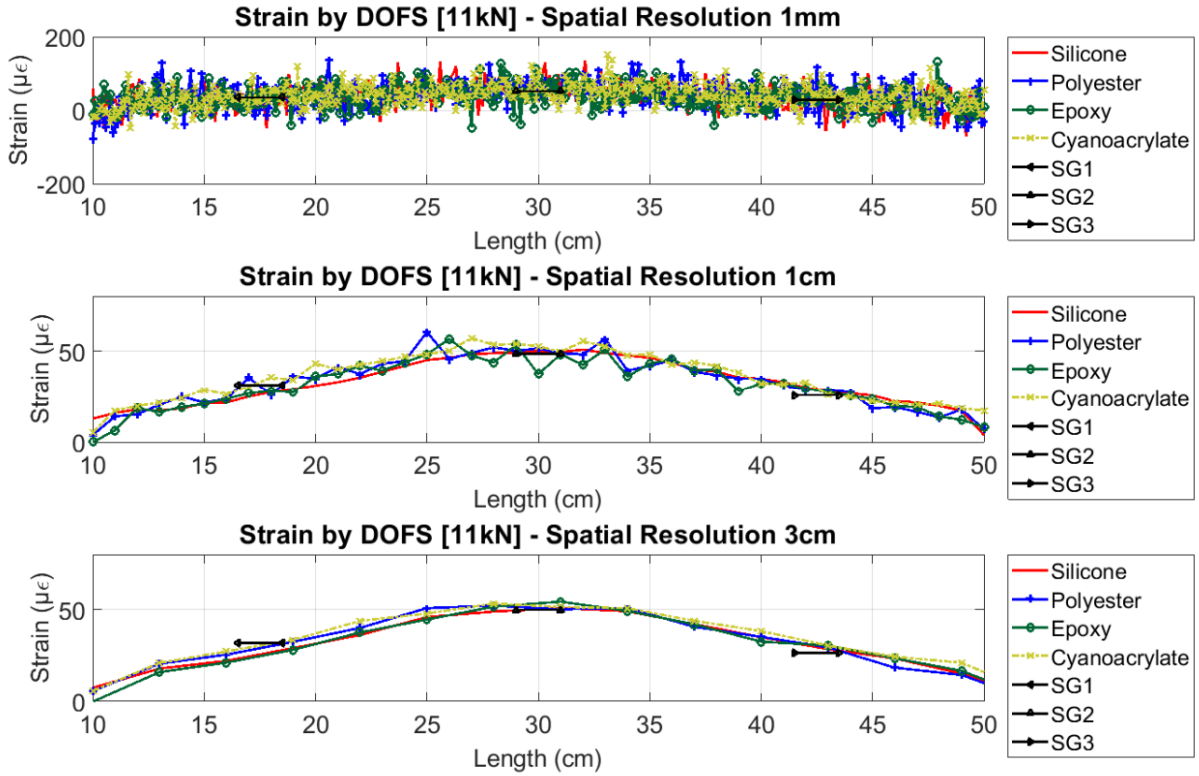

Figure 9. Strain data measured by DOFS with different spatial resolution inputs and adhesives.

As it is possible to observe from this figure, there is a clear difference between the data measured using a 1 mm and the two spatial resolutions, presenting a significantly higher spatial variability. This is due to the heterogeneity of the sizes of the aggregates that constitute the concrete material. A still relatively noticeable variability is observed for the 1 cm spatial resolution (except for the silicone bonded segment) but significantly smaller than the one verified with 1 mm and that presents a good agreement with the strain gauges and the measurements observed with a 3 cm spatial resolution.

Having this in mind, it was decided to assess if even initially inputting a random spatial resolution it would be possible to obtain equal or similar results as using a different resolution. This is done by means of performing a moving average that would represent the desired resolution.

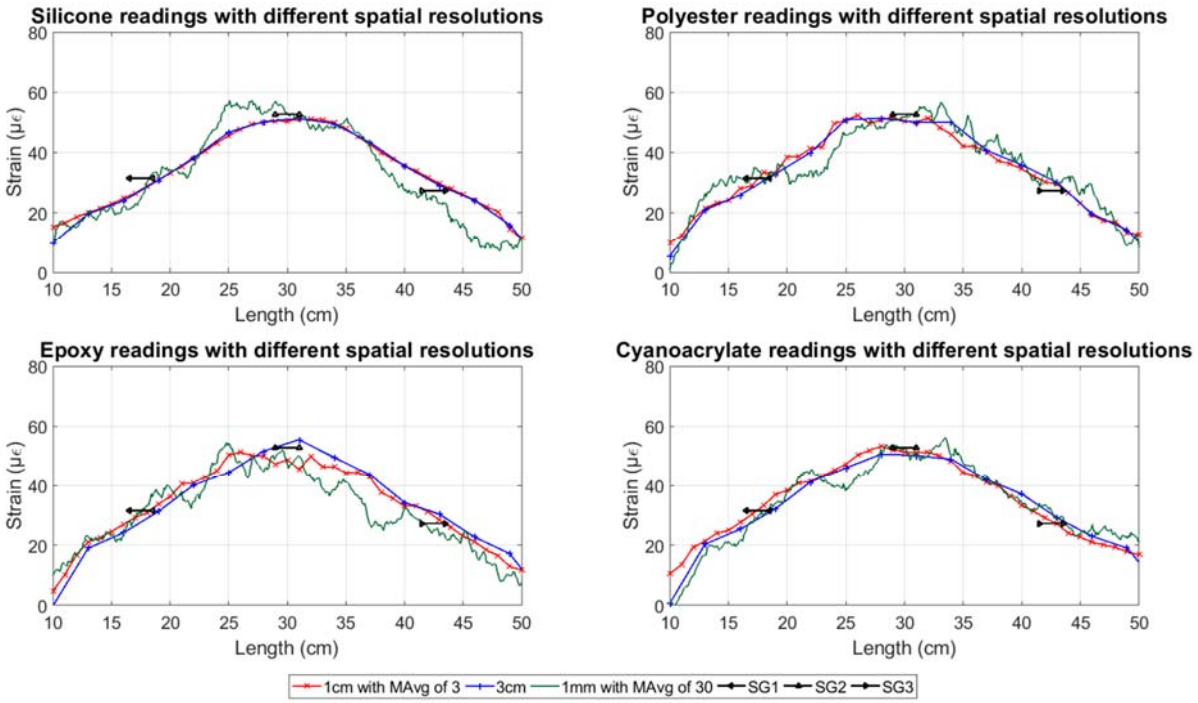

Figure 10. Data measured by each DOFS adhesive segment with different spatial resolutions while performing a moving average to the 1 mm and 1 cm data in order to directly compare it with the 3 cm spatial resolution data

In this way, the measurements obtained with a 3 cm spatial resolution were directly compared with the other two sets by conducting a moving average with a window of 30 units to the 1 mm measurements and another with a window of 3 for the 1 cm. The obtained graphs are depicted in Figure 10.

It is possible to observe how the averaged 1 mm obtained data improved significantly from before resembling the data from the other sets and the strain gauges but still presenting a noticeable erratic spatial variability. It is also perceived that apart the epoxy bonded DOFS segment, the set of averaged 1 cm data fits almost completely the one obtained using an initial 3 cm spatial resolution.

The conclusion is that no real advantages are originated by using a sub-cm spatial resolution. Furthermore, due to good agreement between the averaged 1 cm and 3 cm sets, it is decided to use the 1 cm spatial resolution, which provides a greater flexibility and better results considering the spatial resolution-accuracy-variability trade-off.

5.2. Comparison of different adhesives under elastic loading behaviour

The test cycles 1 to 3 are also used to analyse the performance of the different adhesives used to bond the DOFS to the concrete surface under non-cracked conditions.

In Figure 11 the strain measurements obtained through strain gauge 1 (SG1), strain gauge 2 (SG2) and strain gauge 3 (SG3) are compared with the corresponding points of each adhesive bonded segment of the DOFS. Since the deployed strain gauges have a 3 cm length, an average of the points of the DOFS, which are located at the same position of the length of the strain gauges is performed in order

to more correctly compare both set of sensors. The applied load is also plotted using the right y-axis. A good agreement between the data from the DOFS and the strain gauges is observed.

At mid-span, where the strains are higher it is seen on Figure 11 and Figure 12 how apart from a small difference of 5.54 με (11.70%) of the epoxy bonded DOFS segment to SG2 all other adhesives have a difference around or below 2 με. This corresponds to the resolution of the used DOFS acquisition system as mentioned before. Furthermore, as seen in Figure 12, all adhesives bonded DOFS segments present an average difference at the three locations below 13% which goes in agreement with what was verified in a previous test where a similar DOFS was compared with foil gauge strain sensors at different locations of a wind turbine blade [18].

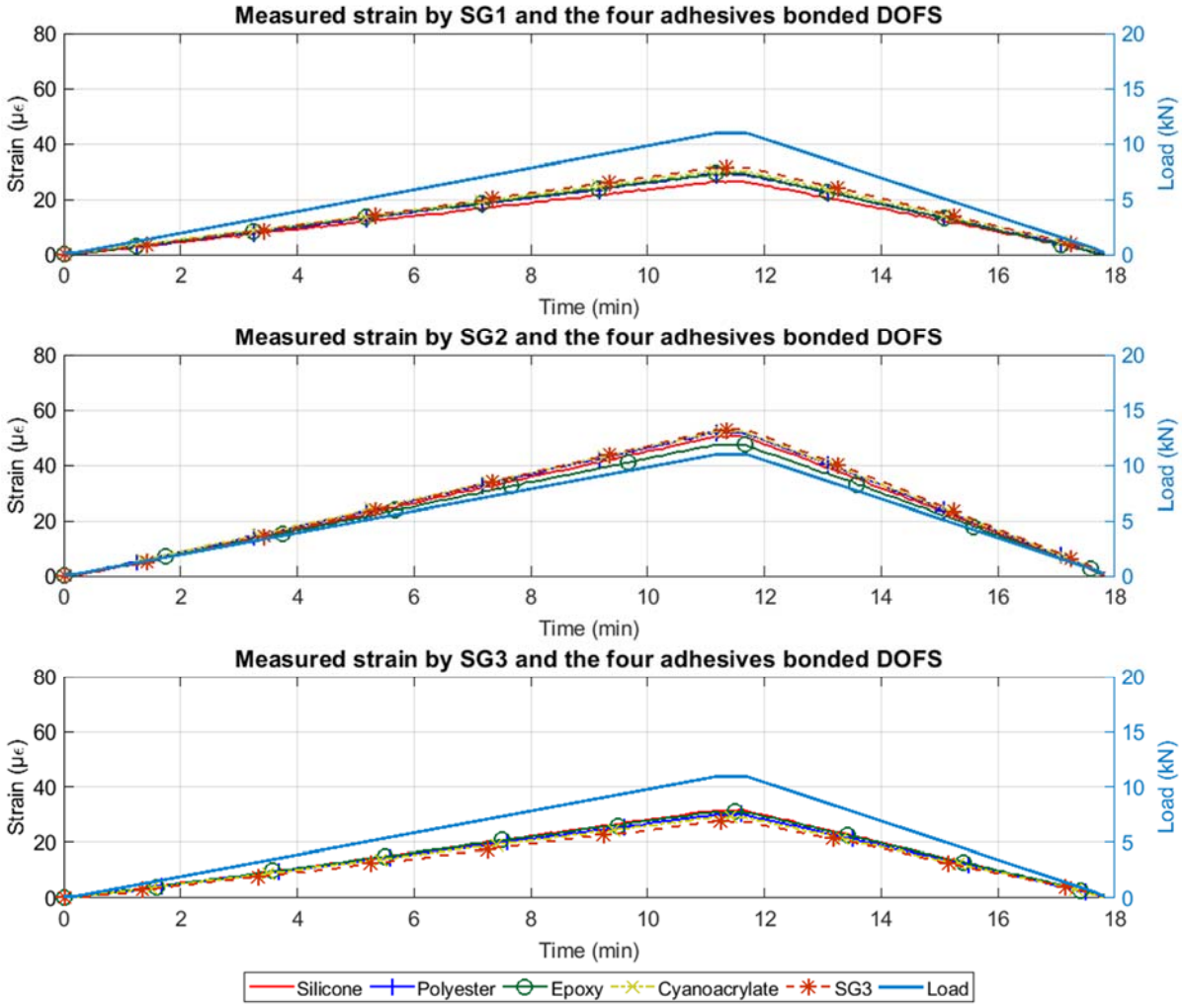

Figure 11. Comparison of strain measured by DOFS and SG1, SG2, SG3 with inputted load

Nevertheless, when assessing the overall distribution of the DOFS measurements for each segment over time, the surface plot of Figure 13 is obtained. Here it is seen a slightly smoother and homogenous reading at the neutral cure silicone segment when compared with the other adhesives by means of clearer increase of the contour lines of its surface plot.

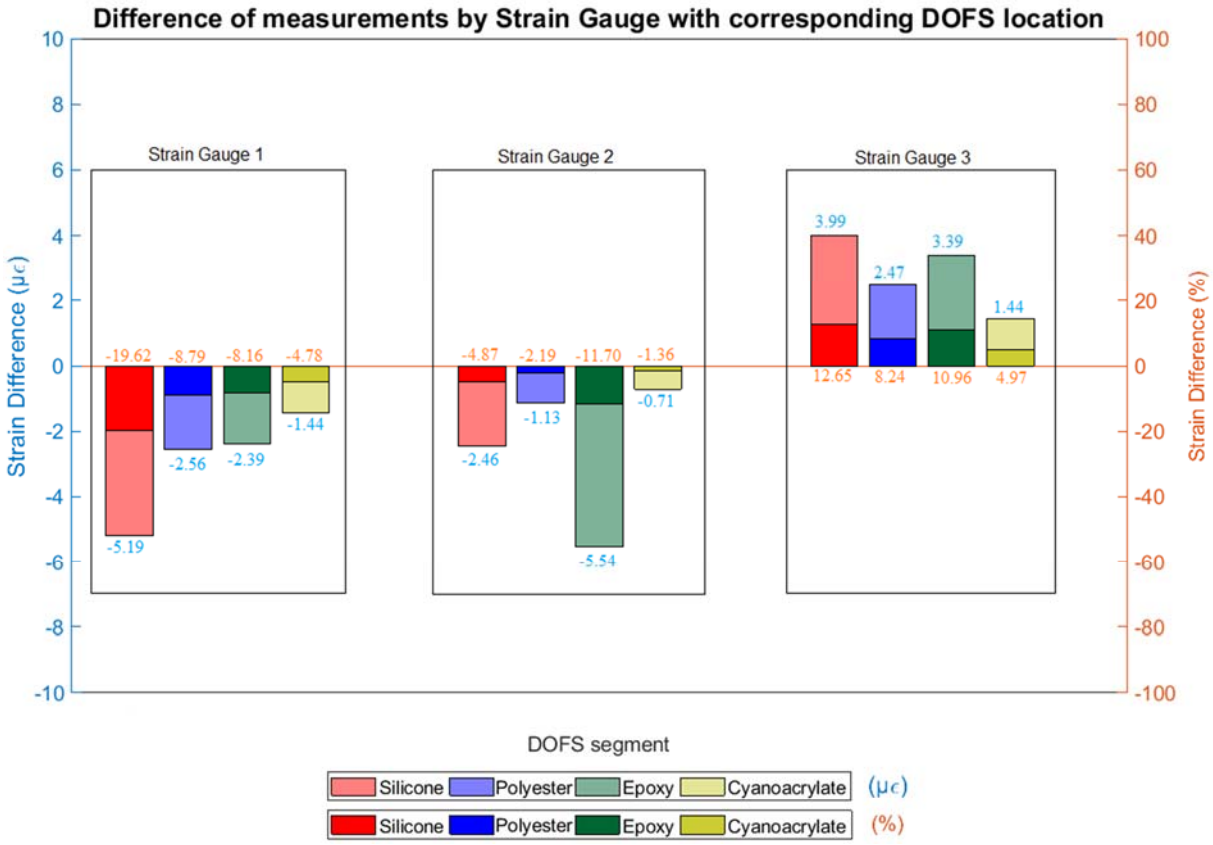

Figure 12. Strain difference of measurements by each DOFS bonded segment to corresponding Strain Gauge

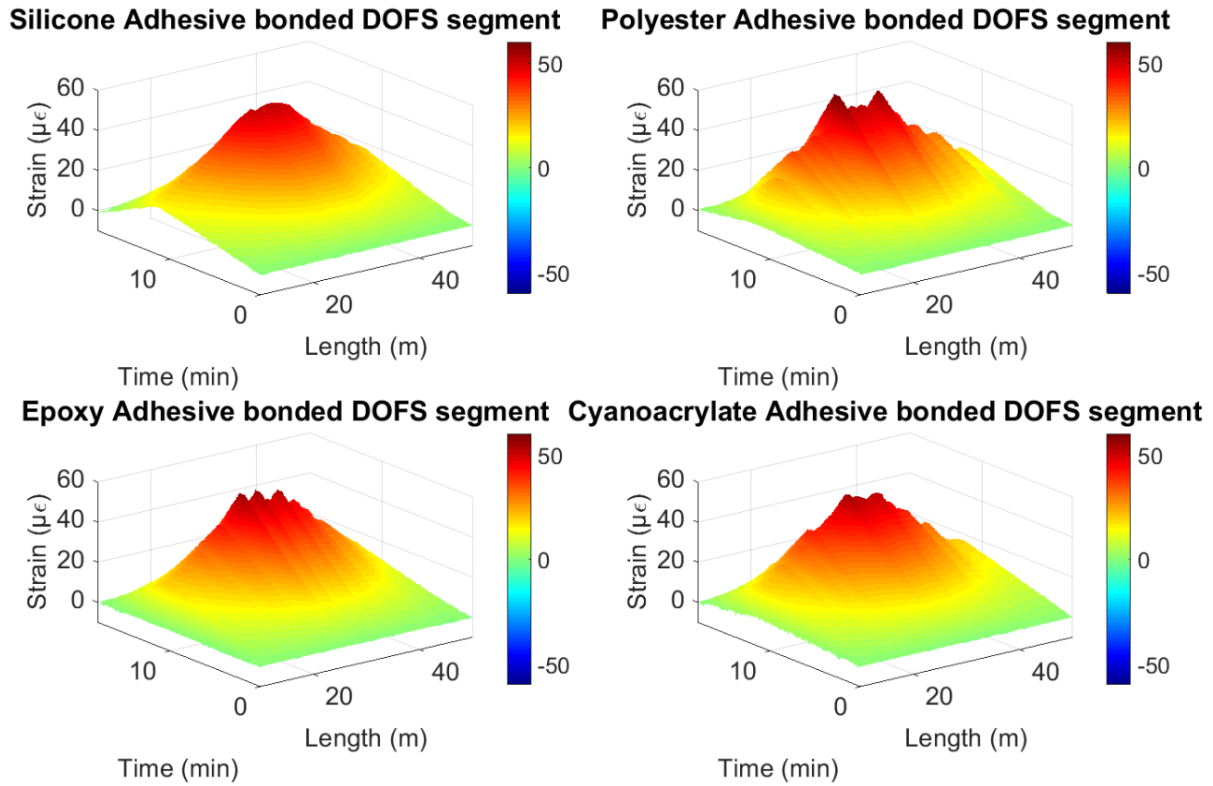

Figure 13. Strain measured for elastic load test cycle with different adhesive bonded DOFS segments

The other used adhesives - Polyester, Epoxy and Cyanoacrylate - display a significant higher spatial variability especially at the point corresponding to the maximum strain value.

5.3. Comparison of different adhesives when inducing cracking

After conducting the load test cycles under non-cracked conditions a load test cycle inducing cracking was performed as depicted in Figure 8. Here, as mentioned before, the load was applied initially up to 20 kN, then decreased to zero and increased again until failure.

According to the mechanical properties obtained through the tests conducted to the cylindrical specimens and presented in Table 1, the cracking load would be close to 18 kN. Therefore, in the test, it was also desired to assess the performance of the different adhesives after cracking during the unloading stage. Nevertheless, during the execution of the load cycle it was verified that, the resistance of the beam specimen was relatively higher from what was expected.

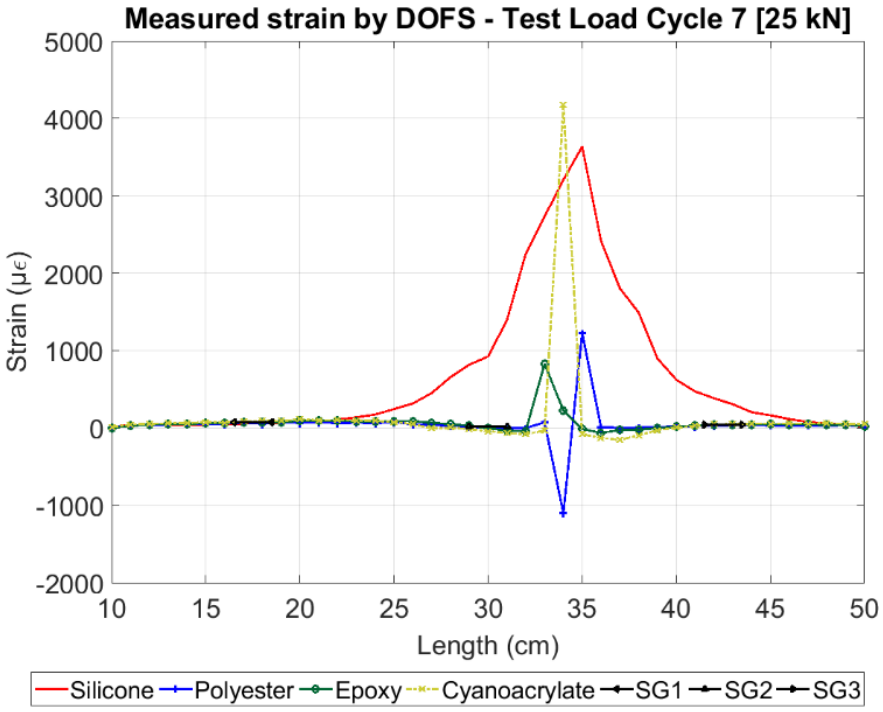

Figure 14. Detection and localization of cracking at concrete by DOFS

In reality, as in Figure 15, cracking only started to occur around the 24 kN load, being firstly detected by the silicone and cyanoacrylate bonded segments. In Figure 14 is displayed the detection of cracking by all segments at load level of 25 kN. Figure 15 depicts the evolution of the strain measurements by the four different adhesives bonded segments for different load stages and compared with the data obtained by the strain gauges.

As seen for the first part of the test (under un-cracked condition), before the occurrence of cracking, the silicone bonded segment presents significantly smoother spatial measurements when compared with the other adhesives.

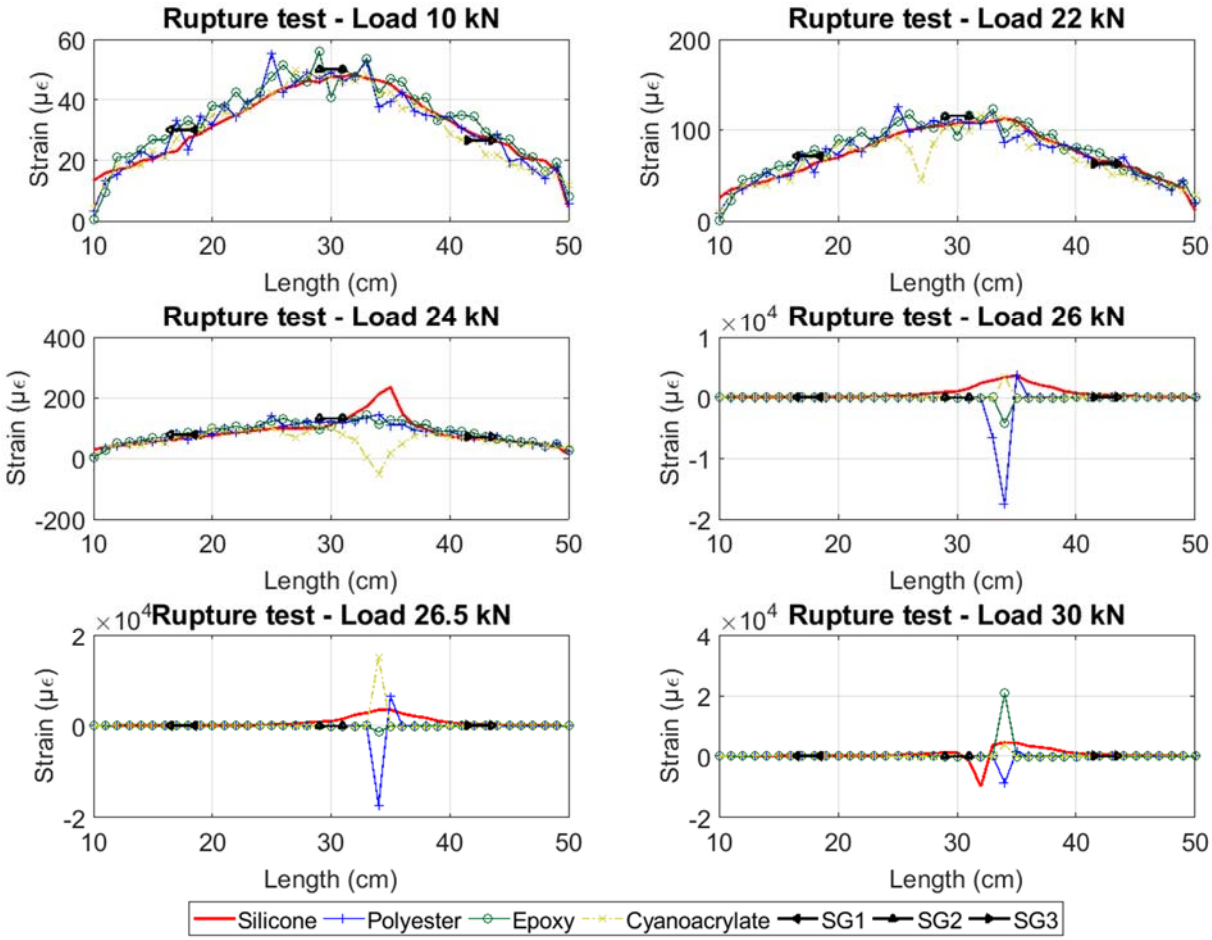

Figure 15. Evolution of the measured strain for different load levels until failure

After the initiation of cracking, all segments detect this damage at relatively the same location. This is in accordance to what was observed visually as the developed crack was not formed in a straight line orthogonal to the bonded DOFS segments.

Afterwards, once the cracking occurs, all segments, apart from the silicone bonded one, start producing peak values with either positive or negative strain for subsequent load levels at the crack location. According to the loading sequence, only positive growing peaks should be observed.

This is related with the aforementioned Spectral Shift Quality (SSQ) values, which are associated with the DOFS measurements during the crack formation. This parameter is a quantitative measure of the correlation between the conducted measurement and the original baseline reflected spectra. Therefore, its value should theoretically be always between 0 and 1. As mentioned before, the system manufacturer suggests the consideration of SSQ values below 0.15 as inaccurate, being that these values correspond to a change in strain or temperature that has likely exceeded the sensor measurable range [19].

Although the silicone bonded segment does not follow this trend, it should be highlighted that it presents, on the other hand, a significantly wider area around the location of the originated crack. This

make it impractical to detect further cracks within this segment in the event of the fiber not being broken at that stage.

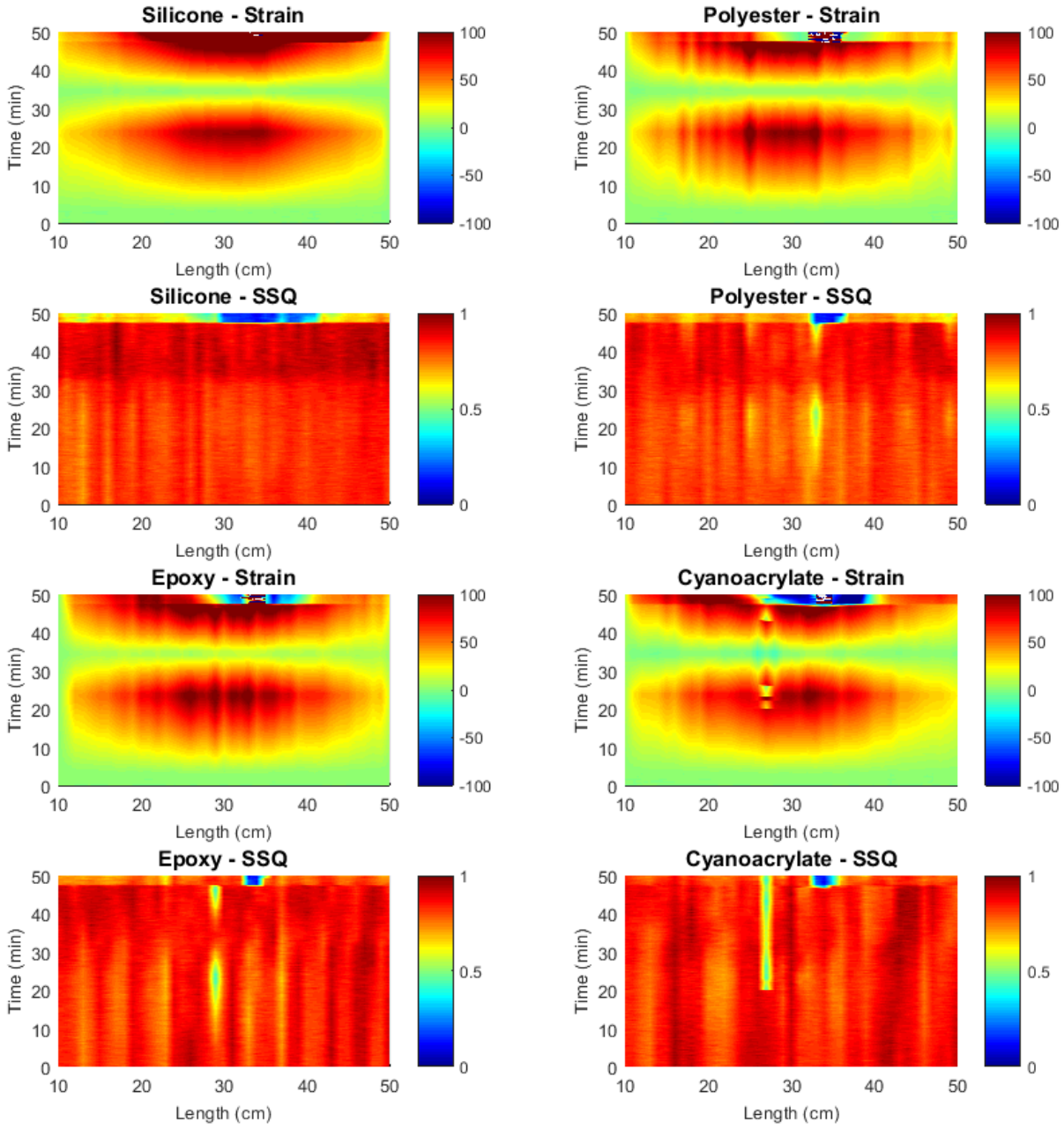

Figure 16. Comparison of SSQ values of each segment with different adhesives when cracking occurs

By analysing the measured strain the associated SSQ matrix, Figure is obtained. It is observable how for all segments, a sharp and sudden change is detected both by the strain measurements and the SSQ matrix values at minute 47.33, which corresponds to a load level of 24.65 kN. Slightly afterwards, the cracking initiation is detected by the silicone and cyanoacrylate segments (see Figure 14). The fiber broke very shortly after minute 50.17, which corresponded to a load of 31.1 kN.

Moreover, it is possible to also observe in Figure 16 that, apart from the silicone bonded DOFS segment, before minute 47.33 there are some segment points, which display a relative smaller SSQ

value than what is verified for the majority of the length of the fiber but also above the suggested 0.15 threshold. This happens close to the mid-span of the beam.

In the polyester and epoxy bonded segments it is seen how these SSQ values increase again during the unloading sequence of the beam before decreasing again with the second loading stage. However, in the cyanoacrylate bonded segment this recovery is not observed. Furthermore, it seems that although above the threshold of 0.15, in the later segment this drop of the SSQ values has an influence in the strain measurements since at this location the measured strain displays some incoherencies.

An additional take away from this analysis is that in the polyester, epoxy and cyanoacrylate bonded segments, the sudden decrease of the SSQ values in the post-cracking stage, is limited to the immediate whereabouts of the crack location and translates in extremely high strain peaks. On the other hand, in the silicone bonded segment, the area that corresponds to low SSQ values is relatively wider but with strain values within a reasonable range.

In an attempt to better assess the performance of the DOFS measurements after the occurrence of cracking, the authors decided to perform a post-processing routine where the DOFS data points corresponding to a SSQ value below 0.15 were removed. Moreover, after the conduction of this action, there were still some data points, which presented negative values. Naturally, this is not coherent to what is expected in a load test where the entire length of the bottom surface of the beam is in tension. This is due to the proximity of these points to the aforementioned inaccurate values (with SSQ lower than 0.15). In this way, these values are also removed in this routine. Finally, a surface interpolation is conducted replacing the removed data points. This is done along the same lines as the authors have conducted successfully in the past [6].

The results of this routine are depicted in Figure 17 and Figure 18, where the measurements between minute 45 and 50 of the load sequence are displayed. As it is possible to observe from these illustrations, considering the conditions mentioned above, the silicone bonded segment is the one presenting less inaccurate data and consequently having less removed measurements. For the other segments, especially due to the removing of negative strain measurements, more data had to be removed. This is then reflected in the interpolated data displayed in Figure 18, especially on the cyanoacrylate bonded segment.

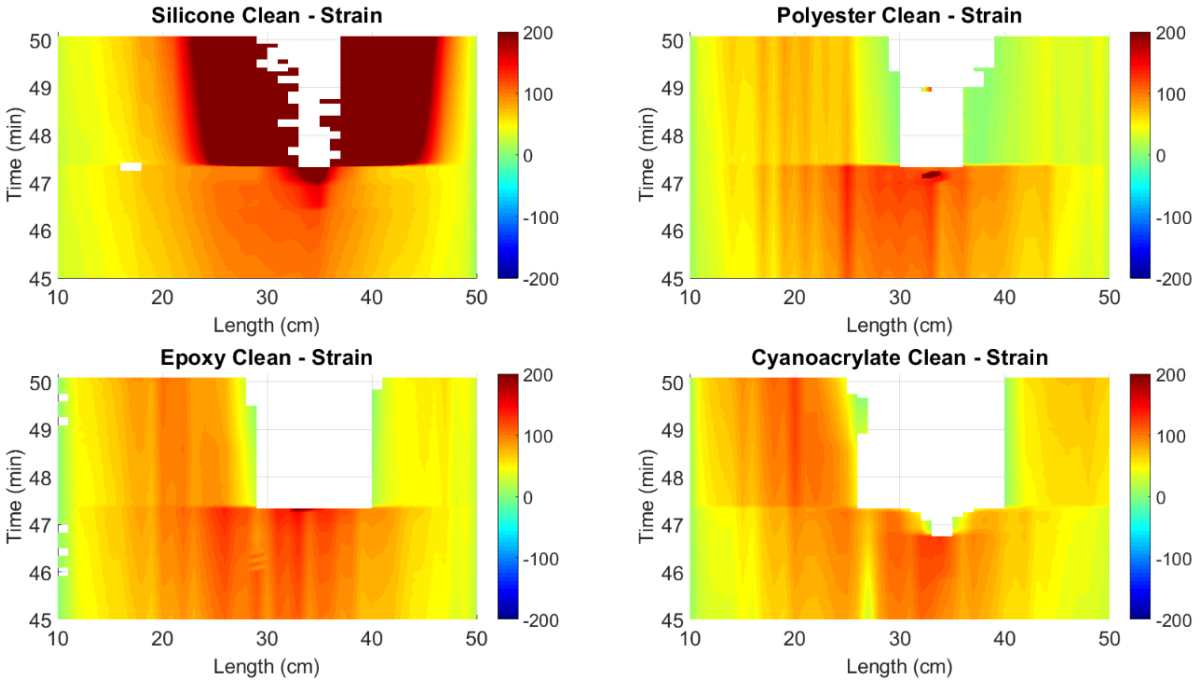

Figure 17. Cleansed DOFS data using SSQ values bellow 0.15 and negative strain

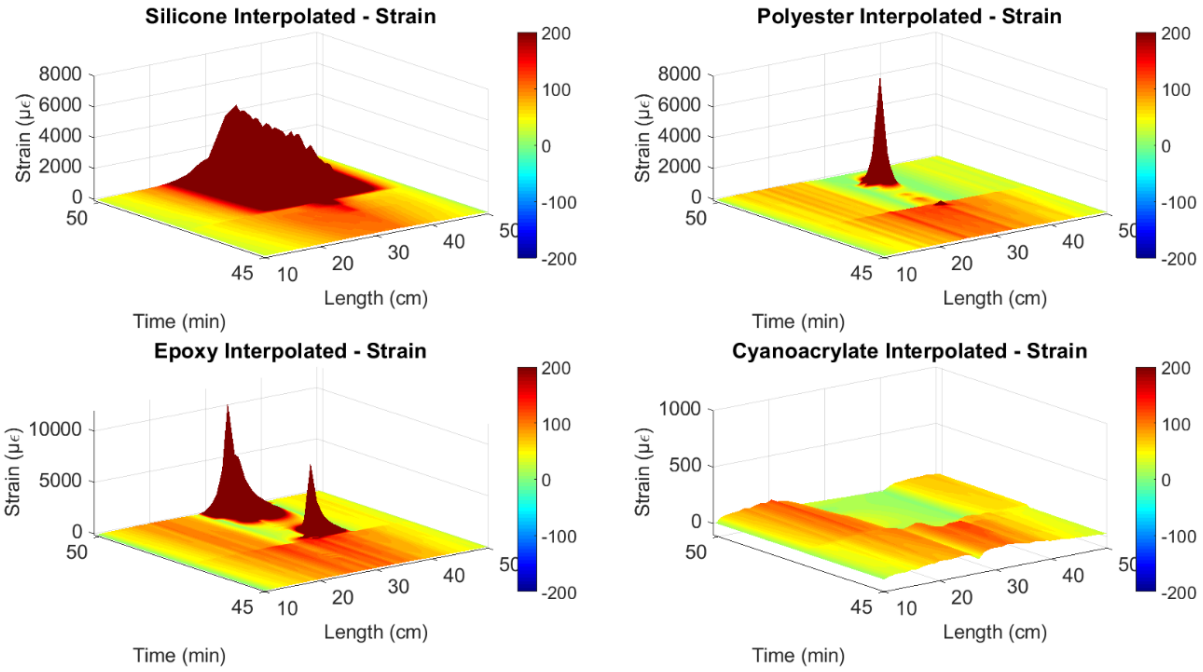

Figure 18. Interpolated strain data

In summary, it is observed a relative smoother performance of the neutral cure silicone during the elastic loading of the concrete beam. All bonded segments presented an acceptable agreement with the data collected from the strain gauges where the difference between both set of sensors was around the resolution of the used system of ±2 με.

When cracking appears, all segments are able to detect the formation of the crack. However, this is followed by a sharp decrease of the spectral shift quality (SSQ) at the location of the crack. Moreover, apart from the silicone segment, the measurements become erratic at this location of the beam until the

rupture of the fiber. By performing a post-processing routine where the data points corresponding to inaccurate or incoherent values are removed and replaced by interpolating the surrounding accurate data points, it is observed how the silicone segment displays information that is more reliable.

The authors are currently conducting a parallel study with the goal of identifying the possible causes of the drop of SSQ and will present further results in the future.

6. Conclusions

In this paper, an experimental campaign to assess the performance of different adhesives for the bonding of polyimide distributed optical fiber sensors in concrete surfaces was presented. Additionally, the influence of the spatial resolution of the DOFS used in the data acquisition was conducted as well.

A three-point load test was carried out on a reinforced concrete beam where a DOFS was bonded to the bottom surface with four segments using different adhesives. Initially, the beam is tested under elastic regime (un-cracked condition) and in second part, the beam is cracked and loaded up to failure.

The results show how the use of a spatial resolution of 1 mm, although theoretically better for an enhanced strain measurement presented an undesired high spatial variability due to the heterogeneity of the aggregates present in the concrete. This does not occur with a spatial resolution of 1 cm, which presented a good correlation with the data measured by the strain gauges.

Additionally, after performing a moving average of both the strain data acquired using a 1 mm and 1cm spatial resolution in order to directly compare it with the 3 cm measured strain, it was seen how the use of 1 cm resolution provided very similar results. In conclusion, the use of a spatial resolution of 1cm is suitable and recommended for this type of applications.

Moving forward to the comparison of the different used bonding adhesives, it was observed how in un-cracked condition, all segments compared fairly well with the data measured by strain gauges along the bottom surface of the concrete. Nevertheless, the silicone bonded segment presented a smoother and more uniform data than the other bonded segments. Therefore, if cracking is not foreseen, all adhesives can be used to obtain accurate and reliable results.

Afterwards, when the tensile capacity of the concrete was exceeded, it was verified how all the segments were able to detect and locate the crack formation. Notwithstanding, the associated SSQ values of the measurements quickly dropped below an acceptable threshold (0.15) shortly after this crack initiation in the whereabouts of the crack location. Therefore, the measurements at this location became erratic in all segments except for the silicone bonded one. Nevertheless, in this later segment the length influenced by the crack formation is relatively wider which compromises the detection on new possible cracks that can have origin in the immediate surroundings of the first detected one.

When removing and replacing the inaccurate and incoherent measurements and replacing them in an interpolation routine, the silicone bonded segment also provide the most realistic results.

Finally, it is important to mention the importance of the viscosity and time of curing of each of the adhesives used. In real and larger structural elements, these parameters are of great importance on the decision of the optimal adhesive for each particular application, which may sway the preference of one adhesive over another.

Acknowledgements: This project has received funding from the European Union's Horizon 2020 research and innovation programme under the Marie Sklodowska-Curie grant agreement No. 642453.

Conflicts of Interest: The authors declare no conflict of interest.

References

[1] P. Ferdinand, "The Evolution of Optical Fiber Sensors Technologies During the 35 Last Years and Their Applications in Structure Health Monitoring," in EWSHM-7th European Workshop on Structural Health Monitoring, **2014**.

[2] A. Barrias, J. Casas, and S. Villalba, "A Review of Distributed Optical Fiber Sensors for Civil Engineering Applications," Sensors, vol. 16, no. 5, p. 748, May **2016**.

[3] S. Villalba and J. R. Casas, "Application of optical fiber distributed sensing to health monitoring of concrete structures," Mech. Syst. Signal Process., vol. 39, no. 1, pp. 441–451, **2012**.

[4] G. Rodriguez, J. R. Casas, and S. Villalba, "Cracking assessment in concrete structures by distributed optical fiber," Smart Mater. Struct., vol. 24, no. 3, p. 35005, **2015**.

[5] A. Barrias, G. Rodriguez, J. R. Casas, and S. Villalba, "Application of distributed optical fiber sensors for the health monitoring of two real structures in Barcelona," Struct. Infrastruct. Eng., **2018**.

[6] A. Barrias, R. J. Casas, and S. Villalba, "Embedded Distributed Optical Fiber Sensors in Reinforced Concrete Structures—A Case Study," Sensors, vol. 18, no. 4. **2018**.

[7] M. Davis, N. A. Hoult, and A. Scott, "Distributed strain sensing to determine the impact of corrosion on bond performance in reinforced concrete," Constr. Build. Mater., vol. 114, pp. 481–491, **2016**.

[8] R. Regier and N. A. Hoult, "Concrete deterioration detection using distributed sensors," Proc. Inst. Civ. Eng. Build., vol. 168, no. 2, pp. 118–126, **2015**.

[9] S. T. Kreger, D. K. Gifford, M. E. Froggatt, B. J. Soller, and M. S. Wolfe, "High resolution distributed strain or temperature measurements in single-and multi-mode fiber using swept-wavelength interferometry," in Optical Fiber Sensors, **2006**, p. ThE42.

[10] LUNA, "Fiber optic sensing," **2014**.

[11] Luna Innovations Incorporated, "High-Definition Fiber Optic Strain Sensors." **2016**.

[12] F. Ansari and Y. Libo, "Mechanics of bond and interface shear transfer in optical fiber sensors," J. Eng. Mech., vol. 124, no. 4, pp. 385–394, **1998**.

[13] K. T. Wan, C. K. Y. Leung, and N. G. Olson, "Investigation of the strain transfer for surface-attached optical fiber strain sensors," Smart Mater. Struct., vol. 17, no. 3, p. 35037, **2008**.

[14] J. M. Henault, J. Salin, G. Moreau, M. Quiertant, F. Taillade, K. Benzarti, and S. Delepine-Lesoille, "Analysis of the strain transfer mechanism between a truly distributed optical fiber sensor and the surrounding medium," in Concrete Repair, Rehabilitation and Retrofitting III: 3rd International Conference on Concrete Repair, Rehabilitation and Retrofitting, ICCRRR-3, 3-5 September 2012, Cape Town, South Africa, **2012**, p. 266.

[15] R. Regier, "Application of fibre optics on reinforced concrete structures to develop a structural health monitoring technique," Canadian theses, **2013**.

[16] G. Rodríguez, J. R. . Casas, S. Villalba, and A. Barrias, "Monitoring of shear cracking in partially prestressed concrete beams by distributed optical fiber sensors," in Proceedings 8th International Conference on Bridge Maintenance, Safety and Management, IABMAS 2016, **2016**.

[17] TML, "TML STRAIN GAUGES 2017." Tokyo Sokki Kenkyujo Co., Ltd., **2017**.

[18] J. R. Pedrazzani, S. M. Klute, D. K. Gifford, A. K. Sang, and M. E. Froggatt, "Embedded and surface mounted fiber optic sensors detect manufacturing defects and accumulated damage as a wind turbine blade is cycled to failure," Luna Innov. Inc, **2012**.

[19] Luna Innovations Incorporated, "ODiSI-A Users Guide," Blacksburg, VA, **2013**.

Journal Article V

Fatigue performance of distributed optical fiber sensors in reinforced concrete elements

Submitted to Smart Structures and Systems in August 2018

António Barrias [1], Joan R. Casas [1] and Sergi Villalba [2]

[1]Department of Civil and Environmental Engineering, Technical University of Catalonia (UPC), c/ Jordi Girona 1-3, 08034 – Barcelona, Spain

[2]Department of Engineering and Construction Projects, Technical University of Catalonia (UPC), c/ Colom 11, Ed. TR5, 08022 – Terrassa (Barcelona), Spain

Abstract: In this paper, the authors present the results of a laboratory test where two reinforced concrete beams were instrumented with Distributed Optical Fiber Sensors (DOFS) to allow the monitoring g of strain in four different longitudinal segments bonded to their bottom surface. The test objective was to confirm the ability and good performance of the DOFS to monitor bridge structures in a long-term basis. To this end, the two specimens were submitted to a fatigue test up to 2 million load cycles. The amplitude of the stress range applied during the fatigue test was representative of what is expected on a standard highway bridge under vehicular traffic. Additionally, each of the four DOFS segments was bonded using a different adhesive to also investigate on the fatigue performance of the adhesive agents normally used. Finally, the collected data is checked against the data recorded with strain gauges also deployed on the beam specimens.

Keywords: Distributed optical fiber sensors, Rayleigh backscatter, structural health monitoring, sensor bonding, fatigue, cycle-loading

1. Introduction

All civil engineering infrastructures are subjected to the passage of time and its associated decay as well as a number of different external adverse effects, which compromises their structural integrity, causes important economic losses, severe environmental impact and finally affects the safety of their users. As of 2016, in the United States alone, 39% of the highway bridges in the National Bridge Inventory were older than 50 years and 9,1% of the total number of bridges were considered structurally deficient. As a result, an average of 188 million trips were performed daily across these structurally deficient bridges and the most recent estimate projects the backlog of rehabilitation projects for these infrastructures at $123 billion [1].

It is therefore of paramount importance to properly monitor and maintain these infrastructures by the deployment of effective and adequate management strategies that optimize their use and extend their lifetime service. It is in this context that the field of Structural Health Monitoring (SHM) has been researched and developed during the past decades. Nonetheless, SHM has not been practiced in a large scale and in a systematic manner quite yet in civil engineering structures, mostly due to the lack of reliable and affordable generic monitoring solutions [2].

Traditionally, monitoring practices have been conducted by means of visual inspections and through the use of a limited number of electric based sensors such as accelerometers, inclinometers, displacement transducers and strain sensors. All of these techniques present different challenges when applied in real world conditions [3].

It is in this way, that optical fiber sensors (OFS) have been one of the most popular research topics within SHM practices in the last two decades. These type of sensors when compared with the conventionally used electrical sensors provide the enhanced advantages of being immune to electromagnetic interference, withstanding wide range of temperature variations, chemically inert and also being small and lightweight which facilitates its handling and transport [4]. As of today, the most popular applications of this technology have been made through the use of discrete or quasi-distributed Fiber Bragg Grating (FBG) sensors [5].

Nevertheless, for a wide range of applications, especially when dealing with large-scale infrastructures, the number of point sensors that are required in order to obtain a complete strain information monitoring can increase dramatically. Additionally, for the specific case of concrete structures, where it is practically impossible to know beforehand with certainty the exact location of possible crack formations, these point sensors present obvious limitations. If the instrumented point sensors are not properly located, important data is going to be absent from the sensors' acquired data. Furthermore, looking into the logistics and more practical side of these applications, a large number of sensors also present the difficulty of requiring an associated large number of connecting cables making the full monitoring system more complex.

Distributed optical fiber sensors (DOFS) overcome this by providing distributed strain and temperature measurements with the unique advantage of doing so over the entire length of the optical fiber cable while sharing the same advantages of the other optical fiber sensors. In this way, virtually every cross-section of the structural element is being monitored while only requiring up to one single sensor and one corresponding connecting cable.

These sensors can be either bonded or embedded into the monitored structure and when strain or temperature variations occur, the scattered signal being reflected within the fiber cable is proportionally altered and in this way distributed sensing is achieved. This is the phenomenon behind this distributed optical fiber sensing as defined by the interaction between the emitted light and the physical optical medium. There are three types of scattering processes which allow for distributed sensing, namely Raman, Brillouin and Rayleigh scattering [6].

The Brillouin scattering based DOFS have been the most used and researched among the distributed sensors practiced in civil engineering SHM applications due to the large-range capability of several kilometers provided by these type of sensors. Nonetheless, as being deployed mostly using optical time domain reflectometry (OFDR), this scattering technique inherently provides a relatively low spatial resolution of 1 m, which is not acceptable for numerous applications, including crack detection in reinforced concrete elements.

On the other hand, Rayleigh scattering based DOFS, which uses optical frequency domain reflectometry (OFDR), enable an intrinsic higher spatial resolution, which can be as high as one millimetre being in this way suitable for damage detection and location. Notwithstanding, it currently presents a significantly lower range of 70 m although this is expected to be greatly enhanced in the near future.

Consequently, this later is the scattering technique being researched by the authors in reinforced concrete elements SHM applications, through the use of an optical backscattered reflectometry (OBR) system based on the aforementioned Rayleigh OFDR. This technology is presented in greater detail in [6], [7].

2. Fatigue load test: motivation

Despite successful and promising applications where distributed optical fiber sensing technology based on Rayleigh scattering OFDR was used [8]-[10], due to its relatively novelty there are still several important challenges regarding its use in the monitoring of civil engineering infrastructures.

Several aspects still present some uncertainties and lack of knowledge that must be addressed before a more reliable use and wider application could be foreseen. This is, for instance, the case of the bonding techniques to different surfaces (concrete, steel) and the most appropriate bonding agents, where important developments were achieved recently [11], [12]. However, a still open issue is the

performance of these sensors regarding the accuracy and reliability of the measurements over time when monitoring real world structures during long-term periods.

Actually, to the author's knowledge, very few publications can be found regarding the performance of Rayleigh based OFDR DOFS under fatigue loading. One of this few cases is an engineering note from LUNA Innovations Incorporated, [13]. In this document, is described an experiment where polyimide coated distributed DOFS were instrumented to fiberglass coupons and subjected to a ± 2000 με and ± 4000 με cyclic load for 1000 cycles each. The fiber sensors were interrogated by their ODiSI B model. The results revealed a superior performance of the distributed optical fiber sensors when compared with resistive gauges since the applied DOFS survived the fatigue tests and demonstrated consistency in their strain measurements through the end of the test in opposition to what was verified on the also instrumented resistive strain gauges' measurements. These later sensors presented displayed cumulative zero-shift in microstrain from an early period of the fatigue test, which just increased in magnitude throughout the test cycle.

Another publication from the manufacturers of the ODiSI system reported on the use of polyimide-coated, low-bend-loss fibers embedded in four layers of a carbon fiber spar cap and surface of a 9 m CX-100 wind turbine blade [14]. The DOFS were used to detect and monitor intentionally introduced defects in the blade and follow the accumulated damage that resulted from these defects with the blade under fatigue loading until failure. The results of the fiber sensor displayed clear evidence of the increasing strain around the defect locations and were able to predict the failure location. Moreover, the DOFS compared well with also instrumented electric foil gauges.

More recently, Wong et al, 2016 described the use of also a similar Rayleigh based OFDR distributed sensors to monitor the fatigue in a flush step lap joint composite structure used in aerospace engineering [15]. This publication demonstrated that it was possible to monitor the fatigue damage propagation until failure with the used DOFS being also able to follow the crack propagation due to the fatigue loading.

All the previous experiences apply to composite elements, where surface characteristics of the material which may highly affect the fatigue response are completely different from the case of concrete elements. Consequently, the authors decided to perform a study to assess the fatigue performance of this technology when applied to reinforced concrete structures. An experimental campaign was devised where a fatigue test was performed on Rayleigh based DOFS instrumented reinforced concrete beams where the load reprised expected real world conditions for the case of highway bridges. As far as the authors know, this is the first time that this subject has been investigated. The devised experimental campaign is introduced and described in the following section.

3. Experimental test setup

Two concrete beams were casted, beam FA1 and beam FA2. These beams had identical properties and geometry and were characterized by having a 600 mm length and a square cross-section of 150 mm width by 150 mm height, Figure 1. As depicted in this figure, the reinforcement of each specimen was constituted by two longitudinal ϕ12 rebars and four ϕ6 stirrups of S500 grade steel.

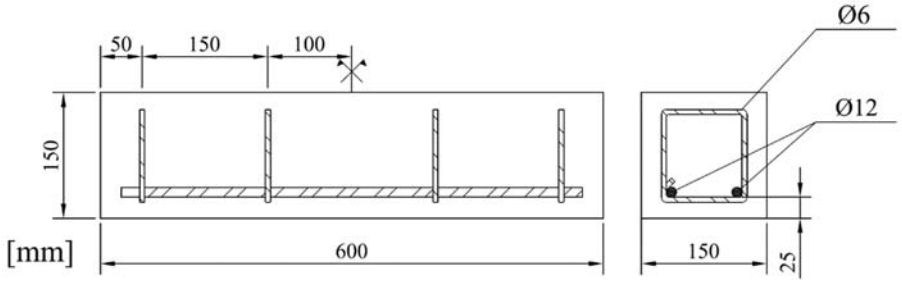

Figure 1. Beam definition scheme (All dimensions in mm)

In each of the specimens, it was adhered a 5.2 m long polyimide DOFS performing a pattern with three horizontal segments in its lateral surface and four equal horizontal segments in its bottom surface, Figure 2 and Figure 3. Notwithstanding, for the purposes of this paper, only the collected data from the four bottom surface bonded segments are considered.

As an additional point of study in this experiment, four different adhesives were used to attach each of the four segments to the bottom surface of the concrete beams, namely neutral cure silicone, polyester, epoxy and cyanoacrylate. This arrangement was the same for both tested beam specimens.

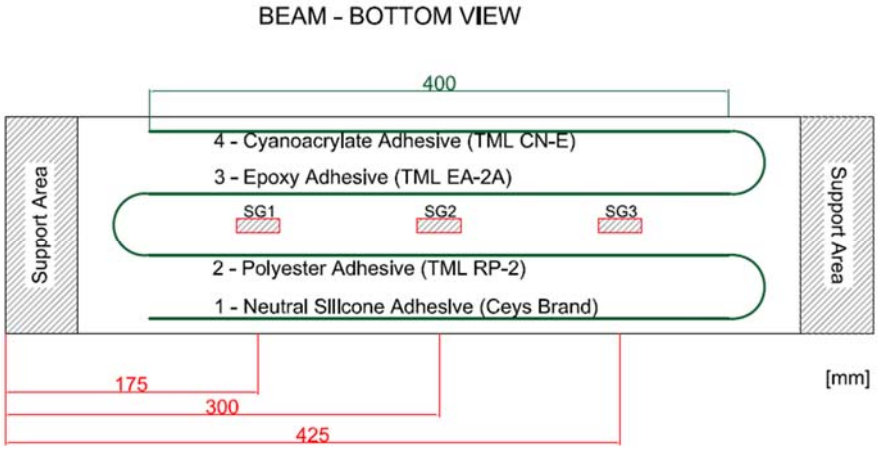

Figure 2. Definition of the sensors attached to the beams and adhesives used

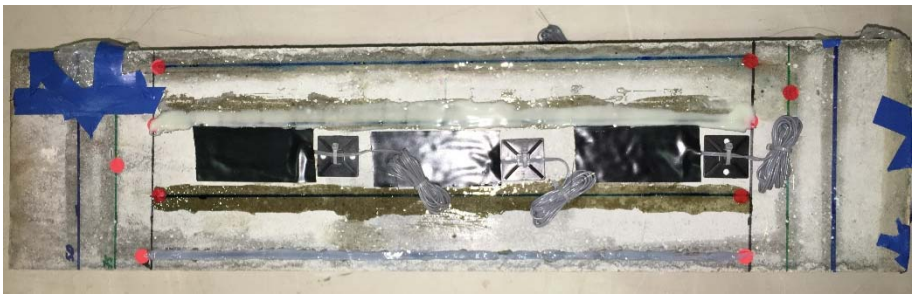

Figure 3. Photograph of the bottom surface of one of the beams with the DOFS and strain gauges

Furthermore, three 30 mm length electrical strain gauges (SG1, SG2 and SG3) from Tokyo Sokki Kenkyujo Co., Ltd were also attached to the bottom surface of each beam as seen from Figure 3 and Figure 4 for comparison purposes with the DOFS data. As the specimens were loaded using a three-point bend test configuration, the measurements obtained by each segment of the DOFS could be directly compared between them and the three strain gauges. A displacement transducer (LVDT) was also deployed at mid-span to follow the deflection of each beam.

At the time of the production of beams FA1 and FA2, in order to obtain the mechanical properties of the concrete, additional cylindrical samples were also produced. These samples were tested close to the date of the load test on the beams. Therefore, the mean compressive strength (f_{cm}), the mean tensile strength (f_{ctm}) and the mean Young modulus of the concrete (E_c) were obtained. With this, the expected strain where cracking is expected to occur (ε_{ct}) was also obtained, as shown in Table 1.

Table 1. Concrete mechanical properties

Properties	f_{cm} **[MPa]**	f_{ctm} **[MPa]**	E_c **[MPa]**	ε_{ct} **[με]**
Concrete	48.027	3.944	37886.64	104.1

As mentioned above, the goal was to subject the specimens to a stress range that would closely replicate the real world conditions observed in a standard highway bridge due to vehicular loads. As a result, for the load input and stress range calculation, the reinforced concrete bridge depicted in Figure 4 was assumed.

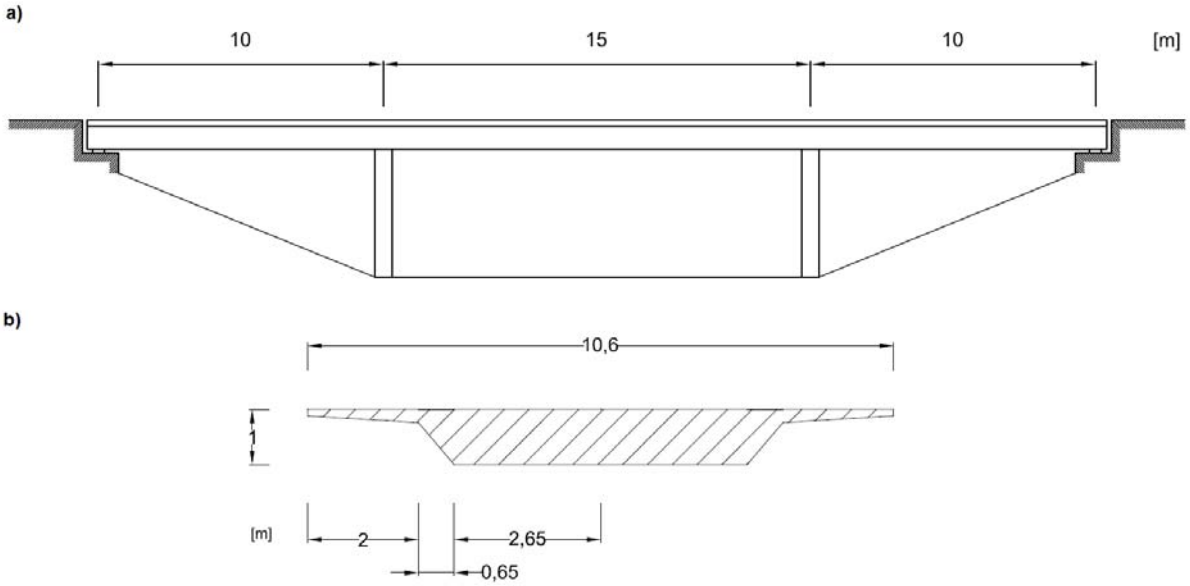

Figure 4. Standard bridge dimensions assumed for the calculation of the load cycles range input – a) elevation; b) cross-section

In this way, two different load stages were considered for the stress range of the load cycles. The lower stress limit reproduced the sole actuation of the structure's self-weight and permanent loads. The upper stress limit was calculated by adding the traffic load as defined in the live load model to the lower limit. As we were dealing with a fatigue problem, the assumed additional load traffic relevant for fatigue was represented as a four-axle truck with a load of 120 kN by axle and multiplied by a dynamic factor of 1.3 as described in Fatigue Load Model 3 of EN 1991-2 [16].

Table 2. Lower and Upper limits for load cycle range

	Load combination	**Maximum bending moment [kN.m]**	**σ [MPa]**	**Equivalent load to apply to beam specimen [kN]**	**Expected strain [με]**
Load Cycle Level [inf]	permanent load	3712.9	2.612	11.75	68.9
Load Cycle Level [sup]	permanent load + additional traffic	4336.3	3.050	13.73	80.5

As a result, the considered minimum and maximum load levels and corresponding stress range and the load to be inputted in the fatigue test is described in Table 2.

The cycling load was introduced with a frequency of 4 Hz and with a sinusoidal profile until reaching 2 million cycles. The frequency was defined such to simulate as much as possible real conditions in concrete bridges when traffic is crossing through. As deduced from tables 1 and 2, the applied load cycles were not expected to generate strains higher than the tensile cracking strain ε_{ct}.

The difference between both beams was that beam FA1 was loaded directly to the 2 million cycles in an un-cracked condition, whereas in beam FA2 the specimen was initially loaded statically until 28 kN (inducing cracking), then unloaded and only afterwards loaded with 2 million cycles identical to beam FA1. The objective was to analyse the fatigue performance in both un-cracked and cracked concrete, simulating the cases where the DOFS will be bonded to prestressed (no cracking) or reinforced (cracking) concrete bridges.

A spatial resolution of 1 cm was selected, what implied an acquisition of strain data from 520 different points along the fiber. It was also defined a sampling acquisition frequency of 0.2 Hz for the DOFS and 1 Hz for the strain gauges and load cell information. Finally, due to the extensive duration of the test and the large amount of collected data, the DOFS's measurements were stored for a duration of 5 minutes (1200 load cycles) every 50 thousand cycles. A photo of each tested beam specimen is depicted in Figure 5.

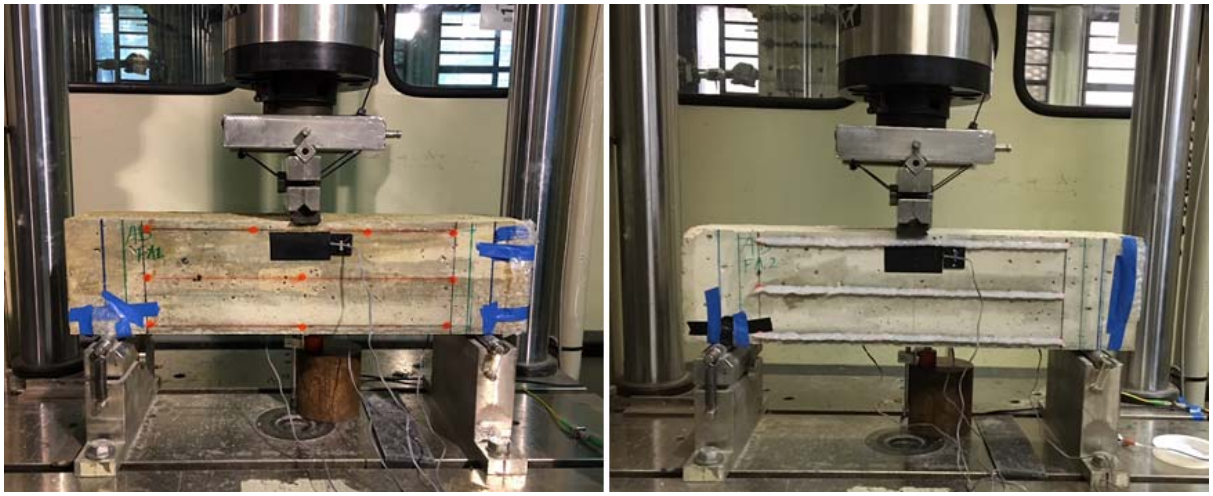

Figure 5. Load arrangement – beam FA1 (left) and beam FA2 (right). The segments of interest for the fatigue analysis are in the bottom surface and cannot be seen in this figure

4. Discussion of Results

The duration of each fatigue test was around 6 days. Afterwards, the collected data was processed and analysed. The results are presented and discussed in the following sections.

4.1. Beam FA1

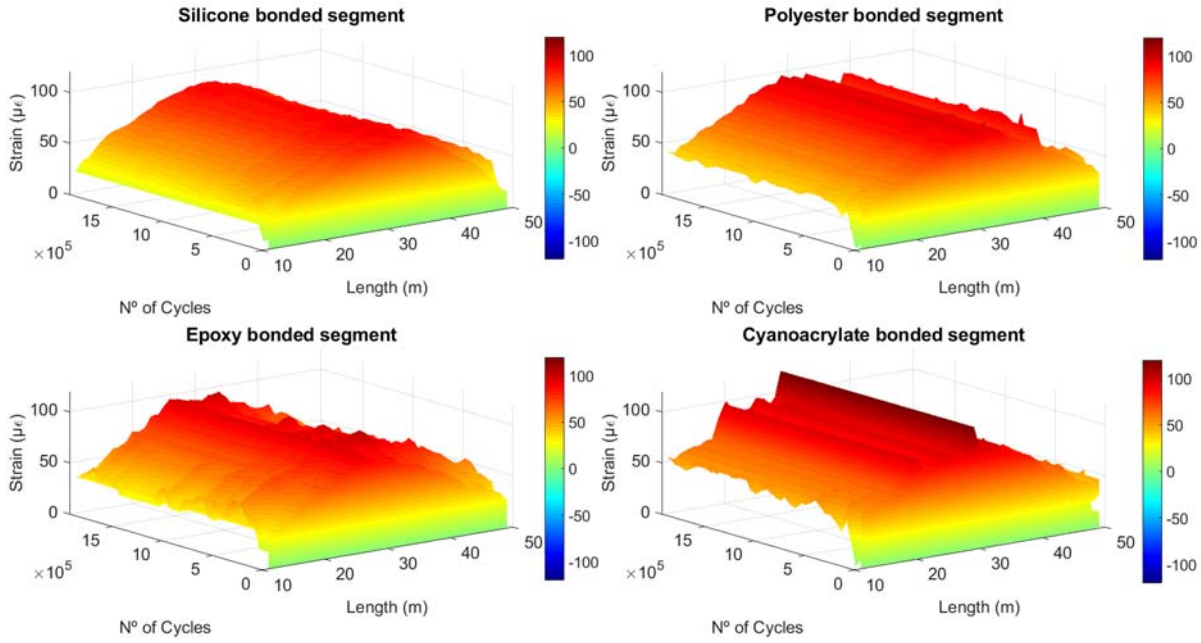

Figure 6. Strain measured by type of bonded segment over the number of load cycles

When analysing the results of this beam, it is important to mention that during the execution of the load test there was an electrical power shut-off which occurred at the 180664 cycles mark. Afterwards, the test resumed from this point and continued smoothly until it was intentionally stopped shortly after 1,925,000 cycles. This was due to logistic reasons, which didn't allow for the completion of the total number of 2 million cycles as intended.

In Figure 6, it is possible to observe the DOFS' measured strain over the performed number of load cycles and over the bonded length of the DOFS for each adhesive type segment located at the bottom surface of the tested beam. Here it is seen how the different DOFS segments were able to follow the developed strain over the cycling load with different levels of stability. Moreover, it is observed how, in general, the silicone bonded segment presents smoother distributed readings when compared with the other deployed adhesives especially when compared with the cyanoacrylate one. This behaviour was also observed in other tests carried out by the authors [11], [12].

Figure 7 summarizes and compares the results obtained by the DOFS and the strain gauges in the centre of the beam, while also plotting the measured displacement at mid-span.

In this figure, it is observed how several interesting events occurred in the first 200k cycles. The measured displacement by the LVDT was progressively increasing, for the same applied load range, from 0.164 mm to 0.182 mm in the first 50k cycles, suggesting an adjustment of beam supports during

this period. SG2 and the DOFS' segments also reveal some atypical strain readings during this time period.

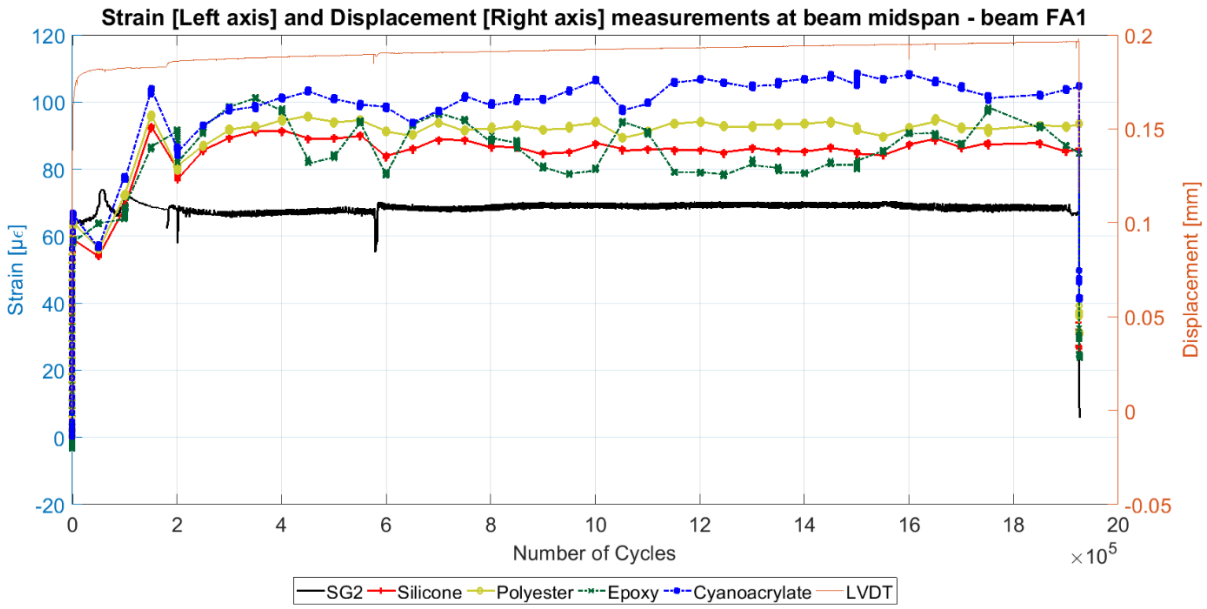

Figure 7. Measured strain and displacement at beam FA1 mid-span over the applied load cycles

It is also observed how all set of sensors seemed to have been affected by the occurrence of the electrical shut off, which occurred around the 180k cycle mark. Close to the 600k cycles mark it is also seen some atypical readings from SG2, which are then quickly recovered.

Finally, and in the context of the goals of the present study, in Figure 7, it is seen how between the 100k and the 150k cycle, the readings from the DOFS segments diverge substantially from what is observed in the strain gauge without any apparent reason, being then sustained and maintained until the end of the load test.

Moreover, this divergence is also observed for the entire length of the deployed DOFS, including the parts of the fiber that are not bonded to the beam, thus discarding any possible influence of a mechanical event. This shift is plotted for the initial unbonded part of the DOFS and for the referred cycles points in Figure 8.

As it is seen in Figure 8, there is a global divergence in the unbonded segment from the first measurements until the 150k cycle mark. On the next DOFS cycle measurement, after the occurrence of the electrical shut off at 180k, which corresponds to the 200k cycle mark, the aforementioned divergence disappears. However, for the remaining bonded parts of the deployed fiber the new measurements after the 200k cycle the shift still remains.

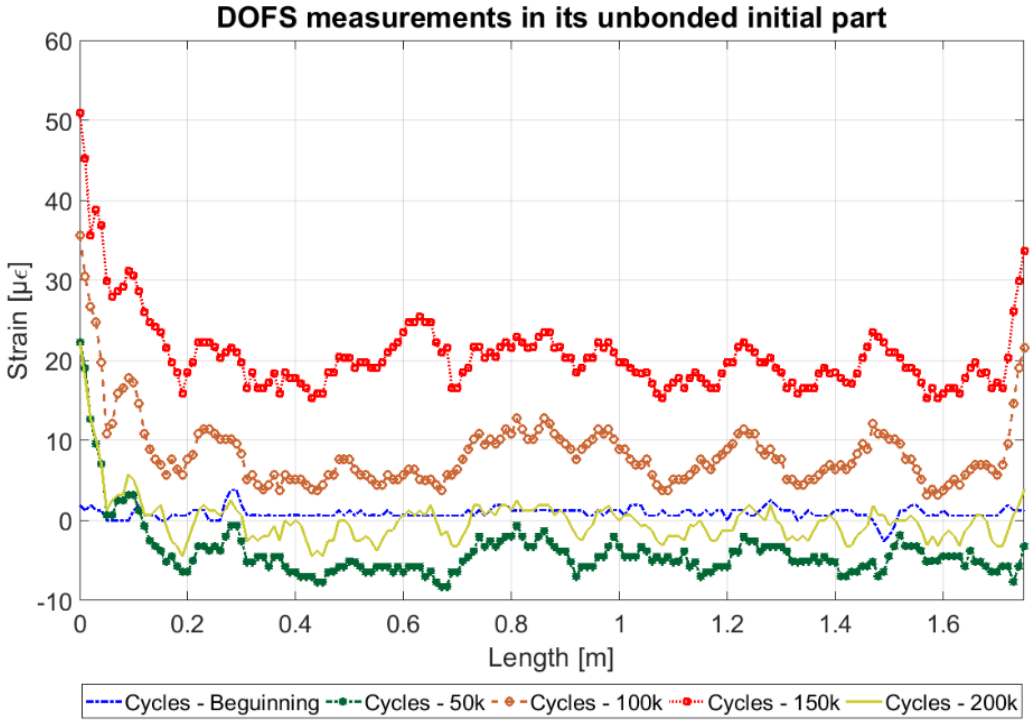

Figure 8. Observed shift of the DOFS measurements observed in its unbonded initial segment

When plotting the longitudinal measured strains by the different bonded DOFS segments at the beginning and end of the applied load cycles jointly with the measurements obtained through the strain gauges, Figure 9 is obtained.

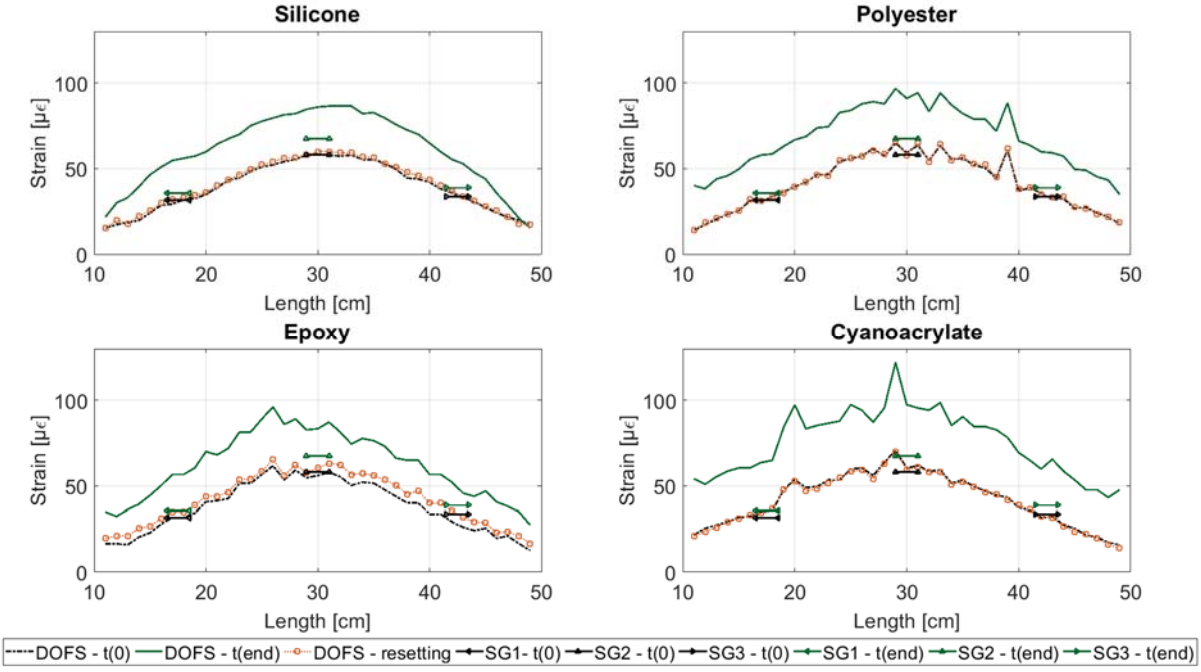

Figure 9. DOFS and strain gauges measurements at the beginning and end of the fatigue test

Here, we can see again how, although both set of sensors agree very well at the beginning of the load cycles, a significant disparity appears at the end. Furthermore, after the end of the load test and the unloading of the specimen (removing of the load representing the permanent state), residual strain

measurements remain present in the DOFS. In Figure 9, it is also plotted the result of subtracting this final residual measurement to the readings at the end of the load cycles (DOFS – resetting). In this case, it is observed how the values from the DOFS match almost perfectly the measurements at the beginning of the load cycles and the values from the strain gauges.

The divergence of the measured data observed for the initial unbonded segment of the DOFS before the occurrence of the electrical shut-off at the 180k cycles mark is responsible of the detected difference between the DOFS measurements and the strain gauges.

In this sense, by calculating the average measured values in the initial unbonded segment of the DOFS (between DOFS length coordinate 0.05m and 1.60 m – Figure 8) before the occurrence of the electrical shut-off and subtracting this value to the remaining measured data of the DOFS, the aforementioned shift is eliminated. This is shown in Figure 10, where after the shift correction is possible to notice how the DOFS measurements better follow the strain gauge with appropriate stability along the number of cycles.

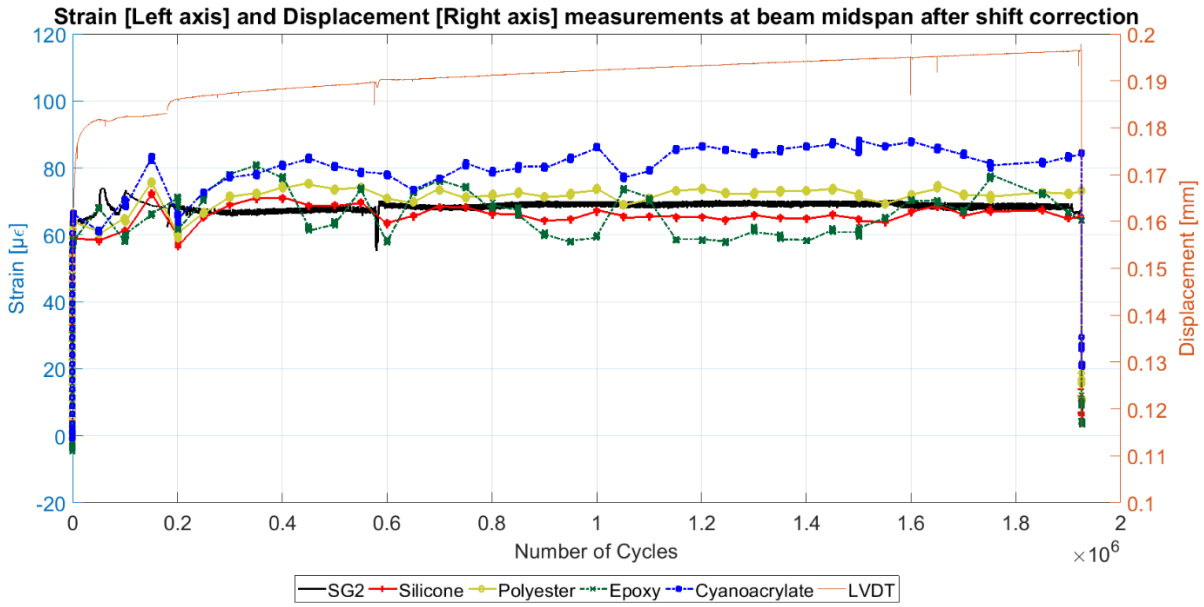

Figure 10. Measured strain and displacement at beam FA1 mid-span over the load cycles after the shift correction

When comparing the results in Figure, it is important to remember that the frequency of the cycling load is 4 Hz, while the sampling rate of the acquisition system of the DOFS is of 1 measurement every five seconds and 1 Hz for the strain gauges. The data was recorded every 50 thousand cycles. Therefore, it was not guaranteed that when recording a result, the strain value obtained in the DOFS coincides at the same point of the sinusoid profile of the load as the strain gauge. A maximum difference in the order of magnitude of the applied strain range (around 12 microstrain) is feasible and this is in accordance to what is seen in Figure, since the differences between DOFS and strain gauge measurements are somewhat within this range.

4.2. Beam FA2

Regarding beam FA2, it was initially and intentionally pre-cracked and only afterwards subjected to the application of two million load cycles with the same load range as beam FA1 and described in Table 2. With this, it was intended to assess the fatigue behaviour of the DOFS measurements when deployed in an existing reinforced concrete structure that may present cracking during its lifetime.

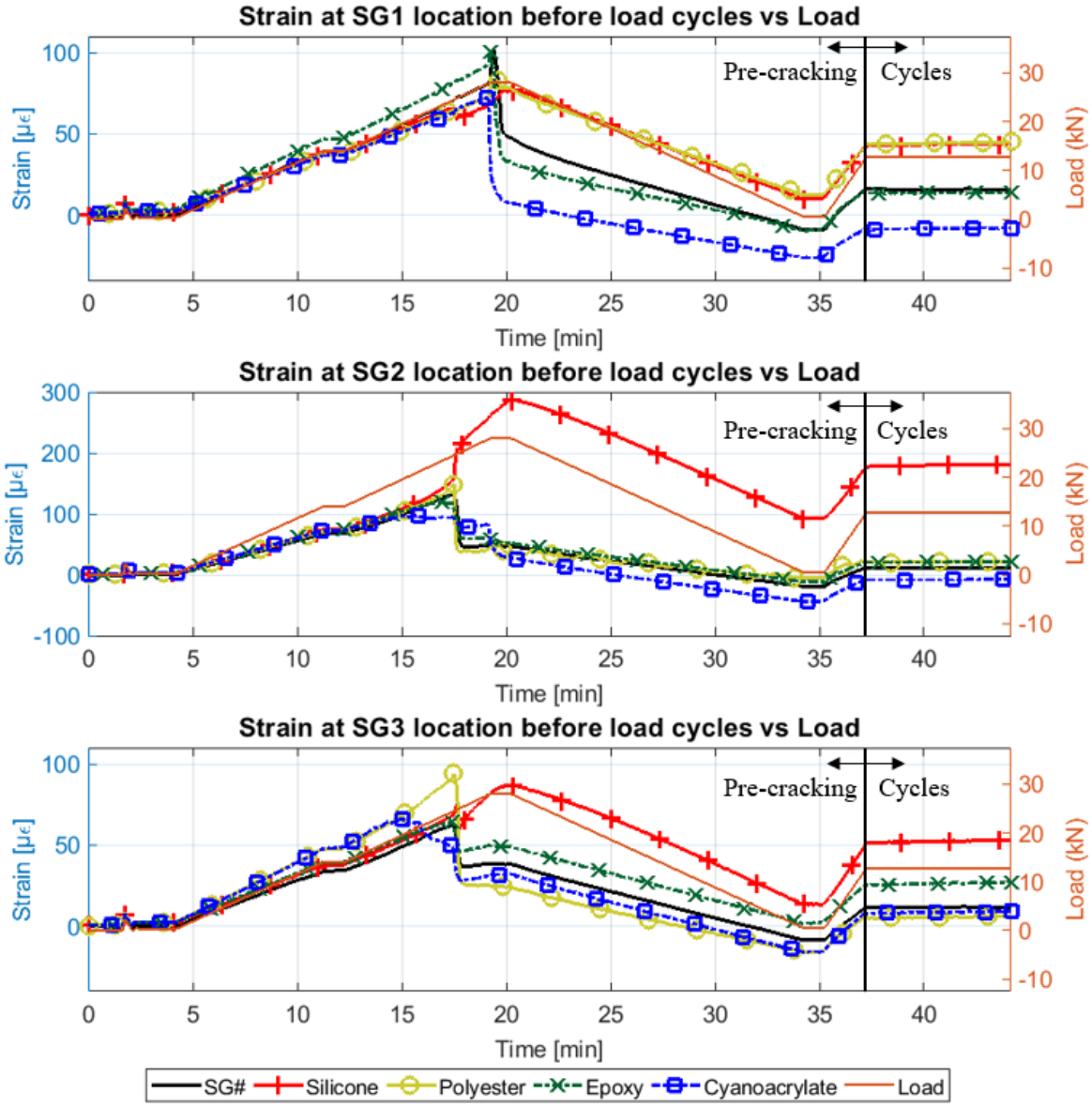

Figure 11. Measured strain vs applied load at SG locations in FA2 pre-cracking stage

In this way, in Figure 11 is depicted the measured strain in the three strain gauges and the corresponding positions of the different bonded DOFS segments for the pre-cracking stage while also plotting the applied load using the right y-axis. It becomes evident how the measurements in the strain gauges are affected by the cracking.

The corresponding measurements by the DOFS at the same locations as the strain gauges display a general good agreement with them, especially at the beam midpoint, (SG2 location) until cracking is

initiated. Cracking is first detected by the cyanoacrylate bonded DOFS segment around minute 15 and then detected by the rest of DOFS segments and SG2 and SG3 at minute 17.5 for a load of 24.67 kN.

As seen in Figure 11, cracking is located between SG2 and SG3 as detected by the different DOFS bonded segments.

Furthermore, after the cracking detection it is seen in Figure 12 how all DOFS bonded segments and strain gauges measurements follow with more or less agreement the applied load until the beginning of the 2 million load cycles application. However, it is observed how after the pre-cracking stage and unloading stage (minute 35 in Figure 12) the strain measurements slightly diverge between the different DOFS segments and the strain gauges this is possibly due to strain redistribution in the element after cracking.

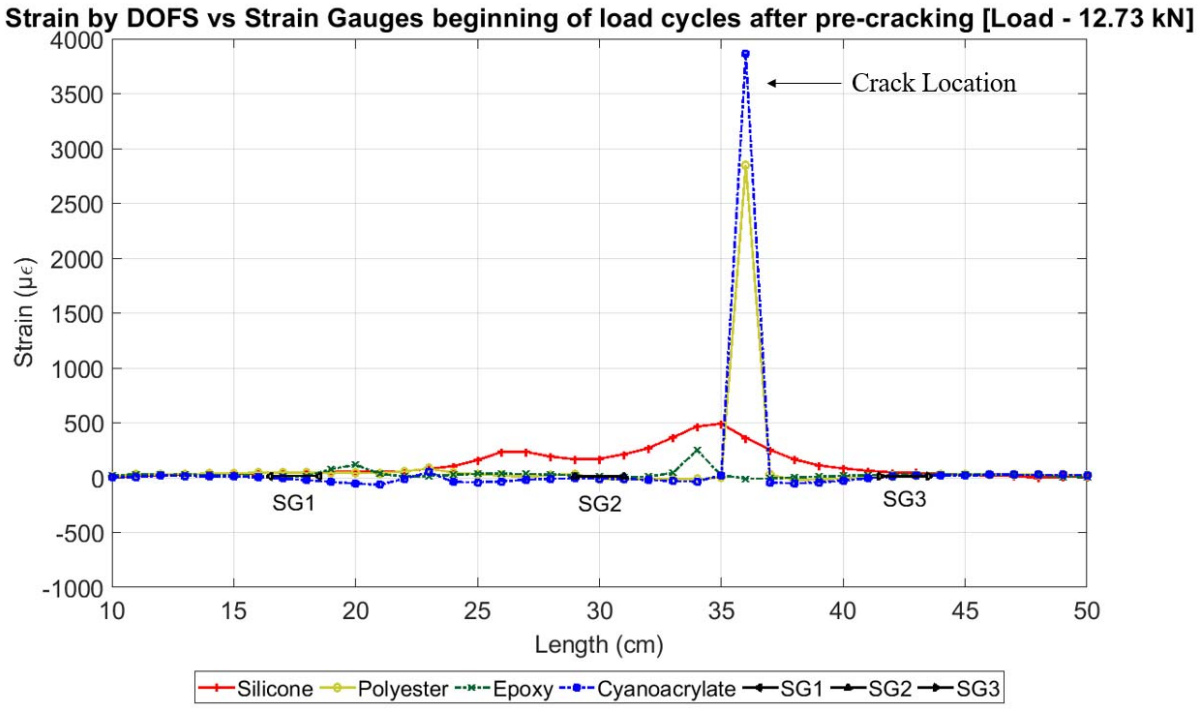

Figure 12. Cracking detection and location at the beginning of the load cycles

In this way, in order to better assess the DOFS performance over the course of the applied number of load cycles, the strain measurements are reset at minute 35 that corresponds to the unloaded stage of the beam after cracking. In Figure 12, due to the scale of the measured strain at the crack location, the measured data of the strain gauges is almost imperceptible; therefore, their location is further highlighted.

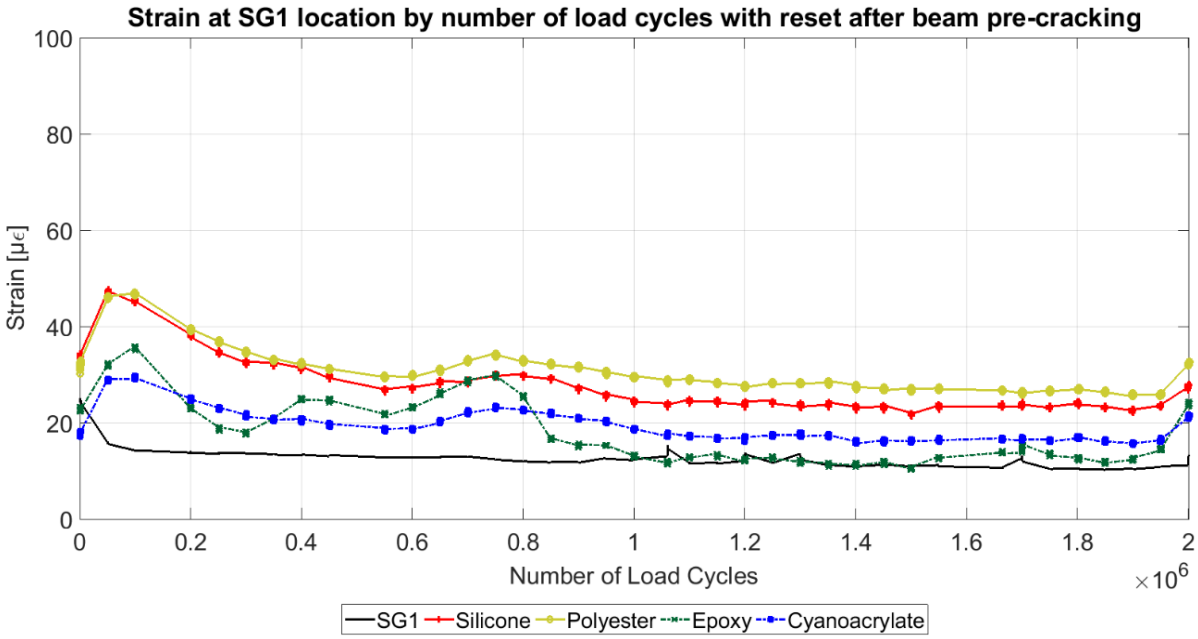

Figure 13. Comparison of strain measurements at SG1 location over load cycles

Moreover, since as seen in Figure 12, cracking is located between SG2 and SG3, to better compare both sets of strain sensors this is done at the SG1 location, as far as possible, from the cracking location to neglect its influence in the strain measurements. This is shown in Figure 13.

The DOFS measurements agree reasonably well with the data obtained by the strain gauges. After a small initial variation within the first measured 50k cycles, despite some small fluctuations, all segments present a stabilization of their measurements The observed difference between both set of sensors is more relevant for the DOFS using silicone and polyester and almost negligible for epoxy and cyanoacrylate. The differences are, as in the case of beam FA1, related with the system strain resolution (± 2 με), different sampling rates in the acquisition systems and strain range due to the amplitude of the load cycles (12 με).

5. Conclusions

In this paper, the performance of DOFS when deployed in reinforced concrete elements subjected to fatigue load was assessed. Two reinforced concrete beams (FA1 and FA2) were instrumented with a 5.2 m long polyimide DOFS as well as three strain gauges. Moreover, four different types of adhesives were used to bond the DOFS to the bottom surface of the beams in order to analyse the quality of the corresponding measurements. The beams were subjected to 2 million load cycles with a stress range representative of actual fatigue loading because of traffic in standard highway bridges.

In beam FA1, which was fatigue loaded in un-cracked state, the results show that the DOFS measurements agreed reasonably with what was expected and measured by the strain gauges as well and for all adhesives tested. The measured differences, in the order of magnitude of 12 microstrains are due to the different sampling rates used in the two sets of sensors, the frequency of the load and the

resolution of the two types of sensors. However, the results show good stability along the number of cycles and no malfunction due to fatigue effects can be observed.

In beam FA2, which was intentionally pre-cracked before the fatigue test, it was observed how after cracking the DOFS continued to provide strain measurements coherent with the applied load. These values were, however, different depending on the bonding agent used in the DOFS segment and also different of the readings from the strain gauges. In the stage of static load application, before the start of the fatigue test, the best match of the DOFS with the values from the strain gauges is obtained with the epoxy, cyanoacrylate and polyester, whereas the worst is in the DOFS segment bonded with silicone. Afterwards, during the fatigue test, the best performance is obtained for the epoxy and cyanoacrylate adhesives, whose measurements matched perfectly with those from the strain gauges. Larger differences, in the order of 20 microstrains were observed for the other 2 bonding agents. However, in all cases the measurements showed a good stability along the number of cycles, indicating no fatigue failures or debonding in the fibre or the adhesive.

In this way, this test provided encouraging results regarding the use of this novel technology in real world applications for long-term monitoring periods when a high number of load cycles with low stress range are seen by the monitored concrete structure. The DOFS showed a good performance under fatigue loading, without malfunctions for a number of cycles up to 2 million. The strains measured along the tests were accurate when compared to the results obtained with strain gauges, with good stability and both for the un-cracked and cracked conditions. Therefore, fatigue loading does not affect the performance of the DOFS for obtaining strain profiles along their length. Notwithstanding, it would be interesting in the future to conduct similar tests on larger RC beam specimens and also with higher stress ranges. In order to better compare with the results of strain gauges and to obtain more conclusive results about the accuracy of the strain data, it will be also of interest to carry out tests where the frequency of the cycling load will allow the sampling rate of the DOFS acquisition system to follow the load profile of the variable load.

Acknowledgements: This project has received funding from the European Union's Horizon 2020 research and innovation programme under the Marie Sklodowska-Curie grant agreement No. 642453.

References

[1] A. (American S. of C. Engineers), "2017 Infrastructure Report Card ASCE," **2017**.

[2] B. Glisic, D. Hubbell, D. H. Sigurdardottir, and Y. Yao, "Damage detection and characterization using long-gauge and distributed fiber optic sensors," Opt. Eng., vol. 52, p. 87101, **2013**.

[3] J. N. Kudva, C. Marantidis, J. D. Gentry, and E. Blazic, "Smart structures concepts for aircraft structural health monitoring," in 1993 North American Conference on Smart Structures and Materials, **1993**, pp. 964–971.

[4] J. R. Casas and P. J. S. Cruz, "Fiber Optic Sensors for Bridge Monitoring," J. Bridg. Eng., vol. 8, no. 6, pp. 362–373, **2003**.

[5] P. Ferdinand, "The Evolution of Optical Fiber Sensors Technologies During the 35 Last Years and Their Applications in Structure Health Monitoring," EWSHM-7th Eur. Work. Struct. Heal. Monit., **2014**.

[6] A. Barrias, J. Casas, and S. Villalba, "A Review of Distributed Optical Fiber Sensors for Civil Engineering Applications," Sensors, vol. 16, no. 5, p. 748, May **2016**.

[7] G. Rodriguez, J. R. . Casas, and S. Villalba, "SHM by DOFS in civil engineering: a review," Struct. Monit. Maint., vol. 2, no. 4, pp. 357–382, Dec. **2015**.

[8] S. Villalba and J. R. Casas, "Application of optical fiber distributed sensing to health monitoring of concrete structures," Mech. Syst. Signal Process., vol. 39, no. 1, pp. 441–451, **2012**.

[9] G. Rodriguez, J. R. Casas, and S. Villalba, "Cracking assessment in concrete structures by distributed optical fiber," Smart Mater. Struct., vol. 24, no. 3, p. 35005, **2015**.

[10] A. Barrias, G. Rodriguez, J. R. Casas, and S. Villalba, "Application of distributed optical fiber sensors for the health monitoring of two real structures in Barcelona," Struct. Infrastruct. Eng., vol. 14 (7), 967-985, **2018**.

[11] A. Barrias, J. R. . Casas, and S. Villalba, "Performance analysis of distributed optical fiber bonding adhesives to concrete," in Proceedings of 9th International Conference on Bridge Maintenance, Safety and Management, IABMAS **2018**.

[12] A. Barrias, J. R. . Casas, and S. Villalba, "On the bonding performance of distributed optial fiber sensors (DOFS) in structural concrete," in Proceedings of the Sixth International Symposium on Life-Cycle Civil Engineering, IALCCE'18, **2018**.

[13] N. A. A. Rahim et al., "Superior fatigue characteristics of fiber optic strain sensors," LUNA, **2013**.

[14] J. R. Pedrazzani, S. M. Klute, D. K. Gifford, A. K. Sang, and M. E. Froggatt, "Embedded and surface mounted fiber optic sensors detect manufacturing defects and accumulated damage as a wind turbine blade is cycled to failure," Luna Innov. Inc, **2012**.

[15] L. Wong, N. Chowdhury, J. Wang, W. K. Chiu, and J. Kodikara, "Fatigue damage monitoring of a composite step lap joint using distributed optical fibre sensors," Materials (Basel)., vol. 9, no. 5, p. 374, **2016**.

[16] CEN (European Committee For Standardization), “EN 1991-2.” **2002**.